

SAE Baja Dynamic Loading Final Project Report

September 28th, 2015



Team: Get Loaded

Members:

Ryan Flatland (rflatlan@calpoly.edu)
Christian George (chgeorge@calpoly.edu)
Nick Bonafede (nbonafed@calpoly.edu)

Advisor/Sponsor:

Professor Fabijanac

Statement of Disclaimer

Since this project is a result of a class assignment, it has been graded and accepted as fulfillment of the course requirements. Acceptance does not imply technical accuracy or reliability. Any use of information in this report is done at the risk of the user. These risks may include catastrophic failure of the device or infringement of patent or copyright laws. California Polytechnic State University at San Luis Obispo and its staff cannot be held liable for any use or misuse of the project.

Table of Contents

List of Figures	6
List of Tables	8
Abstract	9
Chapter 1 - Introduction	
Sponsor Background	10
SAE Baja Vehicle	10
Objectives	12
Chapter 2 - Background	
Measurement Techniques	13
Strain Gauges	13
Introduction	13
Wheatstone Bridge Circuit	21
Amplification	26
Data Acquisition	31
Error Compensation Methods	32
Calibration	35
Force Transducers	37
Dynamics Based Measurements	37
Accelerometers	37
Potentiometers and Position Sensors	38
Direct Measurements of the Loads on the Wheel	38
Wheel Force Transducer	38
Chapter 3 - Design Development	
Suspension	41
Rear Suspension	42
Front Suspension	43
Chassis	45
Skid Plate	45
Frame Roll Hoop	46
Drivetrain	46
Chapter 4 - Final Design Description	47
Strain Gauges	47

Accelerometer	50
Mechanical Design	51
Amplification/Wheatstone	55
DAQ	59
Packaging	60
Amplifier/Wheatstone Bridge Unit	60
Strain Gauge Attachment	67
Analysis	69
Cost Analysis	74
Safety Considerations	76
Maintenance and Repair Considerations	77
Chapter 5 - Design Verification Plan	
Current Testing Plans	78
Calibration	78
Cal Poly Land Plan	80
Specification Verification Checklist	83
Chapter 6 - Project Management Plan	
Management	84
Key Deadlines	84
Gantt Chart	85
Outstanding Tasks	85
Failure Mode and Effect Analysis	86
Chapter 7 - Manufacturing	
8-Channel Wheatstone Amplifier	87
Shocker Rocker	89
Calibration Jigs	90
Strain Gauge Application	91
Baja SAE Vehicle System	92
Chapter 8 - Calibration, Testing, Troubleshooting and Results	
Calibration	94
Amplifier	94
Front Spindle	96
Rear Links	97
Post Calibration	98
Testing	99

Car Scales	99
Driving Test Cases	101
Troubleshooting	103
Drift Causes	104
Bench Tests	104
Drift Troubleshooting Conclusions	108
Post Calibration	108
Results	109
Chapter 9 - Conclusions and Recommendations	114
References	115
Appendices	
Appendix A: Goal Development	
Appendix B: Drawing Packet	
Appendix C: Purchasing Information	
Appendix D: Manufacturer Specifications and Data Sheets	
Appendix E: Detailed Supporting Analysis	
Appendix F: Gantt Chart	
Appendix G: Other Supporting Material	
Appendix H: Calibration Data	
Appendix I: MATLAB Plots	
Appendix J: MATLAB Code	

LIST OF FIGURES

- Figure 1. Common Metal Foil Strain Gauge
- Figure 2. Various Linear Strain Gauges and Strain Gauge Rosettes
- Figure 3. 45-Degree Rosette Figure used with Equation Strain Determination Equations
- Figure 4. Strain Gauge Life Curve at Varying Alternating Strains
- Figure 5. Strain Gauge Piezoelectric Transducer
- Figure 6. Two FBG optical strain gauges from Micron Optics Inc.
- Figure 7. Typical Wheatstone Bridge Circuit
- Figure 8. Multiple Wheatstone Strain Gauge Configurations
- Figure 9. Basic Positioning of Strain Gauges based on Desired Strain Measurement
- Figure 10. Single Differential Amplifier
- Figure 11. Two Op-Amp Instrumentation Amplifier
- Figure 12. Three Op-Amp Instrumentation Amplifier
- Figure 13. Omega Engineering's DMD-465 Amplifier and Signal Conditioner
- Figure 14. Texas Instruments' INA827 Instrumentation Amplifier
- Figure 15. Race Technology's DL1-MK3 Data Logger/Data Acquisition Device
- Figure 16. Temperature Compensated Wheatstone Bridge Circuit
- Figure 17. Lead Wire Temperature and Resistance Compensated Quarter-Bridge
- Figure 18. Introduction of External Error due to Common Mode Noise
- Figure 19. Visual Representation of Twisted Pair Theoretical Effectiveness
- Figure 20. Shunt Calibration of Strain Gauges
- Figure 21. Michigan Scientific ATV Force Transducer Output
- Figure 22. University of Pretoria in South Africa's Custom Wheel Force Transducer
- Figure 23. Shocker Rocker Concept (Middle hole mounts to current shock mount)
- Figure 24. Spindle strain under front suspension combined loading
- Figure 25. Example Strain Gauge Calibration Plot
- Figure 26. Spindle Strain Gauge Orientation
- Figure 27. Omega's KFH-3-350-C1-11L1M2 Pre-Wired Strain Gauge
- Figure 28. Kionix KXD94-2802 3-Axis Accelerometer
- Figure 29. Final Shocker Rocker Geometry
- Figure 30. Shocker Rocker CNC Component with Bearings and Shoulder Bolt
- Figure 31. Shocker Rocker Tab Jig
- Figure 32. Spindle Calibration Jig
- Figure 33. Linear Technology LTC2053 Precision Instrumentation Amplifier
- Figure 34. Wiring Schematic of a Typical Application for a LTC2053 Amplifier
- Figure 35. 3 Op-Amp Differential Amplifier
- Figure 36. Uncompensated Quarter-Bridge Wheatstone Bridge Circuit

- Figure 37. Schematic for Wheatstone and Amplifier
- Figure 38. Updated Schematic for Wheatstone and Amplifier
- Figure 39. Board Rendering for Wheatstone and Amplifier System
- Figure 40. Polycase Enclosure for Amplifier/Wheatstone Unit
- Figure 41. Location of Mounting Tape on Strain Gauge
- Figure 42. Cut FBD Showing Application Points of Forces on Front Suspension
- Figure 43. Free Body Diagram of Rear Suspension Link Forces and Tire Loads
- Figure 44. Completed 8-Channel Wheatstone Amplifier
- Figure 45. Spindle Strain Gauge Amplifier Location
- Figure 46. Rear Links Strain Gauge Amplifier Location
- Figure 47. Assembled Shocker Rocker with Small Axial Link and Shock
- Figure 48. Front Spindle Calibration Jig
- Figure 49. Prepped Axial Links for Strain Gauge Application
- Figure 50. Rear Links Strain Gauge Wiring and Assembly
- Figure 51. Front Spindle Strain Gauge Wiring and Assembly
- Figure 52. Rear Link Amplifier Offset Calibration Process (Off-Car)
- Figure 53. Rear Link Amplifier Offset Calibration Process (On-Car)
- Figure 54. Front Spindle Calibration Jig Assembly
- Figure 55. Attaching Nut to Spindle Calibration Jig
- Figure 56. Rear Link Clevises and Instron Calibration Testing
- Figure 57. Attaching the DAQ and Recording Weight of Vehicle on Car Scales
- Figure 58. Removal of Induced Side Forces with Suspension Travel using Plastic BBs as Rollers
- Figure 59. Temperature Test: Heated Unstressed Quarter Bridge
- Figure 60. Controlled Temperature Test: Unstressed Quarter Bridge
- Figure 61. Controlled Temperature Test: Unstressed Half Bridge
- Figure 62. Vibration Test: Unstressed Half Bridge on Driving Car
- Figure 63. Post Calibration of Link 3 Exhibiting Nonlinear Behavior
- Figure 64. Matlab Filtered Load Data - Driving over Whoops

LIST OF TABLES

Table 1. Omega Engineering Summary of Multiple Wheatstone Bridge Configurations

Table 2. Maximum and Minimum Predicted Strains from Strain Gauges

Table 3. Predicted Resistance Changes from Strain Gauges

Table 4. Predicted Voltages from Strain Gauges

Table 5. Maximum Ranges Allowed based on $\pm 5V$ DAQ Input

Table 6. Selected Gain Resistors and Location

Table 7. Actual Gain from using Selected Gain Resistors

Table 8. Strain Output Band Predicted

Table 9. Setting Time for Adhesives

Table 10. Full Project Cost Analysis

Table 11. Amplifier/Wheatstone Cost Analysis

Table 12. Checklist for Shaft Diameters

Table 13. Gantt Chart

Table 14. FMEA Table

Table 15. Drift of Zero-Point for Each Run and Each Gauge

Table 16. Peak Load Table (lbf)

Table 17. Peak Load Table (Full Car g's)

ABSTRACT

Cal Poly's SAE Baja team undertook a project to measure the loads applied to an off-road buggy via the ground, including any obstacles. Originally, the ground loads pertaining to suspension, drivetrain, and chassis were based on rough estimates and historical part failures. This led to large safety factors, overbuilt parts, unknown part life, and improperly designed points of failure. In order for the team's designs to advance to the next level of competition, an accurate set of loading cases were required. The main focus of the project was the suspension loads measured with strain gauges and a shock potentiometer, however loading the chassis was also analyzed.

The data collected via an onboard DAQ was analyzed via a MATLAB code in order to recreate the peak loads at the wheel. The table of loads can be found within the results section of this document and is listed below as well. These loads will be used to help future SAE Baja teams design improved parts according to known, experimental test data.

	Front Suspension			Rear Suspension		
Loading Case	Fx [lbf]	Fy [lbf]	Fz [lbf]	Fx [lbf]	Fy [lbf]	Fz [lbf]
Acceleration	60	150	-80	150	150	50
Hard Brake	-200	1500	-1300	-100	-500	-120
Left Turn	-1600	4600	-3200	-250	450	-280
Right Turn	450	-1500	-1300	-160	-1000	-75
Rocks	-1400	4400	-3000	-370	-1000	-250
River Bed	-750	2600	-1800	-350	-1000	-350
Rollers	-750	2500	-1800	-250	300	-350
Whoops	-1200	4200	-3000	-250	2600	-550
Tip Over	-2500	8800	-6500	-250	1400	-300
Jump	-450	2200	-1700	-250	350	-400

CHAPTER 1

INTRODUCTION

The Get Loaded team was assigned a project determining the current unknown loading seen by the SAE Baja vehicle under normal and extreme driving conditions. We focused our efforts to determine quantitative values for loadings within the SAE Baja vehicle's front and rear suspension, chassis, and drivetrain. Finding values for these specific loads will allow the team to refine design specifications for realistic loads - this could lead to a reduction in weight, increase in reliability, and allow the SAE Baja team to accurately predict part fatigue life and assist in predicting component failure.

Direct stakeholders of the project include, but are not limited to, the SAE Baja Team (Primary), Professor Fabijanic and possibly other teams considering similar load test methods. The goal of the project was to produce a set of deliverables including an easy to read load table of multiple components, an in-depth report on testing methods for the included loads to assist in creating load values or conducting future tests for different loads.

SPONSOR BACKGROUND

SAE Baja Vehicle

For the SAE mini-Baja competition, students across the world design, build, test and race a single seat off-road vehicle. Our goal was to compile a list of loading cases and lay out a general design process with typical safety factors in order to optimize Cal Poly's Baja car for use in this competition. The competition consists of several events, each of which is scored based on how quickly your car and driver can complete the course. This means that we want to design a fast yet reliable vehicle for competition. We must therefore know what loads are seen by the car during normal and extreme operating condition as well as how often these conditions occur.

The car consists of 6 main subsystems: chassis, suspension, drivetrain, steering, brakes and ergonomics. Accurate loading cases are essential for each of these systems to function properly and at a high efficiency. This will prevent both the over-design of some parts and the failure of others. In previous years these loads have been estimated based on educated guesses and while some systems (brakes) are relatively certain of their loads with calculations and simple tests,

several others (chassis, suspension, steering, drivetrain) must add large safety factors to compensate for the uncertainty in their loading.

The biggest unknown of the group is the suspension loads. Under general driving, we can consider a quarter car model with weight, normal force and traction. However, this is rarely the true case for an off-road vehicle. Whenever the car becomes airborne, it will invariably impact the ground to recover. During this process we have previously assumed a 5g quarter-car impact load with a safety factor of 3. These are fairly arbitrary numbers which have been justified by the fact that we have been using them for several years with no significant failures.

For example, if only one tire lands before the others, which is often the case, the entire weight of the car would be on one corner of the suspension. However, since the springs allow for compression to disperse the impulse of the impact over time, the peak of the impact might be much lower. Thus, we want the loads at the tire for a typical and extreme frontal, side, and lower impacts on both the front and rear tires. Along the same lines, we want to find the force generated by an impact that would cause the wheel to turn about the steering axis either from diamond shaped ruts forcing the front tires together, or an impact from another car.

Another relatively unknown load is the torque exerted on the drivetrain from hitting the ground after a jump. Currently, the only known load was calculated to be 5500 in-lbf from a key that failed on impact 6 years ago. We would like to more accurately measure this load in order to have a more reliably design and predict the life of the drivetrain. The current gearbox was designed for 25 hours of operation at this load of 5500 in-lbf, so it is probably much stronger than necessary, but as we are unsure of the magnitude and frequency of these extreme loads, it is better to over-design the gearbox to guarantee reliability at the cost of weight.

The final system to focus on is the loads seen by the chassis. Under most loading cases the majority of the load comes from the shocks transferring wheel load to the frame. This can be accurately accounted for by the suspension analysis. However, the main failure situation for the frame is during a rollover or impacting an obstacle or another car. Thus, we wanted to gather data that accurately depicted these scenarios to better design our chassis to keep the driver safe without adding unnecessary weight.

OBJECTIVES

Get Loaded wanted to produce a document explaining typical loading cases of a Baja car for use by future Baja teams at Cal Poly. Our deliverable is a load table of the major loads seen on the SAE Baja vehicle and an in-depth report with easy to use instructions for the use of future Baja teams. It will contain a list of typical loading cases seen on the suspension (tires) and chassis. Due to the limited amount of resources, an in-depth analysis on the drivetrain was considered but later abandoned.

Engineering Specifications:

The loadings of interest are listed in the Appendix G. Our goal was to quantify each of these loads such that we can be confident that our value is $\pm 10\%$ of the load experienced. This was based on the Baja team's desire to declare a safety factor to the precision of one decimal. The included QFD in the Appendix A was used to determine the ranking of importance of each loading case.

Suspension loads were quantified in the frame of reference of the vehicle, meaning that pitching of the car and steering of wheels did not need to be quantified in order to completely define the forces relative to the car. Additionally, it was not our goal to find the exact forces at the contact patch, rather the apparent loads as experienced by the suspension components transferring those loads to the vehicle.

Budget

Our current budget of funding from the Baja team was \$1000. Additionally, we determined that only half of the DAQ repair and upgrade costs fell onto this senior project, since the Baja team needs the repair and will benefit from the increases in functionality from the upgrades needed to complete the Get Loaded project.

CHAPTER 2

BACKGROUND

Loading analysis and quantification is a very well-developed and well-documented science. Strain gauges, force transducers, and accelerometers are common measurement tools to analyze the forces experienced by assemblies. Accurate determination of loads are critical in multiple phases of a system's design, testing, and competition as they can give an insight to failure points within a system and predict fatigue life in critical components.

Forces can be measured in various ways: the easiest of which is to place a force transducer at the point of impact to directly measure the force. However, as the majority of the loads we wished to test were on a rotating and translating object this is not possible. This left us to measure the force indirectly through the reaction induced on subsequent components in the system. The methods considered and discussed were via the use of strain gauges on current members of the car or through the placement of force transducers between members.

Strain Gauges

Introduction

Strain Gauges are an extremely common piece of measuring equipment that are regularly used within commercial, industrial and personal applications. The benefit of strain gauges is that they can convert multiple varieties of applied loading into a simple resistance change. Thus, they convert mechanical properties from a physical system into electrical data value that can then be used to record actual loads and/or pressures for future component design or system setup. Knowing these specific loads from experimental results allowed a comparison with theoretical models which yielded either equation setup errors or unforeseen effects of other components or physical properties.

In order to convert mechanical properties of a system to an electrical value, a strain gauge consists of a simple filament of wire structured within a grid to create a resistor with a predefined resistance. The strain gauge is then attached to a physical component that has induced stress from a loaded force or pressure. As the mechanical component experiences and induced load, the material of the piece will begin to deflect. This deflection then causes the strain gauge to slightly expand or retract. As the strain gauge expands or retracts, the given resistance experiences a slight change due to the deflection of the internal wire. Thus, the change in the deflection of the material will then create a change in resistance within the strain gauge. Since the change in the

both resistance of the strain gauge is directly related to the deflection of the material, the strain of the material (change in length of material) can be measured by this change in resistance.

Gauge Factor

One key component when relating the strain to the resistance is to understand that every gauge has a certain “gauge factor”. The gauge factor, k , determines the ratio of resistance change within a strain gauge to the strain of the material as evident in Equation 1.

$$k = \frac{\Delta R}{\Delta L} = \frac{\Delta R}{\varepsilon} \quad (1)$$

k : Gauge Factor

ΔR : Change in Resistance

ΔL : Change in Material Length

ε : Strain of Material

This factor can vary depending on the design material of the strain gauge or the type of strain gauge chosen. A more in-depth explanation of different types of strain gauges can be found below within the “Types of Strain Gauges” section. The gauge factor can also be related directly to the strain gauge’s sensitivity. A more sensitive strain gauge will yield smaller changes in strain. According to HBM’s “Applying the Wheatstone Bridge Circuit”, the most common strain gauge, the metal foil gauge, normally has a gauge factor of about 2. Also according to the HBM document, the experimentally determined “gauge factor” is commonly written on the packaging of the strain gauge.

Types of Strain Measurement Devices and Equation Derivation

There are various types of strain gauges to choose from depending on a strain gauge’s application and design parameters. Three popular choices for measuring strain are metal foil strain gauges, piezoelectric transducers and FBG optical sensors.

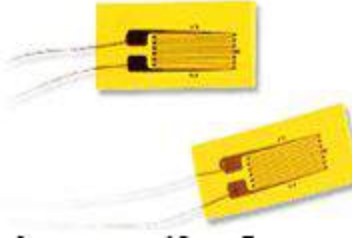


Image courtesy of Omega Engineering

Figure 1. Common Metal Foil Strain Gauge

The most common of the three are metal foil gauges as shown in Figure 1. They consist of a filament wire running through a grid that creates a resistor. According to Omega Engineering's "The Strain Gauge", the nominal resistance value for metal foil strain gauges range from 120 ohms to 5000 ohms depending on the specific application and design parameters. However, the most common resistance for metal foil gauges is either 120 ohm or 350 ohms. The common max induced strain for multiple commercial strain gauges provided by Omega Engineering can range from 30,000 micro-strain to 50,000 micro-strain. Grid length can also range of the gauge can also range from as small as 0.008 in to 4in ("The Strain Gauge"). A longer grid length will simply measure over a larger area of material for an average strain. They generally are cheaper than smaller strain gauges because the tolerances do not have to be so miniscule. However, smaller grid lengths can measure more specific points on a component. Smaller grid lengths would be more beneficial for members in bending or torsion as they will give a more precise measurement value in contrast to purely axial stress where they entire member experiences the same strain (theoretically).

Although the general construction of metal foil gauges is similar except for varying grid length and nominal resistance, the arrangement of multiple strain gauges on a single piece of foil can vary. Figure 1 is an example of a linear strain gauge capable of only measuring linear strain at a given point. However, sometimes it is desirable to measure multiple directions of strain at a specific point to determine a component's complete loading. A strain gauge setup with multiple strain gauges is called a "rosette". Figure 2 below shows multiple strain gauge layouts of various rosettes.

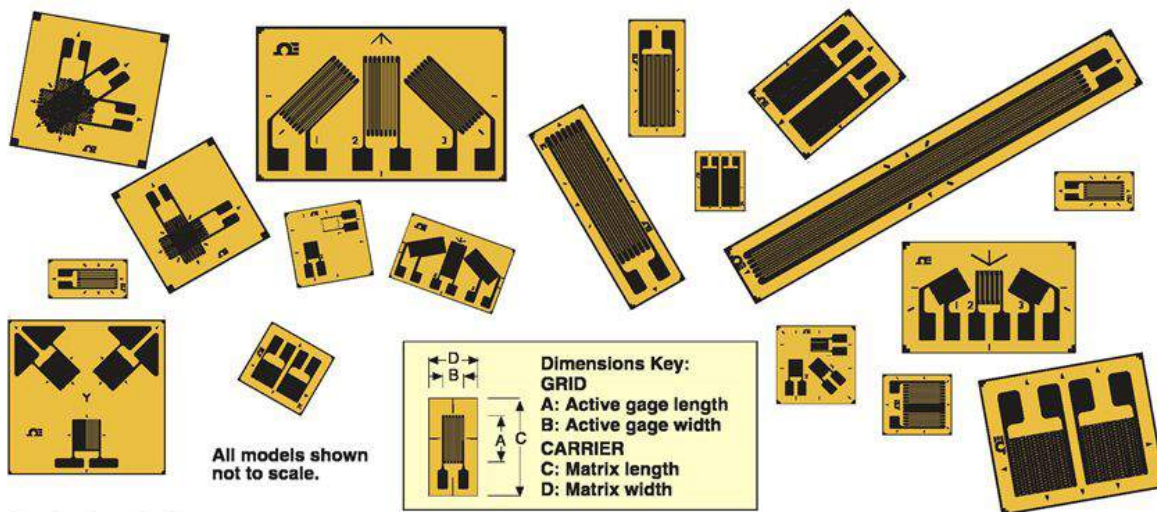


Image courtesy of Omega Engineering

Figure 2. Various Linear Strain Gauges and Strain Gauge Rosettes

If the desired point of measurement is small, but multiple strain locations need to be measured, a layered or stacked rosette (as seen in the top left corner of Figure 2) can be used instead of planar rosette (as seen in the bottom left corner of Figure 2). Rosettes can be beneficial when the direction of the induced stress within the member is unknown or if the loading on the member is completely unknown because the following equations, provided courtesy of Vishay Precision Group's "Strain Gage Rosettes: Selection, Application and Data Reduction", can be used in order to determine the principle strains. The following equations assume that a 45-degree rosette is being used oriented as shown in Figure 3. Get Loaded decided to choose a 45-degree rosette, therefore the equations will relate directly to the conceptual design.

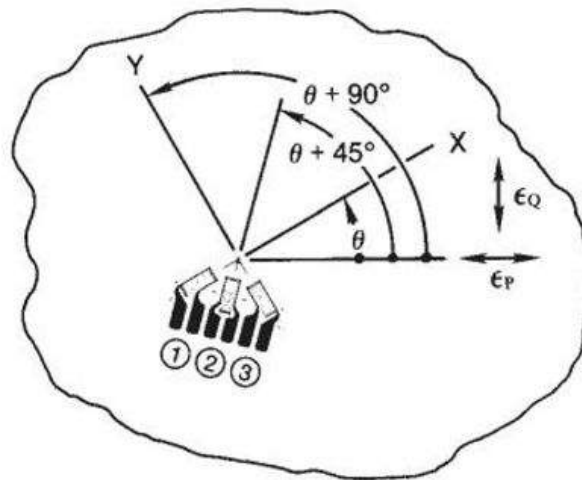


Figure 3. 45-Degree Rosette Figure used with Equation Strain Determination Equations

$$\varepsilon_1 = \frac{\varepsilon_P + \varepsilon_Q}{2} + \frac{\varepsilon_P - \varepsilon_Q}{2} \cos(2\theta) \quad (2)$$

$$\varepsilon_2 = \frac{\varepsilon_P + \varepsilon_Q}{2} + \frac{\varepsilon_P - \varepsilon_Q}{2} \cos 2(\theta + 45^\circ) \quad (3)$$

$$\varepsilon_3 = \frac{\varepsilon_P + \varepsilon_Q}{2} + \frac{\varepsilon_P - \varepsilon_Q}{2} \cos 2(\theta + 90^\circ) \quad (4)$$

ε_1 : Strain in Gauge 1

ε_2 : Strain in Gauge 2

ε_3 : Strain in Gauge 3

ε_P : Strain in the Primary Horizontal Direction

ε_Q : Strain in the Primary Vertical Direction

θ : Angle at which Gauge 1 is Oriented in Relation to Primary Horizontal Direction

Equation 2, Equation 3 and Equation 4 are the standard equations for the strains within the strain gauges shown in Figure 3. The equations can be rewritten to create Equation 5 and Equation 6 below.

$$\varepsilon_{P,Q} = \frac{\varepsilon_1 + \varepsilon_2}{2} \pm \frac{1}{\sqrt{2}} \sqrt{(\varepsilon_1 - \varepsilon_2)^2 + (\varepsilon_2 - \varepsilon_3)^2} \quad (5)$$

$$\theta = \frac{1}{2} \tan^{-1} \left(\frac{\varepsilon_1 - 2\varepsilon_2 + \varepsilon_3}{\varepsilon_1 - \varepsilon_3} \right) \quad (6)$$

Once the principle strains are found, the principle stresses can be found using Equation 7 and Equation 8.

$$\sigma_P = \frac{E}{1-\nu^2} (\varepsilon_P + \nu\varepsilon_Q) \quad (7)$$

$$\sigma_Q = \frac{E}{1-\nu^2} (\varepsilon_Q + \nu\varepsilon_P) \quad (8)$$

σ_P : Stress in the Primary Horizontal Direction

σ_Q : Stress in the Primary Vertical Direction

E : Modulus of Elasticity of Measured Material

ν : Poisson's Ratio of Measured Material

Depending on the geometry of the component being analyzed, the stresses can then be used in order to find the original loading of the member.

The life of typical metal foil strain gauges can extend up into the hundreds of thousands of cycles. However, after a certain amount of use, the accuracy of the strain gauge begins to dwindle as the filament within the strain gauges experiences fluctuating stresses. Fortunately, a presentation completed by HBM documented the life cycle of strain gauges by testing them to failure under varying cyclical loads (Kleckers).

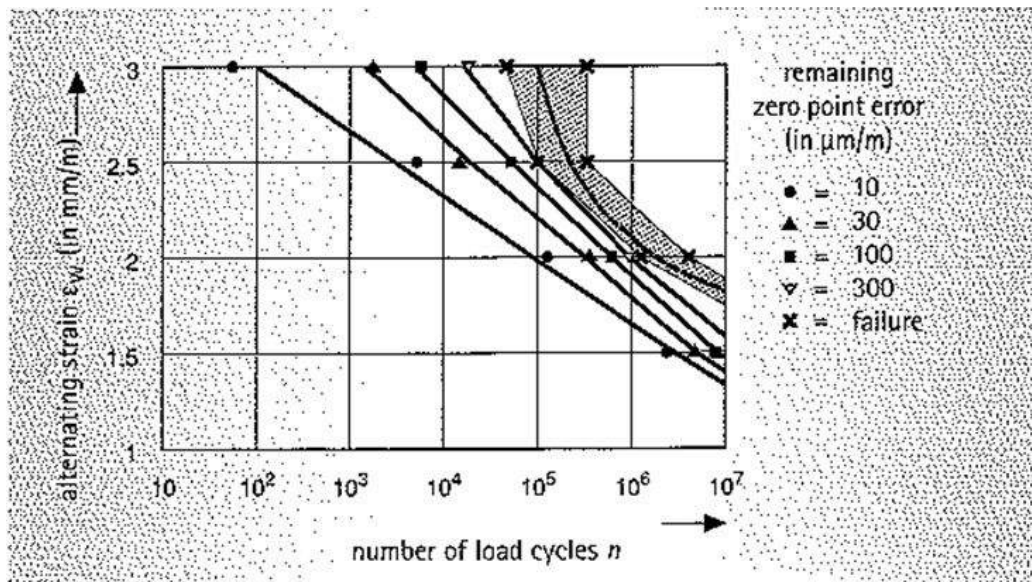


Image and description courtesy of HBM

Figure 4. Strain Gauge Life Curve at Varying Alternating Strains

Taken from Klecker's presentation, Figure 4 identifies a rough life curve of a standard metal foil strain gauge with induced fully reversible loading. As the load cycles and alternating strain increases in magnitude, the zero point of the strain gauge begins to increasingly deviate from center. This was a major concern for the Get Loaded project because all of the measurements used for the project are caused from dynamic loading. Therefore, the design of the Get Loaded project needed to be within an acceptable zero point error for the strain induced and cyclic loading. Also, the amount of tests and the span in which they are conducted was carefully monitored as straining the gauges affected the accuracy and precision of the results. This was compensated by re-calibration before testing.



Image and description courtesy of HBM

Figure 5. Strain Gauge Piezoelectric Transducer

Piezoelectric sensors (Figure 5) could also be used to measure strain within a component. HBM's "Strain Gauges or Piezoelectric Sensors? A Comparison" explains that the piezoelectric sensors can determine strain by a voltage created by a compression of internal crystals. The force applied can then be used to determine the strain within the member. They are more accurate and precise for strain measurements within a given component in comparison to their metal foil strain gauge counterparts. However, they have a huge limitation because the loading force needs to be known in order to determine the induced strain within the component. Therefore, piezoelectric sensors were not further researched for the Get Loaded project as the loading on the Baja vehicle is unknown and the primary objective of the project.



Image and description courtesy of National Instruments

Figure 6. Two FBG optical strain gauges from Micron Optics Inc.

FBG (also known as fiber Bragg grating) optical sensors (Figure 6) are yet another method to analyze the strain within a component. According to National Instruments' white paper "FBG Optical Sensing: A New Alternative for Challenging Strain Measurements", FBG optical sensors use refraction of light within fiber optic cords in order to find the strain at a localized point. Since they do not use any electrical components and determine strain via light, they are not susceptible to any errors or noise via electronic data collection. However, due to the fact that they are a relatively new technology and expensive in comparison to metal foil gauges, FBG optical sensors were not further researched for the Get Loaded project.

Popular Metal Foil Strain Gauge Vendors

Some popular Metal Foil Strain Gauge vendors are Omega Engineering, HBM, National Instruments and Vishay Precision Group. All of the vendors have an extensive selection of strain gauges and measurement devices. Thus, final cost will play a role in the final selection of a specific manufacturer.

Wheatstone Bridge Circuit

Introduction

Typically, a data acquisition device (DAQ) collects and/or analyze a voltage from another device or load. Therefore, in order to be able to read the change in resistance of a metal foil strain gauge, the change in resistance must be converted into a voltage. One method of converting a change in resistance to voltage is by incorporating the strain gauge within a Wheatstone bridge circuit (Figure 7).

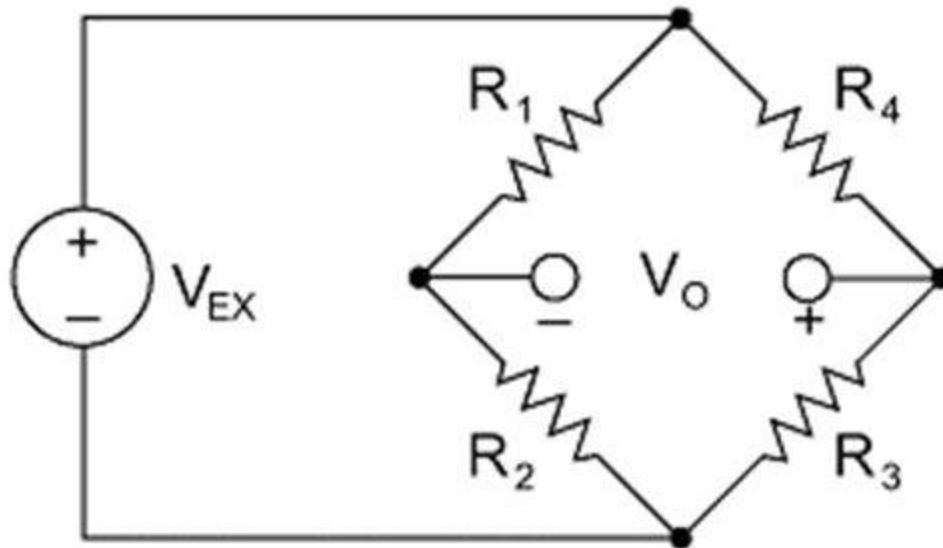


Image courtesy of National Instruments

Figure 7. Typical Wheatstone Bridge Circuit

In order to determine the strain within a member, at least one of the resistors R_1 , R_2 , R_3 or R_4 within the Wheatstone circuit would be replaced with a strain gauge. All of the non-strain gauge resistances would have a value similar to the nominal value of the strain gauge. Thus, the Wheatstone bridge works by “comparing unknown resistances [metal foil strain gauge resistances] with well-defined resistance [non-strain gauge resistances]” (Hoffmann). In order to measure the difference between the known and unknown resistance, an external excitation voltage must be added to the Wheatstone bridge as seen in Figure 7.

Wheatstone Bridge Equation Derivation

Using simple circuitry equations, if all of the resistors equal each other ($R_1=R_2=R_3=R_4$), the voltage drop across all the resistors would be half of the excitation voltage. Since the voltage drop across R_1 and R_4 would be the same, the resulting output voltage (V_o) would equal zero and the Wheatstone bridge would be considered balanced. Some basic assumptions with the Wheatstone circuit is that the bridge is not excited by the measurement device connected to the output voltage (Hoffmann). This is done by having a high impedance by the device connected to these terminals. A further explanation on how this error is avoided can be found within the *Amplification* section.

When the bridge is considered unbalanced, one or more of the resistors within the Wheatstone bridge circuit differ from the one another. Thus, if resistor R_4 was a strain gauge and slightly changed its resistance value from the fixed resistors, a difference within the voltage drop across resistors R_1 and R_4 will occur. The difference in the voltage drop across both resistors R_1 and

R_4 can be found by measuring the voltage difference across the nodes in the middle of the bridge. Hoffmann's "Applying the Wheatstone Bridge Circuit" has a simplified formula to find the output voltage as a function of the excitation voltage and resistances as shown in Equation 8. The labeling for the specific values have been changed slightly to match the same label convention within Figure 8.

$$V_O = V_{EX} \left(\frac{R_3}{R_3 + R_4} - \frac{R_2}{R_1 + R_2} \right) \quad (9)$$

V_O : Output Voltage from Wheatstone Bridge Circuit

V_{EX} : Excitation Voltage Applied to Wheatstone Bridge

R_1 : Fixed Resistor or Strain Gauge 1

R_2 : Fixed Resistor or Strain Gauge 2

R_3 : Fixed Resistor or Strain Gauge 3

R_4 : Fixed Resistor or Strain Gauge 4

Variations of Strain Gauge Wheatstone Bridges and Strain Gauge Positioning

Due to the fact that any of the fixed resistors can be replaced by a strain gauge, multiple configurations of a Wheatstone bridge can be achieved. Three possible configurations are a quarter bridge, half-bridge or full-bridge. The schematic of each bridge can be found within Figure 8. Each configuration has its own benefits and pitfalls. A more full bridge will increase the sensitivity of the Wheatstone bridge, thus increasing the output voltage per micro-strain ("Positioning Strain Gauges").

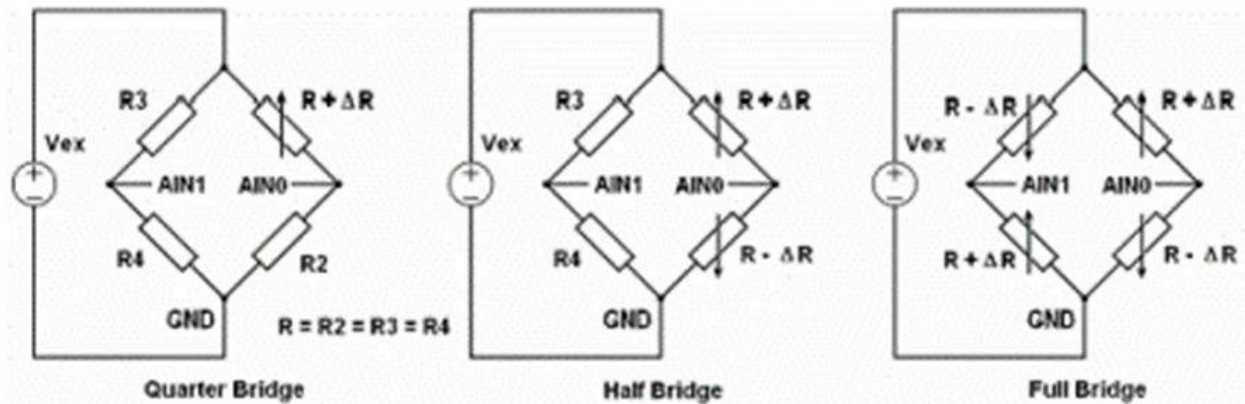


Image courtesy of Emant PTE

Figure 8. Multiple Wheatstone Strain Gauge Configurations

As evident within Figure 8, a quarter-bridge consists of a single stressed strain gauge attached normally to the high end of the Wheatstone bridge. This configuration allows the linear strain of a member at the mounted strain gauge's location on the component to be converted into a voltage. A quarter-bridge Wheatstone bridge configuration produces the lowest sensitivity of all the configurations and does not compensate either temperature effects within the strain gauge compared to the studied material and does not compensate for any other superimposed strain states within the specimen. Compensation methods are described in more detail within the "Compensation Methods" section. The quarter-bridge is also limited because it can measure axial and bending strains but not torsional or shear strain ("Positioning Strain Gages").

A half-bridge consists of two stressed strain gauges on a single side of a Wheatstone bridge. A half-bridge Wheatstone bridge configuration produces a more sensitivity than a quarter bridge but less than a full bridge. A half-bridge compensates for temperature effects within the strain gauge compared to the studied material and can compensate for superimposed strains when measuring bending, shear, or torsional strains. However, it can be used in two different configurations when determining the axial strain. One method involves placing both strain gauges on the same side shown in Figure 9 as strain gauges 1 and 2 within the axial strain figure. This method compensates for temperature effects, but does not compensate for any superimposed strains. The other method is to have both strain gauges opposite to each other shown in Figure 9 as strain gauges 1 and 3 within the axial strain figure. This method compensates for a superimposed bending strain, but does not compensate for any temperature effects within the circuit ("Positioning Strain Gages").

A full-bridge consists of all resistances within a Wheatstone bridge as stressed strain gauges. This configuration yields the greatest sensitivity of all the configurations and automatically

compensates for temperature effects. It also compensates for superimposed axial and bending strains within a stressed member (“Positioning Strain Gages”).

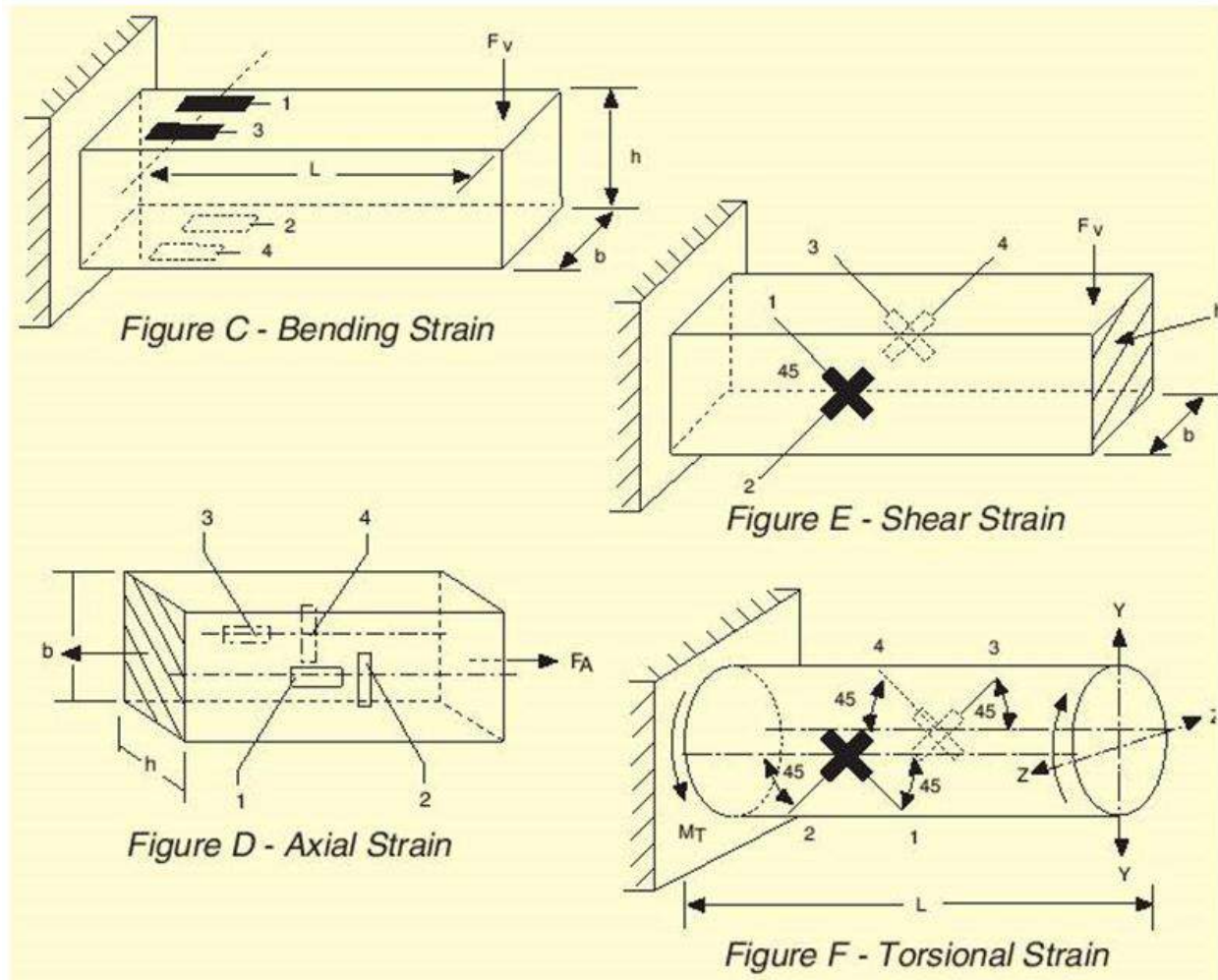


Image courtesy of Omega Engineering

Figure 9. Basic Positioning of Strain Gauges based on Desired Strain Measurement

A full table provided by Omega Engineering and found within their “Positioning Strain Gages to Monitor Bending, Axial, Shear and Torsional Loads” is provided below in Table 1 as a quick summary and verification of the claims mentioned above. For reference, the table “was created assuming a Gauge factor of 2.0, Poisson’s Ratio of 0.3, and it disregards the lead wire resistance”.

Table 1. Omega Engineering Summary of Multiple Wheatstone Bridge Configurations

STRAIN	BRIDGE TYPE	POSITION OF GAGES FIG. C-F	SENSITIVITY mV/V @ 1000 $\mu\epsilon$	OUTPUT PER $\mu\epsilon$ @ 10 V EXCITATION	TEMP. COMP.	SUPERIMPOSED STRAIN COMPENSATED
BENDING	¼	1	0.5	5 $\mu\text{V}/\mu\epsilon$	No	None
	½	1, 2	1.0	10 $\mu\text{V}/\mu\epsilon$	Yes	Axial
	Full	All	2.0	20 $\mu\text{V}/\mu\epsilon$	Yes	Axial
AXIAL	¼	1	0.5	5 $\mu\text{V}/\mu\epsilon$	No	None
	½	1, 2	0.65	6.5 $\mu\text{V}/\mu\epsilon$	Yes	None
	½	1, 3	1.0	10 $\mu\text{V}/\mu\epsilon$	No	Bending
	Full	All	1.3	13 $\mu\text{V}/\mu\epsilon$	Yes	Bending
SHEAR AND TORSIONAL	½	1, 2	1.0	10 $\mu\text{V}/\mu\epsilon$ @ 45°F	Yes	Axial and Bending
	Full	All	2.0	20 $\mu\text{V}/\mu\epsilon$ @ 45°F	Yes	Axial and Bending

Popular Wheatstone Bridge Vendors

As mentioned within the “Popular Metal Foil Strain Gauge Vendors” section above, the primary vendors of Wheatstone bridges are Omega Engineering, HBM, National Instruments and Vishay Precision Group. However, due to the tight budget presented to Get Loaded, another option is to build the Wheatstone bridges and to calibrate and zero balance each bridge.

Amplification

Introduction

Proper amplification of the Wheatstone bridges output voltage is crucial in order to be able to read the voltage at the DAQ. The output voltage from a Wheatstone bridge is typically “in the 10 mv to 100 mv range”. Since these values are relatively low compared to the range that a normal DAQ can read, the output signal must be conditioned and amplified (Karki).

Common Types of Amplifiers used for Signal Gain

Three common amplifiers used for amplification of Wheatstone signals are the one op amp differential amplifier, the three op amp instrumentation amplifier, or the two op amp instrumentation amplifier. The single differential amplifier (Figure 10) and the two op amp

instrumentation amplifier (Figure 11) are cheaper than a three op amp instrumentation amplifier (Figure 12).

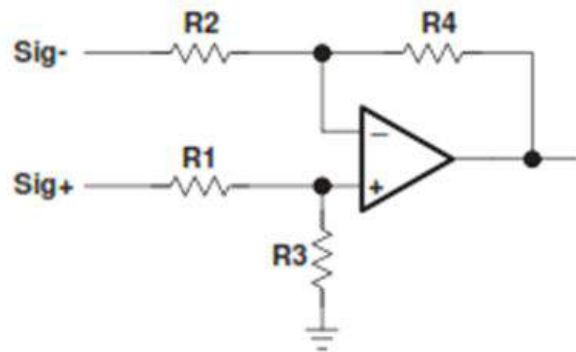


Image courtesy of Texas Instruments

Figure 10. Single Differential Amplifier

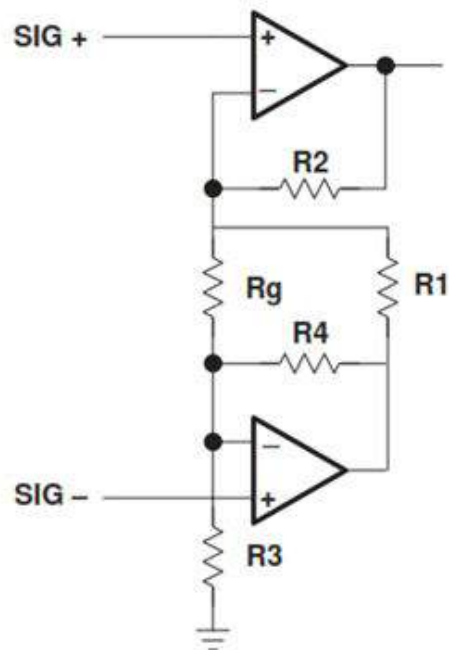


Image courtesy of Texas Instruments

Figure 11. Two Op-Amp Instrumentation Amplifier

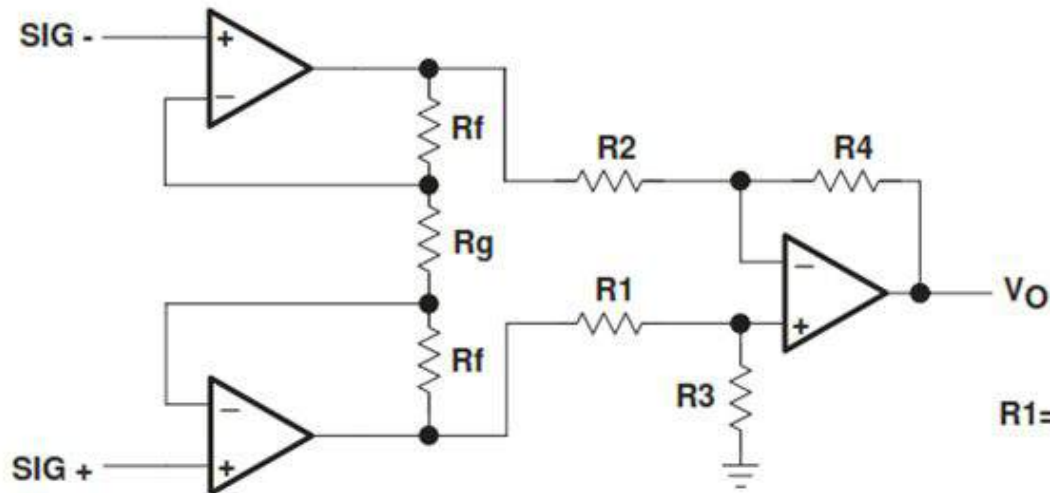


Image courtesy of Texas Instruments

Figure 12. Three Op-Amp Instrumentation Amplifier

A single differential amplifier (Figure 10) will create a gain for the output signal from the Wheatstone bridge. However, the source impedance must be considered in gain calculations. The impedance from the Wheatstone bridge will also change with a change in voltage. Therefore, the results for the gain will be nonlinear in nature (Karki). For ease of calculations and desired accuracy, a single differential amplifier was ignored for the Get Loaded project.

A two op amp instrumentation amplifier (Figure 11) eliminates the need to find the source impedance caused by the Wheatstone bridge. However, as Karki mentions, the bridge is “not as balanced as the 3 op amp instrumentation amplifier”. This is evident as the negative signal shown within the figure goes through both op amps while the positive signal goes through a single op amp (Karki). Due to a small difference in price of a two op amp and three op amp instrumentation amplifier and the necessity to acquire voltages as easily and accurately as possible, Get Loaded chose to continue with a three op amp instrumentation configuration.

The three op amp instrumentation amplifier allows the small millivolt signal from the Wheatstone to experience a gain with minimal effects on the data. As mentioned within the “Wheatstone Bridge Equation Derivation” section, the desired impedance of the amplifier unit would be infinitely large to avoid error caused by an excited Wheatstone bridge. The op amps on the left side of Figure 12 simply take the change in voltage from the Wheatstone bridge (and therefore the change in voltage from the strain gauge) to the amplifier. The impedance of both op amps are high and do not allow for current flow. The source impedance from the Wheatstone will not need to be taken into consideration when calculating the gain of the amplifier (Karki). Therefore, a voltage difference from possible current flow towards the Wheatstone bridge will

not occur, and thus not affect the signal data from the Wheatstone bridge in gain computations. The third op amp of the three op amp instrumentation amplifier seen on the far right of Figure 12 creates a gain for the signal and outputs a signal many times larger than the initial millivolt signal voltage. Therefore, due to the precision needed for the dynamic impact loading with small strains on the Get Loaded project, the three op amp instrumentation amplifier was chosen as the primary choice for signal amplification.

Manufacturing of Instrumentation Amplifiers

Instrumentation amplifiers can be created using the electrical components found within any of the wiring schematics of Figure 10, Figure 11, or Figure 12. However, unaccounted resistances within solder joints, long wires or even high tolerances within the resistors themselves would create a tedious and time consuming process for the large production necessary for the Get Loaded project.

Major measurement companies such as Omega Engineering or HMB provide easy amplification with signal conditioning via low pass filters and capacitors (“DMD-465”). These allow gain adjustments via a potentiometer and easy to connect terminals. An example of a full amplifier with signal conditioning is Omega Engineering’s DMD-465 (Figure 13).



Image courtesy of Omega Engineering

Figure 13. Omega Engineering’s DMD-465 Amplifier and Signal Conditioner

However, the high cost of these amplifiers and the amount of amplifiers needed to conduct specific tests on different facets of the Baja vehicle grossly exceeded the budget available to the Get Loaded project.

Another commercially available instrumentation amplifier are instrumentation amplifiers created using a single integrated circuit (IC) chip. These are low cost alternatives compared to fully amplifiers and signal conditioners, but they do require separate signal conditioning to be added to the circuit. An example of the schematic of an IC instrumentation amplifier is Texas Instruments' INA827 shown in Figure 14.

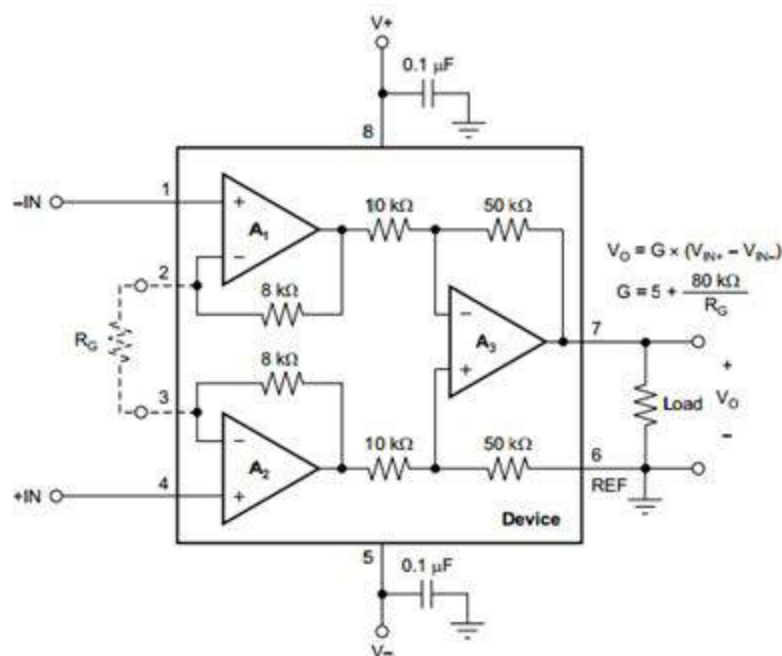


Image courtesy of Texas Instruments

Figure 14. Texas Instruments' INA827 Instrumentation Amplifier

Due to the simplicity of IC instrumentation amplifiers, detailed spec sheets included with each of amplifiers, and low cost, Get Loaded chose to move forward with design considerations using an IC instrumentation amplifier. Each gain computation is different based on the amplifier chosen. Therefore, specific gain equations were used once a specific instrumentation amplifier was chosen during the design process.

Data Acquisition Device (DAQ)

Introduction

Once the signal is amplified, the voltage must be recorded in order to further analyze the loading experienced by the component. Some data acquisition devices have the option to do real-time calculations in order to compute loads directly from the strains logged into the device while others require the data logs to be downloaded and analyzed using additional computation software such as MATLAB or Microsoft Excel (Fabijanic). Due to the tight budget constraint for the Get Loaded project, Baja SAE's data acquisition device, Race Technology's DL1-MK3, shown in Figure 15, needed to be implemented within the system.



Image courtesy of Race Technology

Figure 15. Race Technology's DL1-MK3 Data Logger/Data Acquisition Device

DAQ Considerations

Some major data acquisition specifications that needed to be considered with the dynamic impact loading of the Baja vehicle were the DAQ's sample rate and sensitivity. In order to capture the full impact loads being applied on a component, an absolute minimum of 100 Hz was needed (Fabijanic). Even at a sample rate of 100 Hz, many significant impact loads could have been missed. Expensive wheel force transducers such as those produced by PCB recommend a sampling rate of 90 kHz ("PCB Series 5400 Multi-Axis Wheel Force Transducer"). Wheel force transducers do need to account for telemetry, the orientation of the wheel at any given time, increasing the required frequency. Michigan Scientific recommends a minimum of 500 Hz for measurements using strain gauges. Therefore, due to scope and the budget of the Get Loaded

project, Race Technology's DL1-MK3 was upgraded to 1 kHz and multiple tests were run to capture the impact loads.

Error Compensation Methods

Introduction

Since the deflections of the material during impact loading were within the hundreds of microvolts, many errors could have occurred due the system setup and/or environmental effects. In order to accurately find the loading onto a component of the car, these effects need to be compensated. Some major considerations to compensate for were temperature effects within the strain gauge/specimen interface, temperature effects within the lead wires, and resistance effects within the lead wires.

Strain Gauge/Specimen Temperature Compensation

Temperature can affect the measurement of the loads at the strain gauge. Many mechanical properties or stress/strain states of the strain gauge and specimen material can experience temperature fluctuations which will induce errors within measurements due to thermal effects without proper compensation. Thermal expansion of the specimen, temperature-dependent changes within the strain gauge resistance, thermal contraction of the metal foil of the strain gauge, and temperature response of the connection wires can cause error within the measurement of the loading ("Temperature Compensation for Strain Gauges: Theory and Practical Implementation").

One method to reduce effects of temperature was to select a higher resistance strain gauge ("How Is Temperature Affecting Your Strain Measurement Accuracy?"). Choosing a higher resistance strain gauge would reduce the total deflection and thermal expansion effects of the gauge. Thus, a 10 ohm resistance caused by temperature effects from a 350 ohm thicker gauge strain gauge would have a smaller effect on the strain measurement error than a 10 ohm resistance change from a 120 ohm strain gauge.

Another method to compensate temperature effects was to expand a quarter-bridge Wheatstone to a "quarter-bridge with temperature compensation", also known as a half bridge, with an unstressed strain gauge as shown in Figure 16.

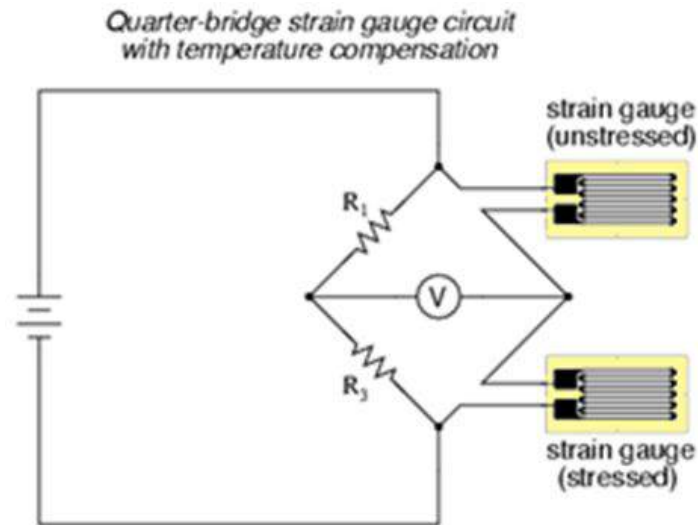


Figure 16. Temperature Compensated Wheatstone Bridge Circuit

The unstressed gauge shown in Figure 16 must be on a similar material to the measuring specimen and must undergo similar temperature changes as the measuring specimen and strain gauge. This compensated configuration cancels out the change in strain due to temperature effects of thermal expansion within the strain gauges, foil or specimen material (“How Is Temperature Affecting Your Strain Measurement Accuracy?”).

Lead Wire Temperature and Resistance Compensation

Changes in temperature of the strain gauge lead wires can cause a resistance difference and therefore a measurement error in strain. Connecting the strain gauge within the Wheatstone bridge with only two wires will cause the “drift caused by lead wire temperature changes [to] be enormous” (“How Is Temperature Affecting Your Strain Measurement Accuracy?”). One way to compensate for the resistance changes was to make all of the wires the same length and have them experience the same temperature changes. In addition, a third wire could have been added to the system in order to reduce drift by moving the collected resistance at the strain gauge instead of after the lead wire leading back to the Wheatstone bridge. Figure 17 shows a wiring diagram a quarter-bridge compensated for lead wire temperature and resistance effects.

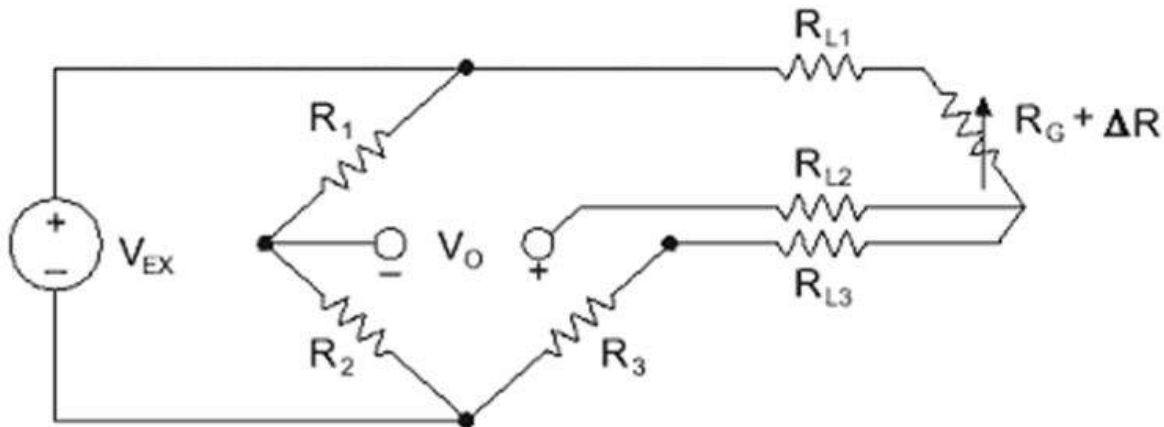


Image courtesy of Dokuz University

Figure 17. Lead Wire Temperature and Resistance Compensated Quarter-Bridge

It should be noted that the three lead wires not only need to be the same length, but also need to be the same gauge size. A larger gauge wire will cause a greater resistance within the wire. Therefore, a measurement error will occur if different gauged lead wires are used.

Twisted Pair Wiring

One method of compensating for noise created by external sources into the wires is to run the wires in a twisted pair fashion. Figure 18 below shows a common setup of the common mode voltage that can occur when running wires between two devices.

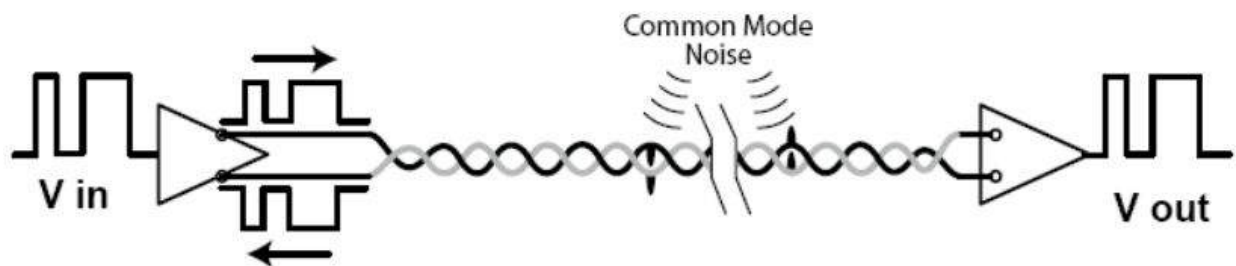


Figure 18. Introduction of External Error due to Common Mode Noise

Essentially, the input signal from V_{in} must be able to travel to V_{out} without any significant change in voltage value. This will be essential when running wires from the strain gauges to the Wheatstone bridges as any introduced error will alter the strain readings at the measuring node resulting in an error when attempting to identify the loading from the ground.

With twisted pair wires, the common mode voltage is both positive and equal on both wires (GEN17-1). Since they are both equal and the use of a differential, rail-to-rail amplifier is essential for strain gauge readings, the difference between the two voltages will not be affected.

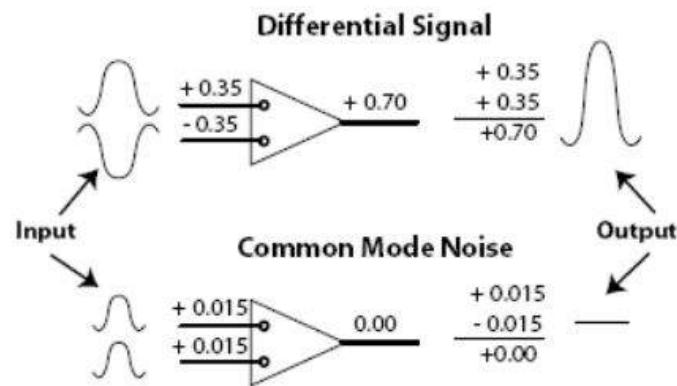


Figure 19. Visual Representation of Twisted Pair Theoretical Effectiveness

Figure 19 shows that the added amplitude of 0.015V from a common mode noise source would be eliminated when entering a differential amplifier. Therefore, running twisted pair wires so that the common mode noise amplitudes are the same on each wire would help in reducing error of data readings from any external EMI sources.

Calibration

Introduction

Certain aspects of the system, especially the Wheatstone bridge needed to be calibrated so that accurate strain readings could be achieved. Two important calibrations that must be done to the strain gauge system are bridge balancing (also known as “Offset-Nulling”) and shunt calibration. Some methods involve computer software compensation while other methods are purely physical compensation.

Also, before the strain gauges can be used within the system, the strains must be verified through bench testing certain components. This can be done by loading a specimen with a pre-determined and verified load. The strains read by the strain gauges can then be verified with the theoretical calculations. Once these bench verification tests are completed and strains are confirmed, the system can be performed on driving tests.

Offset Nulling

Sometimes the Wheatstone bridge will output a voltage at a non-stressed state because some resistors will not be their exact rated value and other assembly methods for the system may lead to unaccounted for additional resistance. In order to correct the error, a potentiometer can be used to set the initial output of the Wheatstone bridge to zero. The bridge is considered “balanced” once the offset is nulled. Some problems that will arise from failing to balance the bridge are inaccurate strain readings and a reduced span of available strain readings (“Measuring Strain with Strain Gages”).

One method of nulling the offset is to compensate with software. Some DAQ systems will read an unstressed state prior to taking stressed readings and have the offset set at zero. Another zeroing method is to place a potentiometer across the output of the Wheatstone bridge and to adjust the resistance to bring the value down to zero (“Measuring Strain with Strain Gages”). This will allow the greatest span of measurement for the current system.

Shunt Calibration

Shunt calibration involves adding an additional resistor to a shunted branch from the stressed strain gauge as shown in Figure 20.

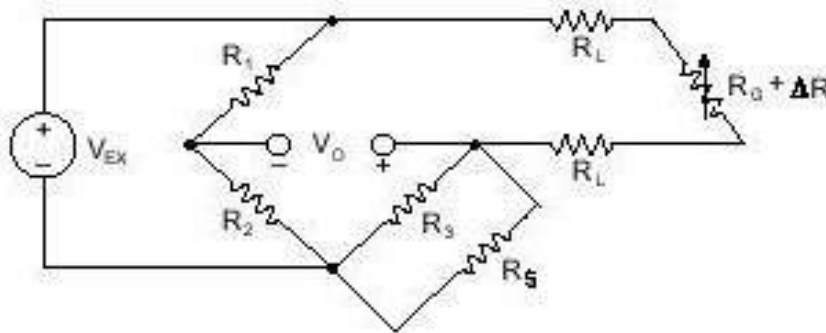


Image courtesy of National Instruments

Figure 20. Shunt Calibration of Strain Gauges

Adding this highly precise resistor simulates a loaded condition for the strain gauge. From this calibration, the gauge factor can be verified or corrected for in the experimental setup. Since shunt calibration affects the gain of the strain gauge directly, it is assumed that other compensation methods are not connected within the system during calibration (“Measuring Strain with Strain Gages”). Any additional compensation methods will error the final output reading from shunt calibration and the output from the specimen testing will be incorrect.

Bench Test Calibration

Shunt calibration can be a very tedious method to calibrate and verify the gauge factor of the strain gauges. An alternative method would be to add a load to the specimen and see if the strains being read are actually the predicted strains for the loading. This method allows for the verification of the gauge factor, any necessary gain adjustments needed for the strain gauge and verification that the theoretical models predict accurate loading.

Force Transducers

Force transducers are essentially strain gauges on members with known parameters (at the factory) to be pre-calibrated and delivered with a calibration sheet. This would significantly cut our manufacturing time by not requiring us to adhere strain gauges to the car. Although this method would circumvent the minor hassle of adhering the strain gauges, it posed a problem in that the design of the components to be measured would have had to be modified to allow for the use of these components. In addition, the only force transducers even close to the budget could only read axial loads. This did not allow us to get all the information required to solve for our loading cases without purchasing many of these systems or absurdly expensive ones. These major setbacks quickly dismissed force transducers as a valid design option.

Dynamics Based Measurements

Introduction

Another way about measuring the loads is to measure the dynamic response of the system. This data can then be transformed into forces through Newton's Laws and the mass properties of the system (mass, geometry, moments of inertia).

Accelerometers

Accelerometers are very similar to force transducers except that they incorporate an internal unit mass that is calibrated by the factory to give highly accurate results. The piezoelectric properties of the accelerometer output a voltage which in turn can determine an acceleration based on the factory's acceleration calibration constant. ("Accelerometers") Specific placement of accelerometers around the point of impact would yield accelerations of each component which could then be calculated back into the force on them and projected toward the wheel in order to determine the load on the car by using the sprung and unsprung masses.

While this is easier to do than the strain gauge calculations, it is a step further away from the result generated by force transducers. It would also also the use of current suspension and frame members for testing, but would not allow for bench testing as the results would be a function of time. This setup of sensors would have been somewhat reusable and required relatively less money and calibration than large scale force transducers.

Linear Potentiometers and Position Sensors

The use of linear potentiometers or position sensors would be possible in the measurement of the suspension travel through an impact. As we have both spring rate and damping rate data from our shocks, this would be a fairly simple calculation to find the force across the shock. These sensors would not be useful in the measurement of the chassis or the load in any suspension member other than the shock. These would therefore have to be complemented by the use of accelerometers on both the sprung (chassis) and unsprung (upright) masses.

As with the force based system, the combination of multiple forms of sensors would be necessary in order to easily and fully define the system. The largest issue with attempting to model this vehicle system is that very small geometry responses must be measured in order to calculate a peak impact load. This can cause the price to increase exponentially as the peak load geometric response is much more subtle than its stress-strain counterpart.

Direct Measurement of the Loads on the Wheel

Wheel Force Transducers

Strain gauges have been specifically applied to ground vehicle dynamics via “wheel force transducers,” which typically output the three forces and three moments that fully define the loading at the spindle - the main target of this project. Several companies produce fully packaged systems to mount to the rim and gather all the data simultaneously for the one wheel. These models come in several sizes, with MTS and Michigan Scientific both offering sizes designed for ATV tires.

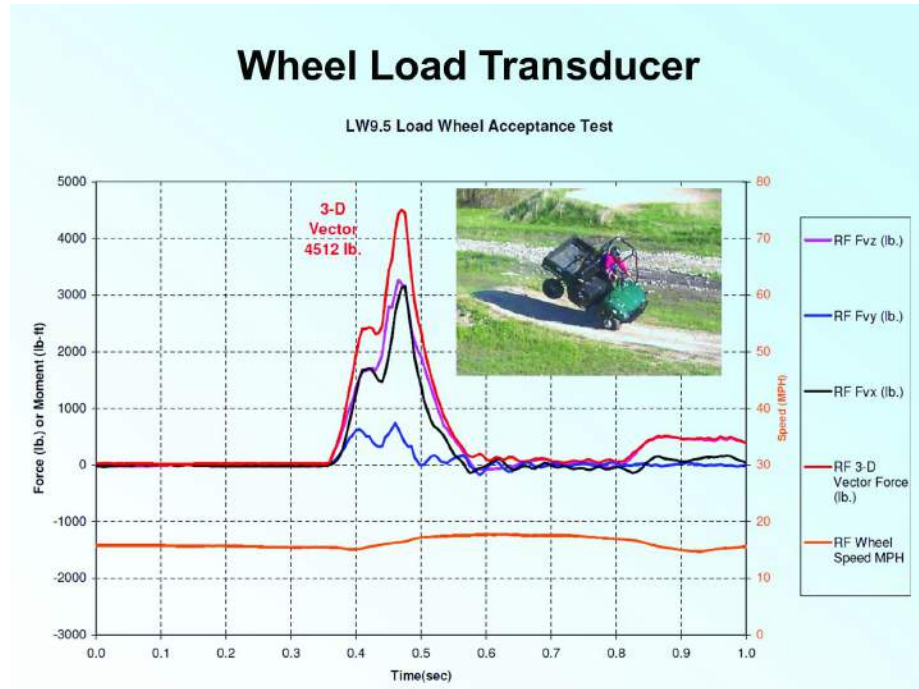


Figure 21. Michigan Scientific ATV Force Transducer Output

Figure 21 shows a sample output from Michigan Scientific’s ATV model wheel force transducer. The standard pricing on these was in the region of \$13,000 for a month rental, with sponsorships we were able to reduce the cost to our team to \$7,800, but this was still far too expensive to consider a viable option. Although the cost was an impediment, a wheel force transducer would have been the quickest and easiest way to obtain the data, and would have allowed our project to get into a deeper and more complete analysis of the loadings. The main bulk of the project would have then shifted from design of a data collection system to design of bench tests and multiple on-car “running” tests. Other projects have had successes at the design and build of a custom wheel force transducer, like the one shown below in Figure 22 from the University of Pretoria in South Africa.



Figure 22. University of Pretoria in South Africa's Custom Wheel Force Transducer

While creating a wheel force transducer would have been capable of collecting the loads we required and achieve the goals of determining loads, the design of a wheel force transducer was sufficiently complex to warrant a senior project on it's own.

The idea of the wheel force transducer did however lead to a different concept for the implementation of strain gauges. Using the dead spindles in the front suspension of the current Baja car for a measurement location made it possible to create a low-cost, simplified wheel force transducer by applying strain gauges directly to the spindle.

CHAPTER 3

DESIGN DEVELOPMENT

Introduction

Competing designs were chosen by a balance of their monetary implication to the team, the team's working knowledge of the type of system (after research), the difficulty of the execution of the design, and the potential accuracy of the result.

SUSPENSION

Introduction

For the suspension, the main design problem was to determine the forces occurring at the tire contact patch by measuring quantities away from the contact patch. The forces on the ground go first into deforming the tire, then into accelerating the suspension, finally into deforming the suspension components (i.e. shocks, links, A-arms, etc.). Since the goal of this project was to improve the design of the components of the car, we assumed that this deformation is insignificant as it will be present in all Baja suspension design and thus the damping due to the tire can be ignored. We did, however consider the effects that tire type and pressure could have on dampening loads.

The choice in how to measure these loads came down to a decision between load cells, strain gauges, accelerometers, shock dynamometer data with kinematic measurement, and creation or purchase of a wheel force transducer. For suspension application, the use of a wheel force transducer would be the most effective use of our time, however due to its price it was not feasible and the design of one for ourselves would not allow enough time to collect the data we needed for our finish date. Load cells would have been the next most effective, but the mounting of load cells for suspension components would have required a major redesign of both suspension systems and we determined that this is far outside of the scope of our project. This left us with a combination of strain gauges and accelerometers for the measurement of suspension forces. Once the decision was made to go in the general direction of strain gauges, there were still significant design decisions to be made as far as how each system would use them to measure the forces.

As the force from the ground interacts with the suspension, some of the force goes into accelerating the suspension and the rest goes into accelerating the rest of the vehicle. Creating an isolated system by making cut FBDs at the point of attaching the strain gauges eliminates the

effect of the accelerating car and replaces it with the measured force in the strain gauged component. This left us with the forces measured from strain gauges, the forces being studied on the ground, and the acceleration of all the mass in between. The effect of acceleration was minimized by placing the strain gauges as close to the contact patch as possible, however it could not be eliminated. Since the goal of the project was to find the loads experienced by the suspension components rather than the real forces at the tire patch, ignoring the forces that go into the acceleration of the suspension was reasonable. This is in accordance with our design specifications, that the desired measurement is the load which affected the suspension components, since the goal of this project was to allow more accurate and efficient design of parts.

Rear Suspension

The simplicity of the five link suspension lends itself to measurement of the forces in each axial link, in addition to the load in the shock. As the links are loaded via a simple pin-pin connection they can be considered two-force members and thus only require a single strain gauge each to find the loading. The only problems arise with the direction of the force vectors depending on the location in the suspension travel, and the load in the shock. The former can be easily measured with a linear potentiometer mounted between a known location on a link and the frame. The measurement of the shock loading becomes more problematic.

The need to measure the shock loading was met with several alternatives including the use of dynamometer data with the position and speed of the suspension travel to calculate the force. This method was deemed unreliable and was quickly replaced by considering strain gauge and load cell setups. A load cell placed between the shock and either the suspension or frame would tell us the load going through it, however it quickly became difficult to design a mounting for this system that would still remain rigid enough to drive on.

We then began to consider strain gauging the shock housing, however calculations would have been incredibly difficult given that we do not have access to the cross section of the housing. Then, looking at FSAE style pushrod suspensions we realized how much easier it would be to simply strain gauge a link that passed through a rocker to the damper. This is not feasible for Baja as our nine inches of suspension travel would have required an unreasonably large rocker (9"+) to redirect the motion. However, if we considered reorienting the solid link mounted from the frame to the rocker and the shock from the now rigid rocker to the suspension we could redirect the force of the shock into a two force member to measure our shock loading, as shown in Figure 23. This system was henceforth referred to as the Shocker Rocker.

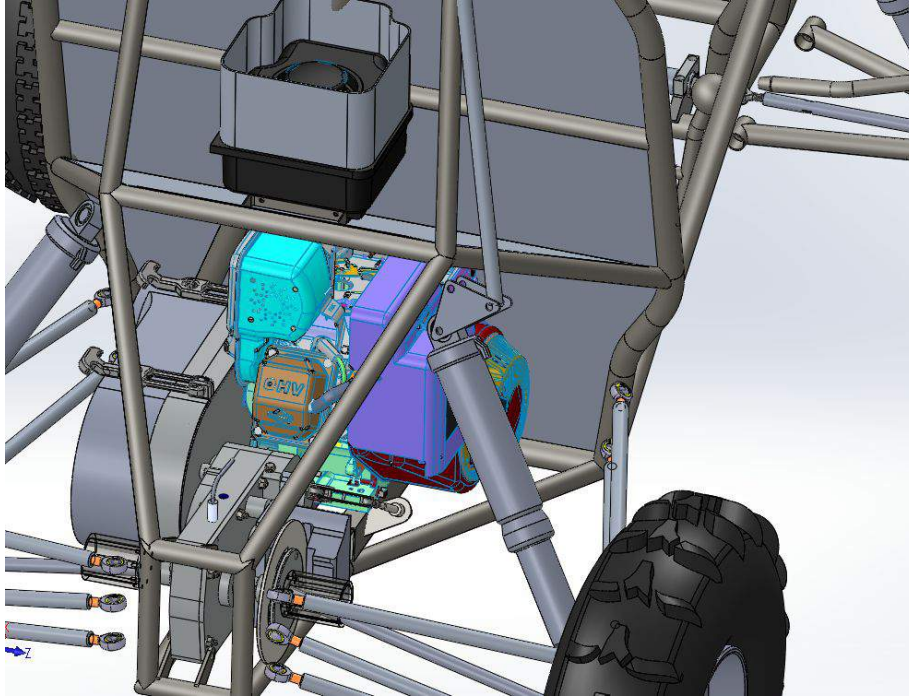


Figure 23. Shocker Rocker Concept (Middle hole mounts to current shock mount)

Once again, we concluded that the part of the force that goes into the acceleration of the unsprung mass can be ignored since it doesn't affect the strength requirements of the frame or suspension components

In summary, we found the load on the rear tire by measuring the strain in each of the links and the shock, and the position of the suspension. This totals to 7 channels which was well within the capabilities of the DAQ. Once all the loads and the suspension angle was calculated we can simply summed all the forces in each direction to find the reaction at the contact patch.

Front Suspension

The placement of the strain gauges went through several iterations beginning with placement in the center of the A-arms and on the shock. It was figured that if we could measure the load in each of the members mounting the suspension to the frame we could calculate the load at the tire. This quickly became very complicated as the suspension is not rigid and therefore we must also calculate the load vector dynamically as well as differentiate between the bending in the lower a-arm due to the shock from the axial loading on each tube. This method would have required the use of 7 strain gauges on each of the 4 main tubes in the a-arms (28 total), measurement of the suspension angle for force vectors via linear potentiometer or position sensor, and a shocker rocker similar to the one discussed in Rear Suspension. The required 30 channels immediately ruled out this strain gauge setup based on the capabilities of our DAQ.

This required us to reduce the number of channels. To do this meant that we had to reduce the number of members connecting the wheel to the rest of the car. We considered strain gauging the steering axis of the upright. This would only require 2 sets of 7 strain gauges to reconcile the load path. It then occurred to us that we could simply strain gauge the spindle and it would reduce the reaction forces to a single tube in combined loading.

In this scenario, we started making assumptions that greatly reduced the number of required channels. Assuming that there was no hoop stresses and very little torque applied through the bearing we removed the need for rosettes. We only needed 3 axial strain gauges (positions shown in Figure 24) to resolve the 2 bending moments and the axial load. A couple simple, static tests calibrated the system and basic structures could let us approximate any Poisson effect. Since the spindle sees all the loads that go to the shock, we no longer had to measure the load in the shock for the front suspension. This setup brought us down to 3 DAQ channels and didn't require any extensive design or fabrication of new parts.

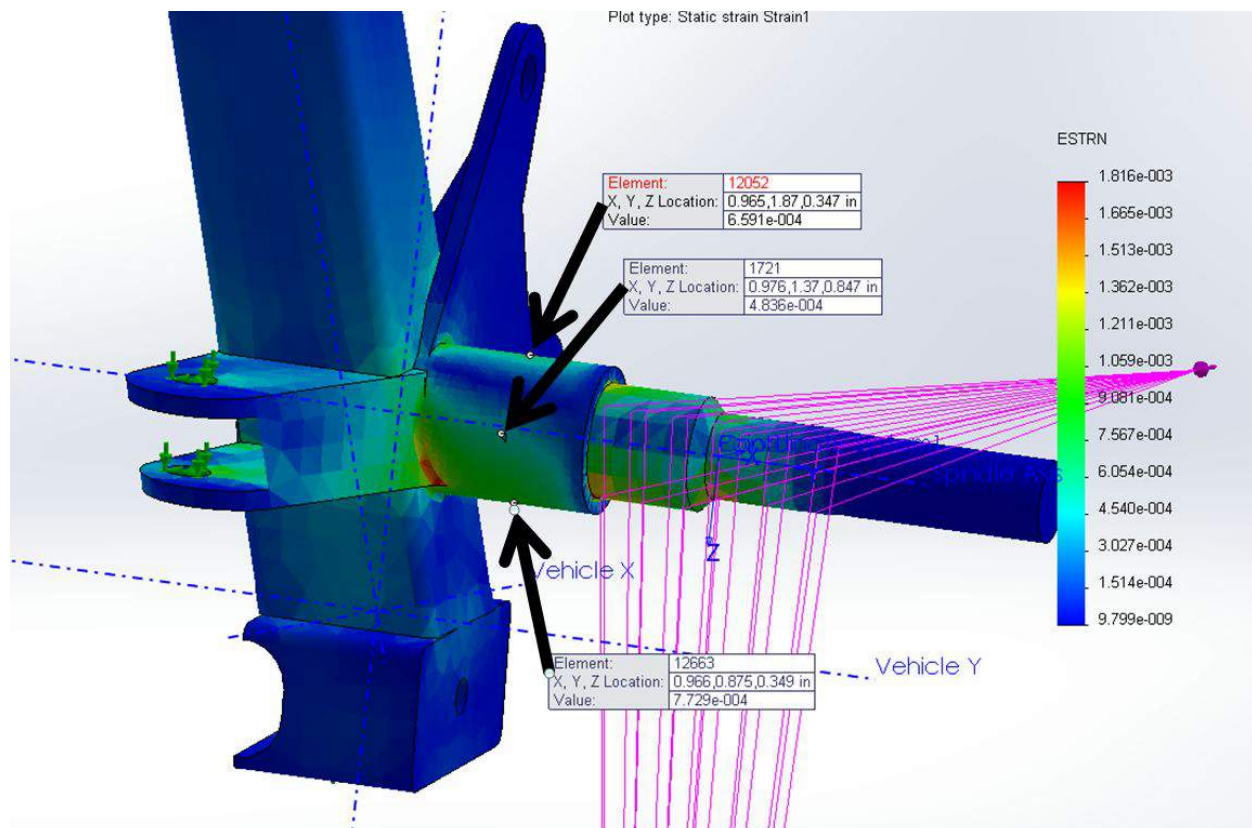


Figure 24. Spindle strain under front suspension combined loading

In summary, the top concept for the front suspension is to find all the loads at the tire by measuring the strain on the spindle. This brings our us down to 3 required channels which is well within the limit of our DAQ.

CHASSIS

Introduction

While suspension loads were our primary goal, we also wanted to find other common loads on the chassis. Excluding suspension, the most common loads seen during operation are skidplate impacts and roll hoop impacts. These can be very difficult to measure due to the uncertain nature of ground impacts on the roll hoop or the skid plate. In addition, the damping effects that make our skid plate useful as a skid plate also make it difficult to get an accurate reading of the peak force. Despite this, these are very severe loading cases that affect the design of the entire roll cage and must therefore be defined more accurately.

Skid Plate

The main concern measuring the loads into the skid plate, when hitting rocks, was to avoid measuring the damped force seen due to the deflection of the skid plate. This, along with the non-homogeneous behavior of composites, and the issues posed by unknown point of loading made strain gauges impractical for this application. The issue of damping caused by a soft skid plate could be solved by replacing it with a stiff one. This replacement would have been ideally be stiff enough that it could be considered rigid. Our first idea consisted of applying strain gauges to the members around the skid plate or to the skid plate itself. We determined that these ideas would require significantly more channels than the DAQ can support (30+) and a knowledge of plane theory not necessary to our project previously. This approach was well outside the scope of this project.

We then thought that the simplest option would be to mount the skid plate to the frame through load cells, quantifying all forces on the plate. We might have been able to use prefabricated button or washer load cells under the main mounting bolts for the skid plate. When we realized that this had become impractical for monetary and simplicity reasons we realized that an additional 3-axis accelerometer could be used to measure the force acting on the car by measuring the acceleration (linear and rotational) experienced during an impact. This method of measurement also accounts for the soft skid plate and therefore no longer requires a stiff one.

Frame Roll Hoop

Measuring loads on the top of the roll cage experienced to during a rollover presented an issue similar to that of the skid plate - where we needed to measure a load that was not precisely applied, since numerous variables when flipping the car made it nearly impossible to guarantee an impact point and direction. Due to this, several frame members likely ended up in bending in various and unknown directions, which made it very difficult to accurately analyze by strain analysis.

Special were taken to design the tests of the rollover case, since intentional rollovers with a driver onboard pose safety issues, but the weight and CG of the driver are significant components of the vehicle and must be accounted for.

DRIVETRAIN

The design issue when attempting to measure the torque loads in the drivetrain was the transfer of data from the spinning shaft to the data acquisition system. One simplifying action was to measure the torque from the output shaft of the gearbox, which didn't articulate with the suspension. While we still had to pick up the data from the rotating shaft via some form of brushed contacts or wireless transmission, the transfer could occur at a location fixed to the frame. The ending concept used strain gauges on the gearbox output shaft with data transfer via a brushed contact.

The drivetrain portion of the project was proposed to an EE project class and should be completed mid-late winter quarter of 2015. This did not leave enough time to do this testing before the writing this final report for senior project. However, regardless of the timing, this testing will be done and the data will be gathered and compiled for the use by the future Baja team.

CHAPTER 4

FINAL DESIGN DESCRIPTION

STRAIN GAUGES

Location and Operation of Strain Gauges

In the rear suspension, six axial strain gauges (five on links in addition to one measuring the shock load) allowed us to define the loads at the ground. For discussion on the measurement of the shock load, see the Shocker Rocker section in Mechanical Design. In the front suspension, three axial gauges on the top, rear, and bottom (Figure 26) of the spindle allowed us to isolate the three loads. Poisson's effects were accounted for by calibrating the gauges with a range of known weights. The resulting plots were similar to Figure 25 and can be found in Appendix H.

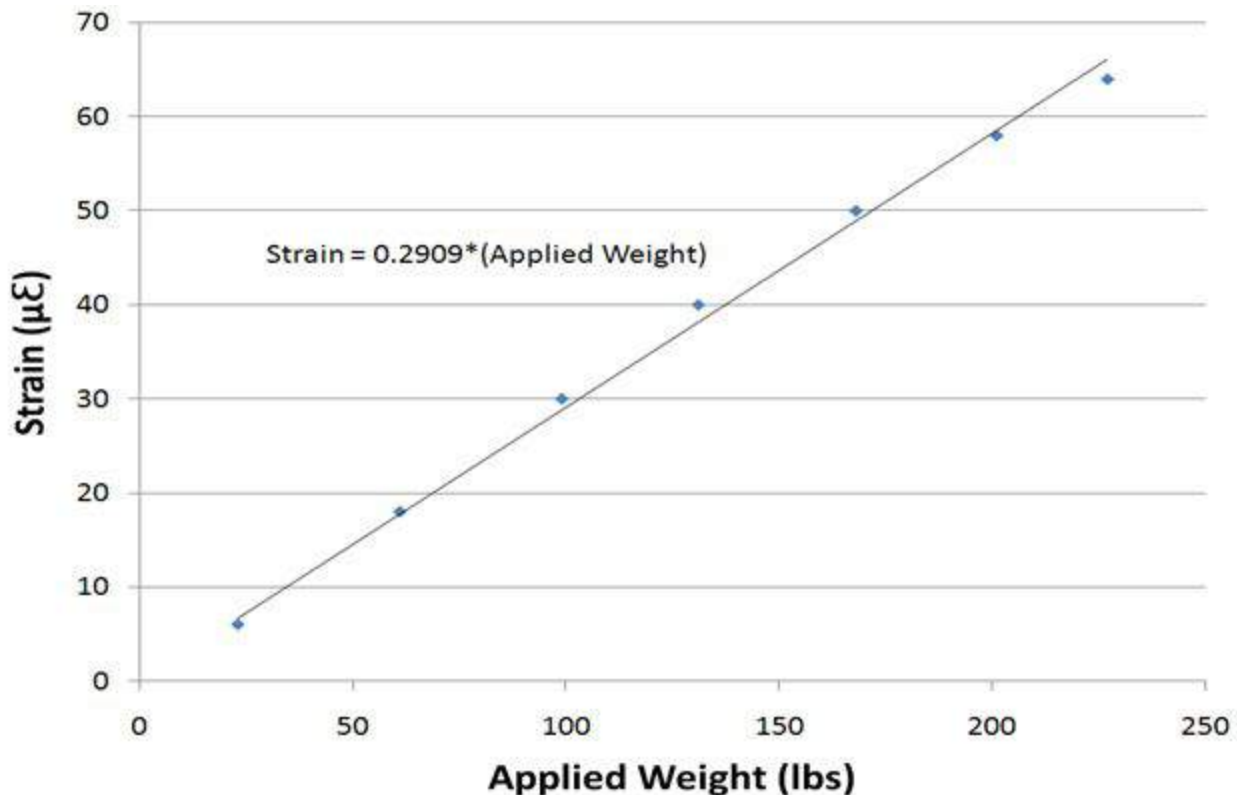


Figure 25. Example Strain Gauge Calibration Plot

Even simpler than this, we had the same correlation of voltage to load (simply scaled by the gauge factor). For the spindle, since we had to separate the axial stress from the bending stress,

we essentially needed a relation between strain gauge readout (voltage) to stress at the gauge. Based on the load - voltage curve, we used the known cross sectional geometry to solve for the stress - voltage curve. With that, it was easy to break out the moments and axial stress and ultimately the loads at the ground based on strain gauge readings. For more discussion of these equations, see the Analysis section.

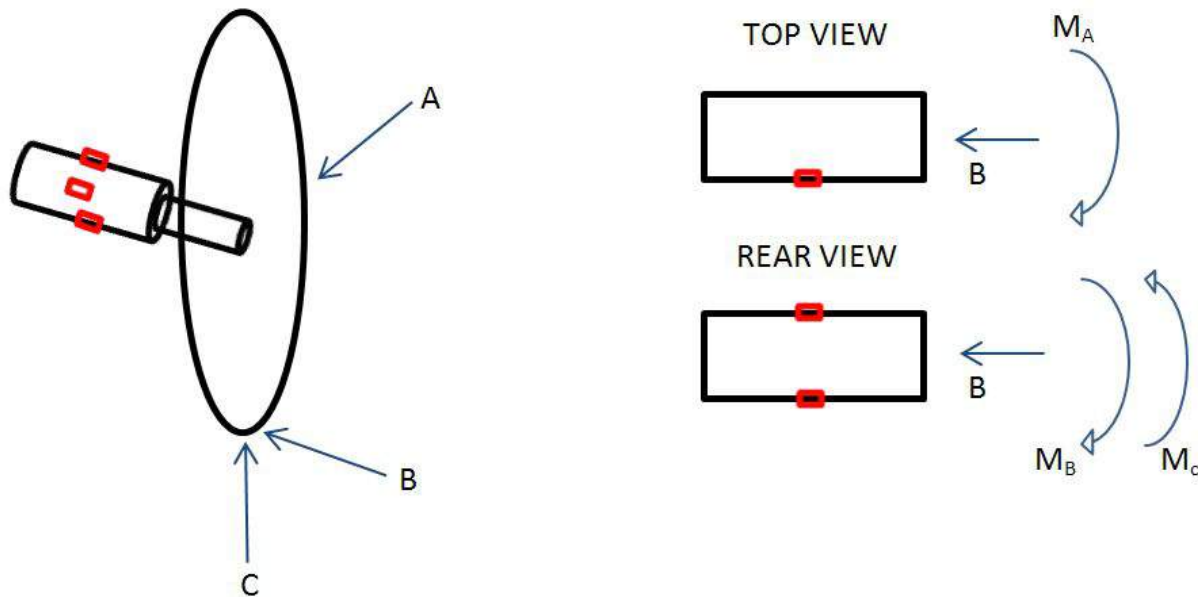


Figure 26. Spindle Strain Gauge Orientation

After comparing the multiple measurement techniques, Get Loaded moved forward with a design that utilized only metal foil strain gauges to measure suspension loading. Other devices such as accelerometers and linear potentiometers were considered but dropped due to specific design selections that were chosen to be used as a final design. The portion of the ground forces that accelerates the unsprung mass did not need to be accounted for since those loads would not affect the strength requirements of suspension components.

Selection and Reasoning of Strain Gauges

The strain gauges chosen were selected from Omega Engineering due to availability, price and overall simplicity of the packaged strain gauges. The gauges chosen Omega Engineering's KFH pre-wired strain gauge series. The specific strain gauge chosen was model number: KFH-3-350-C1-11L1M2 and can be seen below in Figure 27.



Figure 27. Omega's KFH-3-350-C1-11L1M2 Pre-Wired Strain Gauge

Full manufacturer specs and technical details can be found with Appendix D of this report. Due to the fact that our design discussed earlier involved only axial strain measurements, using only KFH-3-350-C1-11L1M2 strain gauges was feasible to complete the design. Using pre-wired strain gauges removed any error that may have been involved with an inexperienced student like ourselves soldering on a very small pad location. Having dirty solder, wrong amount of flux or having the iron too hot could all induce resistance errors reading the strain from the gauges. Incorrect soldering could have caused the gauges to fail prematurely or may have even completely damaged the strain gauge before use. Due to the multiple sources of error that could have been induced through inexperience and the limited amount of budget available for strain gauges, the increase in cost using the more expensive pre-wired strain gauges was justified.

Another benefit of using the KFH series was that the strain gauges were fully encapsulated. This allowed some protection from the natural environment such as water or dirt effects acting on the exterior of the gauges. Since moisture could have bridged the strain gauge and nulled out the resistor, having the gauges encapsulated removed any large errors caused from environmental effects.

The selected gauge was rated at 350 ohms. Therefore, as mentioned in Chapter 2 of this report, the amount of error that could have been induced by external sources such as temperature effects should not have been evident in the collection of data. A 10 ohm change caused by temperature fluctuations should not error the data as much on a 350 ohm strain gauge as it would have on a 120 ohm strain gauge. The 350 ohm pre-wired strain gauge with the smallest grid length was chosen as spindle packaging is about a half of an inch. Also, the smaller the grid length, the more precise the measurement will be at the measuring point. Since the spindle is round and was in bending at times, finding the strain at a point was crucial. Finding an average across a larger grid length would once again result in an error and may not have come close to matching the

theoretical model. Due to the fact that the strain gauges had to be ordered in packages of 10, the linear strain gauges were also used on the rear links.

The strain gauges were all compensated for steel without an option to purchase a compensated pre-wired gauge for another material. A minor issue was that the material property of the spindle was steel while the links were of aluminium which would have induced an error without accounting for the thermal compensation difference. Omega provided information of the temperature response based on the thermal coefficient of multiple materials with their data spec sheets that can be found within Appendix D.

The resistance of the leads were originally going to be accounted for by using 3 leads coming from the strain gauges. However, due to budgetary and time constraints along with the setup of the custom amplifier and Wheatstone bridges, the decision was made to use 2 leads coming from the gauges. The effect of wire resistance should have been relatively small and should have allowed the project to fulfill the error of measuring with 15% error of the actual load. Also, since Omega offered pre-wired strain gauges at 1m in length each, it is safe to assume that the effects of error due to wire resistance is negligible at 1m.

ACCELEROMETERS

After comparison of chassis load measurement techniques, accelerometers came to be the simplest of the solutions that fit within our budget. We chose to use the internal accelerometers on the DAQ unit which are pre-calibrated and rated for up to 6G accelerations. This data is setup to log automatically with 2mG resolution at 100 Hz. This is well within the parameters necessary to gather data on the loads we seek within the established amount of error (see Chapter 1 on *Engineering Specifications*).

As mentioned in the Chapter 2's accelerometer background information, using an additional accelerometer close to the CG allowed the rotational acceleration and inertia to be calculated and used with impulse momentum equations and energy equations. The previously chosen accelerometer will be the Kionix KXD94-2802 shown below in Figure 28.



Figure 28. Kionix KXD94-2802 3-Axis Accelerometer

With a 5V input from the DAQ and the 200mV/g output, this 3-axis accelerometer was adequate for use in skid plate and chassis testing. Using the adhesive from the strain gauges, the accelerometer would have been mounted on the upper-center of the firewall. From this location, the forces can be calculated through dynamics and then converted into impulse and energy transfer for use in bench testing and design of chassis and skid plates. The equations for the required analysis can be found within the Analysis section of Chapter 4.

MECHANICAL DESIGN

Shocker Rocker

As previously discussed, a method was required to find the load in the shock for the resolution of rear suspension loads at the tire contact patch. The conceptual design was only slightly modified due to geometry and packaging constraints, but the theory was the same - a rocker was going to redirect the entirety of the shock force into an axial link which was measured in the same way as the other five axial links of the rear suspension. Design considerations for the shocker rocker included: frictionless interaction at the pivot point, negligible geometry change due to deflections, and precise geometry to ensure accurate transfer of loads.

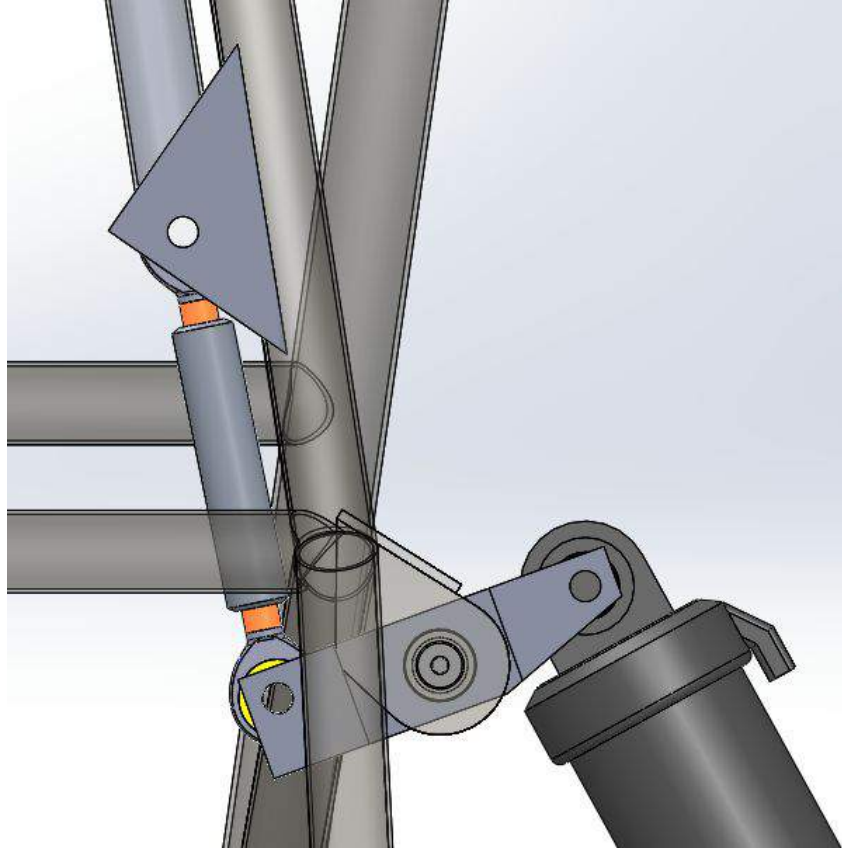


Figure 29. Final Shocker Rocker Geometry

The assumption of a frictionless pivot was necessary despite the fact that the rocker would not actually move significantly. If there were considerable frictional forces, they would manifest as a moment that would resist some of the shock force and keep it from fully transferring to the axial link. The inclusion of bearings satisfied this assumptions, and a shoulder bolt was used to ensure good fitment with the bearing inner diameters.

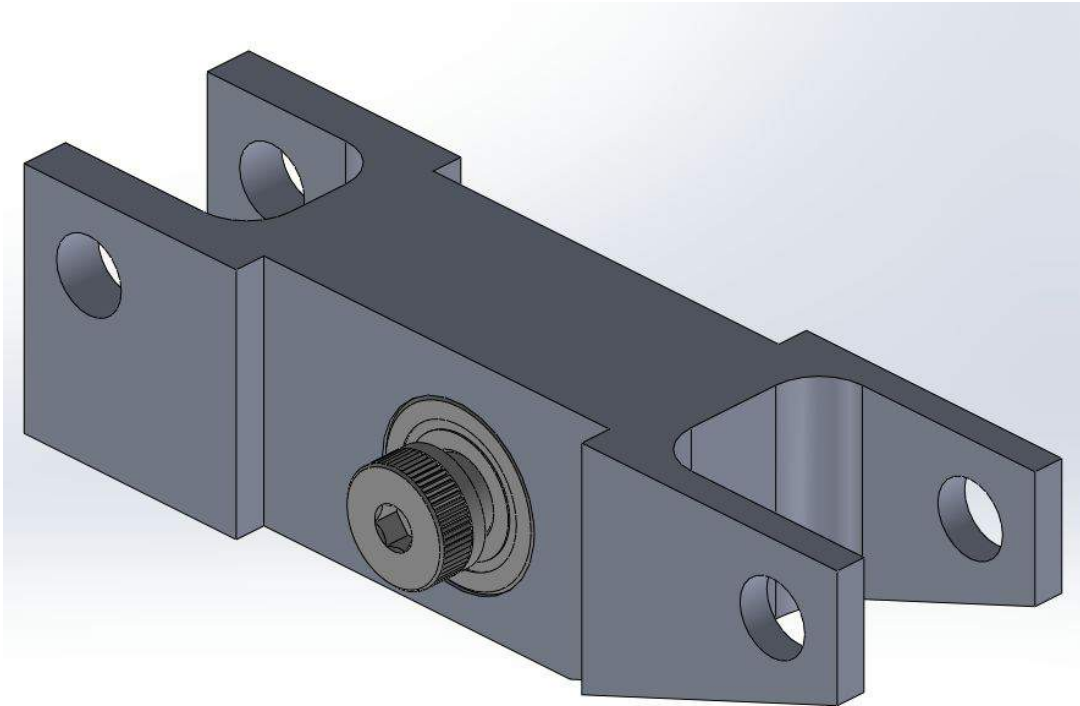


Figure 30. Shocker Rocker CNC Component with Bearings and Shoulder Bolt

Concerns for the accuracy of geometry were solved with careful consideration with machining and jiggging of the components driving the geometry. The rocker itself had the critical spacing of the three bolts, and any error here could have changed the 1:1 ratio. This, as well as the tolerance requirements of the bearing cups, drove us to chose CNC machining for the rocker. Another potential source for error in the geometry came from the location of the tabs where the axial link mounted to the frame. Figure 30 shows how careful jig design and implementation minimized any inaccuracies due to the location of these tabs. As long as the vertical plane of the jig is aligned with the vertical axis of the car (using a T-Square to the floor of the car) then the tabs will be correctly oriented. Finally, the jig piece included a hole that was used to set the length of the axial link, ensuring the geometry is as designed.

It is worth noting that this relocation of shock force put the vertical frame tube in bending, and based on the expected maximum forces in the shock, we would see 27 ksi of bending stress. To mitigate this, an additional tube was added to the frame to support this load directly.

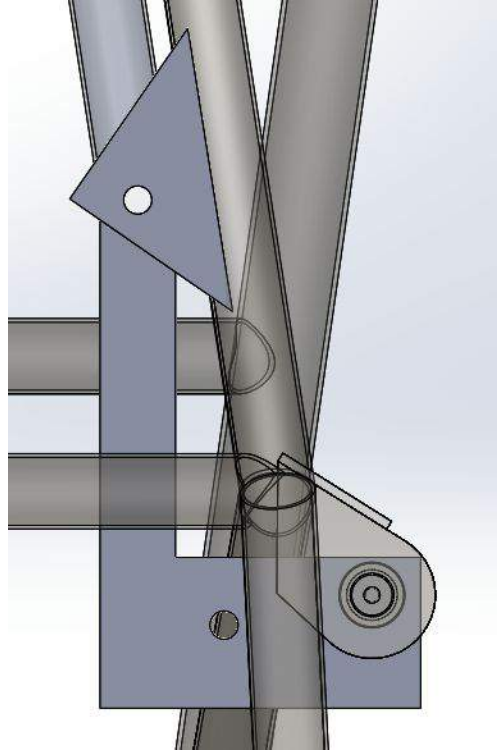


Figure 31. Shocker Rocker Tab Jig

The drawings for all of the components involved in the Shocker Rocker system are included in Appendix B.

Spindle Calibration Jig

We needed to calibrate the spindle to obtain the stress-voltage relation. To ensure the accuracy of the calibration, the known loads must have been applied entirely axially. The setup shown in Figure 32 displays the method used to guarantee that no bending was induced. As long as the flat plane of the jig was parallel to the ground and the rod end was not binding at the edge of its misalignment travel, we confirmed that the load was entirely axial. Further discussion of the calibration procedure can be found in Chapter 5.

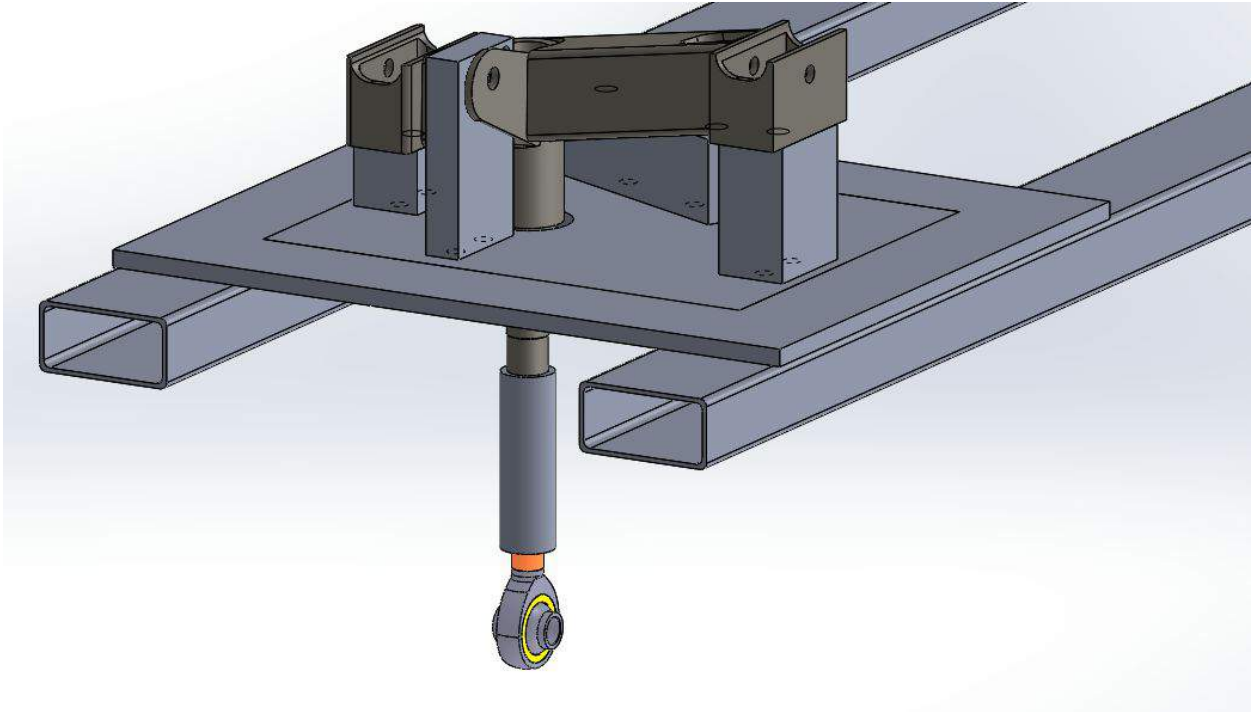


Figure 32. Spindle Calibration Jig

AMPLIFICATION/WHEATSTONE

Amplification Selection and Reasoning

As mentioned in Chapter 3 of this report, 3-op amp instrumentation amplifiers appeared to be one of the more cost effective and simple methods of amplifying a signal from a Wheatstone bridge. The final chosen IC instrumentation amplifier was Linear Technology's LTC2053 amplifier shown below in Figure 33.

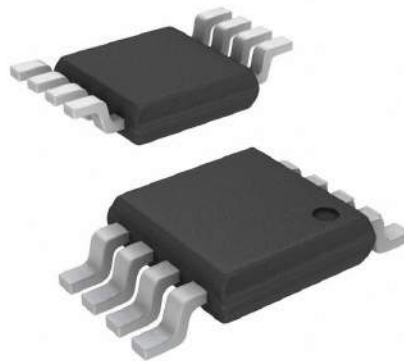


Figure 33. Linear Technology LTC2053 Precision Instrumentation Amplifier

The full manufacturer's datasheet and specs from Linear Technology is provided in Appendix D of this report. The LTC2053 was chosen because one of its primary uses is to amplify signals from a Wheatstone Bridge as shown by the wiring schematic example given with the manufacturer's specs and provided below in Figure 34 as reference.

TYPICAL APPLICATION

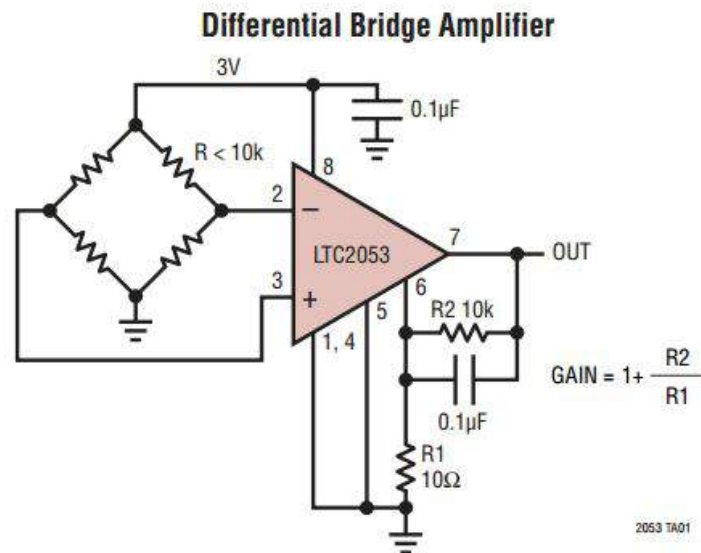


Figure 34. Wiring Schematic of a Typical Application for a LTC2053 Amplifier

One reason for choosing the LTC2053 was the capability of being able to change the gain through the amplifier by changing resistors R1 and/or R2. This is essential as the amount of gain needed for different strain gauge will change depending on the amount of strain that is expected from the spindle or rear axial links. If the theoretical calculations were proven false by seeing the impact peaks cut off from the data, the gain was able to be decreased to allow the peak to fall within the proper range. As mentioned later, the changing of the resistor was simplified by having resistors in parallel and a switch that allowed current to flow through the branch or not.

Having the entire 3 op-amp amplifier within the IC chip also eliminated additional resistances that may have occurred from the additional solder connections needed for a 3 op-amp differential amplifier construction. An image of the required connections can be found in the Amplifier Background Section within Chapter 2 but is also provided below in Figure 35 for convenience.

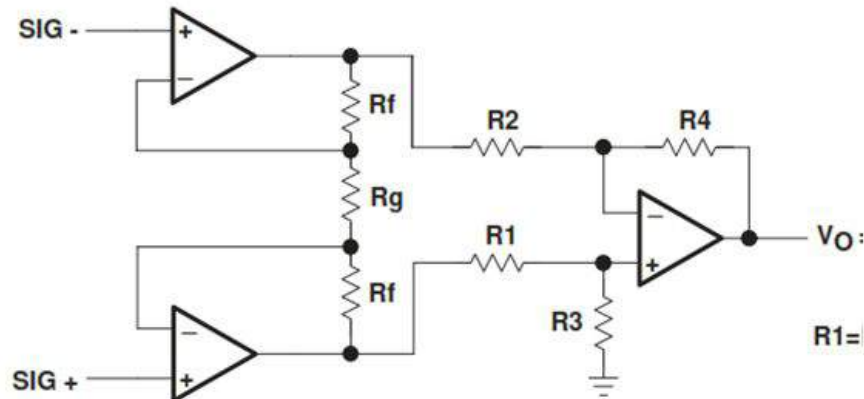


Figure 35. 3 Op-Amp Differential Amplifier

Similar to the strain gauge error avoidance through pre-wired strain gauges, the limited number of solder connections reduced the possibility of having an increase in unknown resistance from dirty solder. Also, avoiding use of multiple resistors when building the 3-op amplifier reduced the error from multiple manufacturing tolerances and instead the LTC2053 offered a single tolerance for the gain of the instrumentation amplifier.

The LTC2053 was also a precision amplifier, rail-to-rail output, with a zero drift operational amplifier. The rail to rail output allowed both positive and negative values to be sent to the DAQ's inputs. The reference output pin was connected to a steady 5V that allowed the voltage sent to the DAQ to be read $\pm 5V$ instead of around 5V. This concept is more clearly defined and shown in the Amplifier/Wheatstone Bridge Unit section under Packaging.

The maximum voltage allowed to the LTC2053 was 11V. The amplifier was powered by a steady, regulated 10V to get an acceptable resolution. A more in-depth analysis on the resolution can be found in the DAQ section. Therefore, the power requirements and resolution requirements were both met using the LTC2053.

The capacitor location seen in Figure 34 was also used in order to smoothen out peaks and filter some noise out of the amplification process. A full schematic of the selected wiring for the amplification unit can be found within the Amplifier/Wheatstone Bridge Unit and with Appendix B.

The LTC2053 was not be purchased directly by Linear Technology, but was instead ordered via DigiKey to consolidate all of the parts for the amplification unit in one simple location. A full cost analysis and bill of materials can be found within Appendix C.

Wheatstone Selection and Reasoning

After carefully considering the cost of strain gauges, any compensated method for strain gauge setup via Wheatstone bridges were abandoned. The final Wheatstone bridge configuration chosen was an uncompensated quarter bridge as shown below in Figure 36.

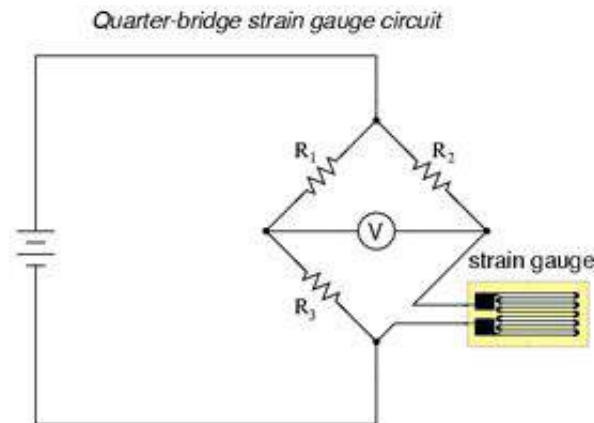


Image courtesy of Dokuz University

Figure 36. Uncompensated Quarter-Bridge Wheatstone Bridge Circuit

Fortunately, temperature compensation was not needed as the selected strain gauges from the KFH series were compensated for steel. Also, since the stress state of a certain point did not have to be fully defined and the only importance was the loads at the tires, the bending/axial/torsional stresses and strain did not have to be removed from the strain readings at the gauges. The quarter bridge setup also allowed the other resistors to be a fixed ohm value and to be located away from the strain gauge mounting location. This is ideal for the Amplification/Wheatstone Bridge Unit discussed in the Amplifier/Wheatstone Bridge Unit section.

Gain Selection

In order to for the DAQ to receive data, the millivolt output from the strain gauges had to be amplified as mentioned in previous sections. However, the DAQ could only read up to a value of $\pm 5V$. Therefore an assumption on max loads had to be made and the correct resistors needed to be selected to create a gain that makes the strain readings within that maximum 5V range.

Ideally, we wanted the maximum strain to output a value of $\pm 5V$ to the DAQ. However, due to the unknown loading and therefore actual strain in the members and resolution of the DAQ, Get Loaded assumed that the maximum load should fall at around 80% of that range. This allowed higher strains to be achieved and still be within the $\pm 5V$ range without any clipping.

An in-depth analysis of the selection of actual resistors for gains is mentioned in the Packaging section as the gain's effects on the system is a more appropriate location for discussion.

DAQ

Introduction

In order to capture the impact load outputs from the strain gauges and accelerometers, a few modifications were made to the currently owned Race Technology's DL1-MK3.

Planned Upgrades

The first improvement was to increase the sample rate from the standard 100 Hz to an improved rate of 1 kHz. As mentioned in the Chapter 3, the additional data points increased the probability of finding the actual peak loads.

Another upgrade to the DAQ was increasing the current 8 channel inputs to 12 channels. The additional channels allowed testing of both the front and rear suspensions at the same time. This greatly increased the amount of test runs that were conducted per testing session.

Resolution

The DL1-MK3 DAQ has 12-bit resolution which leads to a resolution of 6.2mV. A full spreadsheet of the calculations can be found in Appendix E.

PACKAGING

Amplifier/Wheatstone Bridge Unit

Preliminary Design of and Component Combination

After the selection of the LTC2053 amplifier, the entire system from wheatstone bridge to DAQ input needed to be created to ensure that the combination of components between the strain gauge and the DAQ would result in a desirable output to the DAQ. A simplified hand drawing of the system schematic is located within Appendix B.

Once a full grasp of the requirements needed to setup the system were reached, in order to begin construction, Get Loaded chose to consult Thomas Willson, an EE major at Cal Poly San Luis Obispo, who had experience in creating advanced electronic circuits with PCB chips. One reason for reaching out to Thomas was to gain insight in creating the 8 channel strain gauge amplification circuits within a compact, confined space that would fit on the SAE Baja vehicle. Thomas is a member of SAE Formula Electric and saw the potential use of an wheatstone/amplifier circuit for strain gauge readouts. After discussing our overall design with him along with the individual component requirements and functions, he created a simplified schematic of a single channel board shown below in Figure 37.

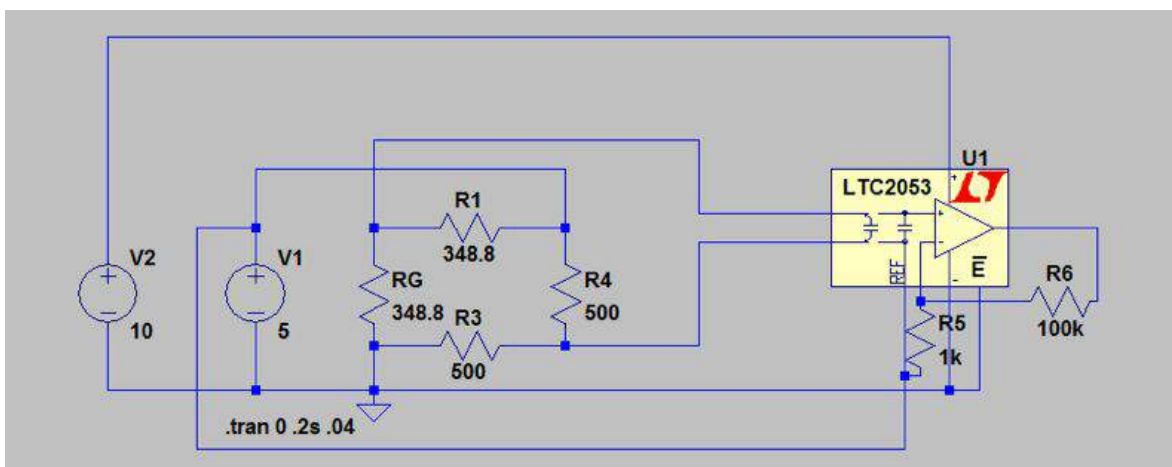


Figure 37. Schematic for Wheatstone and Amplifier

Similar to the hand drawing found in Appendix B, Figure 37 shows that the Wheatstone bridge is excited by a 5V excitation voltage while the amplifier is powered by a 10V power source. Once again, the 10V amount was chosen based on resolution to be seen from the DAQ explained more in depth within the DAQ section above.

Looking at Figure 37, the resistance values of the strain gauge (R_G) and the fixed resistor (R_1) were also matched in order to create a voltage at the output node of half the excitation current. For this model, the value would be 2.5V. In reality there would most likely be a resistance difference between R_1 and R_G . Therefore, putting a lower value for R_1 and adding a potentiometer in series with R_1 allowed the user to increase the resistance of the R_1 branch until the branch was equal to the value of the strain gauge resistance. At this point, the R_1 and R_G side of the bridge would be balanced and the output node on that side of the bridge would be 5V, half of the excitation voltage. The right side could have two higher resistance resistors at R_3 and R_4 as long as R_3 and R_4 are equal. Using a higher resistance decreases the resistor manufacturing percentage error that is greater at smaller resistances.

Continuation of Wheatstone/Amplifier Design

Thomas also added the “gain affecting” resistors at R_5 and R_6 to model where the change in amplifier gain would occur on the board. Lastly, the 5V power source also branched to the reference input of the LTC2053 allowed a $\pm 5V$ value around a 5V base or reference voltage.

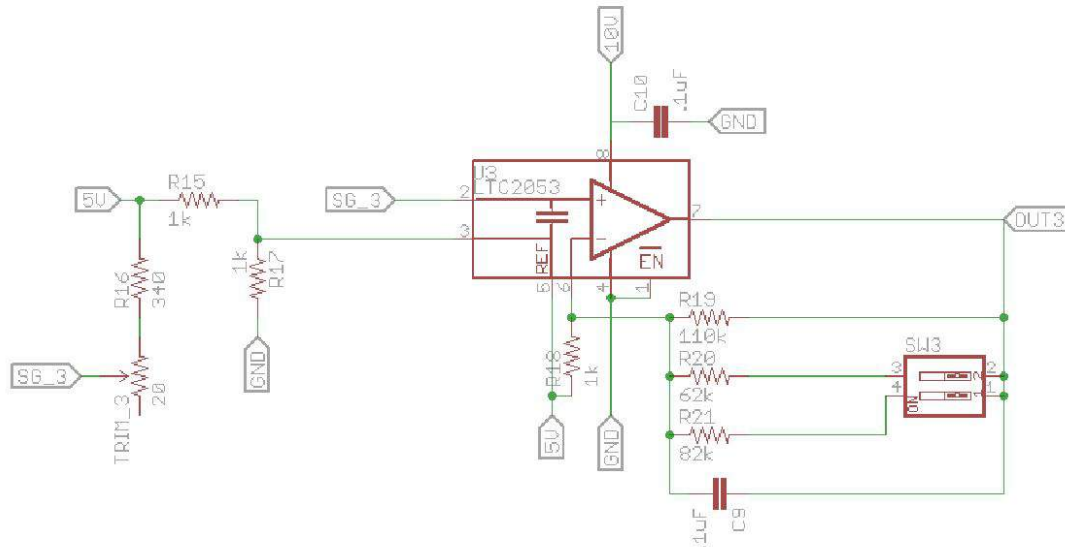


Figure 38. Updated Schematic for Wheatstone and Amplifier

After creating the rough preliminary circuitry for the Wheatstone/Amplifier circuit in Figure 37, Thomas added additional pieces mentioned from the Get Loaded preliminary drawing to the circuitry as shown in Figure 38. For the capability of changing gain, he added multiple dip switches to change the total value of the R_6 resistor value. Capacitors were added in parallel with

the R6 resistance value and to the 10V input to the amplifier in order to smoothen the signal of the amplifier input voltage and the output of voltage to the DAQ. The potentiometer previously mentioned to be used in order to balance the bridge has also been added to the schematic as TRIM_3.

Using EAGLE software, Thomas created a setup on a compact board that allows 10V and 5V regulated voltage to be created from a single 12V source. He also added an LED to turn on while zeroing out each bridge in order to make sure the bridge is balanced along with the differences of resistances in the manufacturing of the strain gauge and fixed gauges. A completed board schematic can be seen below in Figure 39.

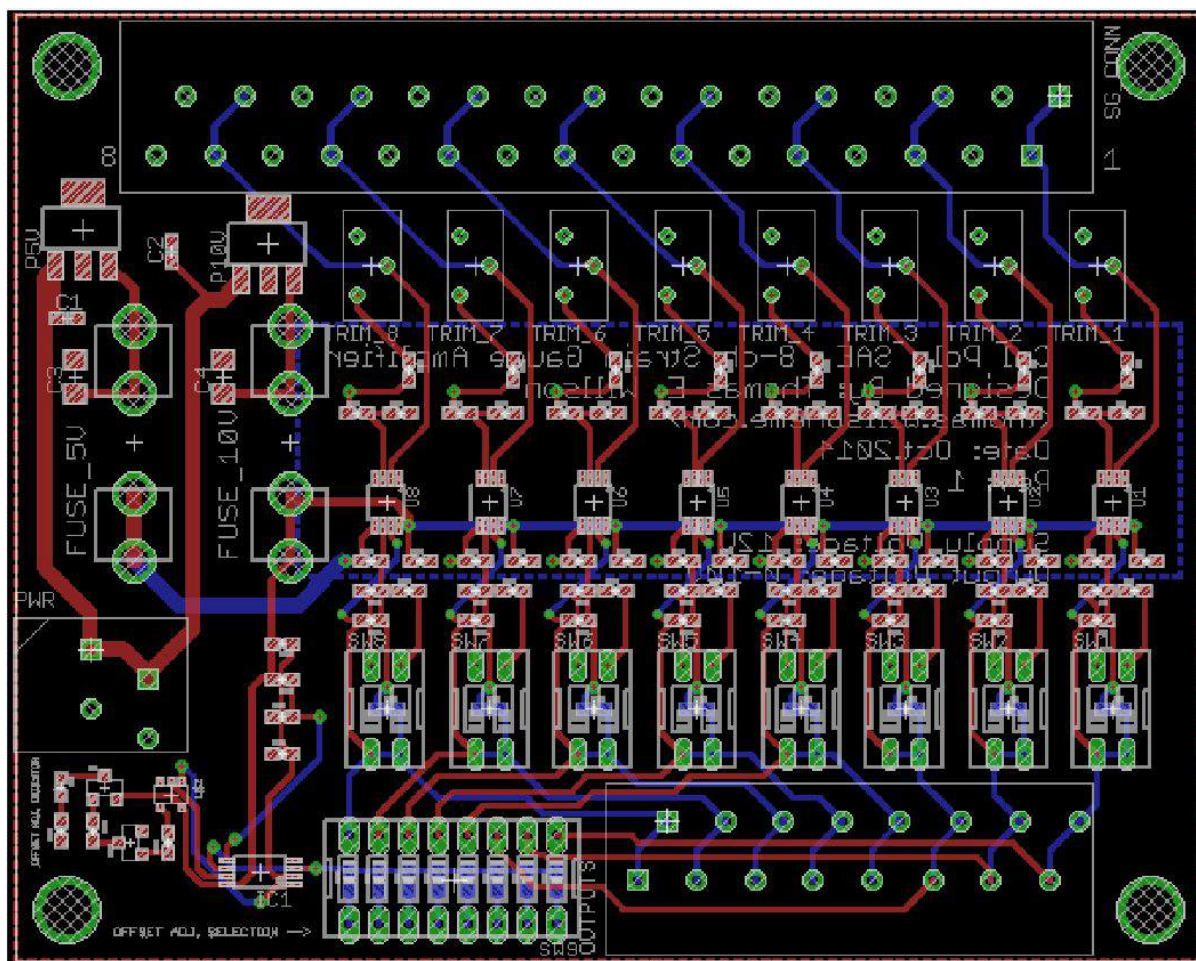


Figure 39. Board Rendering for Wheatstone and Amplifier System

A full documentation along with OSH Park's board renders for a quote and BOM can be found in Appendix B. The dip switches located near the bottom of the board in Figure 39 were used for calibration purposes. All channels were off and the active, calibrating channel was on. This

allowed only 1 LED to be used in order to be a zero-indicator for a balanced bridge instead of having 8 separate LEDs.

The path of the wires can be followed to represent the rough preliminary hand drawing in Appendix B. The open holes on the edge of the board near the dip switches were for the outputs pins to the DAQ. The dual dip switches located more centrally to the board were the switches used for gain control seen in Figure 39. The black square located along the midline of the board were the LTC2053 instrumentation amplifiers. The collection of three clustered red rectangles were the resistors used for the bridge completion. They were connected to the potentiometer labeled as TRIM_(Channel). From the potentiometers, the traces continue to the holes near the top of the board which correspond to the inputs from the channel's respective strain gauges. This completes the path drawn out in simplified hand drawing and rough schematic.

Resistor Gain Selection

As mentioned in the "Gain Selection" section within Amplification/Wheatstone section above, specific resistors were selected to capture the impact stress peaks. The analysis began with looking at the predicted output strains at all of the strain gauges onto the car. This included both the strain gauges on the spindle and the ones on the axial links. Once minimum and maximum strains were found via FEA and a rear suspension program model, an analysis of the "data" path through the gauge, wheatstone, amplifier and DAQ was conducted.

Table 2. Maximum and Minimum Predicted Strains from Strain Gauges

	Rear Max Strain	Front Max Strain
	<u>microstrain</u>	<u>microstrain</u>
Min Gauge Output	30	N/A
Max Gauge Output	350	1000
Worst Case	-	1500

A final conclusion of the assumed maximum and minimum strain outputs from the FEA and rear suspension model are listed above in the Table 2. From these outputs, the gauge factor formula discussed in Chapter 2 was used to create resistance changes seen at the strain gauge for the strains predicted and is collected below in Table 3.

Table 3. Predicted Resistance Changes from Strain Gauges

	Rear Max Resistance	Front Max Resistance
	ohm	ohm
Min Gauge Output	0.021	N/A
Max Gauge Output	0.245	0.7
Worst Case	-	1.05

From the resistance changes, an output voltage from the Wheatstone configuration was created to find the input to the amplifier. The Wheatstone Output voltages are found below in Table 4.

Table 4. Predicted Voltages from Strain Gauges

	Rear Max Voltage	Front Max Voltage
	millivolts	millivolts
Min Gauge Output	0.075	N/A
Max Gauge Output	0.875	2.498
Worst Case	3.744	-

The values from Table 4 must then be multiplied in order to be readable from the DAQ. This was the gain setting needed from the amplifier to multiply the signal. Table 5 below shows the absolute maximum gain allowed to let the predicted strains have a value of $\pm 5V$ (the maximum allowed voltage for the current setup range at the DAQ).

Table 5. Maximum Ranges Allowed based on $\pm 5V$ DAQ Input

	Rear Max Gain	Front Max Gain
Min Gauge Output	66668.67	N/A
Max Gauge Output	5716	2002
Worst Case	1335	-

Seeing the large variation in maximum gains allowed, multiple resistors put in parallel along with dip switches on each branch were used in order to allow to maximum predicted strain output voltage to be around 80% of the full data range. The minimum strain output gain was too high to account for therefore the maximum gauge output at the rear, the maximum gauge output from the front and a worst case scenario were chosen to design the fixed gains. The results for the resistors used for gains are listed below.

Table 6. Selected Gain Resistors and Location

Resistor Gain Selections	Value	Units	Branch
1	110	<u>kohm</u>	hot
2	62	<u>kohm</u>	switch
3	82	<u>kohm</u>	switch

Using the selected values from Table 6 and assuming a 24 ohm resistor for the denominator of the gain ratio, Table 7 was created to show the gains achieved by all possible setups. The 1's and 0's of the table are represented of current flowing through the branch (1) or when no current is flowing (0).

Table 7. Actual Gain from using Selected Gain Resistors

Gain Output	Gain R1	Gain R2	Gain R3	Gain
1	1	0	0	4584
2	1	1	0	1653
3	1	0	1	1958
4	1	1	1	1115

Therefore, in order to find the percentage of the amount of the predicted maximum strain within the maximum strain sweep of the DAQ at multiple settings, the selected gain setup was chosen by picking the closest actual gain output value below the predicted max gain allowed for a full $\pm 5V$ sweep. Table 8 presents this data in a concise summary.

Table 8. Strain Output Band Predicted

Gain (Resistor Created)	Gain (DAQ Allowed)	Percentage of Measured Strain Band Used
4584	5716	80.2
1653	2002	82.6
1115	1335	83.5

As shown by Table 8, the chosen resistors put the maximum predicted load at around 80% of the total available strain band. This met our projected goal of 80% and therefore the selected strain gauges were valid for gain amplification. Simulations were run in EAGLE and the hand calcs confirmed the simulation results.

Amplifier/Wheatstone Enclosure

The enclosure selected for the Amplifier/Wheatstone board was selected from Polycase's selection of waterproof cases. Polycase is a company that specialized in enclosures for electronic components and therefore considered the waterproof and/or water resistant requirements for electrical systems. The enclosure chosen for the unit was similar to Figure 40 below.



Figure 40. Polycase Enclosure for Amplifier/Wheatstone Unit

Twisted Pair Wiring

In order to remove any external sources that may cause error to the voltage inputs at the DAQ, the wires running from the strain gauges, through the Amplifier/Wheatstone unit and into the DAQ must be protected from the environment. The method chosen for Get Loaded's applications was to use "Twisted Pair". Twisted Pair reduces the effect of EMI sources by isolating a common mode voltage from external sources. A more in depth understanding of the method of negating EMI sources via twisted pair wiring can be found in Chapter 2 of this report.

Also, since the spark caused by the engine will emit electrical pulses, this may have caused an apparent noise spike every time the spark is ignited. If the effect of the spark appeared when collecting data via the twisted pair method, we assumed the effect could be easily predicted and compensated by finding the RPM and creating an inverse function to eliminate the peaks. Fortunately, this did not occur.

Strain Gauge Attachment

Introduction

In order to attach the strain gauges to the SAE Baja vehicle, certain precautions were taken. Omega Engineering has provided a full guide to placing the strain gauges using their specific adhesives. A brief overview of the process they recommended is provided below, but the extensive guide can be referenced within Appendix G.

In order to ensure proper adhesion to the spindle and rear axial links, the surfaces needed to be fully cleaned and prepped. This allowed the strain gauge to not slip on the material and read the actual strain state of the point being analyzed on the spindle or axial links.

Prepping the Surface

First, the material needed to be free of any foreign contaminants such as dirt, rust or paint. The most efficient way of removal was to remove any contaminants with sandpaper. The grade of the sandpaper was determined when examining the contaminants.

After the large contaminants were removed from the surface, the surface needed to be free of any layers of chemicals that would affect the adhesive bond between the strain gauge and material to be tested. Acetone was used to remove any oils and scrubbing patterns were considered to ensure that dirt particles were not re-introduced to the testing location and to make sure that a residue would not be left on the strain gauge attachment site.

Once the surface was chemically and physically clean, the location needed to be slightly roughened in order to allow the adhesive to have a strong bond between the strain gauge and material. This roughening step could have been skipped, but the maximum readable strain would have been reduced. Get Loaded chose to roughen the location to ensure high strains from impact could be read. Omega Engineering recommended using sandpaper of different grits for different materials. The recommended sandpaper grade for the aluminum axial links was 220 to 360 grade while the recommended grade for the steel spindle was 80 to 180 grade.

One important consideration when cleaning and roughening the strain gauge attachment location was over-sanding which may have resulted in a substantial decrease in shaft size and possibly induce an error if the diametral change was not accounted for after sanding. The diameter of the shafts were added after full cleaning and roughening to a checklist provided with Chapter 5's Specification Verification section.

After roughening the surface, a light cleaning with acetone was necessary in order to remove any particles created from the roughening.

Prepping the Strain Gauge

Since the KFH strain gauges were already pre-wired, the only prep necessary was to clean the adhesive side of the strain gauge. Omega recommended holding the strain gauge with tweezers and using Freon, Frigen or carbon-tetrachloride soaked on a gauze pad to clean the surface. Due to the availability of these chemicals, Get Loaded chose to skip this step.

Attaching the Gauge

Once the strain gauge was laid onto the surface, it could no longer be removed or adjusted. Therefore, it was crucial that the placement of the strain gauge was as exact as possible. In order to begin placement, a piece of adhesive tape was added to the gauge away from the solder joints. A sample location of the tape can be found below in Figure 41.

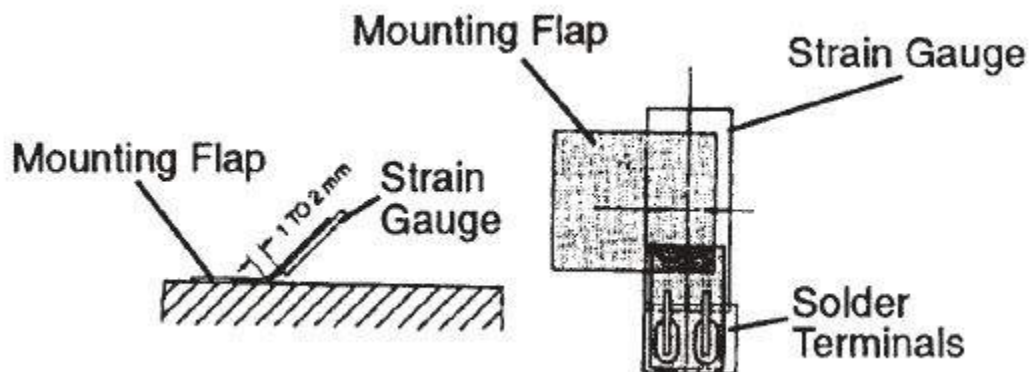


Figure 41. Location of Mounting Tape on Strain Gauge

Once the strain gauge had been placed in the desired location, the tape was pressed down onto the test area to fix the strain gauge and to create a mounting flap as shown in Figure 41. We then lifted the strain gauge up using tweezers and applied one drop of adhesive to the mounting area surface. At this point, a piece of Teflon film was used to spread the adhesive around the area to a uniform thickness. The strain gauge was then be flipped down onto the adhesive and a new piece of teflon tape was used to press down on the strain gauge a secure it to the testing specimen. The strain gauge was pressed down on via the teflon tape until the adhesive set. The correct timing for adhesive setting times are provided by Omega in Table 9 below.

Table 9. Setting Time for Adhesives

MINIMUM SETTING TIME FOR BONDING

Material	Setting Time
Steel	60 to 120 sec.
Aluminum	50 to 100 sec.
Plastics	10 to 60 sec.

Removing Excessive Materials From Strain Gauge Mounting Process

The Teflon tape should be removed minutes after setting to reduce the chance of movement when removing the teflon tape. Once the strain gauges were set, they were left alone for a minimum of 24 hours to fully cure. Once fully cured, removing the adhesive tape used for mounting was required.

ANALYSIS

Once the system was fully integrated in the vehicle, we could begin taking and analysing data. The data was gathered from the sensors via the Race Technology data acquisition unit. Once the data for a given loading case was taken, it was processed according to the appropriate calculations listed below. The differing setups for front suspension, rear suspension and chassis each required a different analysis tool. However, since each of these loading cases were measured separately, this was not a problem.

Front Suspension

The front suspension was a simple system of a stiff member with known (measured) strain on the spindle and unknown (desired) loads on the tire. There were 3 unknown forces with 2 known and 1 unknown point of application as seen in Figure 42. A vertical and a longitudinal load were assumed to be applied at the points directly below and in front of the spindle respectively. This was a safe assumption due to the fact that if either of these forces were translated front/back or up/down (respectively), the only effect would be a rotation of the tire. Since no load was applied to the vehicle due to this error we safely ignored it. The last load was a force acting on the side of the tire, as in a sliding impact with a rock whilst turning. The position of this load could have varied from impact to impact and depending on the location, could cause differing moments on the spindle. All three of these forces as well as the position of the side impact force need to be solved through the use of our strain gauges on the spindle.

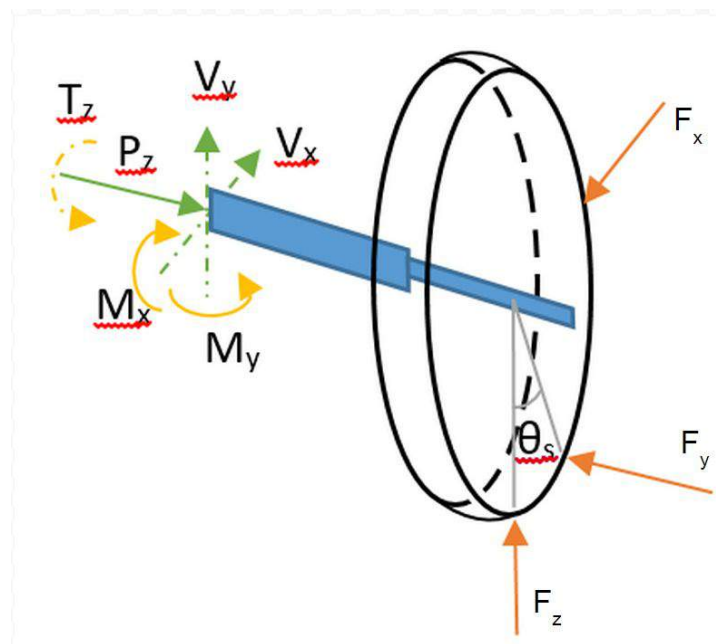


Figure 42. Cut FBD Showing Application Points of Forces on Front Suspension

The three known (measured Pz, Mx, and My) loads shown in Figure 42 were the normal force and moments in the vertical and longitudinal directions. However, since the loading case with an unknown θ was statically indeterminate, we assumed its value. We needed to approximate our θ to within ± 6 degrees in order to maintain an error of less than 10% on the magnitudes of the forces.

$$\sigma_u = -\frac{F_x}{A_s} + \frac{(F_x R_w) \cos(\theta) y}{I} - \frac{(F_z d) y}{I} \quad (10)$$

$$\sigma_t = -\frac{F_x}{A_s} - \frac{(F_x R_w) \cos(\theta) y}{I} + \frac{(F_z d) y}{I} \quad (11)$$

$$\sigma_b = -\frac{F_x}{A_s} + \frac{(F_x R_w) \sin(\theta) y}{I} - \frac{(F_z d) y}{I} \quad (12)$$

These equations were implemented in a MATLAB file to quickly solve for massive amounts of data with minimal user effort. The loads were then plotted against time and correlated to each other to determine peak loads, variance in peak value, and an estimate of how often these loads occur.

This setup employed the use of the DAQ in its regular position (under the steering column) and separate amplifiers which were mounted to the upright in order to minimize noise due to low strength signals travelling long distances (see *Amplifier/Wheatstone Design*).

Rear Suspension

While requiring more design, manufacturing and setup, calculations of forces from the data retrieved by the system was very straightforward. Because each link (including the shock) in the rear suspension were a two force member, once calibrated, we had a simple conversion factor between the voltage read and the force induced on any given link. Since we knew that each link could only act in tension or compression, if we knew the orientation of the link, we would have a complete image of the load it carries. Therefore, we simply used the orientation of the link to convert each of their forces into lateral, longitudinal, and vertical components and summed the results in order to obtain the reaction at the ground for the rear tire. This is summarized in the equations below.

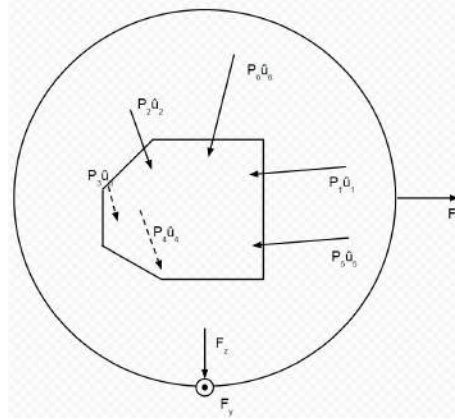


Figure 43. Free Body Diagram of Rear Suspension Link Forces and Tire Loads

$$F_x = \sum_{i=1}^6 P_i \hat{u}_i \cdot \hat{i} \quad (10)$$

$$F_y = \sum_{i=1}^6 P_i \hat{u}_i \cdot \hat{j} \quad (11)$$

$$F_z = \sum_{i=1}^6 P_i \hat{u}_i \cdot \hat{k} \quad (12)$$

Where: F_x is the load from the ground experienced by the suspension

P_i is the magnitude of the force carried by any particular link

\hat{u}_i is the unit vector of the same link

\hat{i} is the global unit vector matching the direction of component force F_x .

As with the front suspension calculations, these equations are currently implemented in a MATLAB file. The results were plotted to determine peak loads, variance in peak value, and an estimate of how often these loads occur.

Chassis

Theory of analysis of data gathered from chassis impact testing was marginally simpler than the previous two systems. For both skid plate and roll hoop, we were measuring the translational and rotational acceleration of the car in order to calculate the force applied on the frame. Geometry and dynamics allowed us to convert the accelerations of two points on the vehicle into translation

and rotation at the CG. Once we had this, the only calculation necessary was to multiply by mass or moment of inertia and do any appropriate unit conversions.

Sum of all Forces

$$F_x = m(a_x) \quad (13)$$

$$F_y = m(a_y) \quad (14)$$

$$F_z = F_{WR} + F_{WF} + m(a_z - g) \quad (15)$$

Sum of all Moments about the CG

$$-F_y(Z_F - Z_{CG}) + F_z(Y_F) = I_{xx}a_x \quad (16)$$

$$-F_{WR}(X_{WR} + X_{CG}) + F_{WF}(X_{WF} - X_{CG}) - F_z(X_F - X_{CG}) - F_x(Z_F - Z_{CG}) = I_{yy}a_y \quad (17)$$

$$F_y(X_F - X_{CG}) - F_x(Y_F) = I_{zz}a_z \quad (18)$$

Once again, these equations were implemented in a MATLAB code. The results were to be plotted to determine peak loads, variance in peak value, and an estimate of how often these loads occur. In addition, the energy associated with these loads was to be quantified in order to help with designing impact bench tests. However, due to electronic miscommunication about the DAQ's capabilities, these formulas were abandoned.

COST ANALYSIS

Table 10 below lists the entire cost analysis of the Get Loaded project. The Amplifier/Wheatstone Unit had a separate BOM shown in Table 11 due to the higher number of parts within the component. These Tables can also be found within Appendix C.

Table 10. Full Project Cost Analysis

System	Item	Details	Part Number	Unit Cost	Number	Total	Date Ordered	Person Ordered
Testing	Gas	87 Octane		25	5	125		
Measurement Eq.	Suspension/Frame	Linear Strain Gauge	KFH-3-350-C1-11L1M2	130	2	260		
Measurement Eq.	Suspension	Amplifier/Wheatstone Unit	N/A (LTC2053 Amp)	163	2	326	23-Oct	N/A
Measurement Eq.	Frame	3 Axis Accelerometer	KXD94-2802	6.45	1	6.45		
Measurement Eq.	Wiring	Extra Instrumentation Wire	28 gauge	20	1	20		
Measurement Eq.	Wiring	Solder		10	1	10		
Measurement Eq.	Wiring	Soldering Iron		40	1	40		
Measurement Eq.	Adhesive	1 oz. Bottle	SG-496	30	1	30		
System	Suspension	Shocker Rocker Raw Material		40	1	40		
DAQ	Repair	None		62.67	1	62.67	28-May	Ryan
DAQ	Upgrades	1kHz		399	1	399	28-May	Ryan
DAQ	Upgrades	4 Additional Ports		250	1	250	28-May	Ryan
Amplifier/Wheatstone	Part	Fuses	<1 Amp	2	10	20		
					TOTAL BUDGET:	1589.12		

The total projected budget needed for the project was approximately \$1600 which is \$600 higher than our original \$1000 budget. However, the available budget was a conservative amount and therefore the extra cost was justified.

Table 11. Amplifier/Wheatstone Cost Analysis

Digi-Key Part Number	Manufacturer	Quantity	Price	Extended Price	Description
GH7212-ND	GRAYHILL INC	1	1.17	1.17	SW DIP RECESSED SEALED 8POS 30V
P430HCT-ND	PANASONIC ELECTRONIC COMPONENTS (VA)	1	0.1	0.1	RES 430 OHM 1/10W 1% 0603 SMD
GH7200-ND	GRAYHILL INC	8	1.14	9.12	SW DIP RECESSED SEALED 2POS 30V
3296Y-200LF-ND	BOURNS INC	8	2.41	19.28	TRIMMER 20 OHM 0.5W PC PIN
TC4S81FT5LFTCT-ND	TOSHIBA SEMICONDUCTOR AND STORAGE (VA)	1	0.57	0.57	IC GATE AND 1CH 2-INP SMV
541-1.60KHCT-ND	VISHAY DALE (VA)	2	0.081	0.162	RES 1.60K OHM 1/10W 1% 0603 SMD
445-5666-1-ND	TDK CORPORATION (VA)	2	0.1	0.2	CAP CER 0.1UF 50V 10% X7R 0603
LM2937IMP-10/NOPBCT-ND	TEXAS INSTRUMENTS (VA)	1	1.85	1.85	IC REG LDO 10V 0.4A SOT223
445-12902-1-ND	TDK CORPORATION (VA)	2	0.45	0.9	CAP CER 10UF 16V 10% X7R 1206
541-1.80KHCT-ND	VISHAY DALE (VA)	2	0.081	0.162	RES 1.80K OHM 1/10W 1% 0603 SMD
MCT0603-1.0K-MDCT-ND	VISHAY BEYSCHLAG (VA)	24	0.178	4.272	RES 1.0K OHM 0.15W 0.5% 0603
445-5666-1-ND	TDK CORPORATION (VA)	16	0.073	1.168	CAP CER 0.1UF 50V 10% X7R 0603
RHM110KCFCT-ND	ROHM SEMICONDUCTOR (PASSIVE) (VA)	8	0.1	0.8	RES 110K OHM 1/10W 1% 0603 SMD
A104568-ND	TE CONNECTIVITY AMP	1	14.43	14.43	CONN 5MM TERMINAL BLOCK 16POS
A104554-ND	TE CONNECTIVITY AMP	1	2.93	2.93	CONN 5MM TERMINAL BLOCK 2POS
A104560-ND	TE CONNECTIVITY AMP	1	8.3	8.3	CONN 5MM TERMINAL BLOCK 8POS
P340HCT-ND	PANASONIC ELECTRONIC COMPONENTS (VA)	8	0.1	0.8	RES 340 OHM 1/10W 1% 0603 SMD
LTC2053CMS8#PBF-ND	LINEAR TECHNOLOGY	8	6.41	51.28	IC OPAMP CHOPPER 200KHZ 8MSOP
P4.70KHCT-ND	PANASONIC ELECTRONIC COMPONENTS (VA)	10	0.1	1	RES 4.7K OHM 1/10W 1% 0603 SMD
LM2937IMPX-5.0/NOPBCT-ND	TEXAS INSTRUMENTS (VA)	1	1.85	1.85	IC REG LDO 5V 0.4A SOT223
F4189-ND	LITTELFUSE INC	2	0.12	0.24	FUSE CLIP CARTRIDGE 250V 10A PCB
P82.0KHCT-ND	PANASONIC ELECTRONIC COMPONENTS (VA)	8	0.1	0.8	RES 82K OHM 1/10W 1% 0603 SMD
MMBT4403-FDICT-ND	DIODES INCORPORATED (VA)	1	0.14	0.14	TRANS PNP 40V 350MW SMD SOT23-3
160-1446-1-ND	LITE-ON INC (VA)	1	0.3	0.3	LED GREEN CLEAR THIN 0603 SMD
296-16806-1-ND	TEXAS INSTRUMENTS (VA)	1	0.42	0.42	IC DUAL DIFF COMPARATOR 8VSSOP
MMBT4401-FDICT-ND	DIODES INCORPORATED (VA)	1	0.14	0.14	TRANS NPN 350MW 40V SMD SOT23-3
P62.0KHCT-ND	PANASONIC ELECTRONIC COMPONENTS (VA)	8	0.1	0.8	RES 62K OHM 1/10W 1% 0603 SMD
Cable Gland	Polycase	2	1.8	3.6	
Enclosure	Polycase	1	14.39	14.39	Not necessarily the best but gives idea of pricing
Custom PCB	OshPark	1	21.33	21.33	Minimum of 3
Unit Price				162.504	

SAFETY CONSIDERATIONS

Introduction

An organized form of possible failure modes can be found within Appendix A of this report. This safety considerations section will reference some risks of various failure modes and how it could have affected the overall goal of collecting loads at the wheel.

Strain Gauge Electrical System

A failure within the electrical system could have caused a loss of data collection or damage to specific components of the system. Some safety considerations were to avoid running the SAE Baja vehicle in wet environments. Moisture could have caused a short somewhere within the system resulting in a error for output at the strain gauge location or a short that could have caused component failure. One way to mitigate the component failures due to a short was to add fuses to the power inputs of components. Therefore if a spike in amperage occurred, the fuse would have blown instead of an internal part of a specific component such as the DAQ or Amplifier/Wheatstone circuit.

Part failures due to manufacturer defects could not be avoided and would have resulted in data error or complete data loss. Part failures could have been remedied quickly by using readily available parts.

A failure within the electrical system would not have been acknowledged by the driver until the data was imported and attempted to be analyzed.

Shocker Rocker

A failure of the shocker rocker would only result in a loss of data collection of the shocker rocker linkage. From a data collection standpoint, this appeared to be an error that could be easily repaired by fixing the shocker rocker. However, the mechanical destruction that could have occurred could have been detrimental to the project. Since the rocker is attached to the shock, a failure from the shock side could have led to a collapse of suspension on that side of the vehicle. Axial links may have become bent and exert additional strain that could have caused strain gauge damage. Deformation in the axial link would have also changed the geometry of the analysis system, therefore new links would have needed to be manufactured. Wiring may also get caught up in moving parts or obstacles from the ground and be removed from their respective input or output locations.

If the shocker rocker would have failed, the driver would have immediately realized a mechanical failure and would stopped testing at that point and time.

General SAE Baja Vehicle Operation

There were many safety considerations when operating the SAE Baja vehicle. Engine sounds, ride feel, throttle response and braking response could have all been indications of failure within the entire Baja vehicle system. Therefore, the driver was aware and familiar with the vehicle's components to identify a soon-to-be source of failure or error.

The driver was also aware of the basic responsibilities and dangers of operating a vehicle. Documents pertaining to responsibilities of operating a university owned vehicle can be reviewed via documentation through Cal Poly's website.

MAINTENANCE AND REPAIR CONSIDERATIONS

Overview

Since Get Loaded's project goal was to find the loads at the tires, the system was not expected to be used extensively or designed to last for any time longer than was required for testing. Therefore, there were not many maintenance or repair considerations.

The only consideration relevant to the project was the effect of zero-drift and life cycle of the strain gauges. Looking at the spec sheet for the KFH series strain gauges within Appendix D, a 120 ohm gauge was tested at cycles of 1000 microstrain per minute. Zero-point drift was recorded and ranges for drift were analyzed. The 120 ohm strain gauge has a maximum life of 5 million cycles in order to have the zero-point drift less than 30 microstrain. For the larger expected strains seen at the spindle, this drift was negligible. However, the rear axial links could have been affected by a 30 microstrain drift. Fortunately, Get Loaded did not expect to see over 5 million cycles and the cycle amplitude for these rear links would be around 30 microstrain instead of 1000 microstrain as seen in the test life cycle test. Also, using a 350 ohm gauge reduced the severity of zero-drift based on the percentage difference of strain. This concept was explained within Chapter 4's discussion of selecting a 350 ohm strain gauge over a 120 ohm strain gauge due to temperature effects. The zero-drift was also be recorded via calibration after testing to see the fatigue of the strain gauge.

CHAPTER 5

DESIGN VERIFICATION PLAN

CURRENT TESTING PLANS

Introduction

This chapter is reserved for the testing plans for the Get Loaded project. The actual testing process undergone by the Get Loaded team is provided with Chapter 7 of this document. A full detailed drawing and model of the created spindle jig mentioned below in “Calibration” is provided in the full design packet within Appendix B. A more detailed explanation of the jig is located in Chapter 4 and analysis of the jig is located within Appendix E.

CALIBRATION PLAN

Location: Cal Poly San Luis Obispo Hangar/Instron Room

Objectives:

- 1) Determine Calibration Constant of Each Gauge
- 2) Strain Output Compared to Load
- 3) Load Cell Creation from Strain Gauges

Equipment:

- 1) Car Scales
- 2) Strain Gauged Linkages
- 3) Strain Gauged Spindle on Vehicle
- 4) Spindle Jig (for front only)
- 5) Instron Machine
- 6) Operating Baja DAQ/Amplifier

Procedure:

Zeroing Wheatstone Bridges

- 1) Using the gain settings on the FRONT amplifier, make sure that the selected output produces the minimum gain possible. (Other settings were proved invalid. See “Chapter 8”)
- 2) Make sure that the strain gauges are all connected into the amplifier channels desired for testing. Record the channel and gauge configuration.

- 3) Turn on the DAQ to power the Wheatstone/Amplifiers
- 4) Make sure the potentiometer is fully shorted causing an imbalance within the bridge. Measure the output of the channel. It should be railed at 0V.
- 5) Slowly turn the potentiometer of Channel 1 until the channel output reads 5V. The output from the Wheatstone bridge at this point is zero and the bridge is balanced.
- 6) Channel 1 bridge balancing is now completed. Do NOT touch the potentiometer for Channel 1. Doing so will cause the bridge to be out of balance.
- 7) Repeat steps 3-6 for each subsequent channel with an attached strain gauge.
- 8) All channel should now have balanced bridges.
- 9) Repeat steps 1-8 for the rear amplifier connected to the axial links.

Spindle Calibration Constant Determination

- 1) Securely fasten the spindle into the spindle jig bar and place the bar on top of two evenly placed bottle jacks placed on car scales.
- 2) Slide the spindle jig piece for the strong floor into the strong floor slots and line it up with the threaded portion of the spindle attached to the bar.
- 3) Place the beveled nut through the spindle end to eliminate a degree of freedom.
- 4) Start the DAQ, increase the bottle jacks to a weight of 200 lbs and hold the load steady.
- 5) Record the actual weight read by the car scales into an excel file.
- 6) Increase the amount by 200 lb and repeat Steps 5-6 until a maximum weight of 2000 lb is reached.
- 7) Observe the voltages of the seen at each load via the DAQ.
- 8) Plot the points on an Excel document to find the calibration constant of the specific strain gauge. Each plot should be linear in nature.

Rear Axial Links Calibration Constant Determination

- 1) Attach the axial link into the clevises for the Instron. Clamp the clevises into the Instron so that there isn't any load bearing on the links.
- 2) Using the displacement setting and button. Begin displacing the upper clevis to induce a tension load within the axial link.
- 3) Set the Instron to 200 lb in tension and wait for 5 seconds,
- 4) Start the DAQ to record the 200 lb voltage and wait an additional 5 seconds.
- 5) Increase the amount 200 lb and repeat Steps 5-6 until a maximum weight of 1400 lb is reached.
- 6) Plot the points on an Excel document to find the calibration constant of the specific strain gauges within the axial links. Each plot should be linear in nature.
- 7) Repeat Steps 1-7 for each axial link.

ON-BOARD TESTING PLANS

CAL POLY LAND PLAN

Location: Pozo Park

Objectives:

- 1) Isolated testing of predicted worst case loadings on Baja SAE vehicle
- 2) Frontal Impact Testing (entire vehicle)
- 3) Frontal Impact Testing (specific systems)
- 4) Side Impact Testing

Equipment:

- 1) Cal Poly Baja SAE vehicle
- 2) On-board RT DAQ
- 3) Strain gauges on front/rear suspension
- 4) Wheatstone Bridge module
- 5) Amplifier for strain measurements
- 6) GoPro camera

Procedure:

Setup

- 1) Record track conditions for the day (muddy, dry, etc.)
- 2) Ensure all strain gauges are reading appropriate loads at a static condition
- 3) Record ambient temperature and weather conditions (sunny, cloudy, rain, etc.)

Frontal Impact Testing (Entire Vehicle)

- 1) Place an obstruction (log/rock/mound/etc) at a distance that allows the vehicle to reach a controlled speed above 20 mph
- 2) Start vehicle, DAQ and GoPro camera
- 3) Bring the vehicle up to speed and hit the obstruction with the wheel pointing forward so that the heading is matched with the vehicle's motion. If a log is being used, the centerline of the car should be perpendicular with the log.
- 4) Repeat Step 3 to collect a total of 3 impacts.
- 5) Drive vehicle back to a safe location and retrieve data from the DAQ

Frontal Impact Testing (Specific Systems)

Front Tires

- 1) Place an obstruction (log/rock/mound/etc) at a distance that allows the vehicle to reach a controlled speed above 20 mph
- 2) Start vehicle, DAQ and GoPro camera
- 3) Bring the vehicle up to speed and aim at the obstruction with the wheel pointing forward so that the heading is matched with the vehicle's motion.
- 4) Create a heading that will isolate the front tire with strain gauges on the front suspension. Hit the obstruction.
- 5) Repeat Step 3 and Step 4 to collect a total of 3 impacts.
- 6) Drive vehicle back to a safe location and retrieve data from the DAQ

Rear Tires

- 1) Place an obstruction (log/rock/mound/etc) at a distance that allows the vehicle to reach a controlled speed above 20 mph
- 2) Start vehicle, DAQ and GoPro camera
- 3) Bring the vehicle up to speed and aim at the obstruction with the wheel pointing forward so that the heading is matched with the vehicle's motion.
- 4) Create a heading that will isolate the rear tire with strain gauges on the rear suspension. Hit the obstruction.
- 5) Repeat Step 3 and Step 4 to collect a total of 3 impacts.
- 6) Drive vehicle back to a safe location and retrieve data from the DAQ

Skid Plate

- 1) Place an obstruction (log/rock/mound/etc) at a distance that allows the vehicle to reach a controlled speed above 20 mph
- 2) Start vehicle, DAQ and GoPro camera
- 3) Bring the vehicle up to speed and aim at the obstruction with the wheel pointing forward so that the heading is matched with the vehicle's motion.
- 4) Create a heading that will isolate the skid plate. Hit the obstruction.
- 5) Repeat Step 3 and Step 4 to collect a total of 3 impacts.
- 6) Drive vehicle back to a safe location and retrieve data from the DAQ

Side Impact Testing

- 1) Find or create ruts similar to those created by typical Baja SAE vehicles
- 2) Start vehicle, DAQ and GoPro camera
- 3) Bring the vehicle up to speed and have the tires enter the rut.
- 4) Turn the tires to create a moment on the vehicle that induce heavy loading on the strain gauged side of the vehicle.
- 5) Repeat Step 3 and Step 4 to collect multiple runs. On the last run, tip the vehicle.
- 6) Right the vehicle and drive vehicle back to a safe location to retrieve DAQ data.

Heavy Whoops Testing

- 1) Find or create whoops similar to those experienced by typical Baja SAE vehicles
- 2) Start vehicle, DAQ and GoPro camera
- 3) Bring the vehicle up to speed and ride across the whoops so that the motion of the vehicle is perpendicular to the longitudinal axis of the whoops.
- 4) Keep the tires straight while going through the whoops. Then go through the whoops again while steering the vehicle heavily to the left and right.
- 5) Repeat Step 3 and Step 4 to collect multiple runs for going over the whoops straight and while turning.
- 6) Drive vehicle back to a safe location and retrieve data from the DAQ

Jump/Drop Impact Testing

- 1) Find a jump that will allow to Baja SAE car to have a hang-time greater than 1 second. If no jump is found, raise the front and then rear of the vehicle.
- 2) Start vehicle, DAQ and GoPro camera
- 3) Bring the vehicle up to speed and go off of the jump so that the motion of the vehicle is perpendicular to the longitudinal axis of the jump. If there is no jump, drop the vehicle.
- 4) Keep the tires straight while in the air and when impacting the ground. Then go off the jump again, slightly angled to allow the majority of the impact force to be carried by the strain gauged suspension.
- 5) Repeat Step 3 and Step 4 to collect a total of 6 runs for going through the jump straight and while turning.
- 6) Drive vehicle back to a safe location and retrieve data from the DAQ.

SPECIFICATION VERIFICATION CHECKLIST

Table 12. Checklist for Shaft Diameters

Prep Measurement Checklist			
Front	Location	Shaft Diameter at Adhesion Point (in.)	Issues/Comments
	Spindle		
Rear	Location	Shaft Diameter at Adhesion Point (in.)	Issues/Comments
	Link 1		
	Link 2		
	Link 3		
	Link 4		
	Link 5		
	Link 6		

Table 12 is a checklist that was used to verify the shaft diameters prior to mounting the strain gauges, but after sanding and prep had occurred. This ensured that the calculations used to convert stress at the points to loads at the ground were using the correct geometries and reducing any potential source of geometric error.

CHAPTER 6

PROJECT MANAGEMENT PLAN

MANAGEMENT PLAN

Specific team member responsibilities for Get Loaded are as followed:

1. Ryan Flatland (*Communications Officer*)
 - a. Be main point of communication with Professor Fabijanic unless otherwise specified within required deliverables
 - b. Facilitate meeting documentation deadlines for group
 - c. Coordinate fabrication of mechanical components
 - d. Keep schedule up to date and keep the team on schedule

2. Nick Bonafede (*Analysis Officer*)
 - a. Ensure accuracy and credibility of data
 - b. Organize data such that it is easy to visualize
 - c. Ensure that adequate research is conducted and sufficiently documented
 - d. Compare actual data to predicted results and document results
 - e. Determine whether resulting data satisfies our goals for confidence and accuracy

3. Christian George (*Testing Officer*)
 - a. Ensure that official testing procedures are produced and followed
 - b. Maintain clear and organized file management system
 - c. Ensure that all testing is done on time
 - d. Manage design and fabrication of all electrical components
 - e. Keep calibration standards of all equipment up to date
 - f. Manage documentation of final report

KEY DEADLINES

5/8/2014 - Decision on the method of measurement

5/15/2014 - Conceptual Model

6/5/2014 - Conceptual Design Report Draft

October 2014 - Design Report / CDR

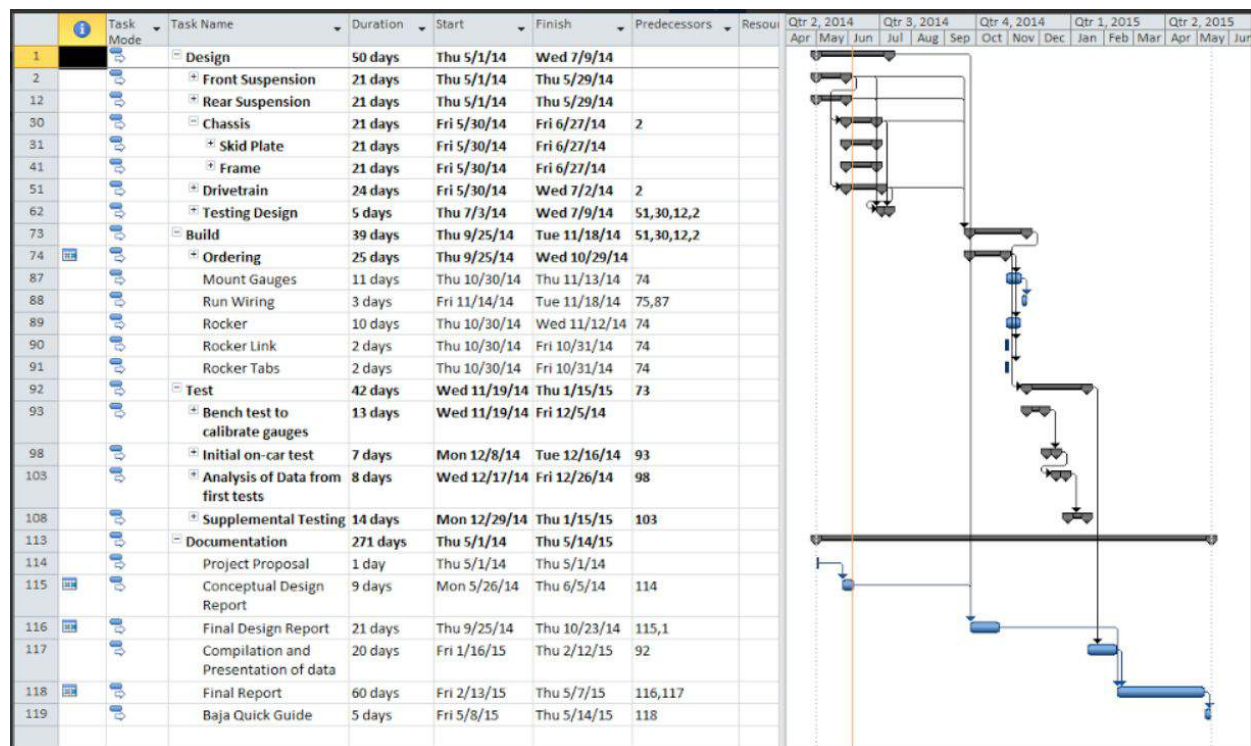
October 2014 - Initial setup of tests

- November 2014 - Manufacturing and Test Review
- December 2014 - Extensive load testing
- January 2015 - Project Update
- February 2015 - Design of bench tests for loads
- March 2015 - Final Report
- May 2015 - Senior Project Expo

Gantt Chart

As our Gantt chart stipulates, we are currently at the middle of the design phase, approaching the detail design for the suspension while only at the preliminary design of the drivetrain and chassis test setups. We will have adequate time over the summer to get to the point where we are ready to begin build immediately after the final design review early Fall quarter.

Table 13. Gantt Chart



Failure Mode and Effect Analysis

The failures with the highest risk codes included: roll hoop failure, front upright failure, and assorted link failures. Our risk codes took severity and probability into account. This analysis did make us think about the numerous “failures” which would manifest as inaccuracies in data. For this reason, more care will be taken with the design, setup, and calibration of the sensor setups.

Table 14. FMEA Table

	A	B	C	D	E	F	G	H	I	
1	System		Item	Failure Mode	Failure Effect	Target	Severity	Probability	Risk	Action Required / Remarks
3	Front Suspension	Upright	Spindle failure	Suspension collapse	E	Critical	Mostly Remote	6	Replace upright, re-do strain gauge setup	
4	Front Suspension	Tie Rod	Buckling failure	Reduction of control	E	Marginal	Remote	6	Replace tie rod	
5	Rear Suspension	Rocker	Bearing failure	Data inaccurate	M	Marginal	Remote	6	Replace bearing	
6	Rear Suspension	Toe Link	Buckling failure	Reduction of control	E	Marginal	Remote	6	Replace toe link, re-do strain gauge setup	
7	Rear Suspension	Rocker	Link buckling failure	Rocker moves until it hits sc	E	Marginal	Remote	6	Replace link / re-do strain gauge setup	
8	Rear Suspension	Rocker	Shock mount to rocker breaks	Suspension collapse	E	Marginal	Remote	6	Rebuild rocker better	
9	Chassis	Frame	Buckling failure on rollover	Driver seriously injured	P	Catastrophic	Extremely Remo	4	Go to the hospital, give up on senior project, or make a new car	
10	Measurement device	Strain Gauges	Bad Adhesion	Data inaccurate or no data	M	Negligible	Reasonably Prot	4	Replace strain gauge	
11	Measurement device	Strain Gauges	Inaccuracy of placement	Data inaccurate	M	Negligible	Reasonably Prot	4	Replace strain gauge or adjust calculations	
12	Measurement device	Strain Gauges	Temperature compensation gauge is str	Data inaccurate	M	Negligible	Reasonably Prot	4	Relocate strain gauge	
13	Measurement device	Amplifiers	Connection break due to vibration	Data stop	M	Negligible	Reasonably Prot	4	Dampen Vibrations / improve wiring	
14	Measurement device	Wiring	Wires caught or stretched due to moving	Data inaccurate or no data	M	Negligible	Reasonably Prot	4	Replace and route wire better	
15	Rear Suspension	Rocker	Deformation of frame	Data inaccurate	M	Negligible	Reasonably Prot	4	Reinforce frame	
16	Measurement device	Strain Gauges	Plastic Deformation of strain gauge	Data inaccurate	M	Negligible	Remote	3	Replace strain gauge	
17	Measurement device	Wiring	Short due to moisture	Data inaccurate	M	Negligible	Remote	3	Paper towels / electrical tape	
18	Measurement device	Wiring	Temperature affecting resistance of wiri	Data inaccurate	M	Negligible	Remote	3	Compensate or isolate wiring	
19	Measurement device	Wiring	Wire gauge affects resistance of wiring	Data inaccurate	M	Negligible	Remote	3	Design wiring right	
20	Measurement device	Wiring	Wire connections break	Data stop	M	Negligible	Remote	3	Make the connections better	
21	Measurement device	DAQ	Short the fuse on the battery input	Data stop and possible corr	M	Negligible	Remote	3	Replace fuse / check for short on input wires	
22	Measurement device	Strain Gauges	Exceed Gauge strain limit	Data stop	M	Negligible	Extremely Remo	1	Replace strain gauge	

CHAPTER 7

MANUFACTURING

Introduction

This chapter is reserved for the documentation and process of manufacturing for the Get Loaded project. Construction of the required components for primary data collection on the Baja vehicle and calibration jigs will be discussed. Detailed drawings of the parts to be manufactured is found within Appendix B while explanations of the individual constructed parts can be found within Chapter 4. Actual calibration procedures used with the manufactured components can found within Chapter 8.

8-CHANNEL WHEATSTONE AMPLIFIER

Once the PCB's were ordered through OshPark, they were given to Thomas Willson along with the components required for the 8-channel amplifier. Thomas hand soldered each electrical component to the board. The final result is seen below in Figure 44.

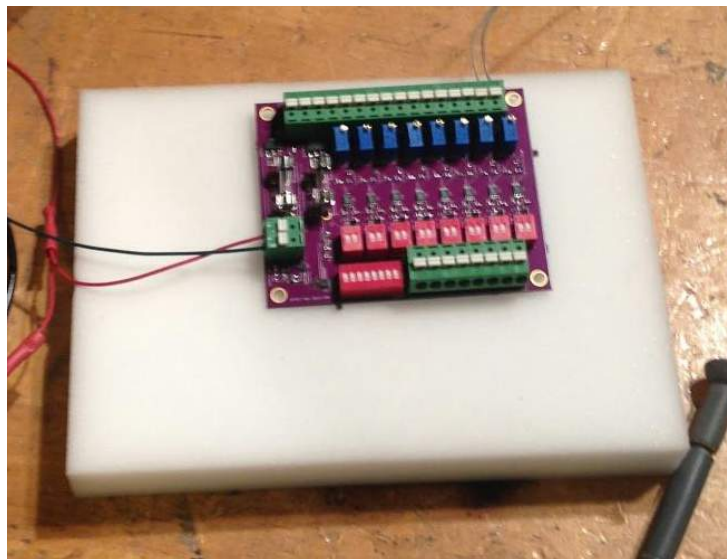


Figure 44. Completed 8-Channel Wheatstone Amplifier

There were not any immediate issues with constructing the amplifiers. However, testing showed that numerous solder connections had failed and needed to be resolved by resoldering and/or extending the trace pads from various electrical components.

Polycase case's were ordered in order to protect the amplifiers from the environments encountered by the SAE Baja vehicle. Mounting locations within the Polycases were used in order to minimize the amount of vibrations delivered through the amplifier/wheatstone board. The location of the amplifier for the spindle strain gauges is shown below in Figure 45.



Figure 45. Spindle Strain Gauge Amplifier Location

The second 8-Channel Wheatstone Amplifier responsible for the rear links and shock potentiometer was located on the rear of the vehicle by the gas tank as shown in Figure 46. Some concerns about this location was an accidental spill over with fuel and exhaust gas causing voltage fluctuations within the strain gauges.



Figure 46. Rear Links Strain Gauge Amplifier Location

Each amplifier was securely fastened to the vehicle using zip ties. The zip ties were able to reduce the amount of vibrations experienced by the amplifiers in addition to the hard mounts within the Polycases. Any movement of the Polycases that would induce any error within measurement values were deemed acceptable prior to any on-car testing.

SHOCKER ROCKER

The shocker rocker provided the force seen within the shock to be transferred to a small axial link that had a strain gauge attached to it. Therefore, the shocker rocker needed to be manufactured with tight tolerances that did not allow any larger or smaller loading to the small axial link. If the pivot point was slightly off center, this would induce an undesired force into the smaller axial link. The imbalance would cause a loading error within the system that would only appear post-testing when calculating the appropriate ground forces. Due to the multiple passes required by a mill and the necessity for tight tolerances, a CNC machine was used to produce the part. The CNC shocker rocker is seen assembled on the vehicle with the smaller axial link, strain gauge, and shock in Figure 47.



Figure 47. Assembled Shocker Rocker with Small Axial Link and Shock

The shocker rocker did not contain any major manufacturing flaws. The surface was slightly uneven with a minor step caused by resetting the piece within the CNC machine. The sizing of the part was still deemed acceptable and the mounting locations remained unaffected.

CALIBRATION JIGS

The manufactured portion of the calibration jig used to calibrate the front spindle strain gauges was essentially a beam and can be seen below in Figure 48.



Figure 48. Front Spindle Calibration Jig

The square 2" x 2" beam had a hole drilled through the center in order to allow the spindle to travel through it. Then, two aluminum blocks were milled and fastened to the top of the beam in order to level out the spindle.

The rear links used an Instron machine in order to perform calibration of their strain gauges. Therefore, the only manufactured parts were steel clevises to hold each rod end within the machine. They were created with a 1/4" thick steel plate and welded together.

STRAIN GAUGE APPLICATION

Omega's strain gauge application method found within Appendix G "Attaching Strain Gauges" was followed carefully when applying strain gauges to both the rear axial links and front spindle. The area of application was first sanded in small circular movements and then cleaned with acetone. The prepped links are shown below in Figure 49.



Figure 49. Prepped Axial Links for Strain Gauge Application

A single drop of adhesive was applied to the application area and the strain gauges were laid down by hand. The wires were held in order to position the strain gauge to avoid contaminating the strain gauges with hand oils or accidentally induced stress. Teflon tape was then laid over the top of the strain gauge to add pressure to the adhesive surface.

Once the teflon tape was held for 45 seconds to a minute, the pressure was slowly released from the strain gauge and precautions were taken to make sure not to accidentally rub the strain gauge.

The strain gauge wires were then taped down approximately 1-2 inches above the solder locations on the gauge to allow for strain relief within the gauges. The links were left to cure overnight for a full 24 hours before reassembling them onto the Baja vehicle.

BAJA SAE VEHICLE SYSTEM

In order to connect the entire strain gauge system together, specific wiring routes that avoided possible signs of error. The errors that were negated through specific routes were thermal errors, electromagnetic errors, and mechanical errors.

The routing for the rear links is shown below in Figure 50. The strain gauge wires for the rear three links were routed towards the main frame of the vehicle. Some slack was given in order to prevent any mechanical errors caused by tension within the wires. The wires were then routed upwards along the frame to the amplifier box shown earlier in Figure 46.



Figure 50. Rear Links Strain Gauge Wiring and Assembly

The wiring route along the frame attempted to minimize any thermal effects from the engine or exhaust. However, the wires were forced to be within the path of the thermal heat released from convection while moving. The frontal 2 links in the rear were routed along the rear plate up the frame and to the rear amplifier box. The thermal effects along with any electromagnetic effects from the spark plug were considered negligible before testing.

The front spindle, as shown below in Figure 51, was routed in a similar fashion with the same error concerns. The spindle's strain gauge wires were give enough slack to allow the steering to go full-lock both ways. Thermal and electromagnetic effects were assumed negligible prior to testing.



Figure 51. Front Spindle Strain Gauge Wiring and Assembly

The wiring for the front spindle was routed along the upper A-arm to the front amplifier box shown earlier in Figure 45. This short path helped to alleviate any thermal effects along the wires.

The outputs for the two amplifier boxes used CAT9 cable to route the amplified strain gauge signals to the DAQ box located centrally in the vehicle. All thermal and electromagnetic effects were deemed negligible as the strain gauge signal was amplified and any changes in resistance would not be considered problematic.

CHAPTER 8

CALIBRATION, TESTING, TROUBLESHOOTING AND RESULTS

Introduction

This chapter is reserved for the documentation and process of calibrating strain gauges, testing the system for peak loads, troubleshooting any sources of errors and final results for the Get Loaded project. Calibration of the axial links, front spindle, amplifier potentiometer offsets and vehicle weight “zeroing” will be discussed. Errors encountered post-testing will also be discussed along with actions taken to minimize discovered errors. The manufacturing of the components used for testing and calibrating, such as calibrations jigs, can be found previously in Chapter 7.

CALIBRATION

In order to record accurate data, various components within Get Loaded’s SAE Baja system must be calibrated as precisely as possible. The primary calibrated components throughout the project were the front and rear amplifiers via potentiometer offsets, the front spindle strain gauges and the rear axial links. In attempts to remain within a low budget, calibration was conducted entirely by the Get Loaded team.

Amplifier

The built amplifiers for the Get Loaded project needed to be calibrated prior to off-car strain gauge calibration and prior to on-car testing. Both amplifier calibration procedures involved offsetting the potentiometer in series with each wheatstone circuit’s strain gauge. In order to make sure that all values were captured within the 10V range, the potentiometers were offset to be centered to allow the output of the amplifiers to be centered at 5V.

The off-car amplifier calibration were centered at 5V without any loading induced on the members as shown below in Figure 52. This allowed the collected data from the rear links and spindle to be fully captured and used to calibrate the member’s strain gauges as force transducers. The method of converting the strain gauges to force transducers will be discussed within the individual strain gauge calibration sections labeled “Front Spindle” and “Rear Links” within the “Calibration” section of this chapter.



Figure 52. Rear Link Amplifier Offset Calibration Process (Off-Car)

Once the amplifier's potentiometers were calibrated to allow the testing for strain gauges to force transducers, the amplifiers had to be recalibrated once they were reconnected to the Baja SAE vehicle prior to testing as shown below in Figure 53.



Figure 53. Rear Link Amplifier Offset Calibration Process (On-Car)

Similar to the off-car calibrations, the front spindle and rear links were calibrated to 5V while on the car. By doing so, the loading from the vehicle's weight was essentially "zeroed" out. Any readings from the strain gauges at this point would correspond strictly to induced loading from the ground. Thus, Get Loaded's initial project requirement of finding ground forces would be fulfilled. The on car calibration was performed immediately prior to testing at the testing locations.

Front Spindle

The 3 strain gauges on the front spindle were calibrated in order to be used as force transducers on the vehicle. Therefore, instead of a voltage only being equivalent to a strain amount, a voltage would also be equivalent to a certain force. The force induced on the spindle strain gauges would then be used to determine stress induced in the spindle. This stress ratio would then be used with recorded data from testing runs and the ground forces on the front tire would be back calculated.

The force transducer calibration required a calibration jig that induced a purely axial force on the spindle. The manufactured front spindle calibration jig discussed in Chapter 7 (Manufacturing) used for this procedure is shown below in Figure 54.



Figure 54. Front Spindle Calibration Jig Assembly

The setup included the spindle with strain gauges, DAQ, two car scales, two bottle jacks, manufactured beam with mounts, and a fabricated nut to reduce induced moments when applying a load. The bottle jacks were evenly spaced from the spindle and centered on the car scales. This allowed the same moment to be applied from each bottle jack. This is essential as the same weight needed to be applied on each scale. Similar loads with different spacing would induce a moment in the spindle and errors would occur when determining a calibration curve.

To reduce the effects any moments induced from distance or mismatched force errors, a nut was created with angled edges. The drawing of the nut can be found within Appendix B. The nut held on the lower manufactured jig that fit into the strong floor. The location of the nut can be seen being applied in Figure 55 below.



Figure 55. Attaching Nut to Spindle Calibration Jig

The calculated stress range the strain gauges would experience under driving conditions was used in order to determine the maximum force applied for the force transducer calibration. The maximum force applied to the spindle was 2000 lb as limited by the car scales. The starting applied load to the spindle was roughly 400 lb and was increased by 400 lb increments. At each increment, the gain settings were changed in order to create 3 separate linear equations for each gain on the tested strain gauge.

After recording the data on the DAQ, the results were analyzed via laptop. The data was confirmed to be linear, within the same magnitude when comparing strain gauges and thus, the equations were assumed valid. All of the results for both the front spindle and rear link calibrations can be found within Appendix H.

Rear Links

Similar to the front spindle, the rear links were calibrated to be force transducers. However, the required loading for calibration was much smaller than the front spindle. This is because the rear suspension only allowed the links to experience purely axial loads. It was assumed that the axial loads would also be small enough to negate any moments caused by a buckling failure mode.

Due to the fact that the calibration loads were much smaller and that the loading was purely axial, an Instron machine was able to be utilized to apply a steady load to each of the rear suspension's links. The only fabrication required for the testing were the clevises to interface the link with the Instron. A visual of a rear link calibration test is shown below in Figure 56.



Figure 56. Rear Link Clevises and Instron Calibration Testing

The starting load for the rear links was determined to be 200 lb. The load was then increased in 200 lb increments via displacement control of the Instron. Similar to the front spindle calibration, the gain was switched to different settings at each load increment to create calibration curves in a single run. Once the maximum loading of 1600 lb was reached, the data was checked on a laptop for linearity.

The calibration test was repeated for each axial link. The results, calibration equations, calibration curves and calibration tables can be found with Appendix H.

Post-Calibration

All of the rear links were calibrated after testing to ensure linearity and equations of the strain gauges remained valid through testing. The results of this processes is further discussed within the “Troubleshooting” section below with all the data included in Appendix H.

TESTING

Once the rear links and front spindle were properly calibrated, testing of the instrumentation system could begin. The system was tested in a stationary configuration on car scales and various specified tests while driving. This section will discuss in detail the stages of each testing scenario and touch on any possible considerations of error adjusted for while testing. Any source of errors identified post-testing will be discussed in the following “Troubleshooting” section. All tests completed on the Baja SAE vehicle were completed entirely by the Get Loaded team.

Car Scales

Vehicle scales were used in order to record the static weight of the Baja vehicle both before and after testing. While awaiting approval to test at the testing facility, the Get Loaded team tested the static weight at the Cal Poly hanger as shown in Figure 57 below.



Figure 57. Attaching the DAQ and Recording Weight of Vehicle on Car Scales

The amplifiers were re-calibrated to make all of the strain gauge outputs to as close to 5V as possible. However, due to the high sensitivity of the potentiometers and gain selections on the amplifier, the amplifiers could not be assumed to be at 5V on a static load. The actual baseline voltage would be found while reviewing the data with a higher resolution. Setting the strain gauges to output 5V on a 0-10V scale would correlate to the car’s weight being negligible when the loads were determined. Thus, all loads calculated would be ground loads and the objective of the Get Loaded team would be fulfilled.

Multiple static loading test were taken while the vehicle was on the scales. The DAQ was set to begin logging data and the initial weight of the vehicle without a driver was recorded via the scales. The driver was then asked to sit still in the vehicle and the scales were recorded while the DAQ recorded the strain gauge voltage differences. Then, one member of the Get Loaded team jumped onto the front of the vehicle to add additional weight. The scales were recorded and the weight distribution was held steady to allow the DAQ to record the values. The last Get Loaded team member jumped on the rear of the vehicle and the weight and data was recorded. Finally, all of the Get Loaded team members were removed and the static weight distribution after applying the weight of the team members was recorded and held constant.

After analyzing the data, an unpredicted trend occurred when additional weight was added to the front of the vehicle. The moment applied to the spindle had a sign convention opposite to what the team expected. Upon further investigation and hypotheses, the team reached a conclusion that the travel of the suspension along with the lack of movement at the tire contact patch caused an induced side force on the spindle. In order to reduce the effects of the side force, a board placed on top of BBs, as shown below in Figure 58, was used to allow the wheel to translate outwards with the travel of the suspension.



Figure 58. Removal of Induced Side Forces with Suspension Travel using Plastic BBs as Rollers

The car scales testing was done both in the hanger and immediately before the on-car testing at the testing facility as shown in Figure 58. The data was collected and immediately analyzed on a laptop to confirm relative validity of the strain gauge outputs. Once the outputs were deemed acceptable, on-car testing was immediately started to avoid errors caused differing environmental conditions. Scale testing was also conducted after on-car testing.

Driving Test Cases

After the scale testing was completed to establish a baseline, the Get Loaded instrumentation system was tested under normal and extreme driving conditions. The extreme cases were conducted in order to capture peak loads that could be experienced by the Baja SAE vehicle. The individual driving tests performed are listed below along with a description of the test and the peak loads they intended to isolate.

Flat Ground Circles

The first test was completed was on flat ground at the entrance of the Pozo course. The DAQ was turned on and the driver (Ryan Flatland) proceeded to make a circular path in a clockwise direction. The run lasted approximately 3-4 minutes before the vehicle was stopped and the DAQ run was shut off. The same procedures of restarting the DAQ and making a circular path was repeated in a counterclockwise direction. The vehicle was stopped, the SD card removed from the DAQ and the data saved onto a laptop to ensure a valid capture of data.

Attempting circles on flat ground attempted to re-create a relatively constant loading on the Baja SAE vehicle while in motion. The test also attempted to isolate the induced side forces from deep ruts that could appear in a Baja SAE competition. Although shallow ruts were created from the constant turning, the effects on the vehicle were assumed negligible in comparison to the deep rut test.

Rock Bed

Once the test for the flat ground circles was deemed acceptable, the Get Loaded instrumentation system was then tested on a small river rock bed along with several small jumps. The DAQ was started on flat ground and the driver (Ryan Flatland) completed a 3-5 minute run driving over rocks within the bed of the river and jumping over small jumps. The run was conducted two times to compare results. After the run, the vehicle was stopped, the SD card removed and the data saved onto a laptop to ensure a valid capture of data.

The rock bed test was conducted in order to recreate erratic and quick loading that can be induced on the Baja SAE vehicle. This test would also confirm that the recording frequency of 1 kHz was high enough to capture peak loads. This test aimed to capture rough terrain that the Baja SAE vehicle could take at sufficient speed.

Post Impact

Another major test conducted by the Get Loaded team was running the Baja SAE vehicle's tire into a post. The tire used to impact the post was the tire with the front spindle that had strain gauges attached to it (front right). The run lasted approximately 20 seconds and involved the vehicle starting, gaining speed to approximately 15-20 mph and impacting the post. After the

run, the data was assumed to be valid and the vehicle was driven to the next location for the deep rut test.

The post impact test was conducted in order to find an extreme and severe impact case caused by poor choices from the driver. These errors could include anything from the driver impacting a large rock, a post or approaching a log at an incorrect angle and high rate of speed.

Deep Rut/Rollover

The Get Loaded team drove the vehicle to an open clearing and proceeded to make a circular path to create deep ruts in preparation for the test. Once the ruts were deemed equivalent to ruts seen on a typical Baja SAE competition course, the DAQ was turned on and the vehicle proceeded around the course in a clockwise direction. The run lasted approximately 5 minutes before the vehicle was rolled over onto its side from a very tight turning in deep ruts. At this point the kill switches were turned on and the DAQ was shut off. The same procedures of restarting the DAQ, making a circular path and tipping over was repeated in a counterclockwise direction.

The deep rut test was conducted to test the Baja SAE vehicle's strength against side forces induced by ruts typically seen on a competition course. The rollover aimed at collecting data where the load of the vehicle was focused on only two points (tires). The rollover test was conducted in a safe location at low speeds. Once the vehicle had rolled over, the driver and a member of the Get Loaded team immediately cut off all fuel and electrical going to the engine of the vehicle.

Pozo Course

After the deep rut and rollover test, the Get Loaded instrumentation system was tested on Pozo's full course. The DAQ was started at the entrance and the driver (Ryan Flatland) completed the course in a approximately 8 minutes. The run was conducted two times to compare results. After the run, the vehicle was stopped, the SD card removed and the data saved onto a laptop to ensure a valid capture of data.

The Pozo course test was conducted in order to recreate a typical competition environment for a Baja SAE vehicle. The course consists of ruts, high speed sections and full lock turns that can induce variable loading into onto the vehicle's suspension. This test would also confirm the reliability of the instrumentation system over an extended amount of time.

Jump

The Get Loaded instrumentation system was then tested within a small motocross/ATV course that contained medium sized jumps. The DAQ was started at the entrance of the course and the

driver completed the data run in a approximately 5 minutes. After the run, the vehicle was stopped, the SD card removed and the data saved onto a laptop to ensure a valid capture of data. The jumps test was conducted in order to recreate the loading caused by normal sized jumps found on a typical competition course for a Baja SAE vehicle. This test also confirmed the reliability of the instrumentation system over many gradual ground impacts.

Drop Impact

The Get Loaded instrumentation system was tested while dropping the front and rear of the vehicle with a driver in the seat. The vehicle was driven to a flat area and shut off. The DAQ was started and the front of the vehicle was lifted to a 90 degree angle with respect to the ground. The vehicle was then dropped with force onto the ground. The same procedure was conducted for the rear of the vehicle. The process was completed 3 times for accuracy and certainty of the data and the run of the data took approximately 5 minutes. After the drop tests, the SD card removed and the data saved onto a laptop to ensure a valid capture of data.

The drop test was conducted to recreate a larger-than-normal jump scenario for a Baja SAE vehicle. This test would also confirm the reliability of the instrumentation system during a sharp and sudden impact.

TROUBLESHOOTING

After the data analysis, we found that there was significant amount of strain gauge drift: the links' readings would change values with no load applied to them. A Matlab script was created to measure the zero-point drift on each channel for each run to find any correlations. If we could prove that the drift acted linearly over the course of a short run, the data we gathered could be salvaged with a little extra analysis. If linearity could be proven, a linear interpolation of the calibration constants from two static points at the start and end of each run could result in fairly accurate loads plots.

Table 15 shows the results of the offset analysis. The main conclusion we drew from this was that the drift was very significant in magnitude - drifting 1 to 6 times the magnitudes experienced when the vehicle is at rest (1 to 6 g's of drift). Additionally the channels didn't seem to drift in a consistent direction and the magnitude of drift didn't seem to be correlated with the length of the run. Link 3 for Run #18 (in red) had a huge drift since we lost the signal mid-run. This information was disconcerting, as it seemed to indicate that the drift was likely due to nonlinear effects.

Table 15. Drift of Zero-Point for Each Run and Each Gauge

Run #	Discription	Zero-point drift over duration of run (axial load in lbf)						Zero-point drift over duration of run (Axial stress in psi)		
		Link1	Link2	Link3	Link4	Link5	Link6	Spindle Top	Spindle Rear	Spindle Bottom
1	Set1_Run1_AccelX20x2BLHCircle'	-7	-12	93	12	3	-18	-396	-99	-1654
2	Set1_Run2_LHCircle'	-63	0	0	-87	-49	-24	-4156	-388	2576
3	Set1_Run3_RHCircle'	86	0	41	15	67	-50	735	-625	1121
4	Set1_Run4_StaticCalibRearRollers'	76	-53	-42	16	56	44	2264	315	-2624
5	Set1_Run5_StaticCalibFrontRollers2'	147	14	27	26	63	60	1110	191	-1086
6	Set1_Run5b_StaticCalibFrontRollers1'	120	40	17	-31	33	75	1664	-38	-1657
7	Set2_Run1_Left_Turns'	121	117	139	87	53	85	-6756	-2133	7800
8	Set2_Run2_Right_Turns'	57	14	73	-9	34	-39	4003	-173	-3025
9	Set2_Run3_Toward_S0x2BT'	-2	91	-62	-53	6	67	-2953	1234	1412
10	Set2_Run4_Whoopses'	3	116	-26	-109	-3	-119	957	-194	644
11	Set2_Run5_Playin_In_The_Rocks'	13	-48	4	89	83	39	-4673	-1329	3967
12	Set2_Run6_Hitting_White_Rock'	57	199	24	-146	21	95	108	1076	-1958
13	Set3_Run_01_Riverbed'	138	65	45	128	107	180	-985	-1727	6695
14	Set3_Run_02_Post'	-23	-28	13	89	2	89	1083	-707	-1594
15	Set3_Run_03_LHRuts'	51	-50	-284	142	58	56	179	-462	-1484
16	Set3_Run_04_RHRoll'	33	127	384	17	31	89	-2100	24	1668
17	Set3_Run_05_LHRoll'	127	17	13	87	113	162	-1580	-2941	7063
18	Set3_Run_06_Endurance'	127	179	-8026	52	36	261	3498	-786	-3616
19	Set4_Run_01_Jumps'	205	19	2	114	109	55	-1339	65	4196
20	Set4_Run_02_LiftAndDrop'	77	87	0	42	-13	9	-3748	1541	2160
21	Set4_Run_03_RearStatic'	-60	96	-1	-181	-29	-22	-531	-263	608
22	Set4_Run_04_FrontStatic'	27	-43	2	-33	19	24	-442	-90	616
	Average drift	74	64	61	71	45	76	2057	745	2692
	Magnitude Comparison: 1g quarter car load	-27	-19	-10	88	98	199	-2300	0	2300

Drift Causes

We initially hypothesized that this drift could be due to temperature and vibration of the potentiometers used to center the zero-load gauge readings. In order to confirm the causes of drift, we conducted a series of bench tests to isolate the cause so we could potentially use the data, or at least produce an updated procedure that would yield better results. While conducting bench tests, one of the important focuses was the magnitude of drift on unstressed links over time. We determined that the acceptable margin of error for the zero point of an unstressed link was around 0.01V—about 15 lbf on the links. This number was chosen because it would result in an uncertainty of less than 1 g at the wheels in all axes.

As the background section Error Compensation Methods discussed, temperature can have a range of effects on strain gauge measurements, and our decision to use a quarter bridge made our readings particularly susceptible. During the bench tests, our first goal was to prove how much of an effect temperature could have, then resolve temperature issues by modifying our measurement technique - specifically by changing to a half bridge.

As a part of the initial design, a small rotary potentiometer was incorporated into each channel of the amplifier to adjust the balancing resistance in the quarter bridge, placing the zero-load reading in the center of the measurement range. While these potentiometers were rated for vibration, we believed that this could still be a point of variation in our zero-point.

Bench Tests

Our first bench test was conducted to prove that temperature alone could have had a significant effect on our readings; we expected to see the large change shown in Figure 59. At 1200 seconds, a heat lamp was turned on next to link B, then it was turned off at 3600 seconds. The temperature change was about 50 degrees Fahrenheit to cause that magnitude of effect on the voltage readings.

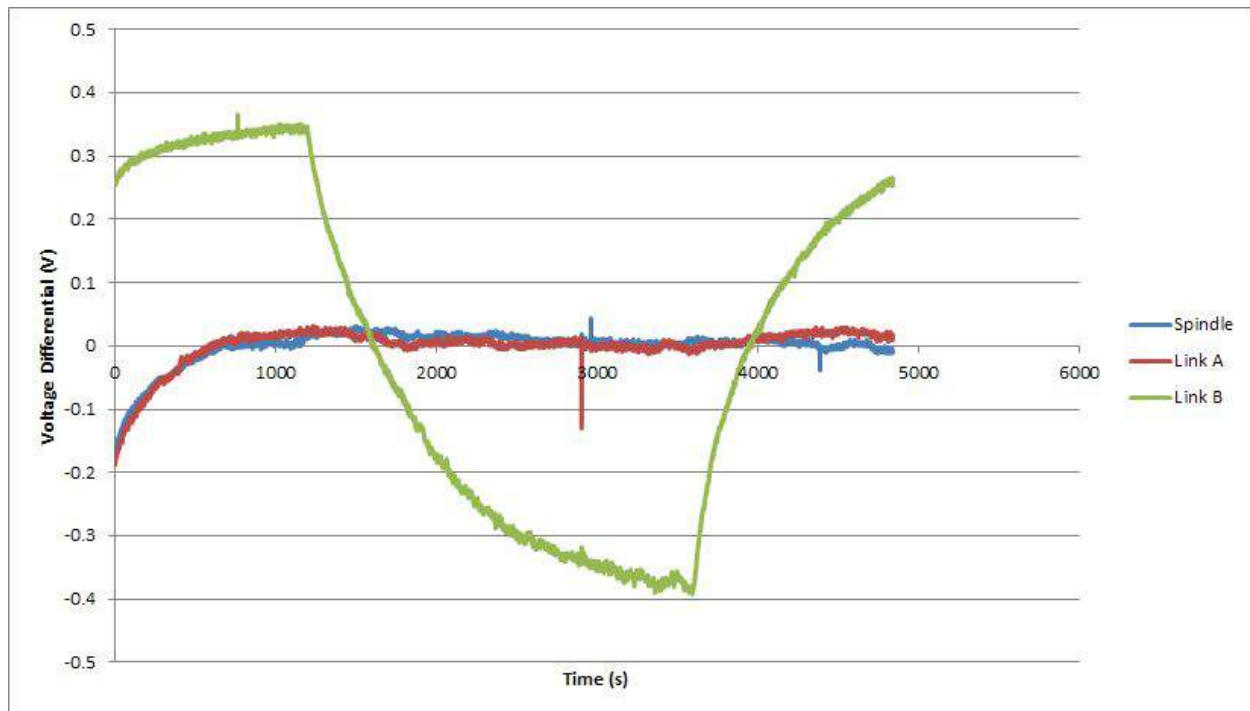


Figure 59. Temperature Test: Heated Unstressed Quarter Bridge

Having confirmed that changes in temperature would cause drift, we moved on to a controlled temperature test with the quarter bridge setup to see if anything other than temperature compensation was at fault for the drift. As Figure 60 shows, even in a controlled temperature environment, the quarter bridge setup was getting exceptionally high drift. It appears that the effect is time dependent, and related to the 5 and 10 volt regulators which we also recorded. After about 1000 seconds, the regulators and link gauge readings were more stable, but still varied within a range of about 0.02V, still a bit higher than our acceptable variance.

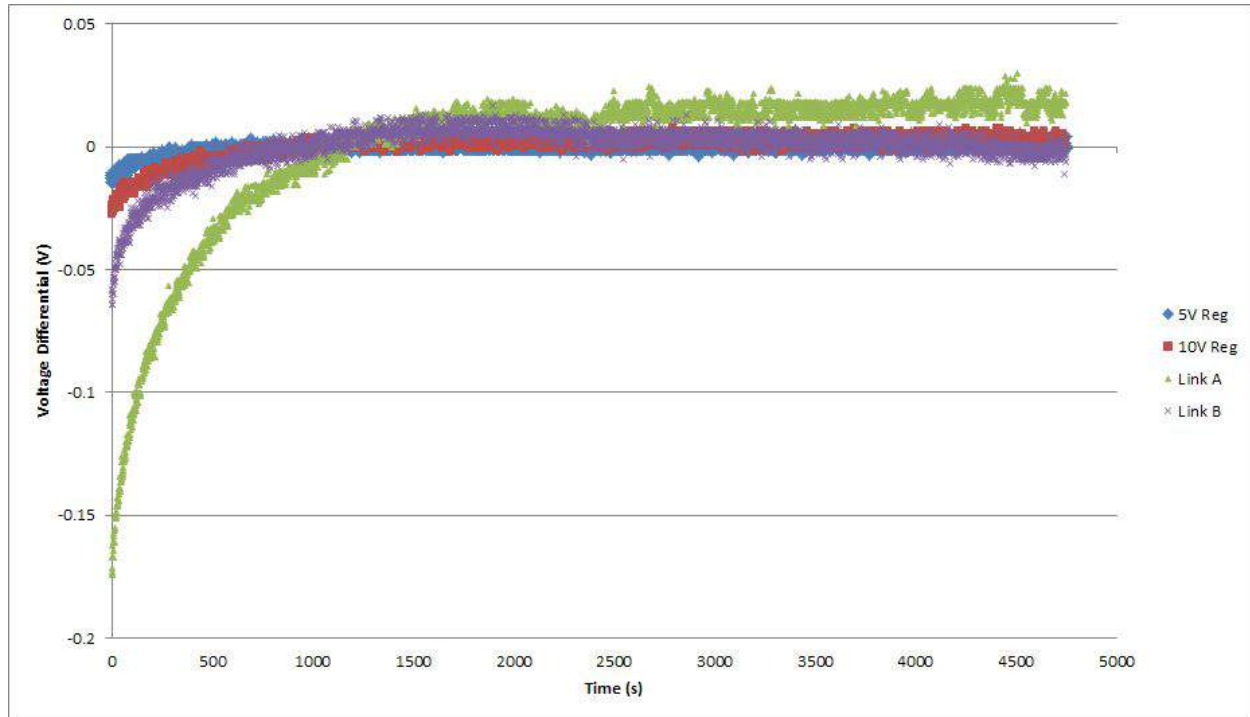


Figure 60. Controlled Temperature Test: Unstressed Quarter Bridge

We modified a channel of our amplifier to operate in a half bridge configuration, with the two strain gauges on two different links. This test was still conducted off the car, in an unstressed, temperature controlled environment. Figure 61 shows that the half bridge was significantly more stable, with a little initial drift that was directly related to the 5 and 10 volt regulators. We also isolated the drift at the beginning of the test: it was not caused by battery voltage changes, so it must have been the warming of the amplifier circuitry due to current flow. This means that a new revision of the board could operate in half bridge configuration, and record the 5 and 10 volt on board regulators to mathematically cancel the drift effects caused by the board heating up. With this test, the variation in our readings was reduced to 0.015V, almost to our goal of 0.01V.



Figure 61. Controlled Temperature Test: Unstressed Half Bridge

Our final test added the violent conditions of the Baja vehicle into the test while still keeping a half bridge configuration, and an unstressed link. Figure 62 shows the significant drift due to vibration in the potentiometers, which was the only variable not affected by the prior static tests. Unfortunately, the potentiometer moves randomly and in both directions, and in magnitudes large enough to move outside our reasonable range of variance by an order of magnitude.

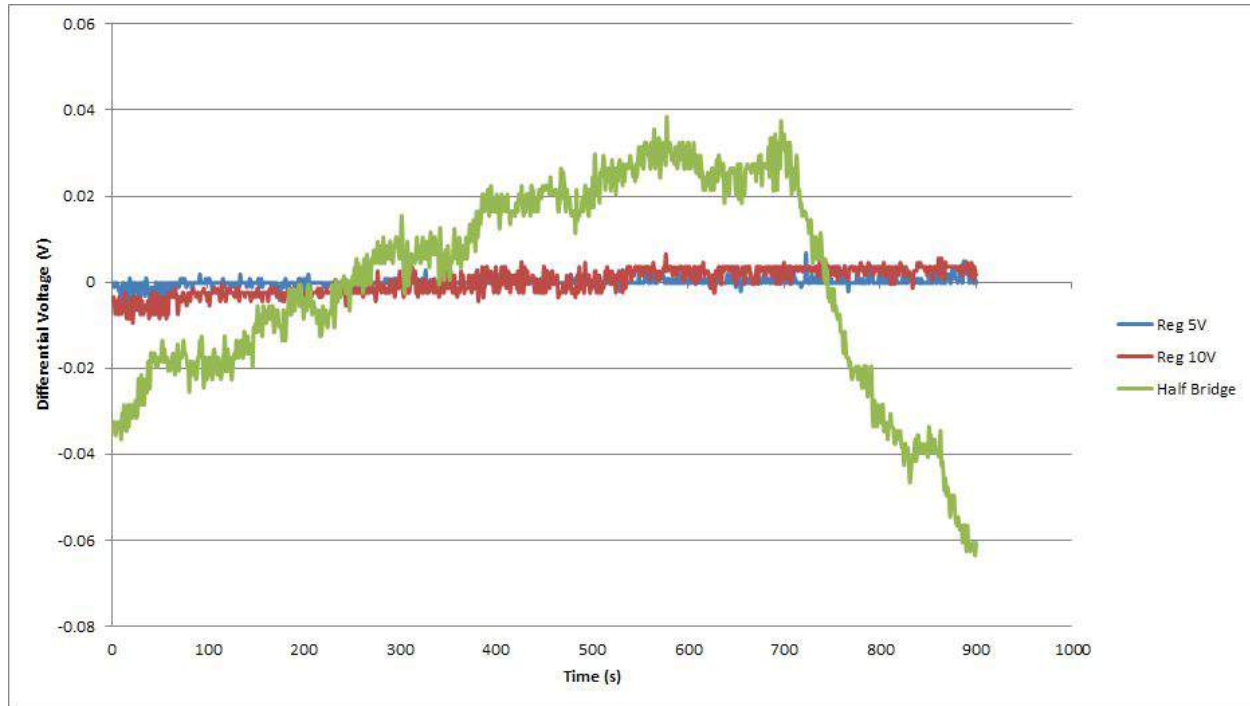


Figure 62. Vibration Test: Unstressed Half Bridge on Driving Car

Drift Troubleshooting Conclusions

The goal of the troubleshooting was to see if we could use all the existing data despite the significant drift. The only way that this could be possible was if the drift was relatively linear, so that we could zero the readings for each run based off the static loads experienced at the beginning and end of the run, and assume a linear interpolation for the drift over the relatively short run. For the temperature effects that exist due to the quarter bridge, that would be a reasonable assumption since the temperature of the link itself wouldn't change significantly in a two minute run. The changes due to vibration, however are more random and cannot be approximated as linear across the run. Due to this, the conclusion of the drift troubleshooting analysis was that we were unable to extract the accurately corrected loads for entire runs.

All the data we collected is still useable however since magnitude changes occurring over very short durations (less than a second) still represent accurate measurements of magnitudes experienced. This concept and application will be discussed further in the Results section.

Post-Calibration

In addition to the investigation of drift, we conducted post-calibration on each of the gauges. Appendix H details the results. All the post calibration was relatively similar to the initial calibration, with two specific exceptions: the rear spindle gauge and the link 3 gauge. Both of these gauges exhibited symptoms of changes during testing.

We believe we exceeded the strain limit of the spindle gauge with the frontal load test where we hit the post. The post calibration showed that the slope of the gauge readings was reduced by 47% from 17159 to 9034 psi/V. Since only this gauge position exhibits this behavior, and it was the only gauge which was loaded so significantly, we concluded that the overloading caused the change in the calibration constant.

We lost the signal of link 3 towards the end of our testing, so we suspected that something was awry. During the post calibration, the data recorded for link 3 was very different, and is included below.

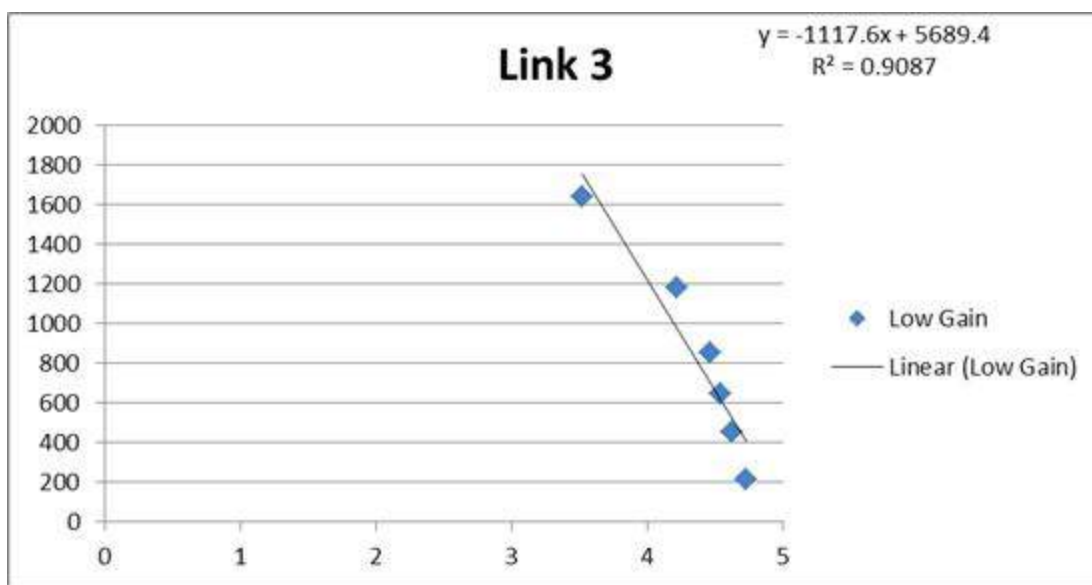


Figure 63. Post Calibration of Link 3 Exhibiting Nonlinear Behavior

Link 3 was the only strain gage that ever exhibited nonlinear behavior for any of the pre or post calibrations. While we are unsure what caused the nonlinearity, or when the calibration changed, we concluded that this was of minimal concern, since the readings on that link were generally below 800 lbf, still in the range that was mostly linear and of a similar slope to the prior calibration.

RESULTS

This section outlines the magnitudes of the loading cases found in the tests described in the above Testing section. Details on how to repeat the tests with increased accuracy are in the above Troubleshooting section. All measured peak loads are shown in the following tables (Table 16 and Table 17) with recommended maximum design loads. There are descriptions below to explain the reasoning, confidence, and how to improve the results of these experiments.

Despite the issues presented in the troubleshooting section, the experiments yielded a fair amount usable data. However, the potentiometer vibration and temperature drift introduced much more uncertainty into the system than previously anticipated. As such, many of the tests did not yield useful results as the uncertainty of the final result is greater than the result itself. This trend, however, extends only to the low impact, cyclical loads (i.e. turning and standard driving). This effect does not extend to the impact loads as these loads have a much larger magnitude and shorter timeframe allowing less time for drift and low frequency noise. Figure 64 shows an example of the vehicle's load output after the data was processed via a MATLAB script file. Appendix I contains MATLAB plots for the other loading cases. Appendix J contains the MATLAB script files used to process the raw data from the DAQ.

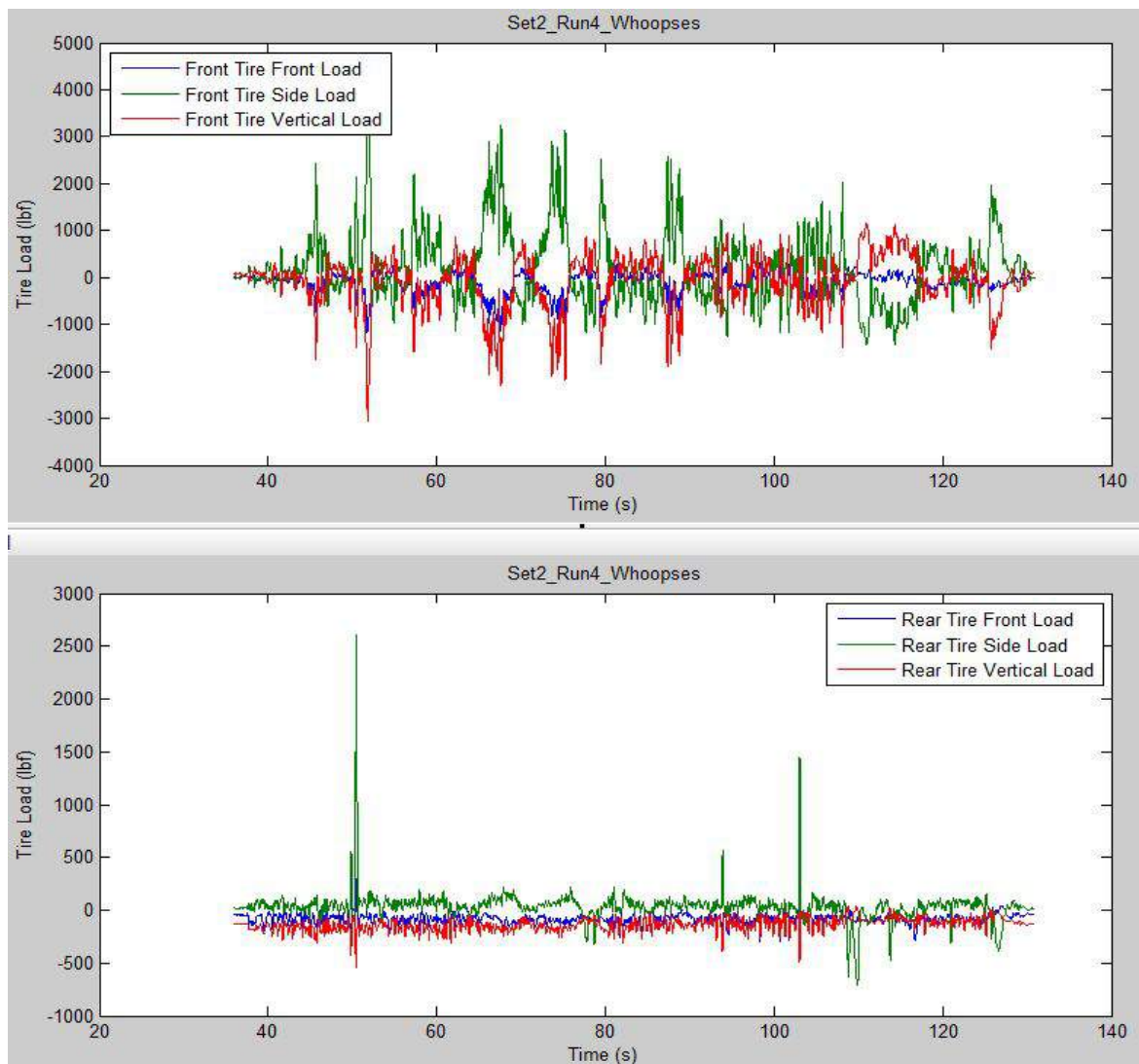


Figure 64. Matlab Filtered Load Data - Driving over Whoops

Furthermore, the loads are taken from the reference frame of the front and rear uprights, including steering for the front. To clarify, the longitudinal load will be directly along the radius of the tire, regardless of the steering angle. Longitudinal forces have been confirmed with hand calculations and acceleration data. Take note that during all turning operations the front tire/upright is rotated about the kingpin axis and that during all suspension travel the tire/upright is rotated about the instant axis. Also note that due to the drifting of the strain gauges, the loads provided are a change in load from static.

Table 16. Peak Load Table (lbf)

Loading Case	Front Suspension			Rear Suspension		
	Fx [lbf]	Fy [lbf]	Fz [lbf]	Fx [lbf]	Fy [lbf]	Fz [lbf]
Acceleration	60	150	-80	150	150	50
Hard Brake	-200	1500	-1300	-100	-500	-120
Left Turn	-1600	4600	-3200	-250	450	-280
Right Turn	450	-1500	-1300	-160	-1000	-75
Rocks	-1400	4400	-3000	-370	-1000	-250
River Bed	-750	2600	-1800	-350	-1000	-350
Rollers	-750	2500	-1800	-250	300	-350
Whoops	-1200	4200	-3000	-250	2600	-550
Tip Over	-2500	8800	-6500	-250	1400	-300
Jump	-450	2200	-1700	-250	350	-400

Table 17. Peak Load Table (Full Car g's)

Loading Case	Front Suspension			Rear Suspension		
	Fx [g]	Fy [g]	Fz [g]	Fx [g]	Fy [g]	Fz [g]
Acceleration	0.1	0.3	-0.1	0.3	0.3	0.1
Hard Brake	-0.4	2.7	-2.4	-0.2	-0.9	-0.2
Left Turn	-2.9	8.4	-5.8	-0.5	0.8	-0.5
Right Turn	0.8	-2.7	-2.4	-0.3	-1.8	-0.1
Rocks	-2.5	8.0	-5.5	-0.7	-1.8	-0.5
River Bed	-1.4	4.7	-3.3	-0.6	-1.8	-0.6
Rollers	-1.4	4.5	-3.3	-0.5	0.5	-0.6
Whoops	-2.2	7.6	-5.5	-0.5	4.7	-1.0
Tip Over	-4.5	16.0	-11.8	-0.5	2.5	-0.5
Jump	-0.8	4.0	-3.1	-0.5	0.6	-0.7

Testing Cases

Flat Ground Circles

Driving in circles on flat ground was intended to yield a constant load typical of that seen by the vehicle while turning. Due to the mild nature of these loads and the large drift and noise inherent in the system, this test was not able to define solid numbers for this loading case. The test was, however, able to determine that these loads are very small when compared to the impacts discussed below. This test can be improve via the means discussed in the Troubleshooting section.

Rock Bed

Driving through the rock bed and small jumps was intended to yield small impact loads similar to those experienced while driving over rough terrain. This test, similar to the Flat Ground Circles, did not yield hard numbers due to noise and drift. Moreover, the small impact nature of this test caused the loads to be completely obscured by the vibrational noise. The test did confirm the magnitude of these loads to be equal to that of the noise. This test can be improve via the means discussed in the Troubleshooting section.

Post Impact

Driving the wheel into a post was intended to measure the high impact load during a major frontal impact. This is the impact when running a wheel into any fixed stationary object at 15 mph. Due to the very high speed and load inherent in any large impact loading case, this load was very clear and discernible. Interestingly, this load is approaching the yield strength of the front upright indicating that the previous design load was about 20% short of the actual load. This test can be improve via the means discussed in the Troubleshooting section.

Deep Rut/Rollover

Driving the vehicle turning through a rut at increasing speeds until rollover was intended to reveal the loads experienced during aggressive cornering, deep ruts, and a typical 90 degree rollover due to a lack of oversteer. These loads can be seen in the table above. This test can be improve via the means discussed in the Troubleshooting section.

Pozo Course

Driving the car around the test track was intended to yield the typical loads seen throughout an endurance race. This can be used to quantify the number of cycles of each type of loading to use in the design life calculations for future years. Due to the mild nature of most of these loads and the large drift and noise inherent in the system, this test was not able to define solid numbers for how many of each cycle to design for. This test can be improve via the means discussed in the Troubleshooting section.

Jump

This test is intended to result in data defining a the load of a typical airborne landing in the vehicle. The loads can be seen in the table above. This test can be improve via the means discussed in the Troubleshooting section.

Drop Impact

This test is intended to be similar to the Jump test. The difference is that the vehicle is not running in an attempt to combat noise and drift. The loads can be seen in the table above. This test can be improve via the means discussed in the Troubleshooting section.

CHAPTER 9

CONCLUSIONS AND RECOMMENDATIONS

This senior project addressed a challenging problem: measurement of loads on a dynamic platform in a harsh environment. While we were successful at salvaging some useful data, there are several aspects we would approach differently if we were to undertake this project again.

1. Half bridge

Our testing showed that the benefits of a half bridge (as far as temperature corrections are concerned) are necessary for the accurate measurement of loads. Including the half bridge by design would have significantly reduced our drift, and improved our confidence in the numbers we did read.

2. Potentiometers

We used potentiometers integrated into the amplifier boards to center the calibration for the strain gauges. These proved to cause significant drift as they were susceptible to shifting with vibration. If using a half bridge of two strain gauges purchased in the same lot, their resistances should be adequately close to remove the need for a calibration potentiometer.

3. Calibration

The calibration proved to be a significant effort off the car, both for pre and post calibration. Designing a new method of calibration on the car, similar to what we did during the test day to account for drift, would probably be a better method. While our scale method works easily for vertical loads, and relatively easy for frontal loads (by pushing the car against a wall with the scales) something would have to be designed to calibrate side loads with a similar method. Another added benefit of this process is the fact that this will cancel out any errors in our static resolution of forces from the wheels to the links.

REFERENCES

"Accelerometers." Accelerometers. Omega, n.d. Web. 01 May 2014.

<<http://www.omega.com/prodinfo/accelerometers.html>>.

"Bonded Foil Strain Gages." Strain Gages. Omega, n.d. Web. 30 Apr. 2014.

<<http://www.omega.com/prodinfo/StrainGages.html>>.

"DMD-465." *Omega Engineering*. Omega Engineering. Web. 27 May 2014.

<<http://www.omega.com/pptst/DMD-465.html>>.

Fabijanac, John. "5-22-2014 Get Loaded Project Update." Cal Poly-Building 192, San Luis Obispo. 22 May 2014. Lecture.

"FBG Optical Sensing: A New Alternative for Challenging Strain Measurements." *National Instruments - White Papers*. National Instruments. Web. 2 June 2014.

<<http://www.ni.com/white-paper/12338/en/>>.

Hoffmann, Karl. "Applying the Wheatstone Bridge Circuit." *Applying the Wheatstone Bridge Circuit*.

HBM. HBM. Web. 20 May 2014. <<http://www.hbm.com.pl/pdf/w1569.pdf>>.

"How Is Temperature Affecting Your Strain Measurement Accuracy?" *National Instruments - White Papers* (2011). - National Instruments. 11 June 2011. Web. 03 June 2014.

<<http://www.ni.com/white-paper/3432/en/>>.

Karki, James. "Signal Conditioning Wheatstone Resistive Bridge Sensors." *The Galpin Society Journal* 45 (1999): 123-30. *Texas Instruments*. Texas Instruments, Sept. 1999. Web. 20 May 2014.

<<http://www.ti.com/lit/an/sloa034/sloa034.pdf>>.

Kleckers, Thomas. "Fatigue Life of Strain Gauges." N.p., n.d. Web. 1 May 2014.

<<http://www.ae.metu.edu.tr/seminar/strain-gage/Day1/fatigue.pdf>>.

"Measuring Strain with Strain Gages." *National Instruments*. National Instruments, 09 Apr. 2014.

Web. 03 June 2014. <<http://www.ni.com/white-paper/3642/en/>>.

Nouwens, OMM. "Modeling, Fabrication, Calibration, and Testing of a six-axis Wheel Force Transducer"

n. d. Web 30 Apr. 2014.

<<http://web.up.ac.za/sitefiles/file/44/1026/2163/noticeboard/Oscar%20complete.pdf>>.

"PCB Series 5400 Multi-Axis Wheel Force Transducer." *PCB*. PCB. Web. 02 June 2014.

<http://www.pcb.com/auto/MultiAxis_Wheel_Force_Transducer.aspx>.

"Positioning Strain Gages." *POSITIONING STRAIN GAGES TO MONITOR BENDING, AXIAL, SHEAR, AND TORSIONAL LOADS*. Omega. Omega Engineering. Web. 1 May 2014.

<<http://www.omega.com/faq/pressure/pdf/positioning.pdf>>.

"Rod-End Compression and Tension Load Cell-Series RDE905." Sensors by Stellar

Technology. Stellar Technology, n.d. Web. 01 May 2014.

<<http://www.stellartech.com/sensors/2013/01/rod-end-compression-and-tension-load-cell-series-rde905/>>

"The Strain Gage." *Omega*. Omega. Web. 15 May 2014.

<<http://www.omega.com/literature/transactions/volume3/strain.html>>.

"Strain Gage Rosettes: Selection, Application and Data Reduction." *Micro-Measurements*. Vishay

Precision Group. Vishay Precision Group. Web. 2 June 2014.

<<http://www.vishaypg.com/docs/11065/tn-515.pdf>>.

"Strain Gauges or Piezoelectric Sensors? A Comparison." *HBM*. HBM. Web. 02 June 2014.

<<http://www.hbm.com/en/menu/tips-tricks/force-measurement/strain-gauges-or-piezoelectric-sensors-a-comparison/>>.

"Temperature Compensation for Strain Gauges: Theory and Practical Implementation." *HBM*. HBM.

Web. 03 June 2014.

<<http://www.hbm.com/en/menu/tips-tricks/experimental-stress-analysis/temperature-compensation-for-strain-gauges/>>.

"Understanding Twisted Pair Cable Technology." *GEN17-1* (n.d.): n. pag. *Vellone*. Minicom

Advanced Systems, 25 June 2005. Web. 21 Aug. 2014.

APPENDIX A:
GOAL DEVELOPMENT

Team: Get Loaded		Engineering Requirements																Benchmarks								
		Weighting (Total 100)																Current Load Estimates	Pretoria College							
Customer Requirements	RESULTS	Suspension	Chassis	Invention	Sketching	Front Susp. / Skew	Front	Sub	Vertical	Rear Susp.	Front	Sub	Vertical	Rear	Chassis	Front	Sub	Rear	Loading / on Shock	Top	Skid Plate	Invention	Current Load Estimates	Pretoria College		
	Repeatability of data collection	4	2	3	3												Δ	Δ	Δ		Δ			0	2	
	Presentation of data	10	11	10	10																			0	2	
	Bench Tests (how much you want it)	10	5	10	10	Δ	Δ	Δ		Δ	Δ	Δ	Δ									■	■	0	1	
	USE OF DATA																									
	Design for reliability (prescribed sf)	10	10	10	10	■	■	■		■	■	■	■		■	■	■	■	■	■	■	■	■	■	0	
	Minimizing weight (prescribed sf)	10	10	10	10	"	"	"		"	"	"	"		"	"	"	"	"	"	"	"	"	"	0	
	Stress Analysis (Sample Calcs?)	10	10	10	10	■	■	■		■	■	■	■		■	■	■	■	■	■	■	■	■	■	0	
	Deflection Analysis	4	2	3	4	"	"	Δ		"	"	Δ											Δ	0	1	
	Bench Tests (how useful?)	10	4	4	4		Δ																■	Δ	0	2
	TYPES OF LOADING																									
	Impact	10	8	9	10	■	■	■		■	■	■	■		■	■	■	■	■	■	■	■	■	■	0	3
	Fatigue	10	5	7	7	Δ				Δ													"	"	0	2
	Sustained loads	10	5	5	5			"			"		"						"		"	"	"	"	0	0
	Cyclic (analyze frequency of each)	10	9	9	9	■	"	■		■	"	■								Δ		Δ	Δ	0	2	
	FAILURE MODES																									
	Point of failure (where load tends to fail)	10	10	7	8	Δ	Δ	Δ		Δ	Δ	Δ											Δ	1	0	
	Mode of failure (fatigue vs impact, tens)	10	5	8	10	"	"	"		"	"	"	"		"	"	"	"	"	"	"	"	"	"	1	0
	Appropriate Life	8	7	7	8	Δ	Δ	Δ		Δ	Δ	Δ											Δ	1	0	
	Current Load Estimates						1	1	1		1	1	1	1		1	1	1	0	0	1	1	1			
Pretoria College										2	2	2											2			

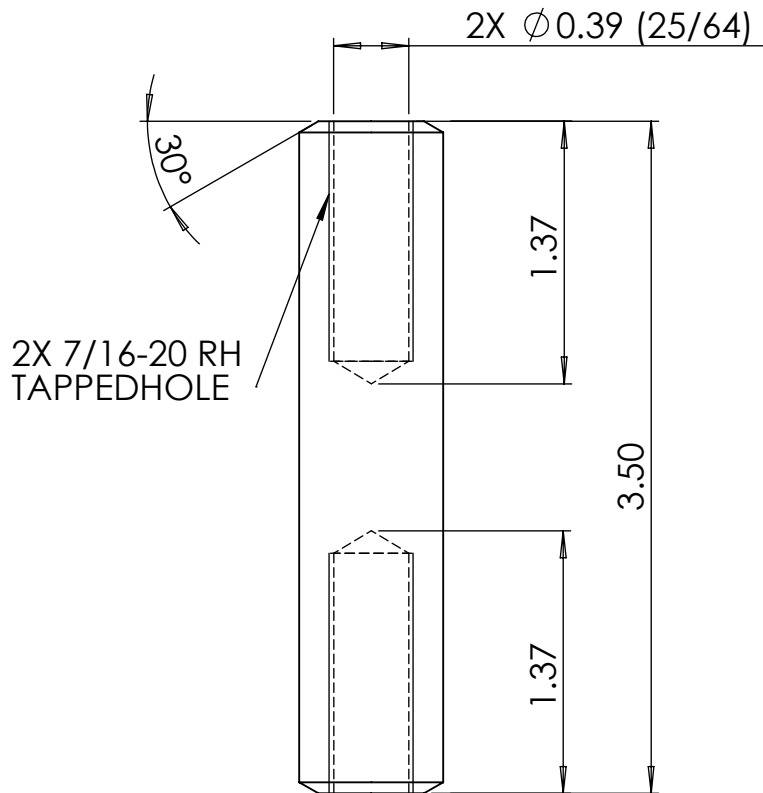
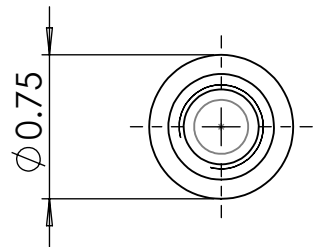
- = 9 Strong Correlation
- = 3 Medium Correlation
- △ = 1 Small Correlation
- Blank = No Correlation

Goal Requirements Decision Matrix

Failure Mode and Effect Analysis Table

1	2	A		B		C		D		E		F		G		H		I
		System	Item	Failure Mode	Failure Effect	Target	Severity	Probability	Risk	Action Required / Remarks								
3	Front Suspension	Upright	Spindle failure	Suspension collapse	E	Critical	Mostly Remote	6	Replace upright, re-do strain gauge setup									
4	Front Suspension	Tie Rod	Buckling failure	Reduction of control	E	Marginal	Remote	6	Replace tie rod									
5	Rear Suspension	Rocker	Bearing failure	Data inaccurate	M	Marginal	Remote	6	Replace bearing									
6	Rear Suspension	Toe Link	Buckling failure	Reduction of control	E	Marginal	Remote	6	Replace toe link, re-do strain gauge setup									
7	Rear Suspension	Rocker	Link buckling failure	Rocker moves until it hits sc	E	Marginal	Remote	6	Replace link / re-do strain gauge setup									
8	Rear Suspension	Rocker	Shock mount to rocker breaks	Suspension collapse	E	Marginal	Remote	6	Rebuild rocker better									
9	Chassis	Frame	Buckling failure on rollover	Driver seriously injured	F	Catastrophic	Extremely Remo	4	Go to the hospital, give up on senior project, or make a new car									
10	Measurement device	Strain Gauges	Bad Adhesion	Data inaccurate or no data	M	Negligible	Reasonably Prof	4	Replace strain gauge									
11	Measurement device	Strain Gauges	Inaccuracy of placement	Data inaccurate	M	Negligible	Reasonably Prof	4	Replace strain gauge or adjust calculations									
12	Measurement device	Strain Gauges	Temperature compensation gauge is str	Data inaccurate	M	Negligible	Reasonably Prof	4	Relocate strain gauge									
13	Measurement device	Amplifiers	Connection break due to vibration	Data stop	M	Negligible	Reasonably Prof	4	Dampen vibrations / improve wiring									
14	Measurement device	Wiring	Wires caught or stretched due to moving	Data inaccurate or no data	M	Negligible	Reasonably Prof	4	Replace and route wire better									
15	Rear Suspension	Rocker	Deformation of frame	Data inaccurate	M	Negligible	Reasonably Prof	4	Reinforce frame									
16	Measurement device	Strain Gauges	Plastic Deformation of strain gauge	Data inaccurate	M	Negligible	Remote	3	Replace strain gauge									
17	Measurement device	Wiring	Short due to moisture	Data inaccurate	M	Negligible	Remote	3	Paper towels / electrical tape									
18	Measurement device	Wiring	Temperature affecting resistance of wiri	Data inaccurate	M	Negligible	Remote	3	Compensate or isolate wiring									
19	Measurement device	Wiring	Wire gauge affects resistance of wiring	Data inaccurate	M	Negligible	Remote	3	Design wiring right									
20	Measurement device	Wiring	Wire connections break	Data stop	M	Negligible	Remote	3	Make the connections better									
21	Measurement device	DAQ	Short the fuse on the battery input	Data stop and possible corr	M	Negligible	Remote	3	Replace fuse / check for short on input wires									
22	Measurement device	Strain Gauges	Exceed Gauge strain limit	Data stop	M	Negligible	Extremely Remo	1	Replace strain gauge									

APPENDIX B:
DRAWING PACKET



PROCESS:

1. CUT TO LENGTH +.125" ON BAND SAW
2. FACE TO LENGTH BOTH SIDES
3. CENTER DRILL BOTH SIDES
4. DRILL 25/64" TO DESIGNATED DEPTH. STEP UP DRILL SIZES
5. TAP HOLE FULL DEPTH IN THE SAME SETUP AS DRILL (DON'T UNCLAMP FROM LATHE)

	NAME	DATE
DRAWN		
CHECKED		
UNLESS OTHERWISE SPECIFIED:		

DIMENSIONS ARE IN INCHES
 TOLERANCES:
 FRACTIONAL: ± 1/32
 ANGULAR: MACH ± 1° BEND ± 1°
 TWO PLACE DECIMAL: ± 0.05
 THREE PLACE DECIMAL: ± 0.005
 TOLERANCING PER: MMC

TITLE:

Rocker Link

REV

A

SCALE: 1:1

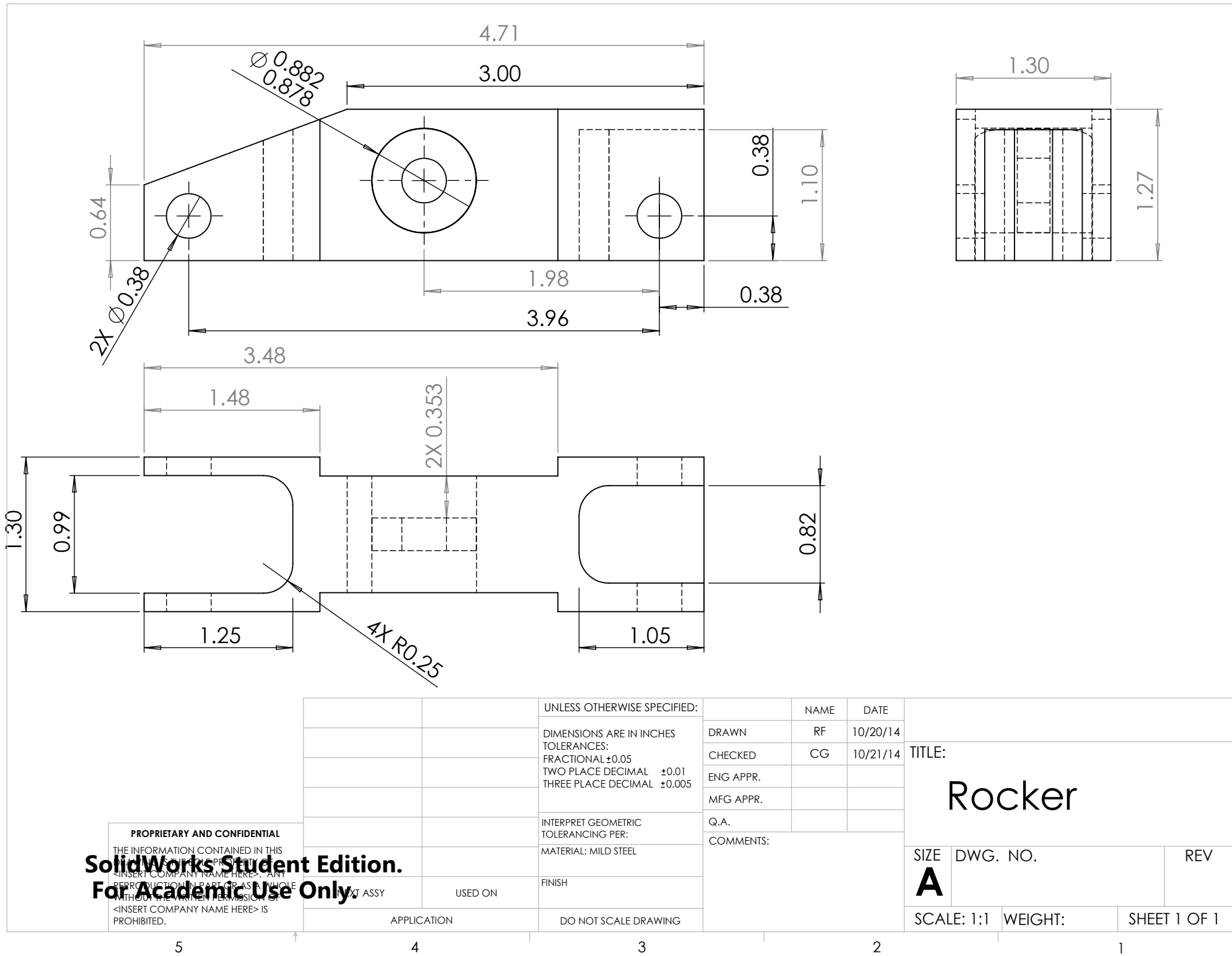
WEIGHT: 0.11 LB

1 OF 1

SolidWorks Student Edition.
For Academic Use Only.

THE INFORMATION CONTAINED IN THIS DRAWING IS THE SOLE PROPERTY OF CAL POLY BAJA. IT IS TO BE USED ONLY IN PART OR AS A WHOLE WITHOUT THE WRITTEN PERMISSION OF CAL POLY BAJA IS PROHIBITED.

PROJECT	ROCKER	LOADS SP	MATERIAL 7075 AL
PROJ NO	NEXT ASSY	SUB-SYSTEM	FINISH STOCK/MACHINE
APPLICATION		DO NOT SCALE DRAWING	

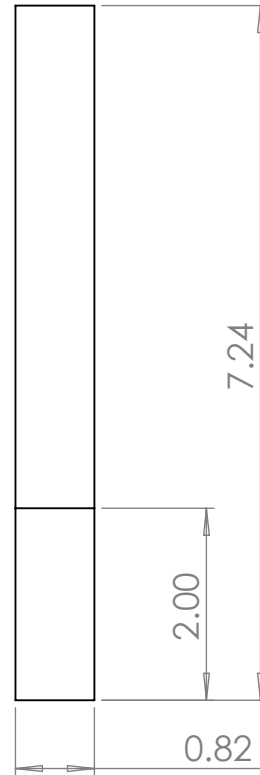
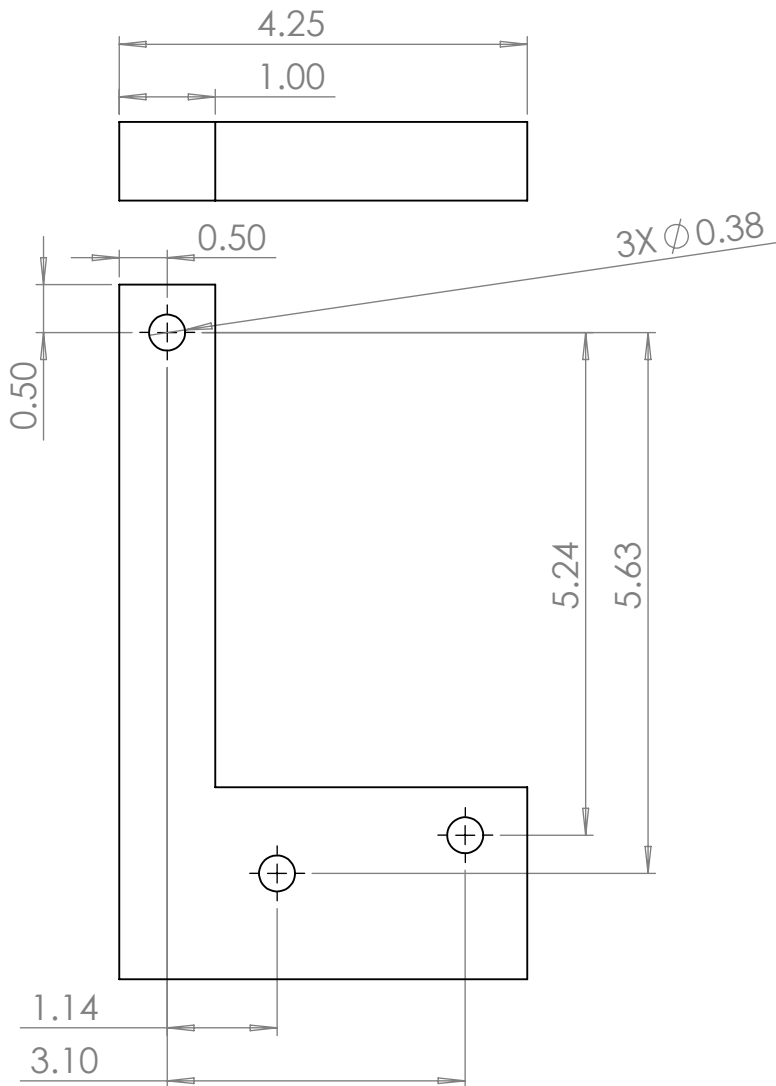


PROPRIETARY AND CONFIDENTIAL
 THE INFORMATION CONTAINED IN THIS DRAWING IS THE PROPERTY OF <INSERT COMPANY NAME HERE>. ANY REPRODUCTION IN PART OR AS A WHOLE WITHOUT THE WRITTEN PERMISSION OF <INSERT COMPANY NAME HERE> IS PROHIBITED.

SolidWorks Student Edition.
For Academic Use Only.

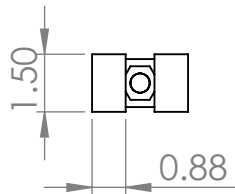
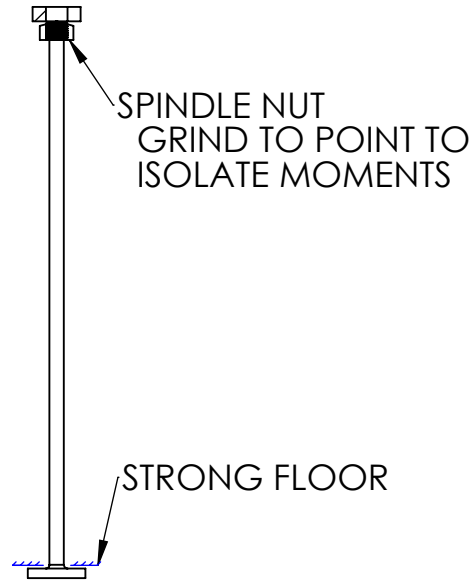
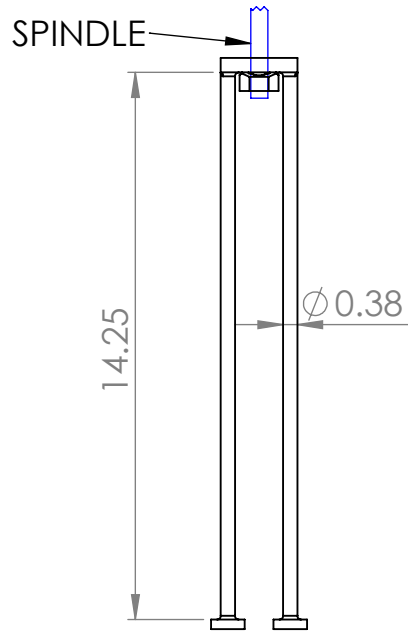
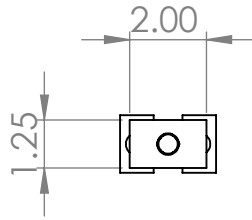
		UNLESS OTHERWISE SPECIFIED:	NAME	DATE
		DIMENSIONS ARE IN INCHES	DRAWN	RF
		TOLERANCES:	CHECKED	CG
		FRACTIONAL ± 0.05	ENG APPR.	
		TWO PLACE DECIMAL ± 0.01	MFG APPR.	
		THREE PLACE DECIMAL ± 0.005	Q.A.	
		INTERPRET GEOMETRIC TOLERANCING PER:	COMMENTS:	
		MATERIAL: MILD STEEL		
		FINISH		

TITLE: Rocker		
SIZE A	DWG. NO.	REV
SCALE: 1:1	WEIGHT:	SHEET 1 OF 1



PROPRIETARY AND CONFIDENTIAL THE INFORMATION CONTAINED IN THIS DRAWING IS THE SOLE PROPERTY OF <INSERT COMPANY NAME HERE>. ANY REPRODUCTION IN PART OR AS A WHOLE WITHOUT THE WRITTEN PERMISSION OF <INSERT COMPANY NAME HERE> IS PROHIBITED.				UNLESS OTHERWISE SPECIFIED:		NAME	DATE	TITLE:	
				DIMENSIONS ARE IN INCHES TOLERANCES: FRACTIONAL ± ANGULAR: MACH ± BEND ± TWO PLACE DECIMAL ± THREE PLACE DECIMAL ±	DRAWN	RF	10/22/14		
				INTERPRET GEOMETRIC TOLERANCING PER:	CHECKED	CG	10/22/14	SIZE DWG. NO. REV ARear Tab Jig	
				MATERIAL 6061	ENG APPR.				
				FINISH	MFG APPR.			SCALE: 1:2 WEIGHT: SHEET 1 OF 1	
				USED ON NEXT ASSY	Q.A.				
		APPLICATION		DO NOT SCALE DRAWING	COMMENTS:				

SolidWorks Student Edition.
For Academic Use Only.



**SolidWorks Student Edition.
For Academic Use Only.**

MATERIAL	STEEL
FINISH	

	NAME	DATE
DRAWN		
MADE		
UNLESS OTHERWISE SPECIFIED:		
DIMENSIONS ARE IN INCHES		
TOLERANCES		
FRACTIONAL:	±1/16	
ANGULAR:	±1°	
TWO PLACE DECIMAL:	±.015	
THREE PLACE DECIMAL:	±.005	
TOLERANCING PER:	MMC	

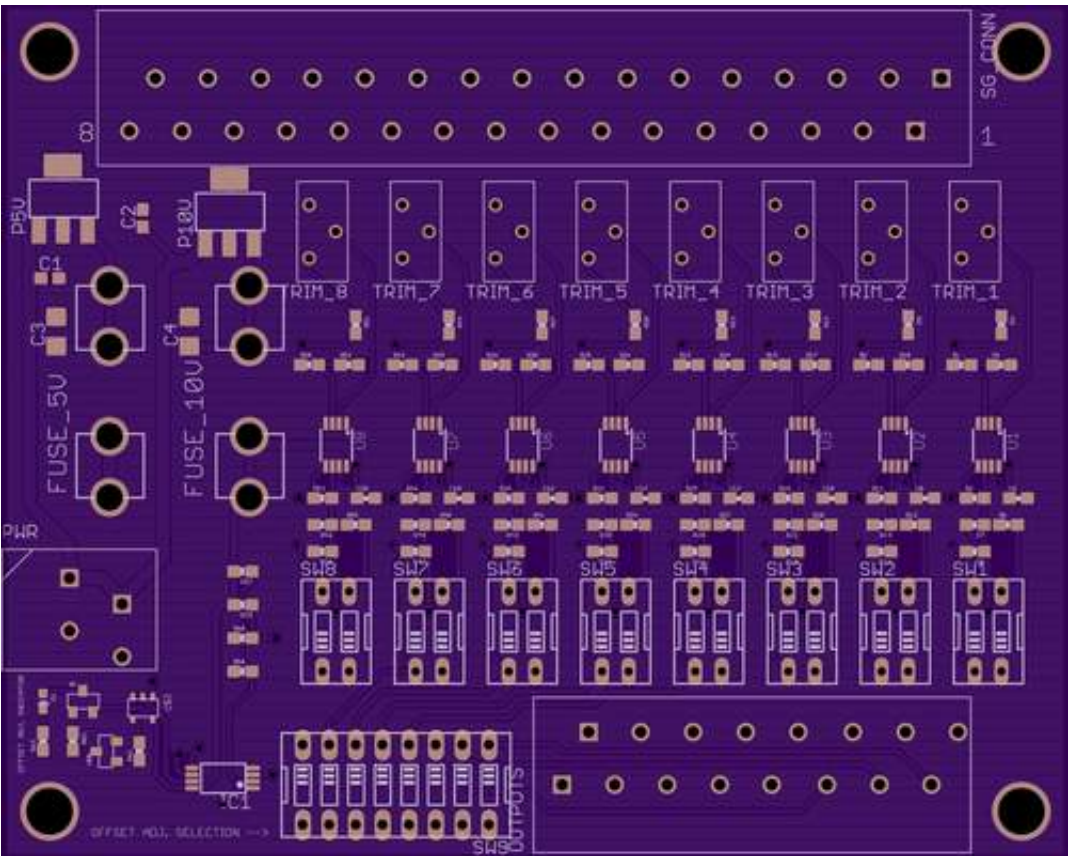
TITLE: SPINDLE CALIBRTION JIG		REV A
SCALE: 1:1	WEIGHT: N/A	1 OF 1

-  Thomas Willson.
- [Home](#) [Shared Projects](#) [Design Rules](#) [Pricing & Specs](#) [Support](#) [Projects](#) [Profile](#) [Log out](#)



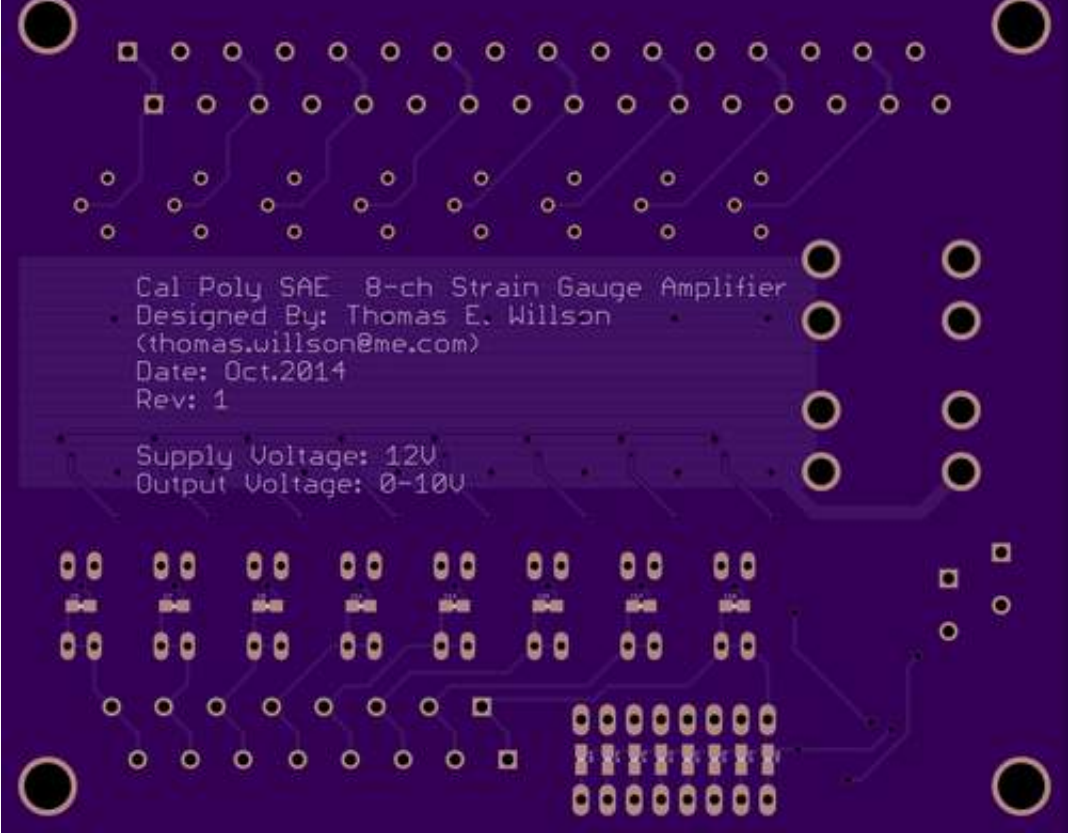
OSH Park

PCB Order - Verify your design



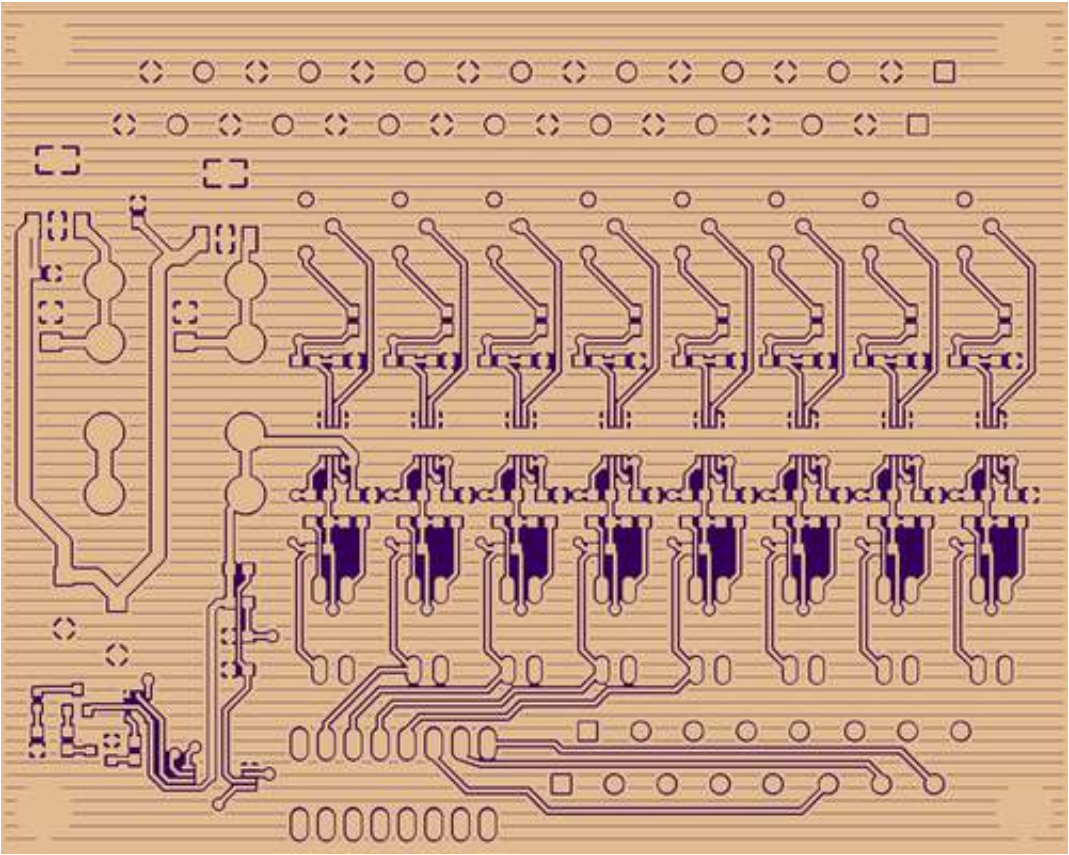
Board Top

This is a render of what we think your board will look like after fabrication as viewed from the top.



Board Bottom

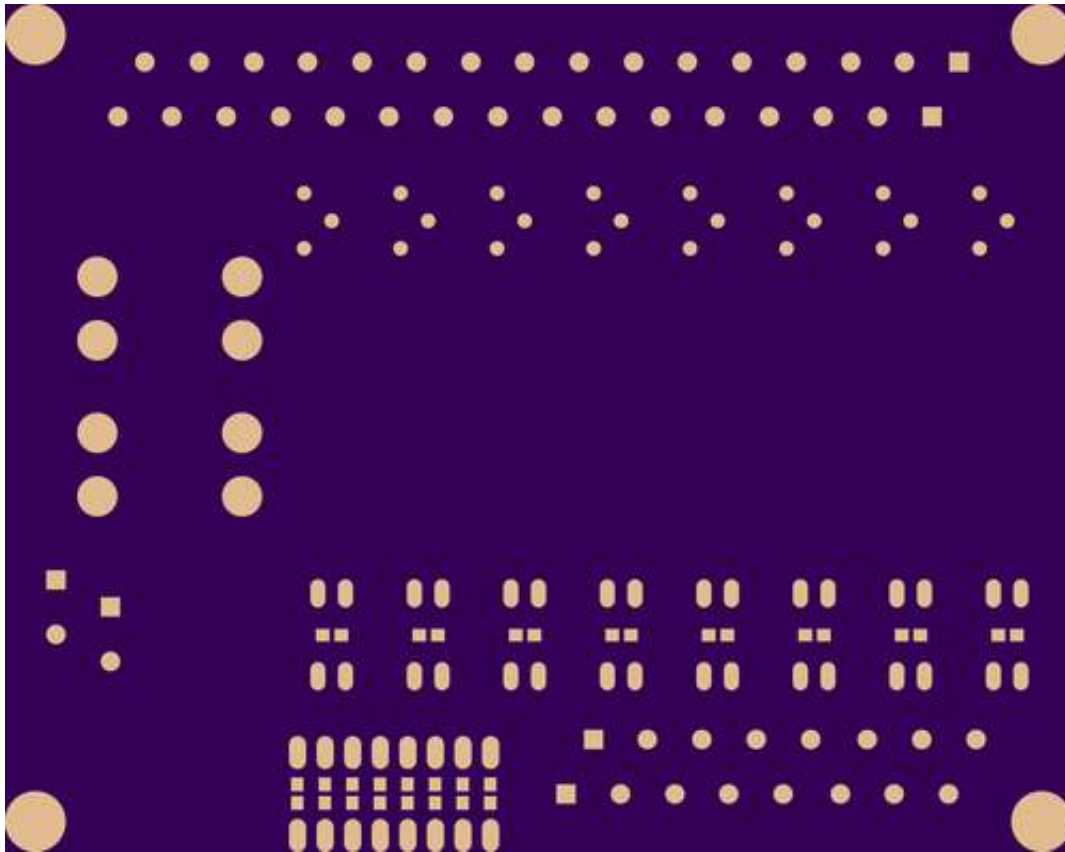
This is a render of what we think your board will look like after fabrication as viewed from the bottom.



Rendered from "Strain_20Gauge_20Amplifier.brd"

Top Layer

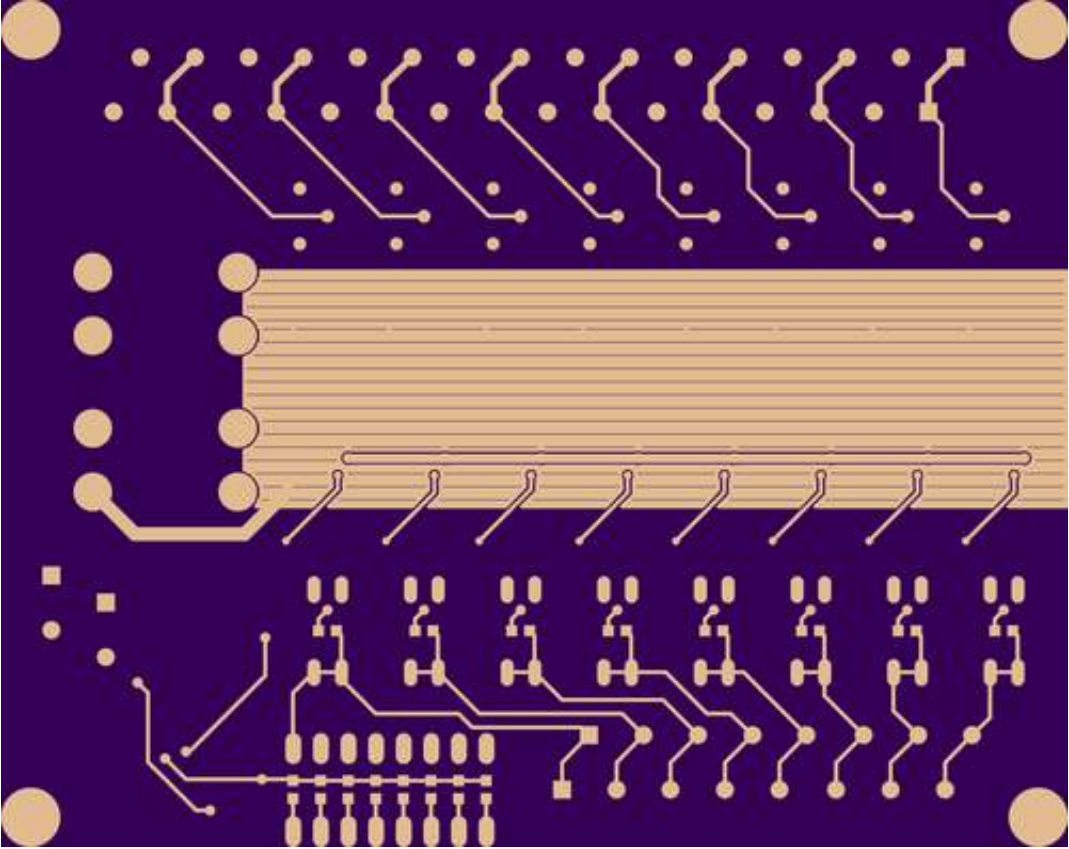
- This is the top layer of copper on your PCB.



Rendered from "Strain_20Gauge_20Amplifier.brd"

Bottom Solder Mask

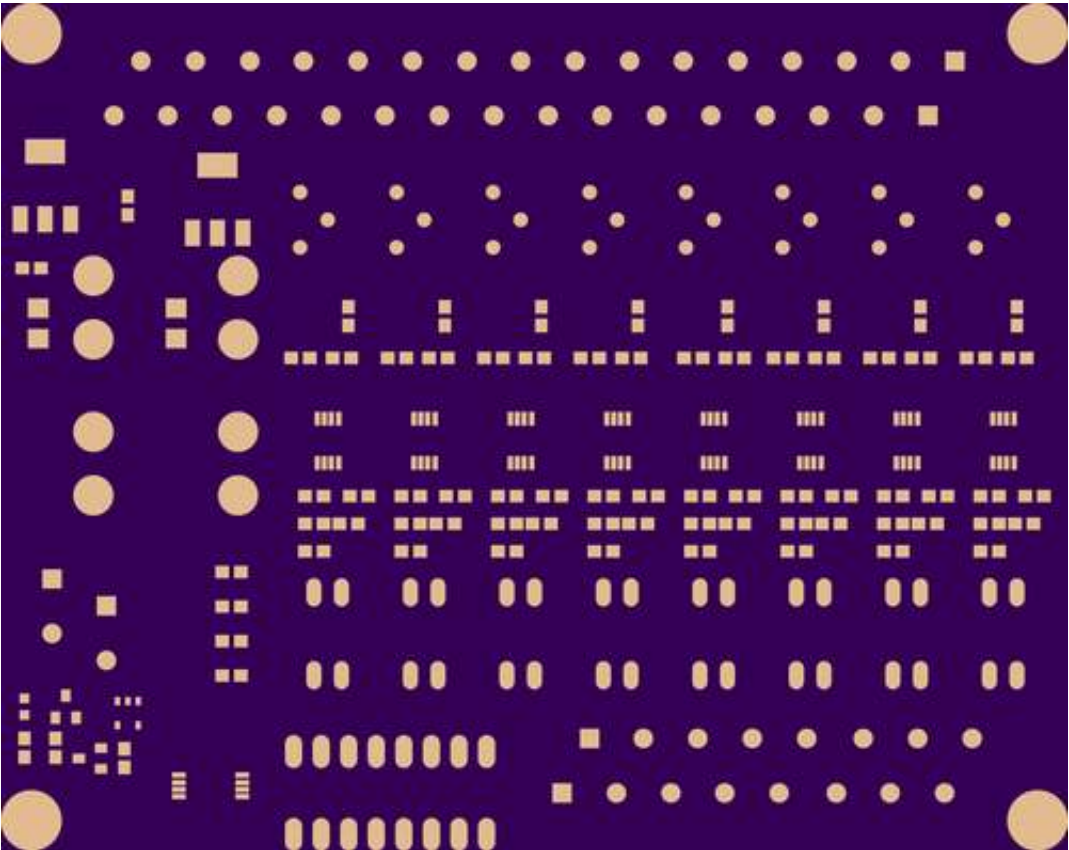
- Soldermask layers are "negative" layers. This layer really designates where there *shouldn't* be solder mask. If you draw on the soldermask layer ("tStop" and "bStop" in Eagle), those areas won't have soldermask.
- If you don't provide a soldermask layer here, this entire side of the board will be coated in soldermask. You probably don't want this.



Rendered from "Strain_20Gauge_20Amplifier.brd"

Bottom Layer

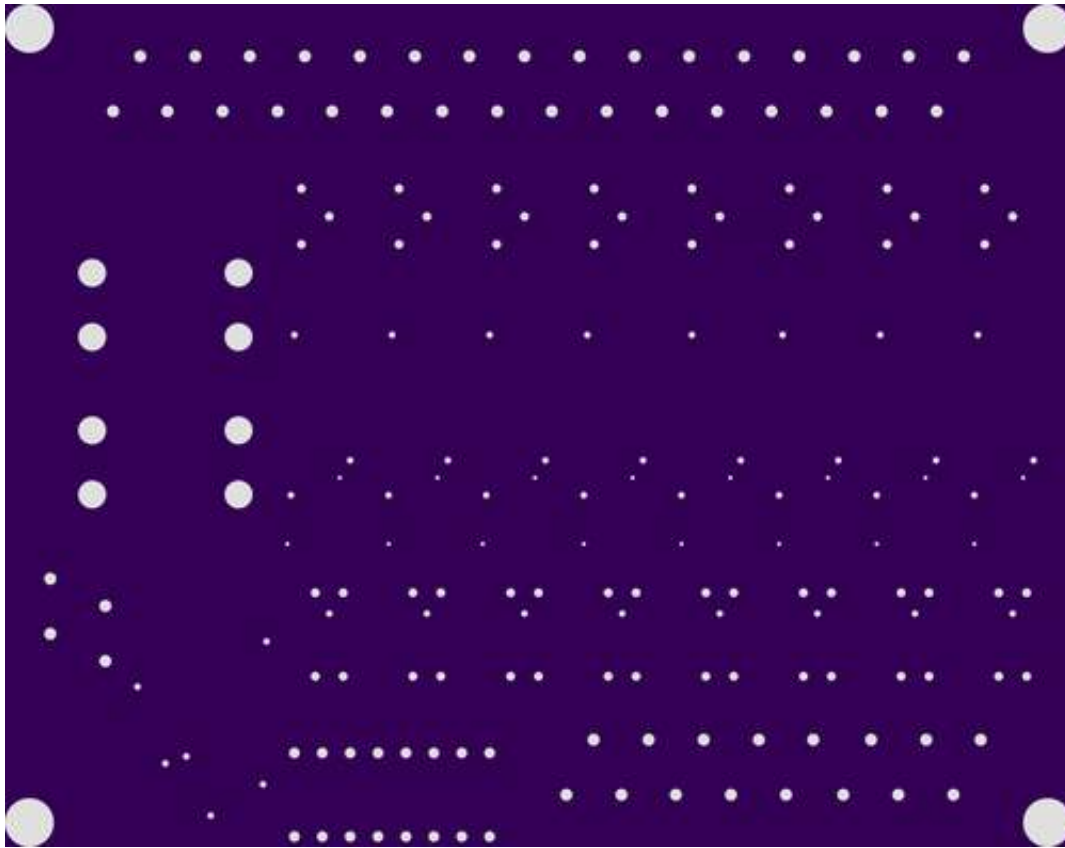
- This is the bottom copper layer of your board.



Rendered from "Strain_20Gauge_20Amplifier.brd"

Top Solder Mask

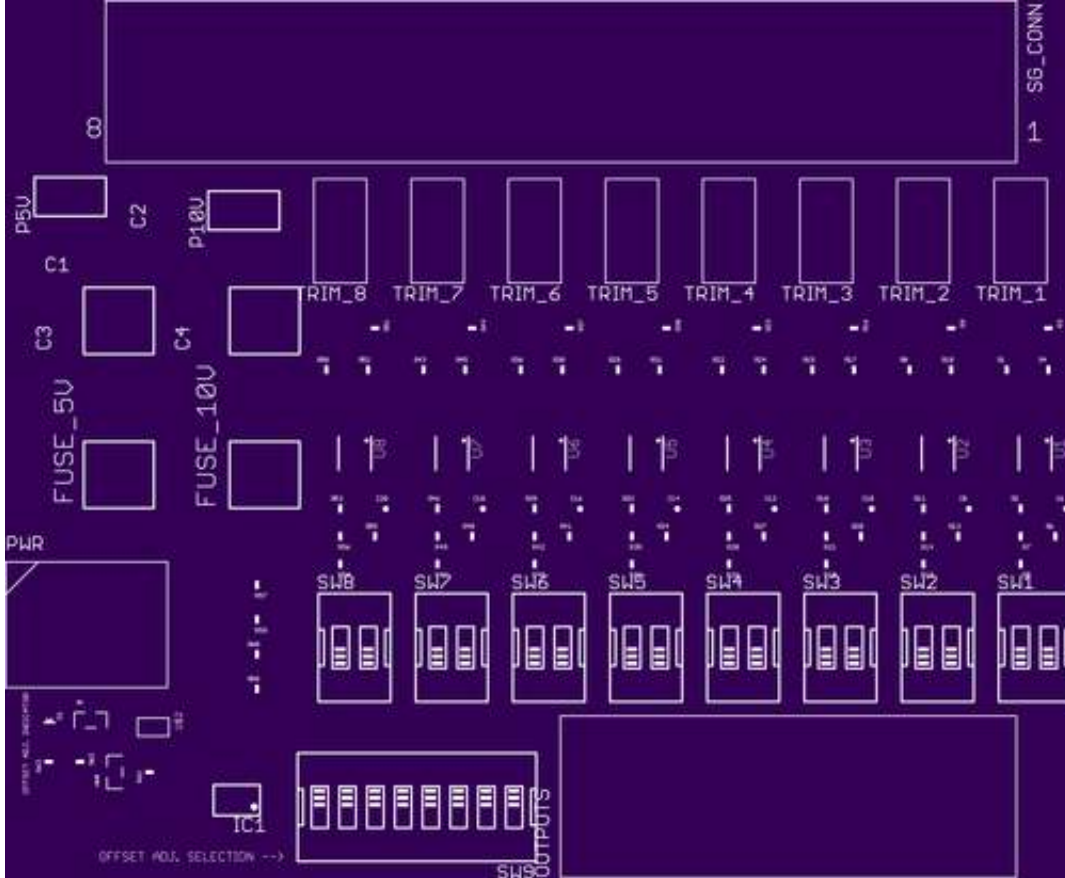
- Soldermask layers are "negative" layers. This layer really designates where there *shouldn't* be solder mask. If you draw on the soldermask layer ("tStop" and "bStop" in Eagle), those areas won't have soldermask.
- If you don't provide a soldermask layer here, this entire side of the board will be coated in soldermask. You probably don't want this.



Rendered from "Strain_20Gauge_20Amplifier.brd"

Drills

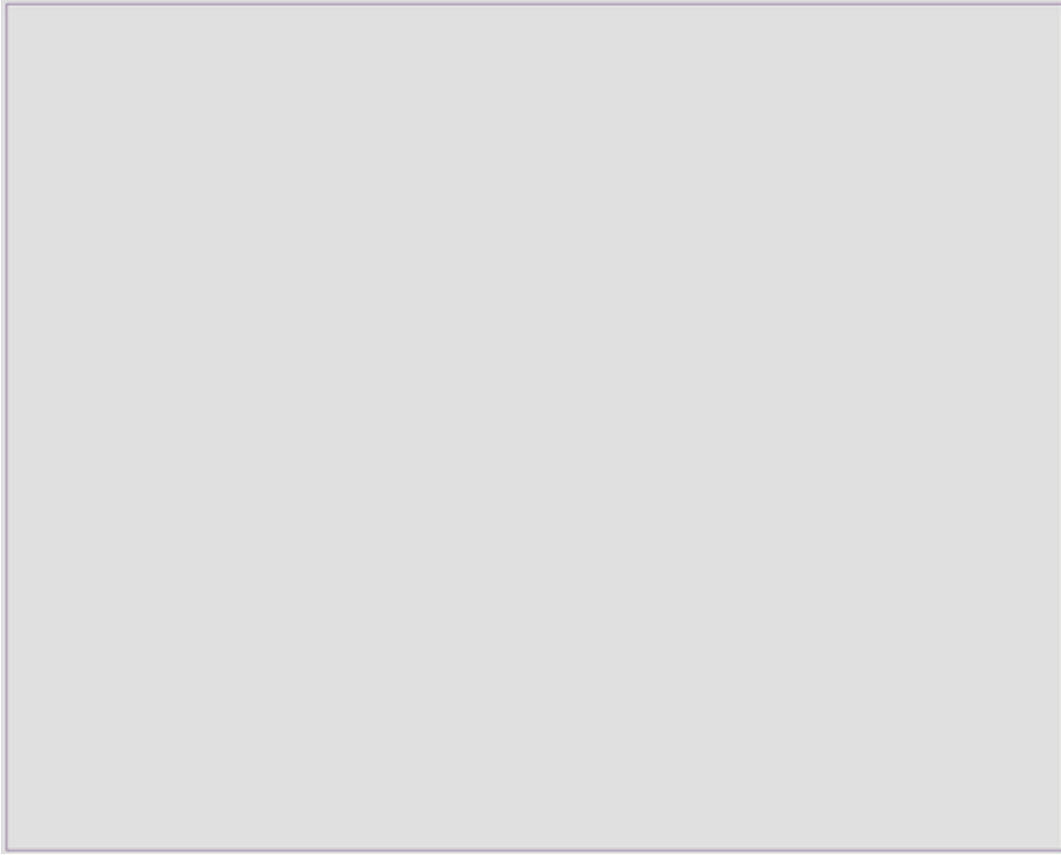
- Your drill file needs to be in text "NC Drills" or "Excellon" format, generated with "2:4" precision, and with "no zero suppression".
- Make sure the center of your drill hits are all inside the board outline. Anything outside of the board outline is automatically removed.
- Overlapping drill hits aren't allowed.
- Minimum drill size is 13 mils. Maximum is 360 mils.
- Plated slots aren't supported.



Rendered from "Strain_20Gauge_20Amplifier.brd"

Top Silk Screen

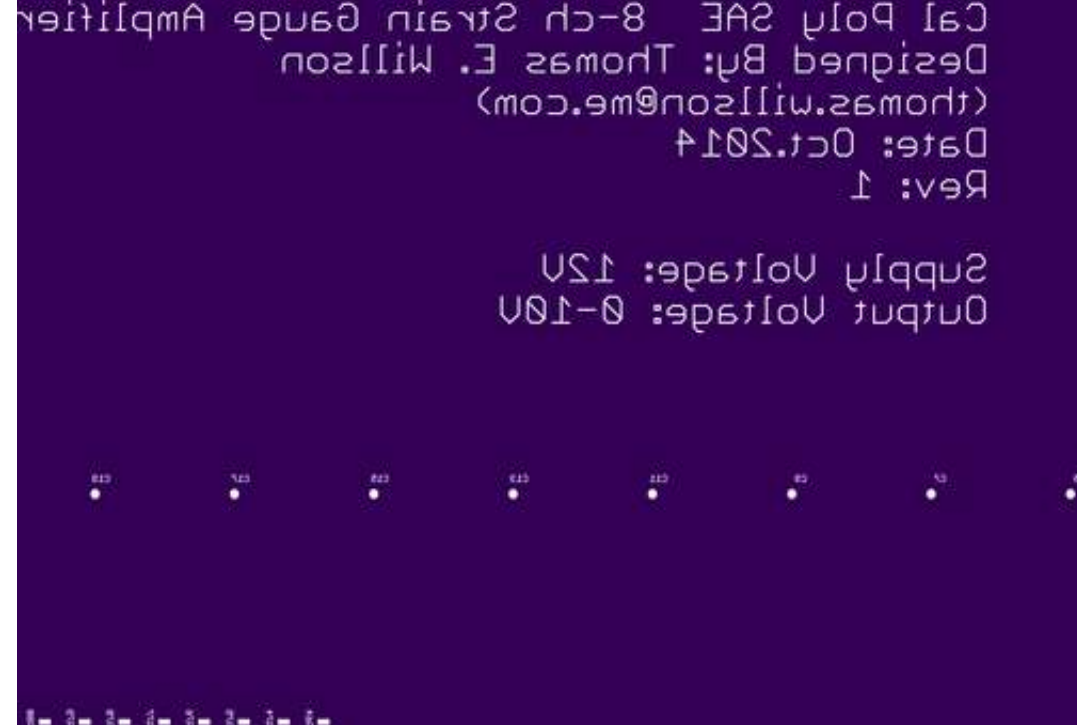
- The silkscreen is put on with what is basically a 200 dpi printer. Lines thinner than 5 mils will be fattened to 5 mils before printing.
- Try to keep your silkscreen inside the board outline. It's okay if it goes out of the board outline, but it will be trimmed with sometimes unpredictable results.
- The fab will automatically remove any silkscreen that crosses drilled holes or exposed metal.



Rendered from "Strain_20Gauge_20Amplifier.brd"

Board Outline

- The board outline needs to go all the way around the edge of the board such that it's "water tight" (no gaps).
- Non-rectangular board shapes are allowed, but you'll be billed for the smallest rectangle that would enclose your design. So a circle two inches in diameter would be billed at 4 square inches.
- Cutouts aren't officially supported, but the fab has been doing them pretty regularly as long as they're drawn on the board outline layer, and are at least 100 mils wide.
- To try making a cutout, draw the outline of the cutout on the board outline layer, or draw the path you'd like the milling tool to make using a 0.1" wide line. Cutouts won't be plated.



Rendered from "Strain_20Gauge_20Amplifier.brd"

Bottom Silk Screen

- The silkscreen is put on with what is basically a 200 dpi printer. Lines thinner than 5 mils will be fattened to 5 mils before printing.
- Try to keep your silkscreen inside the board outline. It's okay if it goes out of the board outline, but it will be trimmed with sometimes unpredictable results.
- The fab will automatically remove any silkscreen that crosses drilled holes or exposed metal.

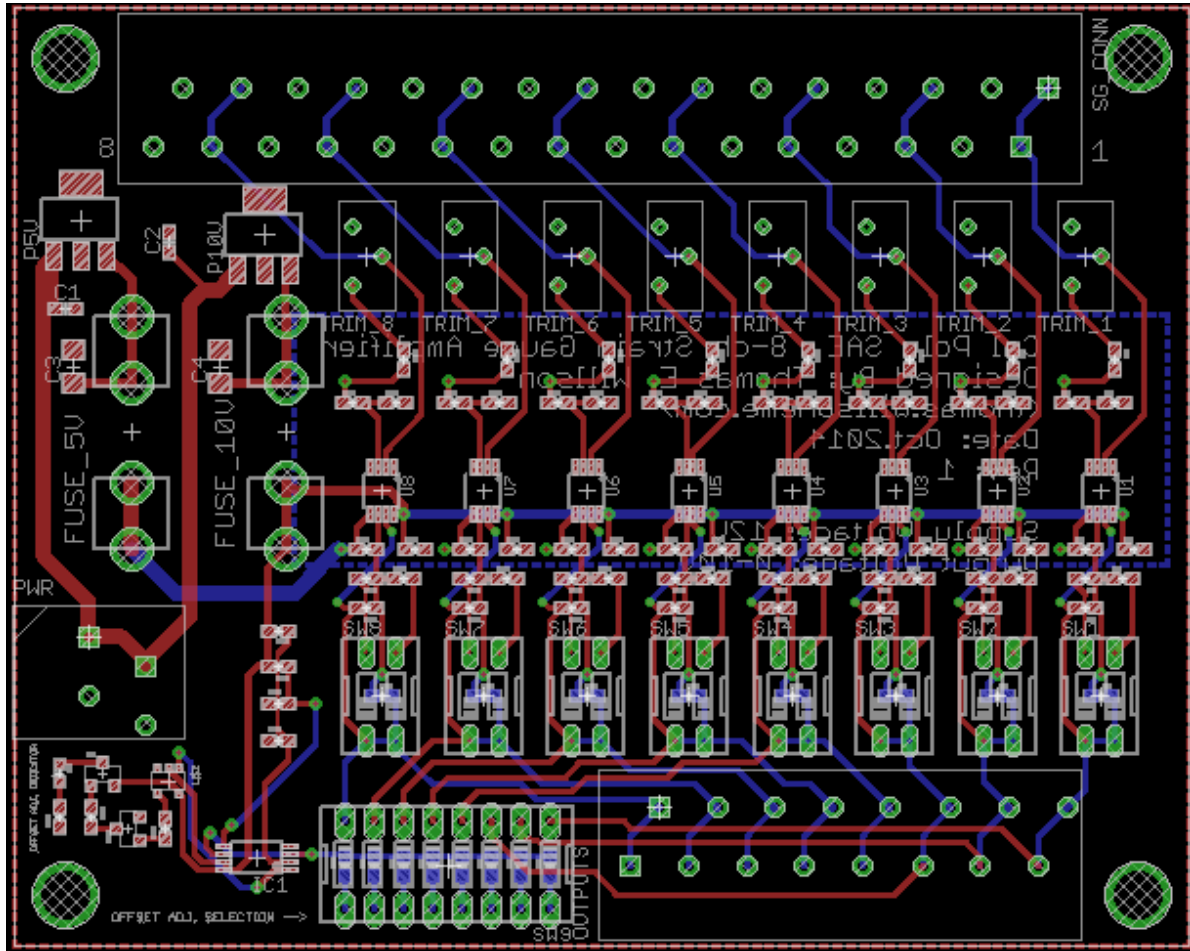
Start Over ↺

Approve →

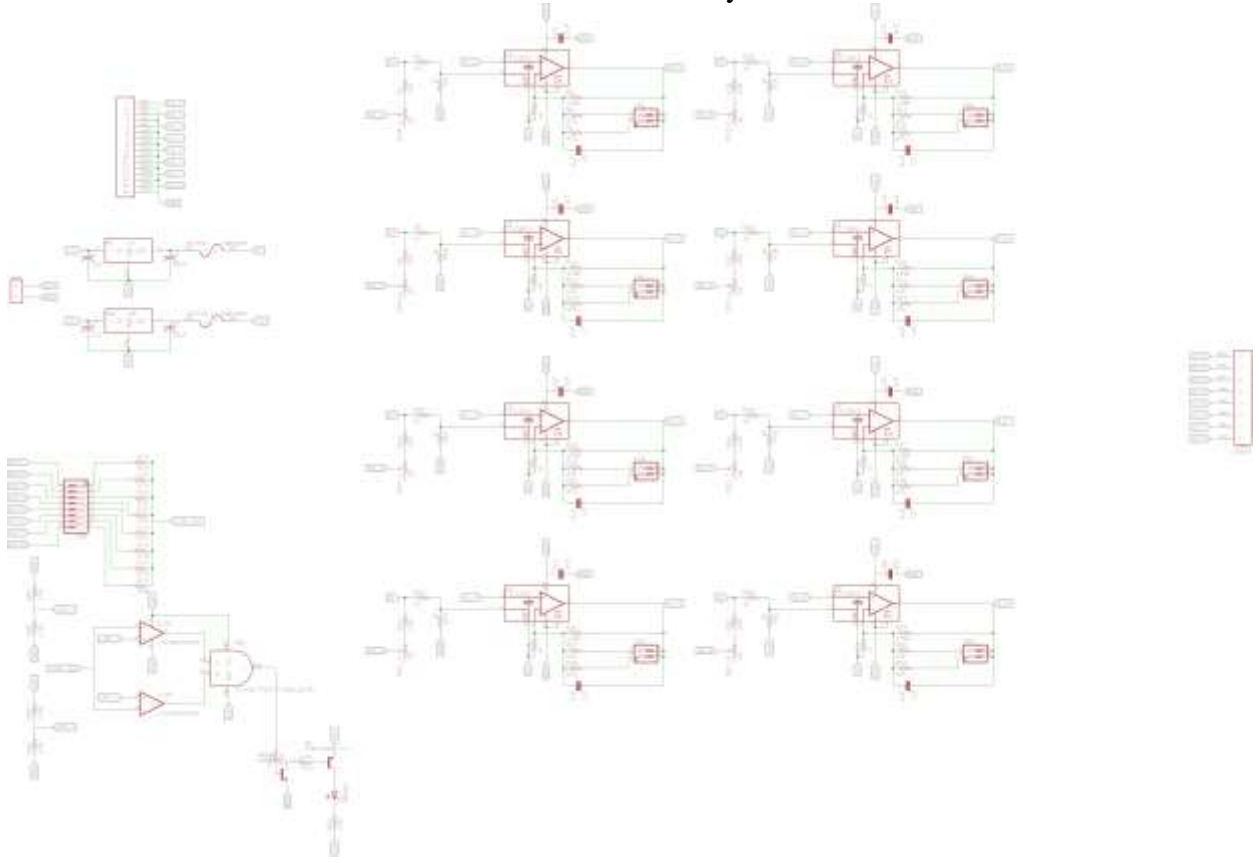
Approve and Order →

Designed and developed by [Resistor](#).

EAGLE Board Schematic



Schematic Board Layouts



APPENDIX C:
PURCHASING INFORMATION

Digi-Key Part Number	Manufacturer	Quantity	Price	Extended Price	Description
GH7212-ND	GRAYHILL INC	1	1.17	1.17	SW DIP RECESSED SEALED 8POS 30V
P430HCT-ND	PANASONIC ELECTRONIC COMPONENTS (VA)	1	0.1	0.1	RES 430 OHM 1/10W 1% 0603 SMD
GH7200-ND	GRAYHILL INC	8	1.14	9.12	SW DIP RECESSED SEALED 2POS 30V
3296Y-200LF-ND	BOURNS INC	8	2.41	19.28	TRIMMER 20 OHM 0.5W PC PIN
TC4S81FT5LFTCT-ND	TOSHIBA SEMICONDUCTOR AND STORAGE (VA)	1	0.57	0.57	IC GATE AND 1CH 2-INP SMV
541-1.60KHCT-ND	VISHAY DALE (VA)	2	0.081	0.162	RES 1.60K OHM 1/10W 1% 0603 SMD
445-5666-1-ND	TDK CORPORATION (VA)	2	0.1	0.2	CAP CER 0.1UF 50V 10% X7R 0603
LM2937IMP-10/NOPBCT-ND	TEXAS INSTRUMENTS (VA)	1	1.85	1.85	IC REG LDO 10V 0.4A SOT223
445-12902-1-ND	TDK CORPORATION (VA)	2	0.45	0.9	CAP CER 10UF 16V 10% X7R 1206
541-1.80KHCT-ND	VISHAY DALE (VA)	2	0.081	0.162	RES 1.80K OHM 1/10W 1% 0603 SMD
MCT0603-1.0K-MDCT-ND	VISHAY BEYSCHLAG (VA)	24	0.178	4.272	RES 1.0K OHM 0.15W 0.5% 0603
445-5666-1-ND	TDK CORPORATION (VA)	16	0.073	1.168	CAP CER 0.1UF 50V 10% X7R 0603
RHM110KCFCT-ND	ROHM SEMICONDUCTOR (PASSIVE) (VA)	8	0.1	0.8	RES 110K OHM 1/10W 1% 0603 SMD
A104568-ND	TE CONNECTIVITY AMP	1	14.43	14.43	CONN 5MM TERMINAL BLOCK 16POS
A104554-ND	TE CONNECTIVITY AMP	1	2.93	2.93	CONN 5MM TERMINAL BLOCK 2POS
A104560-ND	TE CONNECTIVITY AMP	1	8.3	8.3	CONN 5MM TERMINAL BLOCK 8POS
P340HCT-ND	PANASONIC ELECTRONIC COMPONENTS (VA)	8	0.1	0.8	RES 340 OHM 1/10W 1% 0603 SMD
LTC2053CMS8#PBF-ND	LINEAR TECHNOLOGY	8	6.41	51.28	IC OPAMP CHOPPER 200KHZ 8MSOP
P4.70KHCT-ND	PANASONIC ELECTRONIC COMPONENTS (VA)	10	0.1	1	RES 4.7K OHM 1/10W 1% 0603 SMD
LM2937IMPX-5.0/NOPBCT-ND	TEXAS INSTRUMENTS (VA)	1	1.85	1.85	IC REG LDO 5V 0.4A SOT223
F4189-ND	LITTELFUSE INC	2	0.12	0.24	FUSE CLIP CARTRIDGE 250V 10A PCB
P82.0KHCT-ND	PANASONIC ELECTRONIC COMPONENTS (VA)	8	0.1	0.8	RES 82K OHM 1/10W 1% 0603 SMD
MMBT4403-FDICT-ND	DIODES INCORPORATED (VA)	1	0.14	0.14	TRANS PNP 40V 350MW SMD SOT23-3
160-1446-1-ND	LITE-ON INC (VA)	1	0.3	0.3	LED GREEN CLEAR THIN 0603 SMD
296-16806-1-ND	TEXAS INSTRUMENTS (VA)	1	0.42	0.42	IC DUAL DIFF COMPARATOR 8VSSOP
MMBT4401-FDICT-ND	DIODES INCORPORATED (VA)	1	0.14	0.14	TRANS NPN 350MW 40V SMD SOT23-3
P62.0KHCT-ND	PANASONIC ELECTRONIC COMPONENTS (VA)	8	0.1	0.8	RES 62K OHM 1/10W 1% 0603 SMD
Cable Gland	Polycase	2	1.8	3.6	
Enclosure	Polycase	1	14.39	14.39	Not the best but gives idea of pricing
Custom PCB	OshPark	1	21.33	21.33	Minimum of 3
Unit Price				162.504	

Vendors	Phone	Email	Website	Contact Name	Extension #
Omega Engineering	1-888-826-6342	info@omega.com	http://www.omega.com/	Jeff Karwon	2282
DigiKey	1-800-344-4539	webmaster@digikey.com	http://www.digikey.com/	N/A	N/A
OshPark	N/A	N/A	https://oshpark.com/	N/A	N/A

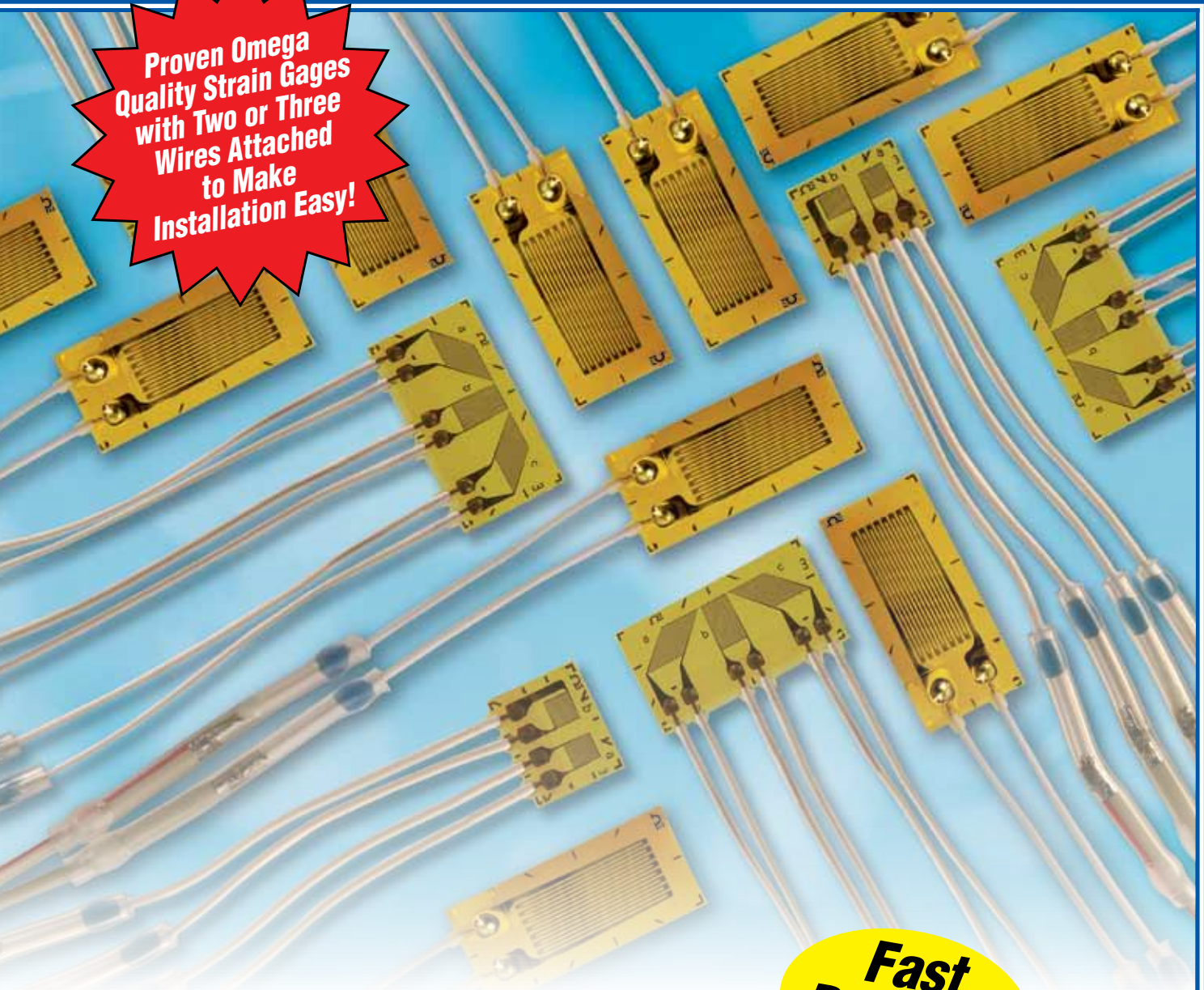
APPENDIX D:
MANUFACTURING SPECIFICATIONS
AND DATA SHEETS

OMEGA® KFH SERIES PRE-WIRED STRAIN GAGES

IN STOCK!
For Fast Delivery
Visit omega.com/kfh

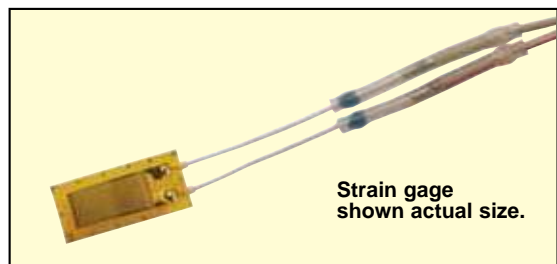


Proven Omega
Quality Strain Gages
with Two or Three
Wires Attached
to Make
Installation Easy!



- ✓ No Soldering at the Measuring Point
- ✓ Each Gage has 50 mm of PTFE Cable before Transitioning to AWG 28 Leads to Prevent Leads from Adhering During Installation
- ✓ Short, Medium and Long Grid Linear Gages
- ✓ Short and Medium Grid XY Gages (T-Rosettes)
- ✓ Short and Medium Grid 0°/45°/90° Planar Rosettes
- ✓ Rugged Polyimide Carrier
- ✓ Fully Encapsulated Gages for Protection from the Environment

**Fast
Delivery!**



Strain gage
shown actual size.

STRAIN GAGES 



PRE-WIRED STRAIN GAGES

PRECISION LINEAR PATTERN

KFH Series

2- or 3-Wire Models

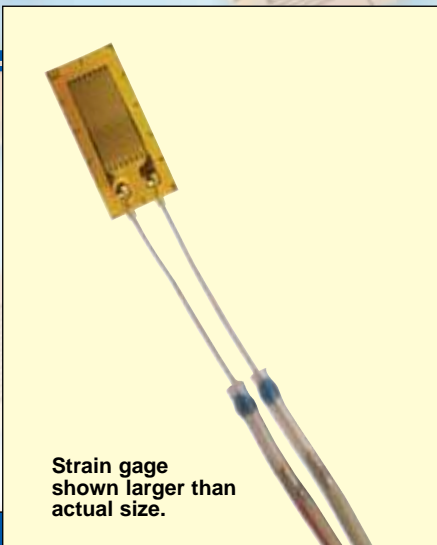
120 or 350 Ω

0.6 to 20 mm Grid Lengths

- ✓ Pre-Wired for Fast Installation
- ✓ No Soldering at Measurement End
- ✓ Broad Temperature Range
- ✓ 2- or 3-Wire Models
- ✓ Clear Alignment Marks

- ✓ Bonds with Hot or Cold Cure Adhesives
- ✓ PTFE Wire at Attachment End Prevents Sticking During Installation

Linear pattern precision gages with miniature and medium length grids are for general purpose and stress analysis applications. Available with either two 1-meter leads or three 3-meter leads and 120 or 350 Ω resistance. All models are compensated for steel.



To Order Visit omega.com/kfh for Pricing and Details

GAGE PATTERN Leads not shown	MODEL NO. Pkg of 10	NOM. RESISTANCE (Ω)	DIMENSIONS mm (inch)				MAX V* (Vrms)	TEMP COMP	TERMINATION AND LEAD LENGTH
			GRID		CARRIER				
			A	B	C	D			
<p>Shown larger than actual size, 0.3 mm</p>	0.3 mm GRID								
	KFH-03-120-C1-11L1M2R	120	0.3 (0.012)	1.96 (0.077)	4.5 (0.18)	3.9 (0.15)	1.5	ST	Two 1 m leads
	KFH-03-120-C1-11L3M2R	120					1.5	ST	Three 3 m leads
<p>Shown larger than actual size, 0.6 mm</p>	0.6 mm GRID								
	KFH-06-120-C1-11L1M2R	120	0.6 (0.024)	1.1 (0.043)	4.8 (0.19)	3.9 (0.15)	1.5	ST	Two 1 m leads
	KFH-06-120-C1-11L3M3R	120					1.5	ST	Three 3 m leads
<p>Shown larger than actual size, 1.5 mm</p>	1.5 mm GRID								
	KFH-1.5-120-C1-11L1M2R	120	1.5 (0.059)	1.5 (0.059)	5.8 (0.23)	3.9 (0.15)	2.5	ST	Two 1 m leads
	KFH-1.5-120-C1-11L3M3R	120					2.5	ST	Three 3 m leads
<p>Shown actual size, 3 mm</p>	3 mm GRID								
	KFH-3-120-C1-11L1M2R	120	3.0 (0.118)	2.0 (0.079)	7.4 (0.29)	3.9 (0.15)	4	ST	Two 1 m leads
	KFH-3-120-C1-11L3M3R	120					4	ST	Three 3 m leads
	KFH-3-350-C1-11L1M2R	350					9	ST	Two 1 m leads
	KFH-3-350-C1-11L3M3R	350					9	ST	Three 3 m leads
<p>Shown actual size, 6 mm</p>	6 mm GRID								
	KFH-6-120-C1-11L1M2R	120	6.0 (0.24)	2.0 (0.079)	10.5 (0.41)	3.9 (0.15)	8	ST	Two 1 m leads
	KFH-6-120-C1-11L3M3S	120					8	ST	Three 3 m leads
	KFH-6-350-C1-11L1M2R	350					15	ST	Two 1 m leads
	KFH-6-350-C1-11L3M3R	350					15	ST	Three 3 m leads
<p>Shown actual size, 10 mm</p>	10 mm GRID								
	KFH-10-120-C1-11L1M2R	120	10 (0.39)	3.0 (0.12)	14.8 (0.58)	4.8 (0.19)	14	ST	Two 1 m leads
	KFH-10-120-C1-11L3M3R	120					14	ST	Three 3 m leads
<p>Shown actual size, 20 mm</p>	20 mm GRID								
	KFH-20-120-C1-11L1M2R	120	20 (0.79)	3.0 (0.12)	25.2 (0.99)	4.8 (0.19)	7	ST	Two 1 m leads
	KFH-20-120-C1-11L3M3R	120					7	ST	Three 3 m leads

ACCESSORIES

MODEL NO.	DESCRIPTION
TT300	Complete heat cure adhesive kit
SG496	1 oz methyl-based cyanoacrylate (approximately 750 gages)
SG401	0.1 oz ethyl-based cyanoacrylate (approximately 50 gages)

* Maximum permitted bridge energizing voltage (Vrms)

Ordering Examples: **KFH-1.5-120-C1-11L1M2S**, a linear 1.5 mm grid, 120 Ω, with two 1 m leads.

KFH-3-350-C1-11L3M3S, a linear 3 mm grid, 350 Ω, with three 3 m leads per grid.

PRE-WIRED STRAIN GAGES

PRECISION PLANAR X-Y PATTERN



KFH Series

2- or 3-Wire Models

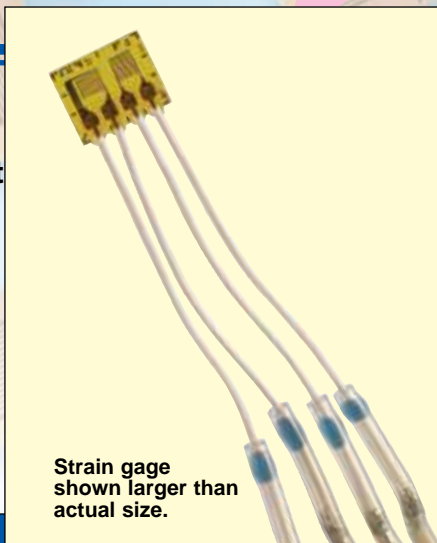
120 or 350 Ω

0.6 to 6 mm Grid Lengths

- ✓ Pre-Wired for Fast Installation
- ✓ No Soldering at Measurement End
- ✓ Broad Temperature Range
- ✓ 2- or 3-Wire Models
- ✓ Clear Alignment Marks


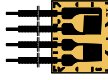

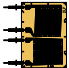
- ✓ Bonds with Hot or Cold Cure Adhesives
- ✓ PTFE Wire at Attachment End Prevents Sticking During Installation

The planar XY pattern allows precision strain measurement by eliminating the errors often associated with a stacked XY pattern. These gages are available with either two 1-meter leads or three 3-meter leads per grid and are compensated for steel.



Strain gage shown larger than actual size.

To Order Visit omega.com/kfh for Pricing and Details

GAGE PATTERN Leads not shown	MODEL NO. Pkg of 10	NOM. RESISTANCE (Ω)	DIMENSIONS mm (inch)				MAX V* (VRMS)	TEMP COMP	TERMINATION AND LEAD LENGTH PER GRID
			GRID		CARRIER				
			A	B	C	D			
 Shown larger than actual size, 0.6 mm	0.6 mm GRID								
	KFH-06-120-D16-11L1M2S	120	0.6	1.0	5.1	6.9	1.5	ST	Two 1 m leads
	KFH-06-120-D16-11L3M3S	120	(0.024)	(0.039)	(0.20)	(0.27)	1.5	ST	Three 3 m leads
 Shown larger than actual size, 1.5 mm	1.5 mm GRID								
	KFH-1.5-120-D16-11L1M2S	120	1.5	1.6	5.8	6.9	3	ST	Two 1 m leads
	KFH-1.5-120-D16-11L3M3S	120	(0.059)	(0.063)	(0.23)	(0.27)	3	ST	Three 3 m leads
Shown actual size, 3 mm 	3 mm GRID								
	KFH-3-120-D16-11L1M2S	120	3.0	3.2	7.5	9.4	5.5	ST	Two 1 m leads
	KFH-3-120-D16-11L3M3S	120					5.5	ST	Three 3 m leads
	KFH-3-350-D16-11L1M2S	350	(0.12)	(0.13)	(0.30)	(0.37)	10	ST	Two 1 m leads
	KFH-3-350-D16-11L3M3S	350					10	ST	Three 3 m leads
Shown actual size, 6 mm 	6 mm GRID								
	KFH-6-120-D16-11L1M2S	120	6.0	6.3	11	16	11	ST	Two 1 m leads
	KFH-6-120-D16-11L3M3S	120					11	ST	Three 3 m leads
	KFH-6-350-D16-11L1M2S	350	(0.24)	(0.25)	(0.43)	(0.63)	20	ST	Two 1 m leads
	KFH-6-350-D16-11L3M3S	350					20	ST	Three 3 m leads

ACCESSORIES

MODEL NO.	DESCRIPTION
TT300	Complete heat cure adhesive kit
SG496	1 oz methyl-based cyanoacrylate (approximately 750 gages)
SG401	0.1 oz ethyl-based cyanoacrylate (approximately 50 gages)

* Maximum permitted bridge energizing voltage (Vrms)

Ordering Examples: **KFH-1.5-120-D16-11L1M2S**, two 1.5 mm grids in a planar XY pattern, 120 Ω, with two 1 m leads per grid.
KFH-3-350-D16-11L3M3S, two 3 mm grids in a planar XY pattern, 350 Ω, with three 3 m leads per grid.



PRE-WIRED STRAIN GAGES

PLANAR 0°/45°/90° ROSETTE PATTERN

KFH Series

2- or 3-Wire Models

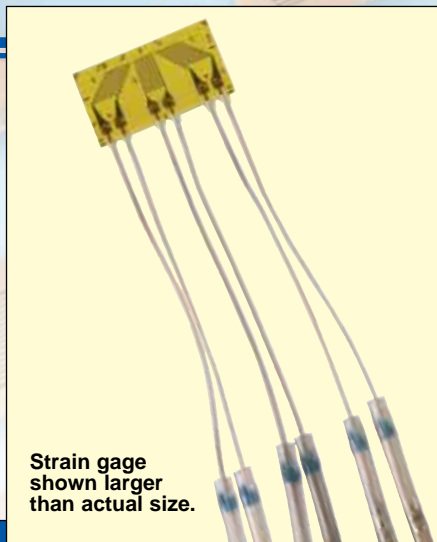
120 or 350 Ω

0.6 to 6 mm Grid Lengths

- ✓ Pre-Wired for Fast Installation
- ✓ No Soldering at Measurement End
- ✓ Broad Temperature Range
- ✓ 2- or 3-Wire Models
- ✓ Clear Alignment Marks

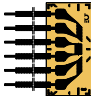
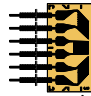

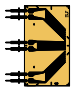
- ✓ Bonds with Hot or Cold Cure Adhesives
- ✓ PTFE Wire at Attachment End Prevents Sticking During Installation

The planar rosette pattern allows precision strain measurement by eliminating the errors often associated with a stacked pattern. These gages are available with either two 1-meter leads or three 3-meter leads per grid and are compensated for steel.



Strain gage shown larger than actual size.

To Order Visit omega.com/kfh for Pricing and Details

GAGE PATTERN Leads not shown	MODEL NO. Pkg of 10	NOM. RESIS- TANCE (Ω)	DIMENSIONS mm (inch)				MAX V* (VRMS)	TEMP COMP	TERMINATION AND LEAD LENGTH PER GRID
			GRID		CARRIER				
			A	B	C	D			
 Shown larger than actual size, 0.6 mm	0.6 mm GRID								
	KFH-06-120-D17-11L1M2S	120	0.6	1.1	4.8	9.9	1.6	ST	Two 1 m leads
	KFH-06-120-D17-11L3M3S	120	(0.024)	(0.043)	(0.19)	(0.39)	1.6	ST	Three 3 m leads
 Shown larger than actual size, 1.5 mm	1.5 mm GRID								
	KFH-1.5-120-D17-11L1M2S	120	1.5	1.5	5.8	10.2	2.5	ST	Two 1 m leads
	KFH-1.5-120-D17-11L3M3S	120	(0.059)	(0.059)	(0.23)	(0.40)	2.5	ST	Three 3 m leads
Shown actual size, 3 mm 	3 mm GRID								
	KFH-3-120-D17-11L1M2S	120	3.0	2.0	7.4	13.9	3	ST	Two 1 m leads
	KFH-3-120-D17-11L3M3S	120					3	ST	Three 3 m leads
	KFH-3-350-D17-11L1M2S	350					5.5	ST	Two 1 m leads
	KFH-3-350-D17-11L3M3S	350					5.5	ST	Three 3 m leads
Shown actual size, 6 mm 	6 mm GRID								
	KFH-6-120-D17-11L1M2S	120	6.0	2.0	10.5	18.7	7.5	ST	Two 1 m leads
	KFH-6-120-D17-11L3M3S	120					7.5	ST	Three 3 m leads
	KFH-6-350-D17-11L1M2S	350					13	ST	Two 1 m leads
	KFH-6-350-D17-11L3M3S	350					13	ST	Three 3 m leads

ACCESSORIES

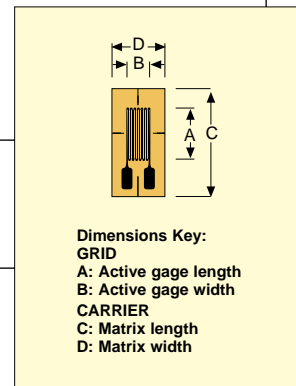
MODEL NO.	DESCRIPTION
TT300	Complete heat cure adhesive kit
SG496	1 oz methyl-based cyanoacrylate (approximately 750 gages)
SG401	0.1 oz ethyl-based cyanoacrylate (approximately 50 gages)

* Maximum permitted bridge energizing voltage (Vrms)

Ordering Examples: **KFH-1.5-120-D17-11L1M2S**, three 1.5 mm grids in a planar 0°/45°/90° pattern, 120 Ω, with two 1 m leads per grid.
KFH-3-350-D17-11L3M3S, three 3 mm grids in a planar 0°/45°/90° pattern, 350 Ω, with three 3 m leads per grid.

SPECIFICATIONS

Strain Gage Construction Measuring Grid Material Thickness Carrier Material Thickness Connections	 μm (microinch) μm (microinch)	Foil strain gage with embedded measuring grid Constantan 3.8 or 5 (150 or 197), depending upon strain gage type Polyimide 45 ± 10 (1.772 ± 394) PTFE wire, Ø - 0.051 mm ² , approximately 50 mm long, connected to AWG 28 ribbon cables (PVC insulated) through solder sleeves in 2- or 3-wire configurations
Nominal Resistance ¹ Resistance Tolerance ¹ with 0.6 mm and 1.5 mm grid length Gage Factor Gage Factor Tolerance with 0.6 mm and 1.5 mm grid length Temperature coefficient of gage factor Nominal value of gage factor temperature coefficient	 Ω % % % % 1/K [1/°F]	120 or 350 depending upon gage ±0.35 ±1 approximately 2 (stated on package) ±1 ±1.5 (115 ± 10) × 10 ⁻⁶ [(64 ± 5.5) × 10 ⁻⁶] Specified on each package
Reference Temperature Operating Temperature Range for static measurement (zero point related) for dynamic measurement (not zero point related)	 °C (°F) °C (°F) °C (°F)	23 PTFE cable -10 to 155 (-14 to 320) -10 to 155 (-14 to 320)
Transverse Sensitivity for linear 3 mm 120Ω gage	%	±0.2
Temperature Response Temperature response as required, adapted to coefficient of thermal expansion α for aluminum α for plastic material α for austenitic steel α for titanium α for molybdenum α for quartz Tolerance of temperature response	 1/K [1/°F] 1/K [1/°F] 1/K [1/°F] 1/K [1/°F] 1/K [1/°F] 1/K [1/°F] 1/K [1/°F] °C (°F)	Specified on each package 10.8 × 10 ⁻⁶ (6.0 × 10 ⁻⁶) 23 × 10 ⁻⁶ (12.8 × 10 ⁻⁶) 65 × 10 ⁻⁶ (36.1 × 10 ⁻⁶) 16 × 10 ⁻⁶ (8.9 × 10 ⁻⁶) 9 × 10 ⁻⁶ (5.0 × 10 ⁻⁶) 5.4 × 10 ⁻⁶ (3.0 × 10 ⁻⁶) 0.05 × 10 ⁻⁶ (0.3 × 10 ⁻⁶) -10 to 120 (-14 to 248)
Mechanical Hysteresis 1) at reference temperature and strain $\epsilon = 1000 \mu\text{m/m}$ (microstrain) on linear 3 mm 120Ω gage at 1 st load cycle and adhesive SG496 at 3 rd load cycle and adhesive SG496	 μm/m (microstrain) μm/m (microstrain)	 1 0.5
Maximum Elongation at reference temperature on linear 3 mm 120Ω gage Absolute strain value for positive direction Absolute strain value for negative direction	 μm/m (microstrain) μm/m (microstrain)	 20,000 ± 2% 25,000 ± 2.5%
Fatigue Life at reference temperature on linear 3 mm 120Ω gage Achievable Number of Load Cycles L_w at Alternating Strain $\epsilon_w = \pm 1000 \mu\text{m/m}$ and zero point variation ≤ 300 zero point variation ≤ 30	 μm/m (microstrain) μm/m (microstrain)	 >1 × 10 ⁷ (test was stopped) 5 × 10 ⁶
Minimum Radius of Curvature, Longitudinal and Transverse, at Reference Temperature within measuring grid area within solder tab area Applicable Bonding Materials Cold Cure Adhesives Heat Cure Adhesives	 mm (inch) mm (inch)	 0.3 (0.012) 10 (0.394) SG496, SG401 TT300





TT300
\$220

TT300, complete strain gage adhesive kit, \$220, shown smaller than actual size.



See Section Y for a Selection of Scientific, Technical, and Reference Books Available from omega.com

KIT INCLUDES

- ✓ Two 1 oz Resin Bottles (½ Filled)
- ✓ Two 1 oz Hardener Bottles (½ Filled)
- ✓ Two Plastic Funnels (35 mm Dia.)
- ✓ Two Brush Caps
- ✓ One 2 oz Bottle of Acetone
- ✓ One 2 oz Bottle of Acid Primer
- ✓ One 2 oz Bottle of Neutralizer
- ✓ One 2 oz Bottle of Resin Solvent
- ✓ Operator's Manual

OMEGA® TT300 cement is a heat-cured, 2-part epoxy adhesive that can be used to bond polyimide-backed strain gages for strain measurement up to 200°C (392°F). Each TT300 kit includes 2 bottles of resin and hardener that are pre-measured to ensure proper mixing proportions. To use, simply pour one bottle of hardener into one bottle of resin and shake for 1 minute.

A bottle each of hardener and resin produce approximately ¾ oz of adhesive. The shelf life of the resin-hardener mixture is 6 weeks at room temperature. The shelf life of the unmixed components is indefinite, provided that the bottles are kept tightly sealed. Each TT300 kit includes 2 oz of acetone, acid primer, neutralizer, and rosin solvent for cleaning and preparing the surface, as well as 2 funnels and 2 cap brushes.

SG496 and SG401 are general purpose cold-curing, 1-part glues. They are the most commonly used adhesives for strain gages. They cure in 1 minute, but require 24 hours to set. SG401 is an ethyl-based cyanoacrylate, and SG496 is a methyl-based cyanoacrylate. They have a 1-year shelf life at room temperature, but shelf life may be longer at colder temperatures. The glue temperature range is -54 to 82°C (-65 to 180°F).

Most Popular Models Highlighted!

To Order (Specify Model Number)

MODEL NO.	PRICE	DESCRIPTION
TT300	\$220	Complete strain gage adhesive kit
SG496	28	1 oz methyl-based cyanoacrylate (approx. 750 gages)
SG401	10	0.1 oz ethyl-based cyanoacrylate (approx. 50 gages)

Note: For strain gage accessories see pages E-56 to E-59.
Ordering Example: TT300, complete strain gage adhesive kit, \$220.



RESISTANCE WIRE FOR TEMPERATURE COMPENSATION AND ZERO BALANCE

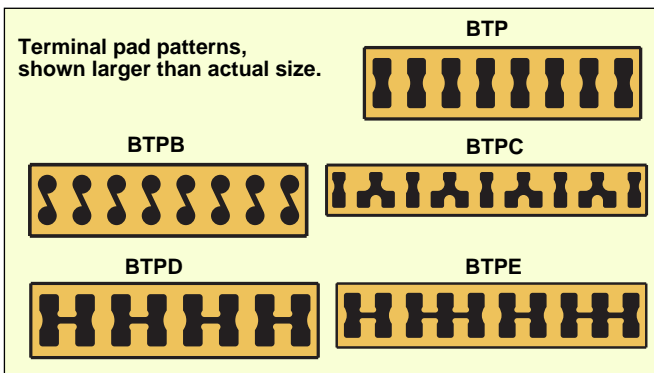
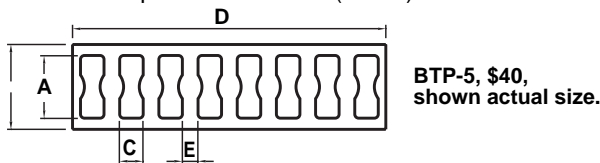
MOST POPULAR MODEL HIGHLIGHTED!

To Order (Specify Model Number)

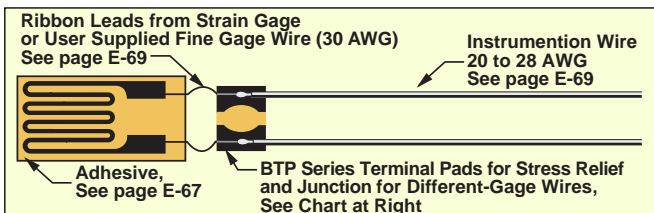
MODEL NO.	PRICE	FUNCTION	MATERIAL	Ω/FT	TEMP COEFF.	SPOOL LENGTH
SGB-36	\$70	Zero and span temp comp.	Balco	19.7	0.45%/°C	500'
SGC-36	20	Zero and span temp comp.	Copper	0.415	0.39%/°C	500'
SGM-36	26	Zero balance	Manganin	15.2	0.002%/°C	200'

BONDABLE TERMINAL PADS

Terminal pads serve 2 main purposes. First, they act as intermediate points for attaching ribbon leads of thin-gage wire to heavier instrumentation wires. Second, they give stress relief to strain gage systems. When the heavy instrumentation wire moves, the terminal pad protects the strain gage. Carrier is polyimide with a thickness of 0.075 mm (0.003"). Minimum bending radius is 2 mm (0.079"). Maximum temperature is 220°C (428°F).



TYPICAL STRAIN GAGE INSTALLATION



BRIDGE COMPLETION RESISTORS

Accuracy: 0.1%

Temperature Compensation: 5 ppm; -20 to 80°C (-4 to 176°F)

Power: ¼ W

MOST POPULAR MODELS HIGHLIGHTED!

To Order (Specify Model Number)

MODEL NO.	PRICE	Ω	MAX BRIDGE EXC.
RES-120	\$7.50	120	10 Vdc
RES-250	7.50	250	15 Vdc
RES-350	7.50	350	18 Vdc

Note: For strain gage accessories see pages E-56 to E-59.

Ordering Example: RES-350, 350 Ω bridge completion resistor, \$7.50.

BONDABLE TERMINAL PADS

To Order (Specify Model Number)

MODEL NO.	PRICE	STRIPS PER PACK	DIMENSIONS mm (in)				
			A	B	C	D	E
BTP-1	\$18.50	70	1.8 (0.07)	2.6 (0.1)	0.7 (0.03)	9.9 (0.39)	0.6 (0.02)
BTP-2	20.50	60	2.4 (0.09)	3.4 (0.13)	0.9 (0.04)	13.2 (0.52)	0.8 (0.03)
BTP-3	29.00	50	3.2 (0.13)	4.5 (0.18)	1.2 (0.05)	17.6 (0.69)	1 (0.04)
BTP-4	32.00	30	4.8 (0.19)	6.5 (0.26)	1.8 (0.07)	24 (0.94)	1.2 (0.05)
BTP-5	40.00	20	6 (0.24)	8.5 (0.33)	2.3 (0.09)	32.4 (1.28)	1.8 (0.07)
BTP-6	40.00	10	9 (0.35)	11.8 (0.46)	3.4 (0.13)	41.4 (1.63)	1.8 (0.07)
BTPB-1	18.50	70	1.8 (0.07)	2.6 (0.1)	0.7 (0.03)	9.9 (0.39)	0.6 (0.02)
BTPB-2	20.50	60	2.4 (0.09)	3.4 (0.13)	0.9 (0.04)	13.2 (0.52)	0.8 (0.03)
BTPB-3	29.00	50	3.2 (0.13)	4.5 (0.18)	1.2 (0.05)	17.6 (0.69)	1 (0.04)
BTPB-4	32.00	30	4.8 (0.19)	6.5 (0.26)	1.8 (0.07)	24 (0.94)	1.2 (0.05)
BTPB-5	40.00	20	6 (0.24)	8.5 (0.33)	2.3 (0.09)	32.4 (1.28)	1.8 (0.07)
BTPB-6	40.00	10	9 (0.35)	11.8 (0.46)	3.4 (0.13)	41.4 (1.63)	1.8 (0.07)
BTPC-1	36.00	30	3.2 (0.13)	4.5 (0.18)	1.2 (0.05)	28.6 (1.13)	1 (0.04)
BTPC-2	36.00	25	3.8 (0.15)	5.4 (0.21)	1.4 (0.06)	34.3 (1.35)	1.2 (0.05)
BTPC-3	36.00	20	4.8 (0.19)	6.5 (0.26)	1.8 (0.07)	39 (1.54)	1.2 (0.05)
BTPC-4	42.00	15	6 (0.24)	8.5 (0.33)	2.3 (0.09)	52.7 (2.07)	1.8 (0.07)
BTPD-1	18.50	25	2.4 (0.09)	3.4 (0.13)	0.9 (0.04)	13.2 (0.52)	0.8 (0.03)
BTPD-2	23.50	25	3.2 (0.13)	4.5 (0.18)	1.2 (0.05)	17.6 (0.69)	1 (0.04)
BTPD-3	26.00	20	4.8 (0.19)	6.5 (0.26)	1.8 (0.07)	24 (0.94)	1.2 (0.05)
BTPE-1	28.50	25	2.4 (0.09)	3.4 (0.13)	0.9 (0.04)	16.5 (0.65)	0.8 (0.03)
BTPE-2	34.00	25	3.2 (0.13)	4.5 (0.18)	1.2 (0.05)	22 (0.87)	1 (0.04)
BTPE-3	35.50	20	4.8 (0.19)	6.5 (0.26)	1.8 (0.07)	30 (1.18)	1.2 (0.05)



UNITED STATES

www.omega.com
1-800-TC-OMEGA
Stamford, CT.

CANADA

www.omega.ca
Laval(Quebec)
1-800-TC-OMEGA

GERMANY

www.omega.de
Deckenpfronn, Germany
0800-8266342

UNITED KINGDOM

www.omega.co.uk
Manchester, England
0800-488-488

FRANCE

www.omega.fr
Guyancourt, France
088-466-342

CZECH REPUBLIC

www.omegaeng.cz
Karviná, Czech Republic
596-311-899

BENELUX

www.omega.nl
Amstelveen, NL
0800-099-33-44



More than 100,000 Products Available!

• Temperature

Calibrators, Connectors, General Test and Measurement Instruments, Glass Bulb Thermometers, Handheld Instruments for Temperature Measurement, Ice Point References, Indicating Labels, Crayons, Cements and Lacquers, Infrared Temperature Measurement Instruments, Recorders Relative Humidity Measurement Instruments, RTD Probes, Elements and Assemblies, Temperature & Process Meters, Timers and Counters, Temperature and Process Controllers and Power Switching Devices, Thermistor Elements, Probes and Assemblies, Thermocouples Thermowells and Head and Well Assemblies, Transmitters, Wire

• Flow and Level

Air Velocity Indicators, Doppler Flowmeters, Level Measurement, Magnetic Flowmeters, Mass Flowmeters, Pitot Tubes, Pumps, Rotameters, Turbine and Paddle Wheel Flowmeters, Ultrasonic Flowmeters, Valves, Variable Area Flowmeters, Vortex Shedding Flowmeters

• pH and Conductivity

Conductivity Instrumentation, Dissolved Oxygen Instrumentation, Environmental Instrumentation, pH Electrodes and Instruments, Water and Soil Analysis Instrumentation

• Data Acquisition

Auto-Dialers and Alarm Monitoring Systems, Communication Products and Converters, Data Acquisition and Analysis Software, Data Loggers Plug-in Cards, Signal Conditioners, USB, RS232, RS485 and Parallel Port Data Acquisition Systems, Wireless Transmitters and Receivers

• Pressure, Strain and Force

Displacement Transducers, Dynamic Measurement Force Sensors, Instrumentation for Pressure and Strain Measurements, Load Cells, Pressure Gauges, Pressure Reference Section, Pressure Switches, Pressure Transducers, Proximity Transducers, Regulators, Strain Gages, Torque Transducers, Valves

• Heaters

Band Heaters, Cartridge Heaters, Circulation Heaters, Comfort Heaters, Controllers, Meters and Switching Devices, Flexible Heaters, General Test and Measurement Instruments, Heater Hook-up Wire, Heating Cable Systems, Immersion Heaters, Process Air and Duct, Heaters, Radiant Heaters, Strip Heaters, Tubular Heaters

FEATURES

- 116dB CMRR Independent of Gain
- Maximum Offset Voltage: 10 μ V
- Maximum Offset Voltage Drift: 50nV/ $^{\circ}$ C
- Rail-to-Rail Input
- Rail-to-Rail Output
- 2-Resistor Programmable Gain
- Supply Operation: 2.7V to \pm 5.5V
- Typical Noise: 2.5 μ V_{P-P} (0.01Hz to 10Hz)
- Typical Supply Current: 750 μ A
- LTC2053-SYNC Allows Synchronization to External Clock
- Available in MS8 and 3mm \times 3mm \times 0.8mm DFN Packages

APPLICATIONS

- Thermocouple Amplifiers
- Electronic Scales
- Medical Instrumentation
- Strain Gauge Amplifiers
- High Resolution Data Acquisition

DESCRIPTION

The LTC[®]2053 is a high precision instrumentation amplifier. The CMRR is typically 116dB with a single or dual 5V supply and is independent of gain. The input offset voltage is guaranteed below 10 μ V with a temperature drift of less than 50nV/ $^{\circ}$ C. The LTC2053 is easy to use; the gain is adjustable with two external resistors, like a traditional op amp.

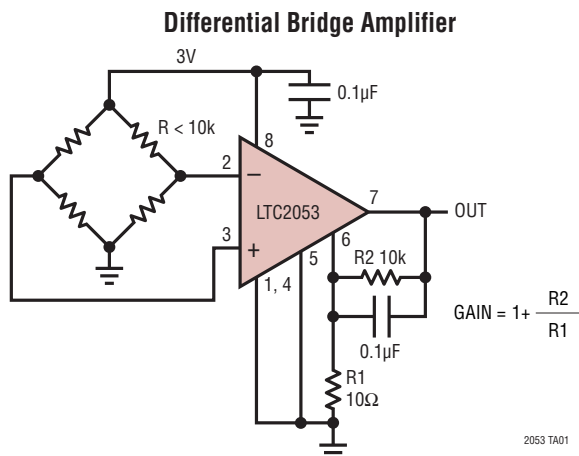
The LTC2053 uses charge balanced sampled data techniques to convert a differential input voltage into a single ended signal that is in turn amplified by a zero-drift operational amplifier.

The differential inputs operate from rail-to-rail and the single-ended output swings from rail-to-rail. The LTC2053 can be used in single-supply applications, as low as 2.7V. It can also be used with dual \pm 5.5V supplies. The LTC2053 requires no external clock, while the LTC2053-SYNC has a CLK pin to synchronize to an external clock.

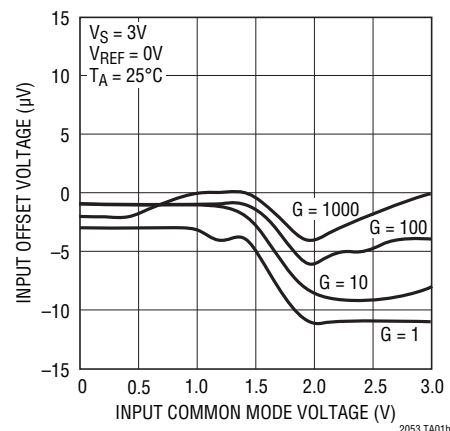
The LTC2053 is available in an MS8 surface mount package. For space limited applications, the LTC2053 is available in a 3mm \times 3mm \times 0.8mm dual fine pitch leadless package (DFN).

LT, LT, LTC, LTM, Linear Technology and the Linear logo are registered trademarks of Linear Technology Corporation. All other trademarks are the property of their respective owners.

TYPICAL APPLICATION



Typical Input Referred Offset vs Input Common Mode Voltage ($V_S = 3V$)

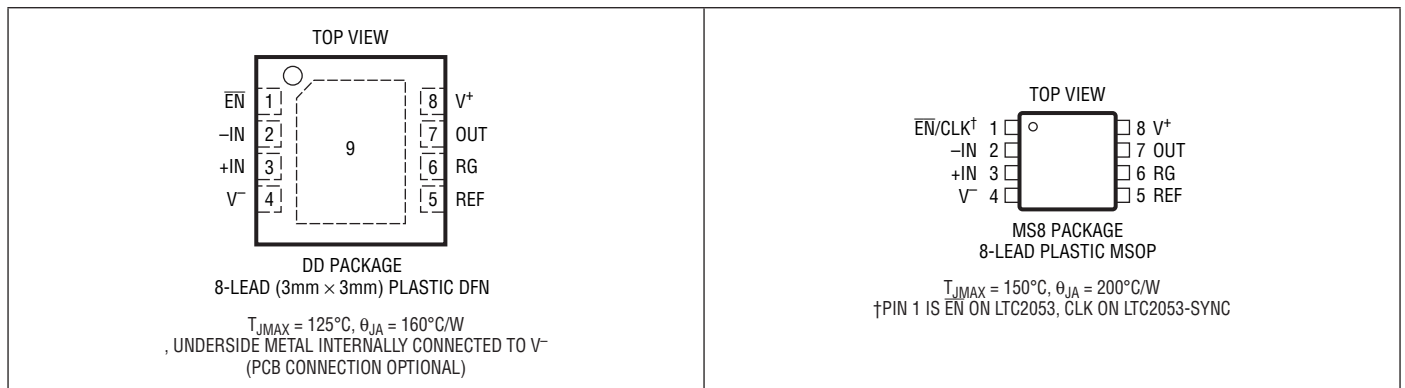


LTC2053/LTC2053-SYNC

ABSOLUTE MAXIMUM RATINGS (Note 1)

Total Supply Voltage (V^+ to V^-).....	11V	Storage Temperature Range	
Input Current.....	$\pm 10\text{mA}$	MS8 Package.....	-65°C to 150°C
$ V_{-IN} - V_{REF} $	5.5V	DD Package	-65°C to 125°C
$ V_{+IN} - V_{REF} $	5.5V	Lead Temperature (Soldering, 10 sec).....	300°C
Output Short-Circuit Duration.....	Indefinite		
Operating Temperature Range			
LTC2053C, LTC2053C-SYNC	0°C to 70°C		
LTC2053I, LTC2053I-SYNC.....	-40°C to 85°C		
LTC2053H.....	-40°C to 125°C		

PIN CONFIGURATION



ORDER INFORMATION

LEAD FREE FINISH	TAPE AND REEL	PART MARKING*	PACKAGE DESCRIPTION	TEMPERATURE RANGE
LTC2053CDD#PBF	LTC2053CDD#TRPBF	LAEQ	8-Lead (3mm × 3mm) Plastic DFN	0°C to 70°C
LTC2053IDD#PBF	LTC2053IDD#TRPBF	LAEQ	8-Lead (3mm × 3mm) Plastic DFN	-40°C to 85°C
LTC2053HDD#PBF	LTC2053HDD#TRPBF	LAEQ	8-Lead (3mm × 3mm) Plastic DFN	-40°C to 125°C
LTC2053CMS8#PBF	LTC2053CMS8#TRPBF	LTVT	8-Lead Plastic MSOP	0°C to 70°C
LTC2053IMS8#PBF	LTC2053IMS8#TRPBF	LTJY	8-Lead Plastic MSOP	-40°C to 85°C
LTC2053HMS8#PBF	LTC2053HMS8#TRPBF	LTAFB	8-Lead Plastic MSOP	-40°C to 125°C
LTC2053CMS8-SYNC#PBF	LTC2053CMS8-SYNC#TRPBF	LTBNP	8-Lead Plastic MSOP	0°C to 70°C
LTC2053IMS8-SYNC#PBF	LTC2053IMS8-SYNC#TRPBF	LTBNP	8-Lead Plastic MSOP	-40°C to 85°C

Consult LTC Marketing for parts specified with wider operating temperature ranges. *The temperature grade is identified by a label on the shipping container. Consult LTC Marketing for information on non-standard lead based finish parts.

For more information on lead free part marking, go to: <http://www.linear.com/leadfree/>

For more information on tape and reel specifications, go to: <http://www.linear.com/tapeandreeel/>

ELECTRICAL CHARACTERISTICS

The ● denotes the specifications which apply over the full operating temperature range, otherwise specifications are at $T_A = 25^\circ\text{C}$. $V^+ = 3\text{V}$, $V^- = 0\text{V}$, $\text{REF} = 200\text{mV}$. Output voltage swing is referenced to V^- . All other specifications reference the OUT pin to the REF pin.

PARAMETER	CONDITIONS		MIN	TYP	MAX	UNITS
Gain Error	$A_V = 1$	●		0.001	0.01	%
Gain Nonlinearity	$A_V = 1$, LTC2053	●		3	12	ppm
	$A_V = 1$, LTC2053-SYNC	●		3	15	ppm
Input Offset Voltage (Note 2)	$V_{\text{CM}} = 200\text{mV}$			-5	± 10	μV
Average Input Offset Drift (Note 2)	$T_A = -40^\circ\text{C}$ to 85°C	●			± 50	$\text{nV}/^\circ\text{C}$
	$T_A = 85^\circ\text{C}$ to 125°C	●		-1	-2.5	$\mu\text{V}/^\circ\text{C}$
Average Input Bias Current (Note 3)	$V_{\text{CM}} = 1.2\text{V}$	●		4	10	nA
Average Input Offset Current (Note 3)	$V_{\text{CM}} = 1.2\text{V}$	●		1	3	nA
Input Noise Voltage	DC to 10Hz			2.5		$\mu\text{V}_{\text{P-P}}$
Common Mode Rejection Ratio (Notes 4, 5)	$A_V = 1$, $V_{\text{CM}} = 0\text{V}$ to 3V , LTC2053C, LTC2053C-SYNC	●	100	113		dB
	$A_V = 1$, $V_{\text{CM}} = 0.1\text{V}$ to 2.9V , LTC2053I, LTC2053I-SYNC	●	100	113		dB
	$A_V = 1$, $V_{\text{CM}} = 0\text{V}$ to 3V , LTC2053I, LTC2053I-SYNC	●		95	113	dB
	$A_V = 1$, $V_{\text{CM}} = 0.1\text{V}$ to 2.9V , LTC2053H	●		100		dB
	$A_V = 1$, $V_{\text{CM}} = 0\text{V}$ to 3V , LTC2053H	●		85		dB
Power Supply Rejection Ratio (Note 6)	$V_S = 2.7\text{V}$ to 6V	●	110	116		dB
Output Voltage Swing High	$R_L = 2\text{k}$ to V^-	●	2.85	2.94		V
	$R_L = 10\text{k}$ to V^-	●	2.95	2.98		V
Output Voltage Swing Low		●			20	mV
Supply Current	No Load	●		0.75	1	mA
Supply Current, Shutdown	$V_{\text{EN}} \geq 2.5\text{V}$, LTC2053 Only				10	μA
$\overline{\text{EN}}/\text{CLK}$ Pin Input Low Voltage, V_{IL}					0.5	V
$\overline{\text{EN}}/\text{CLK}$ Pin Input High Voltage, V_{IH}			2.5			V
$\overline{\text{EN}}/\text{CLK}$ Pin Input Current	$V_{\text{EN}}/\text{CLK} = V^-$			-0.5	-10	μA
Internal Op Amp Gain Bandwidth				200		kHz
Slew Rate				0.2		$\text{V}/\mu\text{s}$
Internal Sampling Frequency				3		kHz

The ● denotes the specifications which apply over the full operating temperature range, otherwise specifications are at $T_A = 25^\circ\text{C}$. $V^+ = 5\text{V}$, $V^- = 0\text{V}$, $\text{REF} = 200\text{mV}$. Output voltage swing is referenced to V^- . All other specifications reference the OUT pin to the REF pin.

PARAMETER	CONDITIONS		MIN	TYP	MAX	UNITS
Gain Error	$A_V = 1$	●		0.001	0.01	%
Gain Nonlinearity	$A_V = 1$	●		3	10	ppm
Input Offset Voltage (Note 2)	$V_{\text{CM}} = 200\text{mV}$			-5	± 10	μV
Average Input Offset Drift (Note 2)	$T_A = -40^\circ\text{C}$ to 85°C	●			± 50	$\text{nV}/^\circ\text{C}$
	$T_A = 85^\circ\text{C}$ to 125°C	●		-1	-2.5	$\mu\text{V}/^\circ\text{C}$
Average Input Bias Current (Note 3)	$V_{\text{CM}} = 1.2\text{V}$	●		4	10	nA
Average Input Offset Current (Note 3)	$V_{\text{CM}} = 1.2\text{V}$	●		1	3	nA
Common Mode Rejection Ratio (Notes 4, 5)	$A_V = 1$, $V_{\text{CM}} = 0\text{V}$ to 5V , LTC2053C	●	105	116		dB
	$A_V = 1$, $V_{\text{CM}} = 0\text{V}$ to 5V , LTC2053C-SYNC	●	100	116		dB
	$A_V = 1$, $V_{\text{CM}} = 0.1\text{V}$ to 4.9V , LTC2053I	●	105	116		dB
	$A_V = 1$, $V_{\text{CM}} = 0.1\text{V}$ to 4.9V , LTC2053I-SYNC	●	100	116		dB
	$A_V = 1$, $V_{\text{CM}} = 0\text{V}$ to 5V , LTC2053I, LTC2053I-SYNC	●		95	116	dB
	$A_V = 1$, $V_{\text{CM}} = 0.1\text{V}$ to 4.9V , LTC2053H	●		100		dB
	$A_V = 1$, $V_{\text{CM}} = 0\text{V}$ to 5V , LTC2053H	●		85		dB
Power Supply Rejection Ratio (Note 6)	$V_S = 2.7\text{V}$ to 6V	●	110	116		dB

LTC2053/LTC2053-SYNC

ELECTRICAL CHARACTERISTICS The ● denotes the specifications which apply over the full operating temperature range, otherwise specifications are at $T_A = 25^\circ\text{C}$. $V^+ = 5\text{V}$, $V^- = 0\text{V}$, $\text{REF} = 200\text{mV}$. Output voltage swing is referenced to V^- . All other specifications reference the OUT pin to the REF pin.

PARAMETER	CONDITIONS		MIN	TYP	MAX	UNITS
Output Voltage Swing High	$R_L = 2\text{k to } V^-$ $R_L = 10\text{k to } V^-$	●	4.85	4.94		V
		●	4.95	4.98		V
Output Voltage Swing Low		●			20	mV
Supply Current	No Load	●		0.85	1.1	mA
Supply Current, Shutdown	$V_{\text{EN}} \geq 4.5\text{V}$, LTC2053 Only				10	μA
$\overline{\text{EN}}/\text{CLK}$ Pin Input Low Voltage, V_{IL}					0.5	V
$\overline{\text{EN}}/\text{CLK}$ Pin Input High Voltage, V_{IH}			4.5			V
$\overline{\text{EN}}/\text{CLK}$ Pin Input Current	$V_{\text{EN}}/\text{CLK} = V^-$			-1	-10	μA
Internal Op Amp Gain Bandwidth				200		kHz
Slew Rate				0.2		V/ μs
Internal Sampling Frequency				3		kHz

The ● denotes the specifications which apply over the full operating temperature range, otherwise specifications are at $T_A = 25^\circ\text{C}$. $V^+ = 5\text{V}$, $V^- = -5\text{V}$, $\text{REF} = 0\text{V}$.

PARAMETER	CONDITIONS		MIN	TYP	MAX	UNITS
Gain Error	$A_V = 1$	●		0.001	0.01	%
Gain Nonlinearity	$A_V = 1$	●		3	10	ppm
Input Offset Voltage (Note 2)	$V_{\text{CM}} = 0\text{V}$			10	± 20	μV
Average Input Offset Drift (Note 2)	$T_A = -40^\circ\text{C to } 85^\circ\text{C}$ $T_A = 85^\circ\text{C to } 125^\circ\text{C}$	●			± 50	nV/ $^\circ\text{C}$
		●			-2.5	$\mu\text{V}/^\circ\text{C}$
Average Input Bias Current (Note 3)	$V_{\text{CM}} = 1\text{V}$	●		4	10	nA
Average Input Offset Current (Note 3)	$V_{\text{CM}} = 1\text{V}$	●		1	3	nA
Common Mode Rejection Ratio (Notes 4, 5)	$A_V = 1$, $V_{\text{CM}} = -5\text{V to } 5\text{V}$, LTC2053C	●	105	118		dB
	$A_V = 1$, $V_{\text{CM}} = -5\text{V to } 5\text{V}$, LTC2053C-SYNC	●	100	118		dB
	$A_V = 1$, $V_{\text{CM}} = -4.9\text{V to } 4.9\text{V}$, LTC2053I	●	105	118		dB
	$A_V = 1$, $V_{\text{CM}} = -4.9\text{V to } 4.9\text{V}$, LTC2053I-SYNC	●	100	118		dB
	$A_V = 1$, $V_{\text{CM}} = -5\text{V to } 5\text{V}$, LTC2053I, LTC2053I-SYNC	●	95	118		dB
	$A_V = 1$, $V_{\text{CM}} = -4.9\text{V to } 4.9\text{V}$, LTC2053H	●	100			dB
	$A_V = 1$, $V_{\text{CM}} = -5\text{V to } 5\text{V}$, LTC2053H	●	90			dB
Power Supply Rejection Ratio (Note 6)	$V_S = 2.7\text{V to } 11\text{V}$	●	110	116		dB
Maximum Output Voltage Swing	$R_L = 2\text{k to GND}$, C- and I-Grades $R_L = 10\text{k to GND}$, All Grades $R_L = 2\text{k to GND}$, LTC2053H Only	●	± 4.5	± 4.8		V
		●	± 4.6	± 4.9		V
		●	± 4.4	± 4.8		V
Supply Current	No Load	●		0.95	1.3	mA
Supply Current, Shutdown	$V_{\text{EN}} \geq 4.5\text{V}$, LTC2053 Only				20	μA
$\overline{\text{EN}}$ Pin Input Low Voltage, V_{IL}					-4.5	V
CLK Pin Input Low Voltage, V_{IL}					0.5	V
$\overline{\text{EN}}/\text{CLK}$ Pin Input High Voltage, V_{IH}			4.5			V
$\overline{\text{EN}}/\text{CLK}$ Pin Input Current	$V_{\text{EN}}/\text{CLK} = V^-$			-3	-20	μA
Internal Op Amp Gain Bandwidth				200		kHz
Slew Rate				0.2		V/ μs
Internal Sampling Frequency				3		kHz

ELECTRICAL CHARACTERISTICS

Note 1: Stresses beyond those listed under Absolute Maximum Ratings may cause permanent damage to the device. Exposure to any Absolute Maximum Rating condition for extended periods may affect device reliability and lifetime.

Note 2: These parameters are guaranteed by design. Thermocouple effects preclude measurement of these voltage levels in high speed automatic test systems. V_{OS} is measured to a limit determined by test equipment capability.

Note 3: If the total source resistance is less than 10k, no DC errors result from the input bias currents or the mismatch of the input bias currents or the mismatch of the resistances connected to $-IN$ and $+IN$.

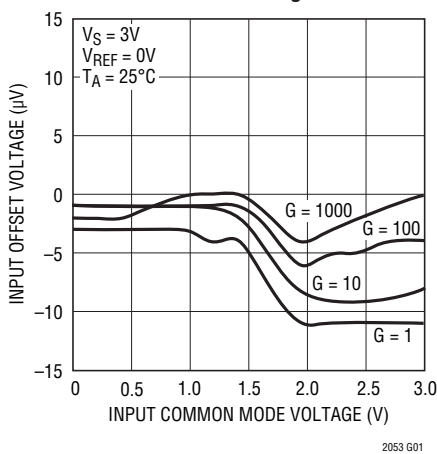
Note 4: The CMRR with a voltage gain, A_V , larger than 10 is 120dB (typ).

Note 5: At temperatures above 70°C, the common mode rejection ratio lowers when the common mode input voltage is within 100mV of the supply rails.

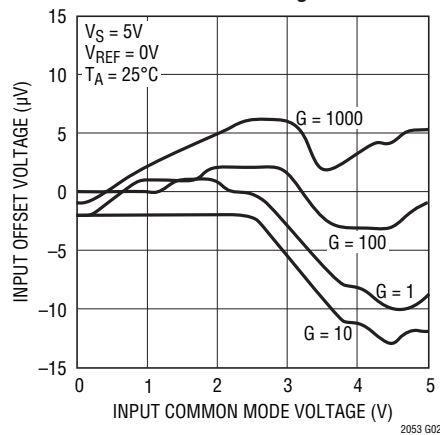
Note 6: The power supply rejection ratio (PSRR) measurement accuracy depends on the proximity of the power supply bypass capacitor to the device under test. Because of this, the PSRR is 100% tested to relaxed limits at final test. However, their values are guaranteed by design to meet the data sheet limits.

TYPICAL PERFORMANCE CHARACTERISTICS

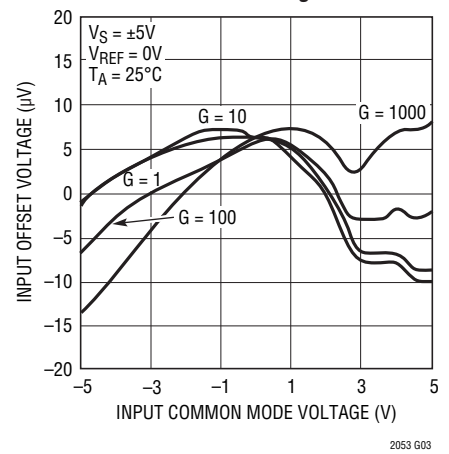
Input Offset Voltage vs Input Common Mode Voltage



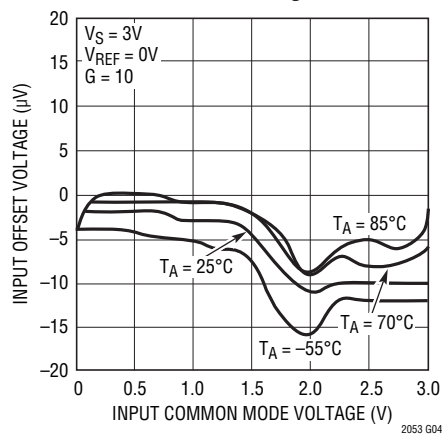
Input Offset Voltage vs Input Common Mode Voltage



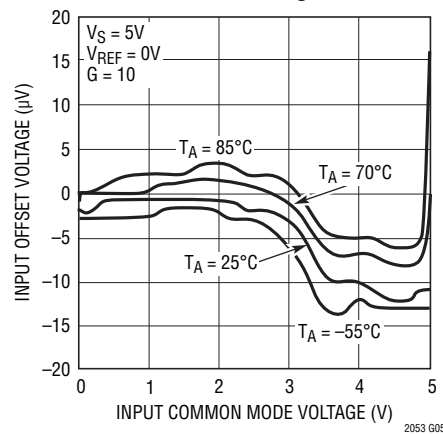
Input Offset Voltage vs Input Common Mode Voltage



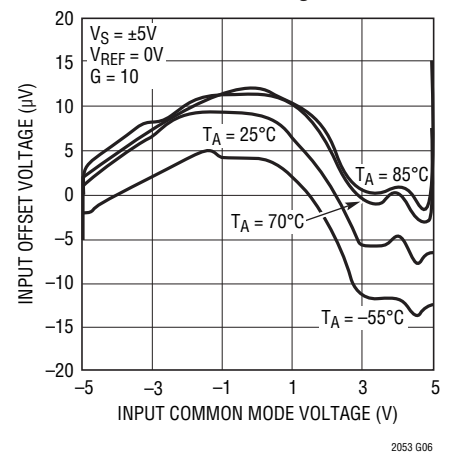
Input Offset Voltage vs Input Common Mode Voltage



Input Offset Voltage vs Input Common Mode Voltage

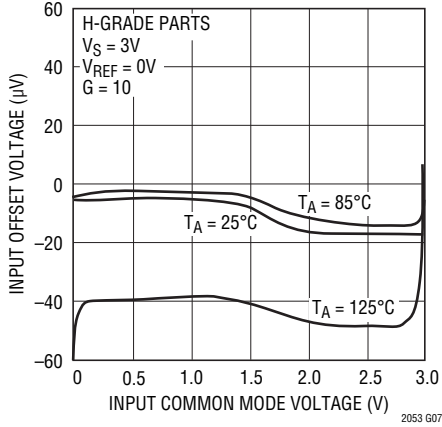


Input Offset Voltage vs Input Common Mode Voltage

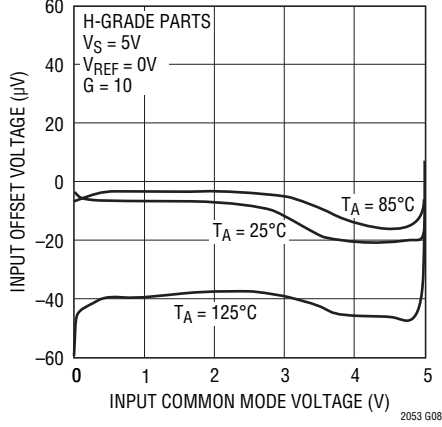


TYPICAL PERFORMANCE CHARACTERISTICS

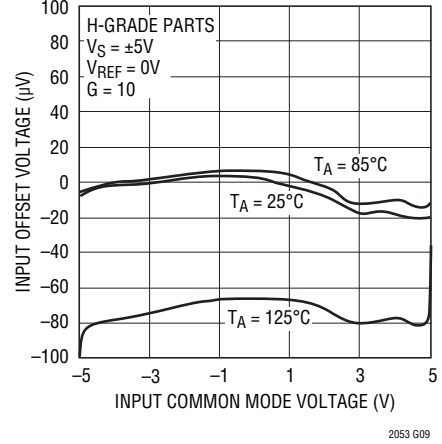
Input Offset Voltage vs Input Common Mode Voltage



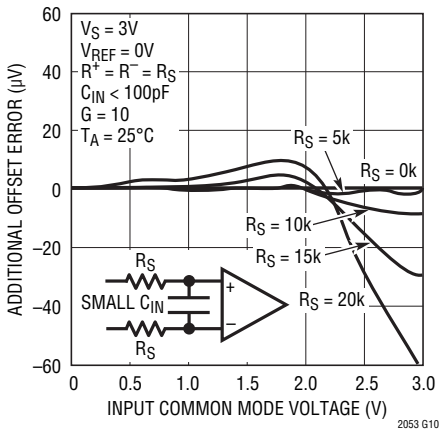
Input Offset Voltage vs Input Common Mode Voltage



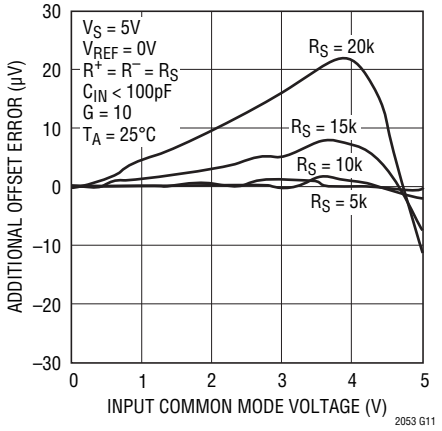
Input Offset Voltage vs Input Common Mode Voltage



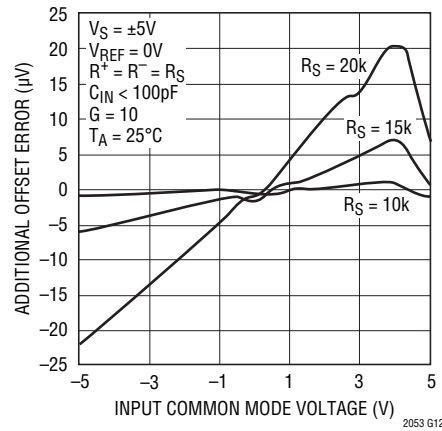
Error Due to Input RS vs Input Common Mode ($C_{IN} < 100pF$)



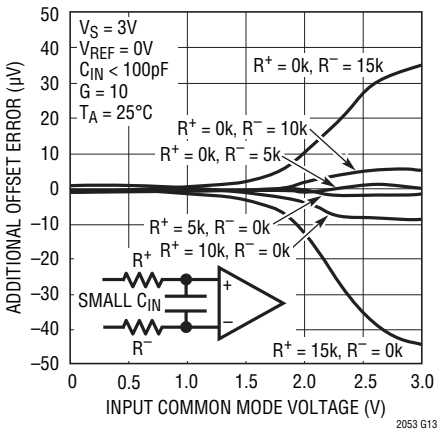
Error Due to Input RS vs Input Common Mode ($C_{IN} < 100pF$)



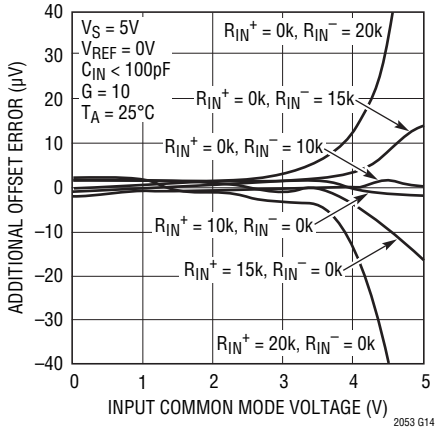
Error Due to Input RS vs Input Common Mode ($C_{IN} < 100pF$)



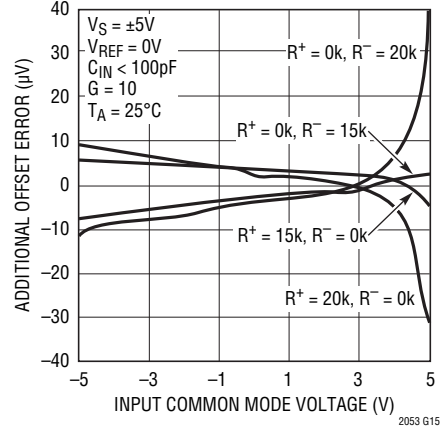
Error Due to Input RS Mismatch vs Input Common Mode ($C_{IN} < 100pF$)



Error Due to Input RS Mismatch vs Input Common Mode ($C_{IN} < 100pF$)

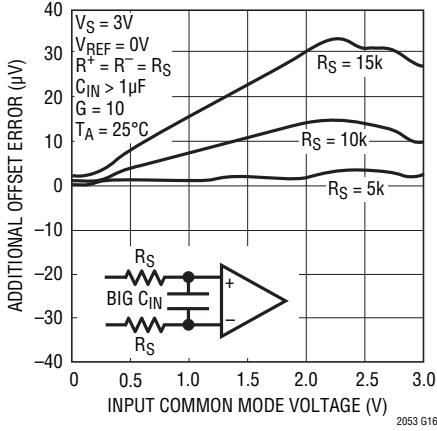


Error Due to Input RS Mismatch vs Input Common Mode ($C_{IN} < 100pF$)

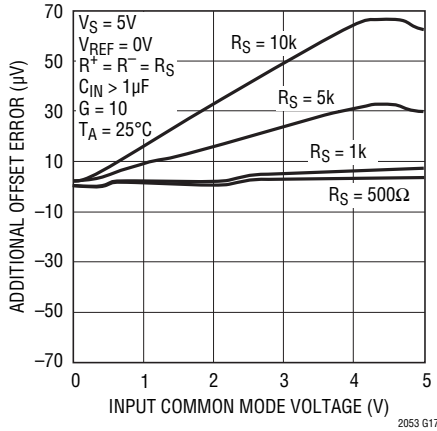


TYPICAL PERFORMANCE CHARACTERISTICS

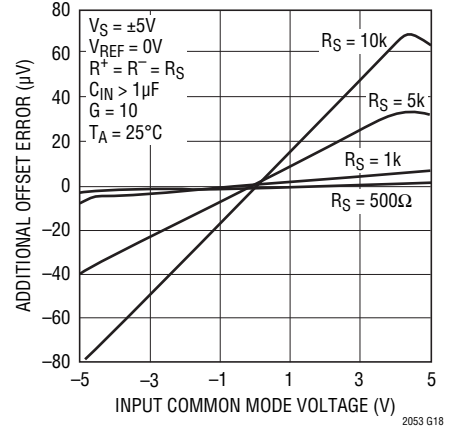
Error Due to Input R_S vs Input Common Mode ($C_{IN} > 1\mu F$)



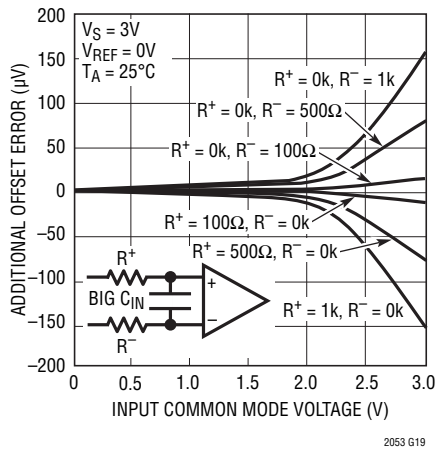
Error Due to Input R_S vs Input Common Mode ($C_{IN} > 1\mu F$)



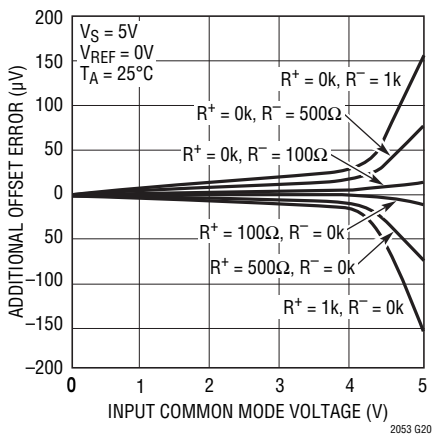
Error Due to Input R_S vs Input Common Mode ($C_{IN} > 1\mu F$)



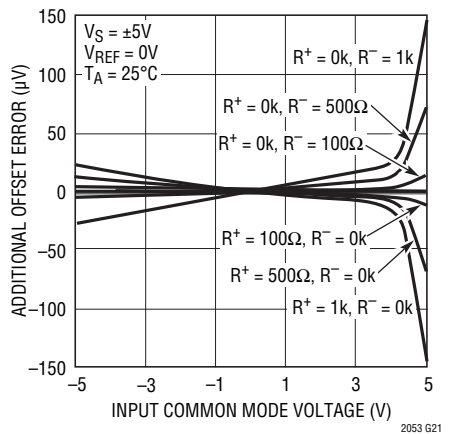
Error Due to Input R_S Mismatch vs Input Common Mode ($C_{IN} > 1\mu F$)



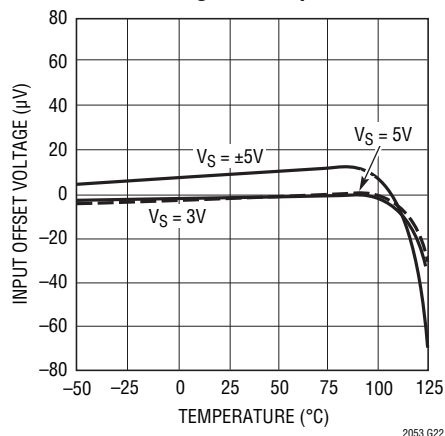
Error Due to Input R_S Mismatch vs Input Common Mode ($C_{IN} > 1\mu F$)



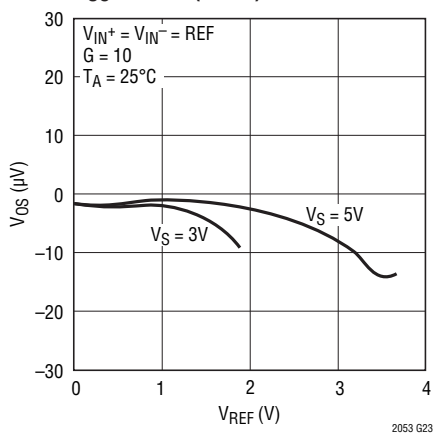
Error Due to Input R_S Mismatch vs Input Common Mode ($C_{IN} > 1\mu F$)



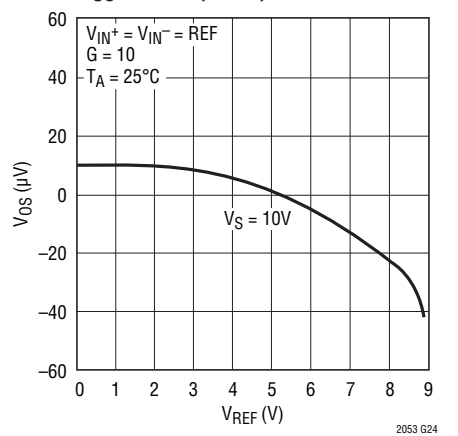
Offset Voltage vs Temperature



V_{OS} vs REF (Pin 5)

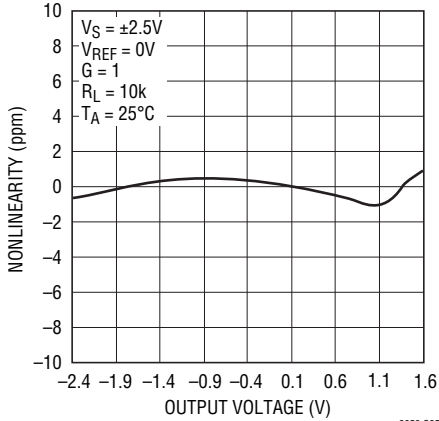


V_{OS} vs REF (Pin 5)

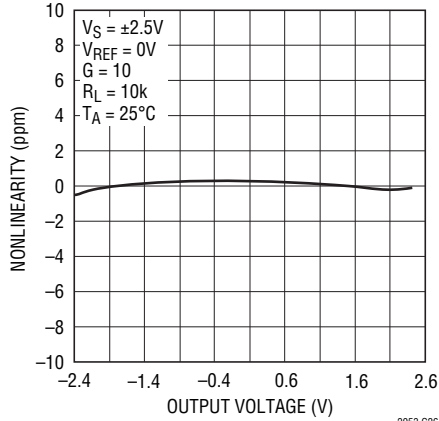


TYPICAL PERFORMANCE CHARACTERISTICS

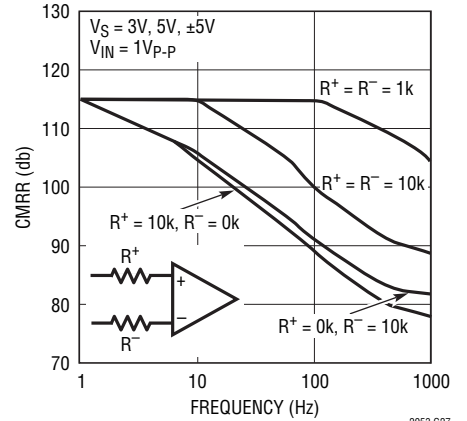
Gain Nonlinearity, G = 1



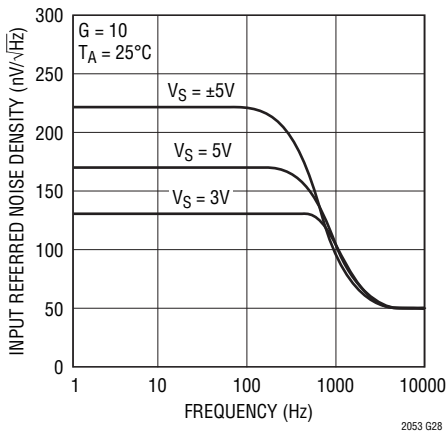
Gain Nonlinearity, G = 10



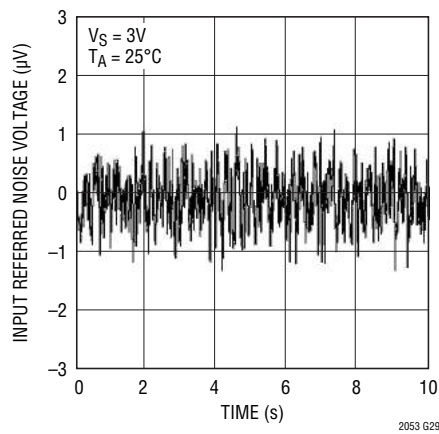
CMRR vs Frequency



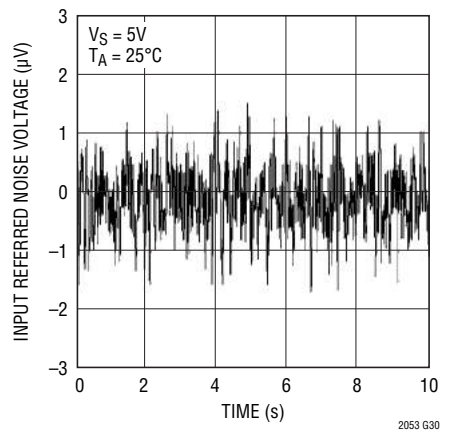
Input Voltage Noise Density vs Frequency



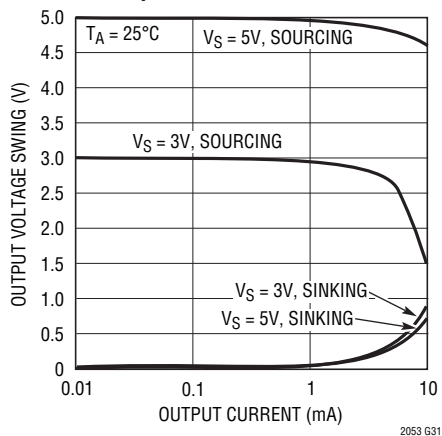
Input Referred Noise in 10Hz Bandwidth



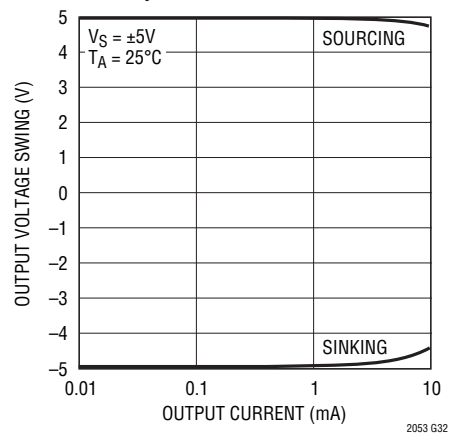
Input Referred Noise in 10Hz Bandwidth



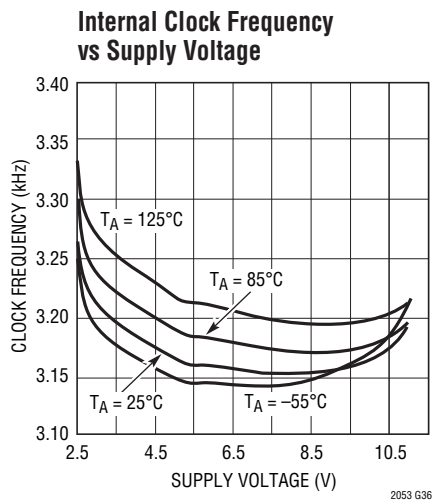
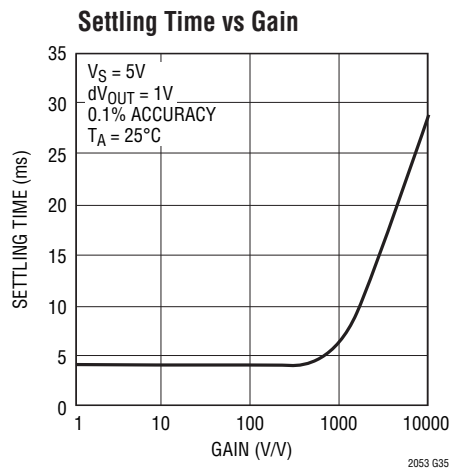
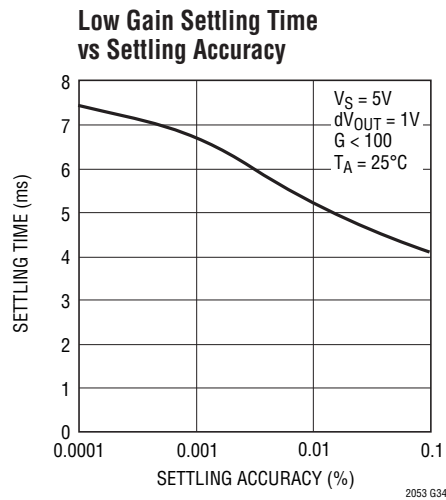
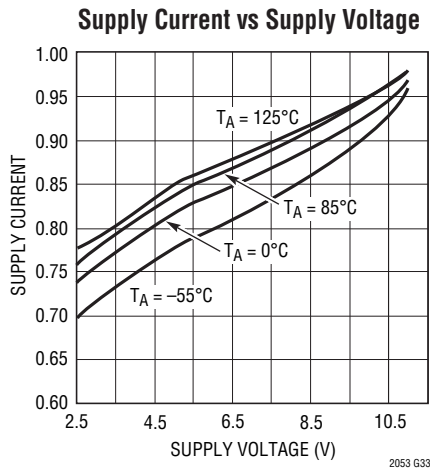
Output Voltage Swing vs Output Current



Output Voltage Swing vs Output Current



TYPICAL PERFORMANCE CHARACTERISTICS



PIN FUNCTIONS

$\overline{\text{EN}}$ (Pin 1, LTC2053 Only): Active Low Enable Pin.

CLK (Pin 1, LTC2053-SYNC Only): Clock input for Synchronizing to External System Clock.

-IN (Pin 2): Inverting Input.

+IN (Pin 3): Noninverting Input.

V^- (Pin 4): Negative Supply.

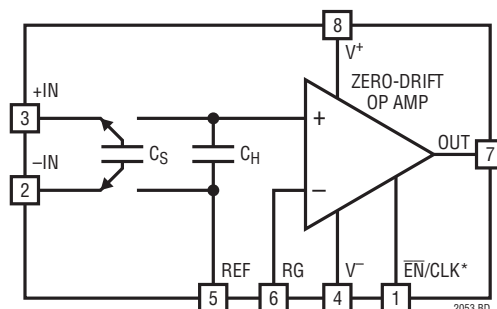
REF (Pin 5): Voltage Reference (V_{REF}) for Amplifier Output.

RG (Pin 6): Inverting Input of Internal Op Amp. See Figure 1.

OUT (Pin 7): Amplifier Output. See Figure 1.

V^+ (Pin 8): Positive Supply.

BLOCK DIAGRAM



*NOTE: PIN 1 IS \overline{EN} ON THE LTC2053 AND CLK ON THE LTC2053-SYNC

APPLICATIONS INFORMATION

Theory of Operation

The LTC2053 uses an internal capacitor (C_S) to sample a differential input signal riding on a DC common mode voltage (see the Block Diagram). This capacitor's charge is transferred to a second internal hold capacitor (C_H) translating the common mode of the input differential signal to that of the REF pin. The resulting signal is amplified by a zero-drift op amp in the noninverting configuration. The RG pin is the negative input of this op amp and allows external programmability of the DC gain. Simple filtering can be realized by using an external capacitor across the feedback resistor.

Input Voltage Range

The input common mode voltage range of the LTC2053 is rail-to-rail. However, the following equation limits the size of the differential input voltage:

$$V^- \leq (V_{+IN} - V_{-IN}) + V_{REF} \leq V^+ - 1.3$$

Where V_{+IN} and V_{-IN} are the voltages of the +IN and -IN pins, respectively, V_{REF} is the voltage at the REF pin and V^+ is the positive supply voltage.

For example, with a 3V single supply and a 0V to 100mV differential input voltage, V_{REF} must be between 0V and 1.6V.

± 5 Volt Operation

When using the LTC2053 with supplies over 5.5V, care must be taken to limit the maximum difference between any of the input pins (+IN or -IN) and the REF pin to 5.5V; if not, the device will be damaged. For example, if rail-to-rail input operation is desired when the supplies are at ± 5 V, the REF pin should be 0V, ± 0.5 V. As a second example, if V^+ is 10V and V^- and REF are at 0V, the inputs should not exceed 5.5V.

Settling Time

The sampling rate is 3kHz and the input sampling period during which C_S is charged to the input differential voltage V_{IN} is approximately 150 μ s. First assume that on each input sampling period, C_S is charged fully to V_{IN} . Since $C_S = C_H$ (= 1000pF), a change in the input will settle to N bits of accuracy at the op amp noninverting input after N clock cycles or 333 μ s(N). The settling time at the OUT pin is also affected by the settling of the internal op amp. Since the gain bandwidth of the internal op amp is typically 200kHz, the settling time is dominated by the switched capacitor front end for gains below 100 (see the Typical Performance Characteristics section).

APPLICATIONS INFORMATION

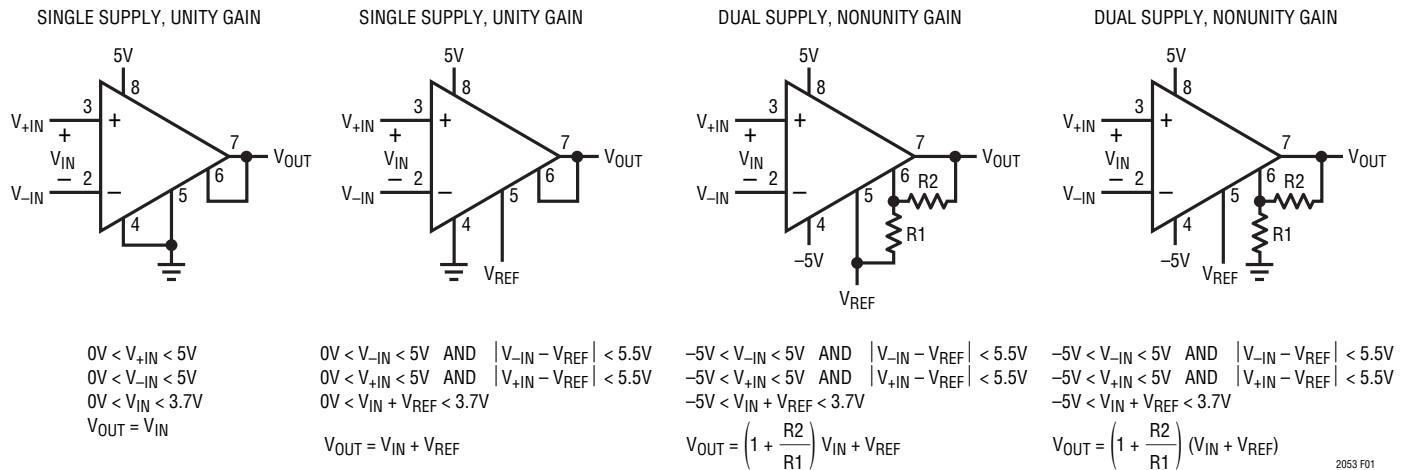


Figure 1

Input Current

Whenever the differential input V_{IN} changes, C_H must be charged up to the new input voltage via C_S . This results in an input charging current during each input sampling period. Eventually, C_H and C_S will reach V_{IN} and, ideally, the input current would go to zero for DC inputs.

In reality, there are additional parasitic capacitors which disturb the charge on C_S every cycle even if V_{IN} is a DC voltage. For example, the parasitic bottom plate capacitor on C_S must be charged from the voltage on the REF pin to the voltage on the $-IN$ pin every cycle. The resulting input charging current decays exponentially during each input sampling period with a time constant equal to $R_S C_S$. **If the voltage disturbance due to these currents settles before the end of the sampling period, there will be no errors due to source resistance or the source resistance mismatch between $-IN$ and $+IN$. With R_S less than 10k, no DC errors occur due to this input current.**

In the Typical Performance Characteristics section of this data sheet, there are curves showing the additional error from non-zero source resistance in the inputs. If there are no large capacitors across the inputs, the amplifier is less sensitive to source resistance and source resistance mismatch. When large capacitors are placed across the inputs, the input charging currents previously described result in larger DC errors, especially with source resistor mismatches.

Power Supply Bypassing

The LTC2053 uses a sampled data technique and, therefore, contains some clocked digital circuitry. It is, therefore, sensitive to supply bypassing. For single or dual supply operation, a 0.1 μ F ceramic capacitor must be connected between Pin 8 (V^+) and Pin 4 (V^-) with leads as short as possible.

Synchronizing to an External Clock (LTC2053-SYNC Only)

The LTC2053 has an internally generated sample clock that is typically 3kHz. **There is no need to provide the LTC2053 with a clock.** However, in some applications, it may be desirable for the user to control the sampling frequency more precisely to avoid undesirable aliasing. This can be done with the LTC2053-SYNC. This device uses Pin 1 as a clock input whereas the LTC2053 uses Pin 1 as an enable pin. If CLK (Pin 1) is left floating on the LTC2053-SYNC, the device will run on its internal oscillator, similar to the LTC2053. However, if not externally synchronizing to a system clock, it is recommended that the LTC2053 be used instead of the LTC2053-SYNC because the LTC2053-SYNC is sensitive to parasitic capacitance on the CLK pin when left floating. **Clocking the LTC2053-SYNC is accomplished by driving the CLK pin at 8 times the desired sample clock frequency. This completely disables the internal clock. For example, to achieve the nominal LTC2053 sample clock rate of 3kHz, a 24kHz external clock should be applied to the CLK pin of the LTC2053-SYNC.**

2053syncfc

APPLICATIONS INFORMATION

If a square wave is used to drive the CLK pin, a $5\mu\text{s}$ RC time constant should be placed in front of the CLK pin to maintain low offset voltage performance (see Figure 2). This avoids internal and external coupling of the high frequency components of the external clock at the instant the LTC2053-SYNC holds the sampled input.

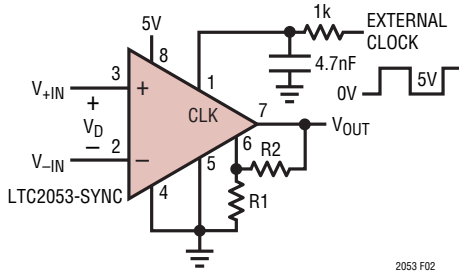


Figure 2. Centered Justified for a Single Line of Text

The LTC2053-SYNC is tested with a sample clock of 3kHz ($f_{\text{CLK}} = 24\text{kHz}$) to the same specifications as the LTC2053. In addition, the LTC2053-SYNC is tested at one-half and 2x this frequency to verify proper operation. The curves in the Typical Performance Characteristics section of this data sheet apply to the LTC2053-SYNC when driving it with a 24kHz clock at Pin 1 ($f_{\text{CLK}} = 24\text{kHz}$, 3kHz sample clock rate). Below are three curves that show the behavior of the LTC2053-SYNC as the clock frequency is varied. The offset is essentially unaffected over a 2:1 increase or decrease of the typical LTC2053 sample clock speed. The bias current is directly proportional to the clock speed. The noise is roughly proportional to the square root of the clock frequency. **For optimum noise and bias current performance, drive the LTC2053-SYNC with a nominal 24kHz external clock (3kHz sample clock).**

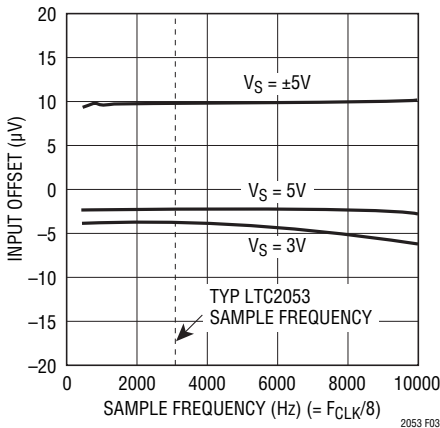


Figure 3. LTC2053-SYNC Input Offset vs Sample Frequency

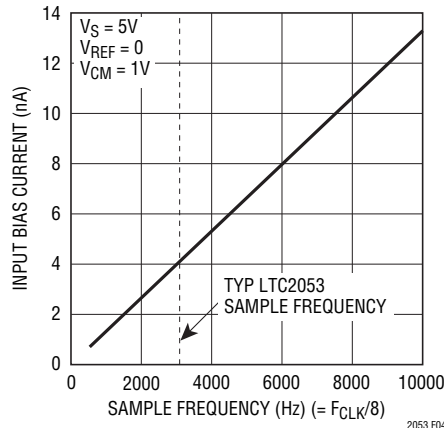


Figure 4. LTC2053-SYNC Average Input Bias Current vs Sample Frequency

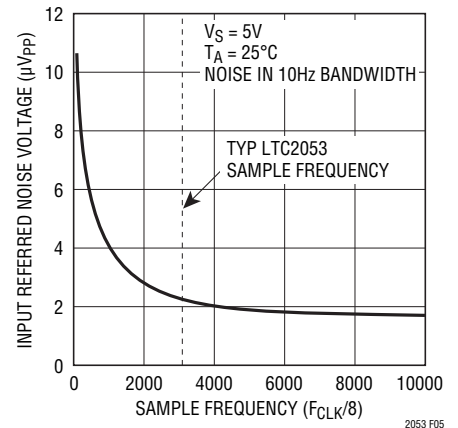
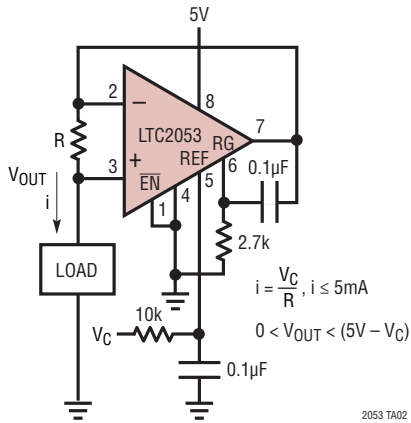


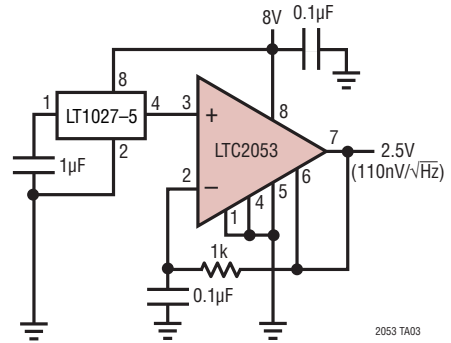
Figure 5. LTC2053-SYNC Input Referred Noise vs Sample Frequency

TYPICAL APPLICATIONS

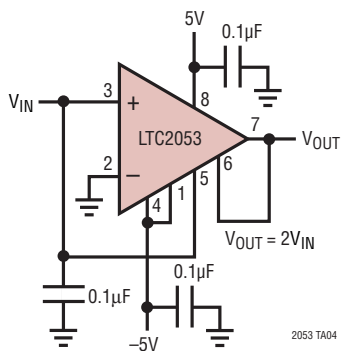
Precision Current Source



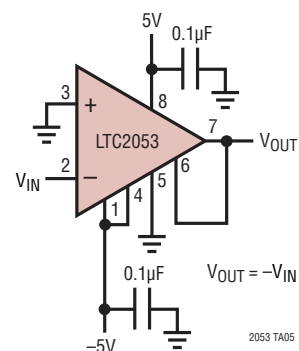
Precision $\div 2$ (Low Noise 2.5V Reference)



Precision Doubler (General Purpose)

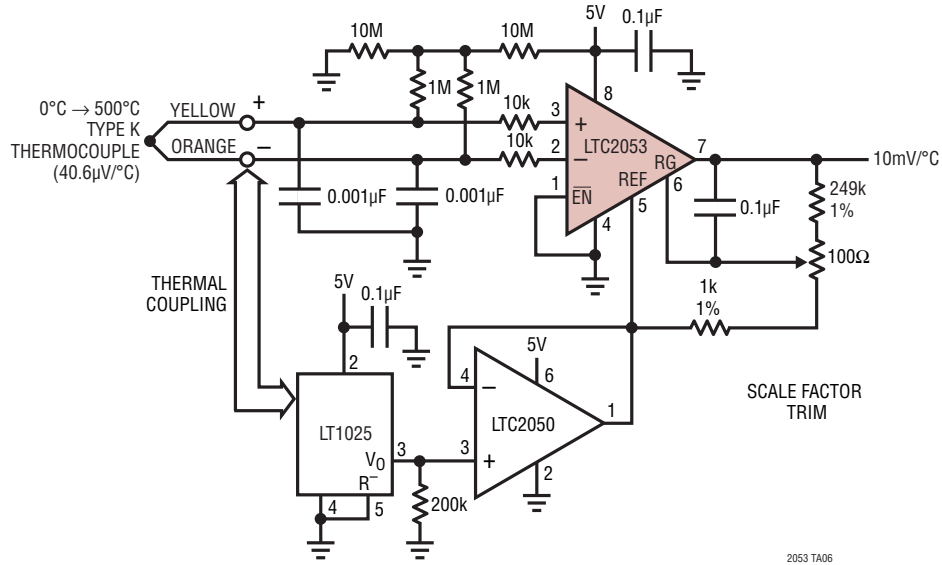


Precision Inversion (General Purpose)

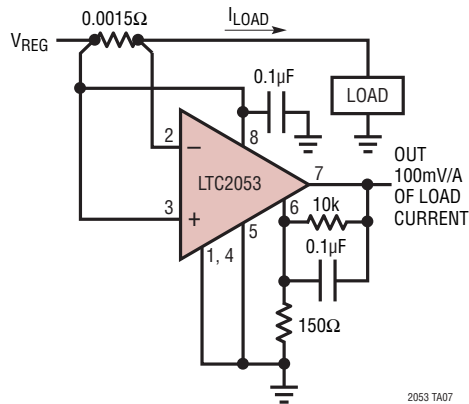


TYPICAL APPLICATIONS

Differential Thermocouple Amplifier

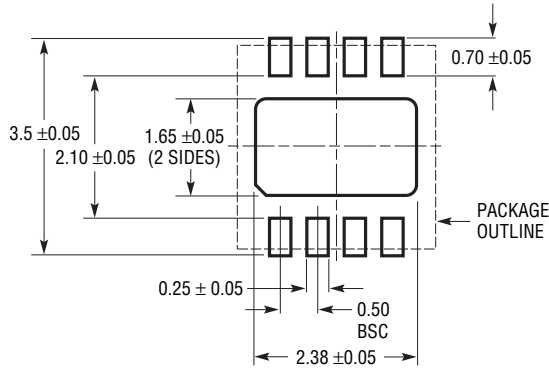


High Side Power Supply Current Sense

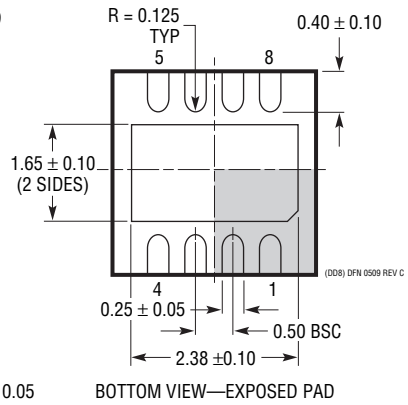
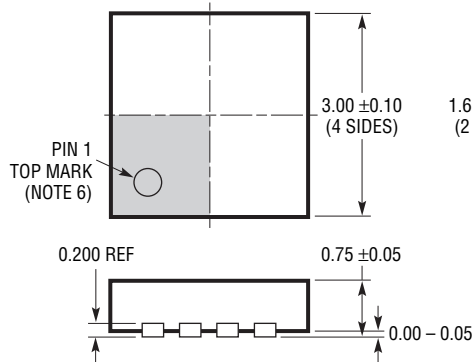


PACKAGE DESCRIPTION

DD Package
8-Lead Plastic DFN (3mm × 3mm)
 (Reference LTC DWG # 05-08-1698 Rev C)



RECOMMENDED SOLDER PAD PITCH AND DIMENSIONS
 APPLY SOLDER MASK TO AREAS THAT ARE NOT SOLDERED



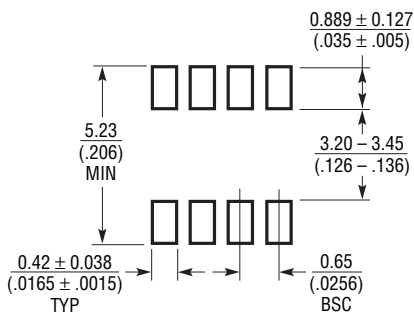
NOTE:

1. DRAWING TO BE MADE A JEDEC PACKAGE OUTLINE M0-229 VARIATION OF (WEED-1)
2. DRAWING NOT TO SCALE
3. ALL DIMENSIONS ARE IN MILLIMETERS
4. DIMENSIONS OF EXPOSED PAD ON BOTTOM OF PACKAGE DO NOT INCLUDE MOLD FLASH. MOLD FLASH, IF PRESENT, SHALL NOT EXCEED 0.15mm ON ANY SIDE
5. EXPOSED PAD SHALL BE SOLDER PLATED
6. SHADED AREA IS ONLY A REFERENCE FOR PIN 1 LOCATION ON TOP AND BOTTOM OF PACKAGE

PACKAGE DESCRIPTION

MS8 Package 8-Lead Plastic MSOP

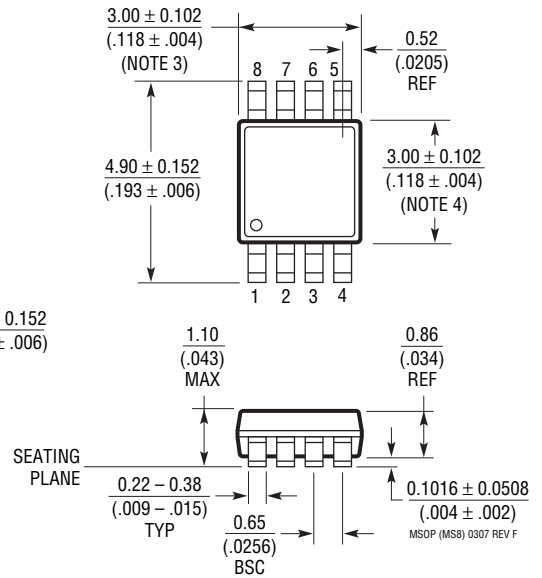
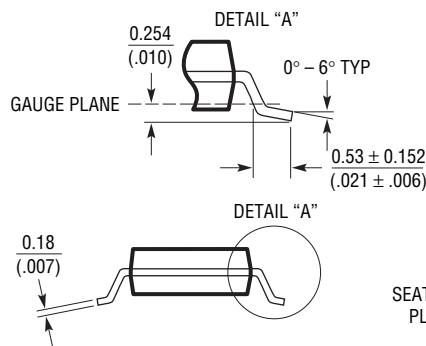
(Reference LTC DWG # 05-08-1660 Rev F)



RECOMMENDED SOLDER PAD LAYOUT

NOTE:

1. DIMENSIONS IN MILLIMETER/(INCH)
2. DRAWING NOT TO SCALE
3. DIMENSION DOES NOT INCLUDE MOLD FLASH, PROTRUSIONS OR GATE BURRS. MOLD FLASH, PROTRUSIONS OR GATE BURRS SHALL NOT EXCEED 0.152mm (.006") PER SIDE
4. DIMENSION DOES NOT INCLUDE INTERLEAD FLASH OR PROTRUSIONS. INTERLEAD FLASH OR PROTRUSIONS SHALL NOT EXCEED 0.152mm (.006") PER SIDE
5. LEAD COPLANARITY (BOTTOM OF LEADS AFTER FORMING) SHALL BE 0.102mm (.004") MAX

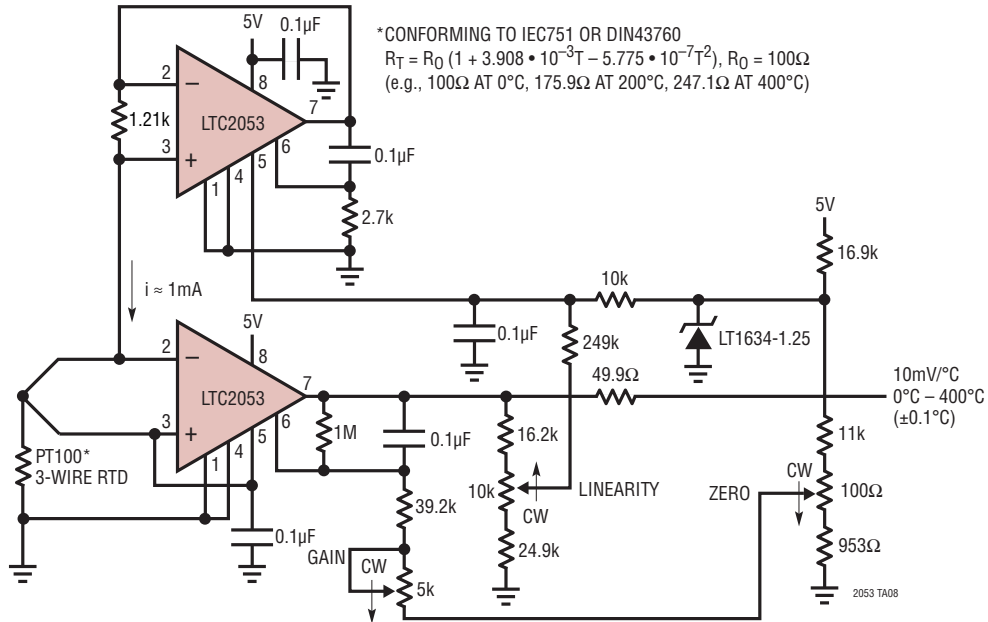


REVISION HISTORY (Revision history begins at Rev C)

REV	DATE	DESCRIPTION	PAGE NUMBER
C	7/10	Corrected text in the Absolute Maximum Ratings section	2
		Updated Pin 6 and Pin 7 text in the Pin Functions section	9
		Replaced Figure 1	11

TYPICAL APPLICATION

Linearized Platinum RTD Amplifier



RELATED PARTS

PART NUMBER	DESCRIPTION	COMMENTS
LT1167	Single Resistor Gain-Programmable, Precision Instrumentation Amplifier	Single-Gain Set Resistor: $G = 1$ to 10,000, Low Noise: $7.5nV/\sqrt{Hz}$
LTC2050/LTC2051	Zero-Drift Single/Dual Operation Amplifier	SOT-23 and MS8 Packages
LTC2054/LTC2055	Zero-Drift μ Power Operational Amplifier	SOT-23 and MS8 Packages, 150 μ A/Op Amp
LTC6800	Single-Supply, Zero-Drift, Rail-to-Rail Input and Output Instrumentation Amplifier	MS8 Package, 100 μ V Max V_{OS} , 250nV/°C Max Drift



± 10g Tri-axis Accelerometer Specifications

PART NUMBER:

KXD94-2802
Rev. 2
May-2014

Product Description

The KXD94-2802 is a Tri-axis, silicon micromachined accelerometer with a full-scale output range of +/-10g (98 m/s/s). The sense element is fabricated using Kionix's proprietary plasma micromachining process technology. Acceleration sensing is based on the principle of a differential capacitance arising from acceleration-induced motion of the sense element, which further utilizes common mode cancellation to decrease errors from process variation, temperature, and environmental stress. The sense element is hermetically sealed at the wafer level by bonding a second silicon lid wafer to the device using a glass frit. A separate ASIC device packaged with the sense element provides signal conditioning and self-test. The accelerometer is delivered in a 5 x 5 x 1.2 mm DFN plastic package operating from a 2.50V - 5.25V DC supply. The three outputs (X, Y, Z) are provided on **analog** output pins. The KXD94 also features an integrated **4-channel multiplexer** (X, Y, Z, and Aux In). The Enable pin must be **high** for normal operation and **low** for power shutdown.



There are 4 factory programmable modes of operation for the KXD94:

- Mode 00** – The three outputs (X, Y, Z) are read through the **digital** SPI interface, which is also used to command Selftest and Standby Mode. The digital I/O pads are powered from a separate power pin, and will interface to 1.8V logic.
- Mode 01** – The three outputs (X, Y, Z) are provided on three **analog** output pins. The KXD94 also features an integrated **3-channel multiplexer** (X, Y, Z). The Enable pin must be **high** for normal operation and **low** for power shutdown.
- Mode 10** – The three outputs (X, Y, Z) are provided on three **analog** output pins. The KXD94 also features an integrated **4-channel multiplexer** (X, Y, Z, Aux In). The Enable pin must be **high** for normal operation and **low** for power shutdown.
- Mode 11** – The three outputs (X, Y, Z) are provided on three **analog** output pins. The KXD94 also features an integrated **4-channel multiplexer** (X, Y, Z, Aux In). The Enable pin must be **low** for normal operation and **high** for power shutdown.

The KXD94-2802 is factory programmed to be in MODE 10.

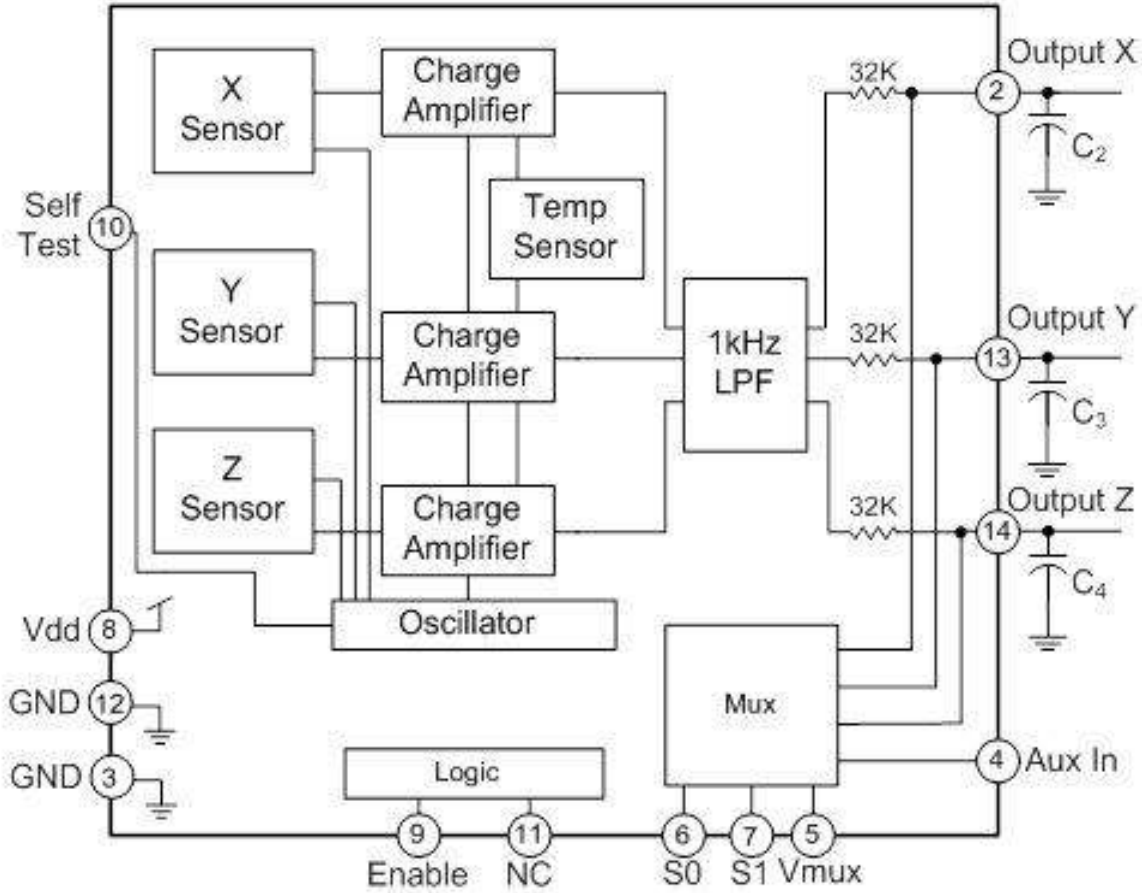


± 10g Tri-axis Accelerometer Specifications

PART NUMBER:

KXD94-2802
Rev. 2
May-2014

Functional Diagram





± 10g Tri-axis Accelerometer Specifications

PART NUMBER:

**KXD94-2802
Rev. 2
May-2014**

Product Specifications

Table 1. Mechanical

(specifications are for operation at 5V and T = 25C unless stated otherwise)

Parameters	Units	Min	Typical	Max
Operating Temperature Range	°C	-40	-	85
Zero-g Offset	! V	2.45	2.5	2.55
Zero-g Offset Variation from RT over Temp.	mg/°C		1	
Sensitivity	! mV/g	193	200	207
Sensitivity Variation from RT over Temp.	%/°C		0.01	
Offset Ratiometric Error (Vdd = 5V ± 5%)	mg		0.2 (xy) 0.1 (z)	
Sensitivity Ratiometric Error (Vdd = 5V ± 5%)	%		1.6 (xy) 0.2 (z)	
Non-Linearity	% of FS		0.1	
Cross Axis Sensitivity	%		2	
Self Test Output change on Activation	g		6.5 (xy) 3.6 (z)	
Bandwidth (-3dB) ¹	Hz	640	800	960
Noise Density (on filter pins)	µg / √Hz		100	

! Denotes Special Characteristics: These characteristics have been identified as important to the customer.

Notes:

1. Internal 1 kHz low pass filter. Lower frequencies are user definable with external capacitors.



± 10g Tri-axis Accelerometer Specifications

PART NUMBER:

KXD94-2802
Rev. 2
May-2014

Table 2. Electrical

(specifications are for operation at 5V and T = 25C unless stated otherwise)

Parameters		Units	Min	Typical	Max
Supply Voltage (V _{dd})	Operating ^{1,2}	V	2.5	5	5.25
Current Consumption	Operating ³	! μA	900	1200	1500
	Standby	μA		-	5
Input Low Voltage ⁴		V	-	-	0.2 * V _{dd}
Input High Voltage ⁵		V	0.8 * V _{dd}	-	-
Analog Output Resistance (R _{out})		kΩ	24	32	40

! Denotes Special Characteristics: These characteristics have been identified as important to the customer.

Notes:

1. Supply voltage must be ramped to 80% of V_{dd} in 60mSec or less. The ASIC does not monitor V_{dd} voltage levels and ramping V_{dd} may result in failure. Note- The voltage can not cycle during the start-up period.
2. The operating voltage range of the KXD94 is 2.5V to 5.25V but the performance for that range is not validated by this specification.
3. Tolerance for current at V_{dd}=5v.
4. Voltage level for logic '0'. I.e. disable selftest function
5. Voltage level for logic '1'. I.e. enable selftest function

	± 10g Tri-axis Accelerometer Specifications	PART NUMBER: KXD94-2802 Rev. 2 May-2014
---	--	--

Table 3. Environmental

Parameters		Units	Min	Target	Max
Supply Voltage (V _{dd})	Absolute Limits	V	-0.3	-	7.0
Maximum Operating Temperature Range		°C	-40	-	125
Storage Temperature Range		°C	-55	-	150
Mech. Shock (powered and unpowered) ⁶		g	-	-	5000 for 0.5ms
ESD	HBM	V	-	-	3000

6. Mechanical shock abuse can cause offset shifts

CAUTION:
ELECTROSTATIC
SENSITIVE COMPONENT



Caution: ESD Sensitive and Mechanical Shock Sensitive Component, improper handling can cause permanent damage to the device.



This product conforms to Directive 2002/95/EC of the European Parliament and of the Council of the European Union (RoHS). Specifically, this product does not contain lead, mercury, cadmium, hexavalent chromium, polybrominated biphenyls (PBB), or polybrominated diphenyl ethers (PBDE) above the maximum concentration values (MCV) by weight in any of its homogenous materials. Homogenous materials are "of uniform composition throughout."



This product is halogen-free per IEC 61249-2-21. Specifically, the materials used in this product contain a maximum total halogen content of 1500 ppm with less than 900-ppm bromine and less than 900-ppm chlorine.

Soldering

Soldering recommendations available upon request or from www.kionix.com.



± 10g Tri-axis Accelerometer Specifications

PART NUMBER:

KXD94-2802
Rev. 2
May-2014

Application Schematic

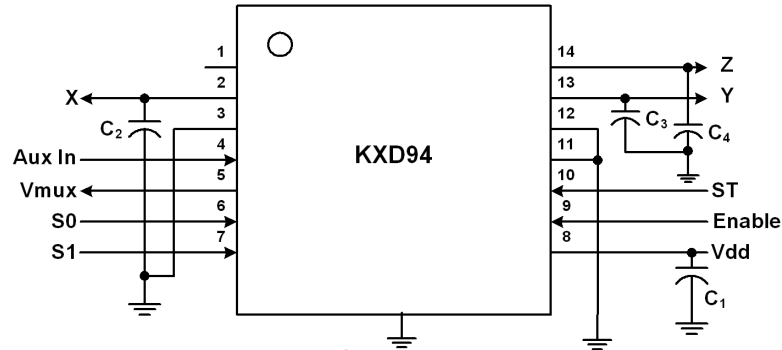


Table 4. KXD94 Pad Descriptions

Pad	Name	Description
1	NC	Not Connected Internally (can be connected to Vdd or Gnd)
2	X output	Analog output of the x-channel. Optionally, a capacitor (C ₂) placed between this pin and ground will form a low pass filter. Connect to Vdd or Ground if not used.
3	GND	Ground
4	Aux In	Auxiliary input for multiplexer. Connect to Vdd or Ground if not used. Input Impedance is 1KΩ
5	Vmux	Multiplexed analog output. Do not connect if multiplexer is not used.
6	S0	MUX selector 0 (See Output Select Table). Connect to Vdd or Ground if not used.
6 ^f	SDO	SPI Serial Data Output
7	S1	MUX selector 1 (See Output Select Table). Connect to Vdd or Ground if not used.
7 ^f	SCLK	SPI Communication Clock
8	Vdd	The power supply input. Decouple this pin to ground with a 0.1uF ceramic capacitor (C ₁).
9	Enable	Enable: High - Normal operation; Low - Device is in standby, power down mode
9 ^f	nCS	SPI Chip Select
10	ST	Self test. The output of a properly functioning part will increase when Vdd is applied to the self-test pin. (see Table 2)
10 ^f	SDI	SPI Serial Data Input
11	NC	Not Connected Internally (can be connected to Vdd or Gnd)
12	GND	Ground
13	Y Output	Analog output of y-channel. Optionally, a capacitor (C ₃) placed between this pin and ground will form a low pass filter. Connect to Vdd or Ground if not used.
14	Z Output	Analog output of z-channel. Optionally, a capacitor (C ₄) placed between this pin and ground will form a low pass filter. Connect to Vdd or Ground if not used.
	Center pad	Ground

Note 1: Pins 6,7,9,and 10 are used for SPI communication when nCS (Chip Select) is low.

Important Technical Note: Power Up / Power Down

Proper functioning of power-on reset (POR) is dependent on the specific Voff and Toff profile of individual applications. It is recommended to minimize Voff and maximize Toff. The application should be evaluated with the range of Voff and Toff expected within the application as POR performance can vary depending on these parameters. In order to guarantee proper reset regardless of Voff and Toff, a software reset can be issued via the SPI protocol. Please refer to Technical Note **KXR94 and KXD94 Accelerometer Reset Sequence** document to ensure proper POR function in your application.



**± 10g Tri-axis Accelerometer
Specifications**

PART NUMBER:

**KXD94-2802
Rev. 2
May-2014**



± 10g Tri-axis Accelerometer Specifications

PART NUMBER:

KXD94-2802
Rev. 2
May-2014

Application Design Equations

The bandwidth is determined by the internal 1kHz low pass filter. The user can lower the bandwidth by placing filter capacitors connected from pins 2, 13 and 14 to ground. The response is single pole. Given a desired bandwidth, f_{BW} , the filter capacitors are determined by:

$$C_2 = C_3 = C_4 = \frac{4.97 \times 10^{-6}}{f_{BW}}$$

The response time (RT) is determined by the equation:

$$RT = 5 \times R_{int} \times C_{ext}$$

R_{int} is the 32K Ω internal resistor. C_{ext} is the external resistor C_2 , C_3 , and C_4 .

Output is a function of t (time) for constant Resistance and Capacitance. Out_{in} is the output during normal operation. The function for output during selftest actuation is described by:

$$Output = Out_{in} * (1 - e^{-t/RC})$$

Power Up / Power Down

Proper functioning of power-on reset (POR) is dependent on the specific Voff and Toff profile of individual applications. It is recommended to minimize Voff and maximize Toff. The application should be evaluated with the range of Voff and Toff expected within the application as POR performance can vary depending on these parameters.



± 10g Tri-axis Accelerometer Specifications

PART NUMBER:

KXD94-2802
Rev. 2
May-2014

Multiplexed Output of the KXD94

Multiplexer Data Select

The KXD94 features an integrated 4-channel multiplexer. This feature reduces system MCU requirements to only 1 ADC and 2 digital I/O's. The KXD94 uses two select inputs (S0, S1) to control the data flow from Vmux, which is a high impedance output. When a microprocessor toggles the select inputs, the desired output is attained based on the Output Select Table 5. Note that logic 0 is GND and logic 1 is Vdd.

Table 5. Output Select Table

S0	S1	Vmux
0	0	X Output
0	1	Z Output
1	0	Y Output
1	1	Aux. In

Data Sampling Rate

When operating in its multiplexed mode, the KXD94 has the ability to achieve very high data sampling rates. Internally, the sensor elements (X, Y) are sequentially sampled in a "round robin" fashion at a rate of 32KHz per axis. Note that this is a differential capacitance sampling of each sensor element, which stores an analog voltage on the filter cap for each axis. Combine this high sensor element-sampling rate with the short 5µs settling time of the integrated multiplexer, and the user can achieve a performance very close to that of the X and Y analog outputs. This is more than sufficient to eliminate any aliasing in the final application since the KXD94 will be operating with a typical bandwidth of ~50Hz and a maximum of 1000Hz.

	± 10g Tri-axis Accelerometer Specifications	PART NUMBER: KXD94-2802 Rev. 2 May-2014
---	--	--

KXD94 Digital Interface

The Kionix KXD94 digital accelerometer has the ability to communicate on a SPI digital serial interface bus. This flexibility allows for easy system integration by eliminating analog-to-digital converter requirements and by providing direct communication with system micro-controllers.

The serial interface terms and descriptions as indicated in Table 6 below will be observed throughout this document.

Table 6. Serial Interface Terminologies

Term	Description
Transmitter	The device that transmits data to the bus.
Receiver	The device that receives data from the bus.
Master	The device that initiates a transfer generates clock signals and terminates a transfer.
Slave	The device addressed by the Master.

The chip will ignore all SPI activity when nCS is held high, and the analog function will run. The analog function is powered down whenever nCS is low, but the SPI bus will function, allowing communication to enable and reset the KXD94.



± 10g Tri-axis Accelerometer Specifications

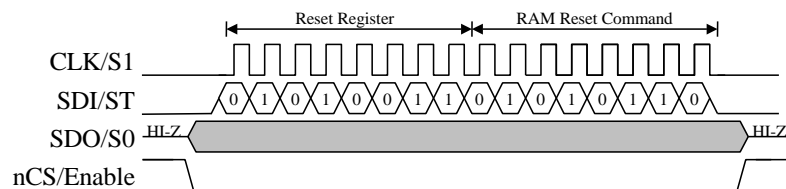
PART NUMBER:

KXD94-2802
Rev. 2
May-2014

Accelerometer SPI Reset Sequence:

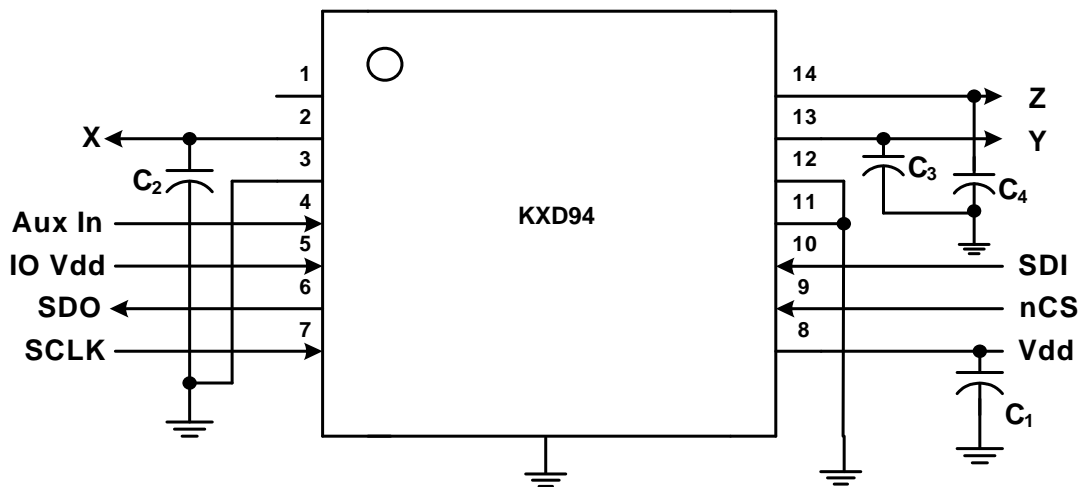
1. Power up KXD94
2. Toggle nCS (Pin 9)
 - a. nCS low to select
 - b. nCS high for at least 200nS (SCLK = 5MHz)
 - c. nCS low to select
3. Send Reset Command per Figure 2 (SDI is latched on rising edges of CLK) Note that it takes 16mSec for the Reset command to execute.

Figure 2. Reset command timing Diagram



4. Set nCS to high (Logic '1') for Normal Analog Operation.

Figure 3. Application Schematic for SPI Reset





± 10g Tri-axis Accelerometer Specifications

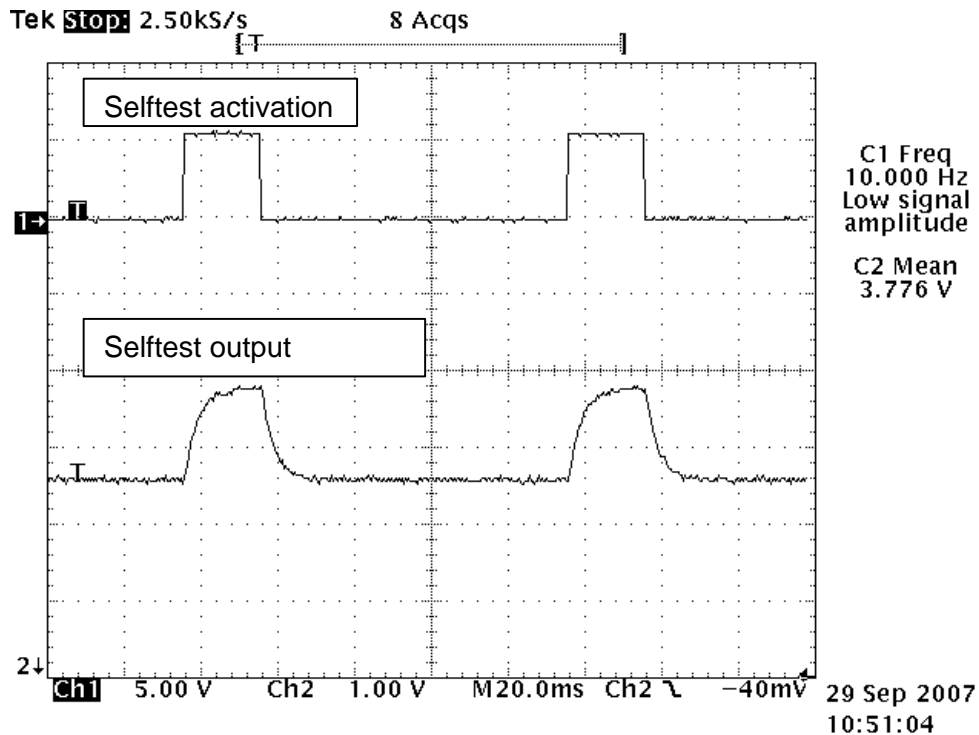
PART NUMBER:

KXD94-2802
Rev. 2
May-2014

Self Test Function

The selftest is activated when 'logic 1' is applied to the ST pin (See Figure 1). An electrostatic force is applied to the sense element that causes the mass to move and the output increases. The selftest function exercises the X and Y sense elements and ASIC blocks. The output change of the selftest function is modified by the internal 1kHz LPF and the external LPF that is defined by the ASIC internal resistance and the external capacitor. Figure 4 is an example of the selftest output with a 50Hz external LPF. The selftest is actuated at 10 Hz and 25% duty cycle.

Figure 4: Selftest Function for KXD94





± 10g Tri-axis Accelerometer Specifications

PART NUMBER:

KXD94-2802
Rev. 2
May-2014

Test Specifications

The performance parameters and characteristics are validated by Design methodology; Design Validation tests; and Product-Production Validation tests. A test control plan has been developed to verify product conformance to specification prior to shipment. Table 7 is a summary of these tests.

Table 7. Test Specifications

Parameter	Specification	Test Conditions
Zero-g Offset @ RT	2.5 +/- 0.05 V	25C, Vdd = 5 V
Sensitivity @ RT	200 +/- 7 mV/g	25C, Vdd = 5 V
Current Consumption -- Operating	900 <= Idd <= 1500 uA	25C, Vdd = 5 V



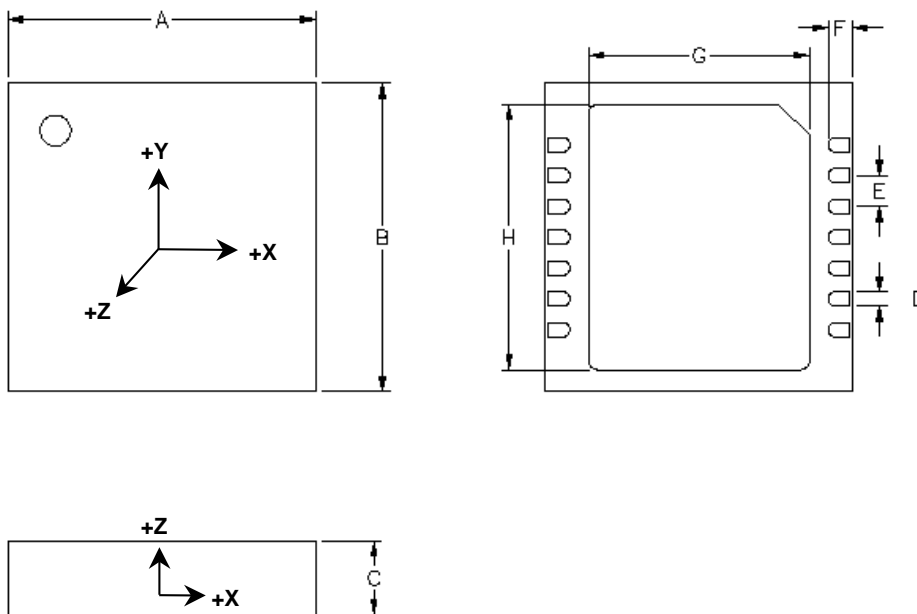
± 10g Tri-axis Accelerometer Specifications

PART NUMBER:

KXD94-2802
Rev. 2
May-2014

Package Dimensions and Orientation

Figure 5. 5x5x1.2mm DFN Package and Acceleration sign convention



All dimensions and tolerances conform to ASME Y14.5M-1994

Dimension	mm			inch		
	Min	Nom	Max	Min	Nom	Max
A		5.00			0.197	
B		5.00			0.197	
C	1.10	1.20	1.30	0.043	0.047	0.051
D	0.18	0.23	0.28	0.007	0.009	0.011
E		0.50			0.020	
F	0.35	0.40	0.45	0.014	0.016	0.018
G	3.50	3.60	3.70	0.138	0.142	0.146
H	4.20	4.30	4.40	0.165	0.169	0.173

When device is accelerated in +X, +Y, and +Z direction, the corresponding output will increase.



± 10g Tri-axis Accelerometer Specifications

PART NUMBER:

**KXD94-2802
Rev. 2
May-2014**

Static X/Y Output Response versus Orientation to Earth's surface (1g):

(Outputs for ±1.33g KXD94)

Position	1	2	3	4	5	6
Diagram					Top Bottom	Bottom Top
X	2.5 V	2.7 V	2.5 V	2.3 V	2.5 V	2.5 V
Y	2.7 V	2.5 V	2.3 V	2.5 V	2.5 V	2.5 V
Z	2.5 V	2.5 V	2.5 V	2.5 V	2.7 V	2.3 V
Polarity	0	+	0	-	0	0
Polarity	+	0	-	0	0	0
Polarity	0	0	0	0	+	-

↓ (1g)

Earth's Surface

	± 10g Tri-axis Accelerometer Specifications	PART NUMBER: KXD94-2802 Rev. 2 May-2014
---	--	--

Revision History

REVISION	DESCRIPTION	DATE
1	Updated approval list. Corrected Table 4 pin description for AUX In.	05-Oct-2009
2	Added POR design note	12-May-2014

"Kionix" is a registered trademark of Kionix, Inc. Products described herein are protected by patents issued or pending. No license is granted by implication or otherwise under any patent or other rights of Kionix. The information contained herein is believed to be accurate and reliable but is not guaranteed. Kionix does not assume responsibility for its use or distribution. Kionix also reserves the right to change product specifications or discontinue this product at any time without prior notice. This publication supersedes and replaces all information previously supplied.

APPENDIX E:
DETAILED SUPPORTING ANALYSIS

Equations Window

Spindle Stress Resolution Equations

$$R_o = 0.5 \text{ [in]}$$

$$R_i = 0.3125 \text{ [in]}$$

$$A_s = P \cdot (R_o^2 - R_i^2)$$

$$I = P / 4 \cdot (R_o^4 - R_i^4)$$

$$y = R_o$$

$$\text{HorizontalOffset} = 1.817 \text{ [in]}$$

$$R_w = 11 \text{ [in]}$$

$$\text{theta} = 10$$

$$S_u = 39879.4 \text{ [psi]}$$

$$S_l = -41358.7 \text{ [psi]}$$

$$S_b = -20683 \text{ [psi]}$$

$$S_u = -B / A_s + M_b \cdot \cos(\text{theta}) \cdot y / I - M_c \cdot y / I$$

$$S_l = -B / A_s - M_b \cdot \cos(\text{theta}) \cdot y / I + M_c \cdot y / I$$

$$M_b = B \cdot R_w$$

$$S_b = -B / A_s - M_a \cdot y / I + M_b \cdot \sin(\text{theta}) \cdot y / I$$

$$A = M_a / \text{HorizontalOffset}$$

$$C = M_c / \text{HorizontalOffset}$$

Hand Calc Equations

DAQ Resolution Results

DAQ Resolution Calculations		
Max Strain	350	Micro-Strain
Volts	5	
Steps	819.2	over full range
Resolution	0.43	Micro-Strain
	0.1%	of max Strain per step
	1.2%	35 Micro-Strain
Full Range	25	V
Full Steps	4096	steps
Used Range	10	V
Steps per range	1638.4	
	0.006104	mV per step [Resolution]

Shocker Rocker Bending Results

Shocker Rocker Bending Calcs		
b	0.1	in
h	1	in
I	0.008333	in ⁴
F	600	
d	0.85	
M	510	
y	0.5	
Bending Stress	15300	psi

Rear Frame Bending Results

Rear Frame Tube Bending		
d	1.5	in
F	600	lbf
Ro	1	in
Ri	0.902	in
I	0.017	in ⁴
A	0.146	in ²
M	900	in-lbf
y	0.5	in
Bending Stress	27118.4	psi
Axial Stress	4098.5	psi
E	29000000	psi
L	25	in
Deflection	0.073	in

APPENDIX F:
GANTT CHART

Task Mode	Task Name	Duration	Start	Finish	Predecessors	Resou
1	Design	50 days	Thu 5/1/14	Wed 7/9/14		
2	+ Front Suspension	21 days	Thu 5/1/14	Thu 5/29/14		
12	+ Rear Suspension	21 days	Thu 5/1/14	Thu 5/29/14		
30	- Chassis	21 days	Fri 5/30/14	Fri 6/27/14	2	
31	+ Skid Plate	21 days	Fri 5/30/14	Fri 6/27/14		
41	+ Frame	21 days	Fri 5/30/14	Fri 6/27/14		
51	+ Drivetrain	24 days	Fri 5/30/14	Wed 7/2/14	2	
62	+ Testing Design	5 days	Thu 7/3/14	Wed 7/9/14	51,30,12,2	
73	- Build	39 days	Thu 9/25/14	Tue 11/18/14	51,30,12,2	
74	+ Ordering	25 days	Thu 9/25/14	Wed 10/29/14		
87	Mount Gauges	11 days	Thu 10/30/14	Thu 11/13/14	74	
88	Run Wiring	3 days	Fri 11/14/14	Tue 11/18/14	75,87	
89	Rocker	10 days	Thu 10/30/14	Wed 11/12/14	74	
90	Rocker Link	2 days	Thu 10/30/14	Fri 10/31/14	74	
91	Rocker Tabs	2 days	Thu 10/30/14	Fri 10/31/14	74	
92	- Test	42 days	Wed 11/19/14	Thu 1/15/15	73	
93	+ Bench test to calibrate gauges	13 days	Wed 11/19/14	Fri 12/5/14		
98	+ Initial on-car test	7 days	Mon 12/8/14	Tue 12/16/14	93	
103	+ Analysis of Data from first tests	8 days	Wed 12/17/14	Fri 12/26/14	98	
108	+ Supplemental Testing	14 days	Mon 12/29/14	Thu 1/15/15	103	
113	- Documentation	271 days	Thu 5/1/14	Thu 5/14/15		
114	Project Proposal	1 day	Thu 5/1/14	Thu 5/1/14		
115	Conceptual Design Report	9 days	Mon 5/26/14	Thu 6/5/14	114	
116	Final Design Report	21 days	Thu 9/25/14	Thu 10/23/14	115,1	
117	Compilation and Presentation of data	20 days	Fri 1/16/15	Thu 2/12/15	92	
118	Final Report	60 days	Fri 2/13/15	Thu 5/7/15	116,117	
119	Baja Quick Guide	5 days	Fri 5/8/15	Thu 5/14/15	118	

Gantt Chart

APPENDIX G:
OTHER SUPPORTING MATERIAL



OMEGA® User's Guide



SG401



SG496

*Shop online at
omega.com®*

*e-mail: info@omega.com
For latest product manuals:
www.omegamanual.info*

**SG401 and SG496
Rapid Cure Strain Gauge
Adhesives**



SECTION 1 - INTRODUCTION

OMEGA's Rapid Cure Adhesives, SG401 and SG496 are modified versions of a solvent-free cyanide-acrylate adhesive specially developed to apply strain gauges of the bonded-resistance type. They are suitable for all series of strain gauges and compatible with most metals of common use and with most synthetic materials. They are not suitable, however, for use with porous materials such as concrete, wood, foam plastic, etc. This series of Strain Gauge Adhesives is supplied in three different packages. Their part numbers and weights are listed below:

Part Number	Net Weight
SG401	0.10 oz.
SG496	1.00 oz.

SECTION 2 - SETTING AND CURING NOTES

Polymerization (setting) of cyanide-acrylate adhesives occurs by the catalytic reaction of moisture absorbed from the air. The most favorable conditions are given by a relative humidity (RH) between 40% and 70%. In the case of RH less than 30%, the reaction is noticeably retarded and in extreme cases, completely stopped. More than 80% RH causes shock setting. Internal stresses in the adhesive layer caused by shock setting reduce the maximum extensibility of the bond. One should, therefore, always ensure that the limit values of 30% and 80% RH are not exceeded.

Complete setting in the given time is achieved only with thin films. Thick layers of adhesive set very slowly and incompletely; therefore, extremely rough contact surfaces are unsuitable.

The setting speed depends on the chemical condition of the components to be bonded. Alkaline materials accelerate polymerization, whereas acid materials not only retard but can completely prevent setting. (In the latter case, a neutralizer should be used.) Representative figures for the setting time and its dependence upon the quoted materials at a temperature of 20°C (68°F) and an RH of 65% are given in Table 2-1. At the end of these periods, the adhesive will have set sufficiently to allow cable connection to be initiated. **Ultimate curing is achieved after some 24 hours.** However, measurements can be taken after the periods quoted in Table 2-2.



**TABLE 2-1
MINIMUM SETTING TIME FOR BONDING**

Material	Setting Time
Steel	60 to 120 sec.
Aluminum	50 to 100 sec.
Plastics	10 to 60 sec.

**TABLE 2-2
MINIMUM CURING TIME FOR MEASUREMENT**

Type of Measurement	Curing Time	
	At 5°C (41°F)	20°C (68°F)
Dynamic	90 min.	10 min.
Static	120 min.	15 min.

SECTION 3 - PREPARING THE SURFACE

The object of preparation is to create a smooth surface that can be wetted. The following steps, which require attention or can be bypassed, depends on the condition of the test piece.

3.1 Coarse Cleaning

Rust, scale, paint, and other such contaminants must be removed from the test area and its surroundings.

3.2 Smoothing Surface

Pitting, protrusions, scratches, and other such imperfections must be removed by grinding, filing, or other suitable methods.

3.3 De-greasing

The choice of a cleaning agent depends on the nature of the contamination and whether the surface is adversely affected by a given cleanser. Powerful grease solvents such as Freon TF, Chlorothene NU, methyl-ethyl-ketone, acetone, and trichlorethylene are normally used. Wax and similar substances dissolve in toluene.

The surface to be cleaned should be washed with gauze pads soaked in solvent. Initial treatment should cover a somewhat larger area than that which is ultimately required. As each new pad of gauze is taken, the zone that receives attention should be progressively reduced to minimize the possibility of continually introducing new particles of dirt from the edges of the zone. Large areas can be brushed with water and an abrasive powder (e.g. AJAX, COMET, etc.). After rinsing, there should remain a surface which is completely wetted with an unbroken film of water. The surface is then dried with a clean cloth (paper towel) or by heat. Ultrasonic cleaning baths or steam degreasing apparatuses can also be used with good effect.



NOTE

The solvent must be chemically clean and should leave no residue. It should never be used directly from the container in which it is stored. A quantity should be transferred to a clean bowl and used from there. Unused fluid in the bowl should never be returned to stock! Use pads of gauze just once and then dispose of them. Never dip a used pad into the solution a second time!

3.4 Surface Roughening

The adhesion between bonded parts depends on the adhesion of the cement with the surfaces wetted by it. Roughening of the surface on the specimen will improve the adhesion by increasing the active surface. Emery paper or cloth should be moved in circles in order to avoid any preferred direction of grooves. Make sure to use only fresh emery paper of a grade that matches the hardness of the specimen material (e.g., for steel use grade 80 to 180; for aluminum use grade 220 to 360). If the roughness becomes too great, air bubbles might form which would prevent effective bonding. The material must be absolutely free of oil and grease. Any surface grooving that might have resulted from the foregoing process must be removed.

If one is familiar with etching processes, this too is possible. If no interference with the surface finish of the test piece is acceptable, the adhesives can be used on smooth or polished surfaces, although its maximum extensibility is then reduced.

3.5 Fine Cleaning

All dirt and dust resulting from the roughening process should be removed carefully. This is achieved with gauze pads soaked in one of the solvents noted in section 3.3. Each pad should be held with clean tweezers and passed over the surface only once. The process should be repeated until the pads show no trace of discoloration. Possible remaining lint should be removed with clean tissue paper. Keep the cleaned area dry! Do not blow with breath or touch with fingers!

To avoid the incidence of new oxidation, the mechanical or chemical treatment of the surface should occur just before adhesion.



SECTION 4 - PREPARATION OF THE STRAIN GAUGE

Prior to attaching the gauge, some users prefer to solder the connections between the gauge and terminal pad, while others prefer to solder after attaching the gauge.

The bonding side of the strain gauge should be carefully cleaned with a gauze pad soaked in Freon, Frigen, or carbon-tetrachloride. Residual moisture must be dried by a radiant heater or a hot-air blower. During this procedure, the strain gauge must be held by tweezers.

SECTION 5 - ATTACHING THE STRAIN GAUGE

Because of the short curing time, it is not possible to readjust the position of the strain gauge once the adhesion process has been initiated.

The gauge width should be extended with a short length of adhesive tape affixed to the upper surface of the gauge, away from the connections. If soldering is to be done after attaching the gauge, protect the solder terminals with tape.

The strain gauge is laid onto the cleaned area of the test piece, and after careful alignment, the protruding part of the adhesive tape is pressed onto the surface (use tweezers). This results in a hinge-like fixture that allows the strain gauge to flap up and down without changing its alignment (see Figure 5-1).

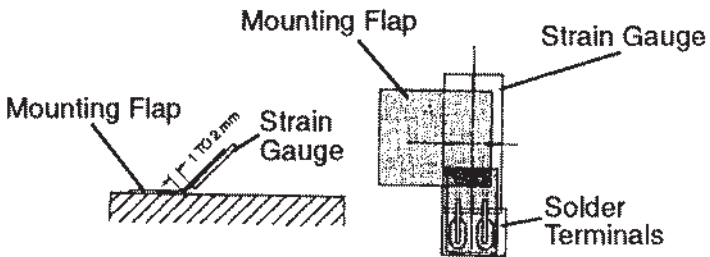


Figure 5-1: Strain Gauge and Mounting Flap

Flip the strain gauge up to expose the adhesion area. Cut off a length of the Teflon® film. If the adhesion area is more than 15 mm (0.6 inch) wide, cut the Teflon strip diagonally. Place one drop of the adhesive onto the adhesion area. Using the Teflon film, distribute the adhesive into a uniformly thin layer by brushing over it just once and lightly pressing the Teflon film downwards. Use as little pressure as possible (see Figure 5-2) because the adhesive will cure immediately if the pressure is too great.

Acid materials delay or inhibit setting of the adhesive. If the bonding surface is acidic, apply a thin coat of neutralizer onto the bonding side of the strain gauge, just enough to wet it. Allow this to dry.

The strain gauge is then carefully flapped over to meet the adhesive surface and covered with Teflon film. Press the Teflon film covering the



adhesive tape and strain gauge until the adhesive has set (see Table 2-1). After a few minutes, remove the Teflon film and carefully release the strain gauge connections from the adhesive. The thickness of the adhesive film in a correctly adhered gauge is 8 micrometers \pm 20%. After curing, remove the alignment adhesive tape by peeling it back onto itself at an acute angle.

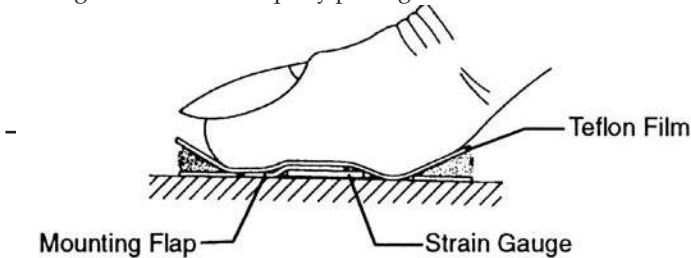


Figure 5-2 : Affixing the Strain Gauge

Experience has shown that problems with the setting of cyanide-acrylates are due mainly to layers of adhesive that are too thick. Therefore, a neutralizer should be used only if a very thin adhesive layer can be guaranteed. The measuring point should be protected against damp chemicals and mechanical damage.

Experience has shown that problems with regard to the setting of cyanide-acrylates are due mainly to layers of adhesive which are too thick. Therefore, a neutralizer should be used only if a very thin adhesive layer can be guaranteed. The measuring point should be protected against damp chemicals and mechanical damage.

SECTION 6 - ATTACHING THE LEAD WIRES

Solder all terminals and secure the instrumentation wire in place, either with adhesive or by mechanical means (see Figure 6-1). After soldering, it is imperative that all soldering points are cleaned of flux residues (even non-corrosive fluxes are hygroscopic and require cleaning).

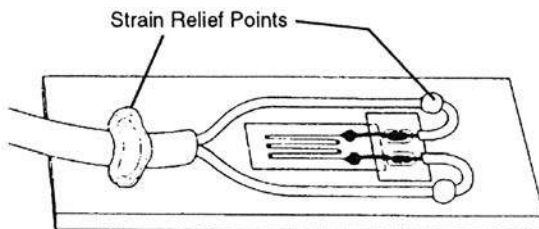


Figure 6-1: Strain Gauge and Lead Wires

A covering should be used to protect the strain gauge from environmental effects. De-grease the entire area and apply the covering (a layer of adhesive) over the strain gauge and lead wire assembly, as shown in Figure 6-2. Cover at least 20 mm (0.8 inch) of the lead wire.

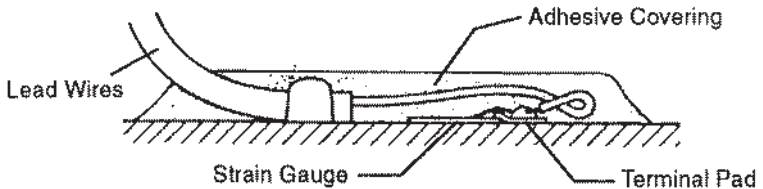


Figure 6-2: Covered Strain Gauge

SECTION 7 - STORAGE

Keep the bottle (or tube) in an upright position, to prevent the adhesive from dripping out and hardening at the drip nozzle and on the screw cap thread. If the adhesive has not been used for a long time, it will harden and seal the tip. Once the tip has been cleaned or cut, the adhesive can be reused.

Protect the adhesive from heat, sunlight, and humidity. Store it in a cool, dry place. The adhesive can be used until its viscosity rises considerably.

A virtually unlimited storage life can be achieved if the adhesive is kept frozen at -15°C (5°F). Before use, defrost the adhesive, making sure it has reached ambient temperature. Repeated freezing does not affect the adhesive.

SECTION 8 - SAFETY MEASURES

Observe the safety regulations, valid in your country, which are designed to avoid accidents associated with the use of adhesives and solvents.

The adhesive itself can do no serious physiological harm. Since it clings to the skin, however, contact should be avoided. Protective goggles should be used. Should, however, the adhesive come into contact with the eyes, rinsing thoroughly with water or boracic solution is necessary. A doctor should be consulted immediately. From previous experience, it has been found that corneal damage heals within a few days and sight remains unimpaired.



omega.com info@omega.com

Servicing North America:

U.S.A.:

Omega Engineering, Inc., One Omega Drive, P.O. Box 4047
Stamford, CT 06907-0047 USA

Toll-Free: 1-800-826-6342 (USA & Canada only)

Customer Service: 1-800-622-2378 (USA & Canada only)

Engineering Service: 1-800-872-9436 (USA & Canada only)

Tel: (203) 359-1660

Fax: (203) 359-7700

e-mail: info@omega.com

For Other Locations Visit omega.com/worldwide

The information contained in this document is believed to be correct, but OMEGA accepts no liability for any errors it contains, and reserves the right to alter specifications without notice.

WARNING: These products are not designed for use in, and should not be used for, human applications.



WARRANTY/DISCLAIMER

OMEGA ENGINEERING, INC. warrants this unit to be free of defects in materials and workmanship for a period of **13 months** from date of purchase. OMEGA's WARRANTY adds an additional one (1) month grace period to the normal **one (1) year product warranty** to cover handling and shipping time. This ensures that OMEGA's customers receive maximum coverage on each product.

If the unit malfunctions, it must be returned to the factory for evaluation. OMEGA's Customer Service Department will issue an Authorized Return (AR) number immediately upon phone or written request. Upon examination by OMEGA, if the unit is found to be defective, it will be repaired or replaced at no charge. OMEGA's WARRANTY does not apply to defects resulting from any action of the purchaser, including but not limited to mishandling, improper interfacing, operation outside of design limits, improper repair, or unauthorized modification. This WARRANTY is VOID if the unit shows evidence of having been tampered with or shows evidence of having been damaged as a result of excessive corrosion; or current, heat, moisture or vibration; improper specification; misapplication; misuse or other operating conditions outside of OMEGA's control. Components in which wear is not warranted, include but are not limited to contact points, fuses, and triacs.

OMEGA is pleased to offer suggestions on the use of its various products. However, OMEGA neither assumes responsibility for any omissions or errors nor assumes liability for any damages that result from the use of its products in accordance with information provided by OMEGA, either verbal or written. OMEGA warrants only that the parts manufactured by the company will be as specified and free of defects. OMEGA MAKES NO OTHER WARRANTIES OR REPRESENTATIONS OF ANY KIND WHATSOEVER, EXPRESSED OR IMPLIED, EXCEPT THAT OF TITLE, AND ALL IMPLIED WARRANTIES INCLUDING ANY WARRANTY OF MERCHANTABILITY AND FITNESS FOR A PARTICULAR PURPOSE ARE HEREBY DISCLAIMED. LIMITATION OF LIABILITY: The remedies of purchaser set forth herein are exclusive, and the total liability of OMEGA with respect to this order, whether based on contract, warranty, negligence, indemnification, strict liability or otherwise, shall not exceed the purchase price of the component upon which liability is based. In no event shall OMEGA be liable for consequential, incidental or special damages.

CONDITIONS: Equipment sold by OMEGA is not intended to be used, nor shall it be used: (1) as a "Basic Component" under 10 CFR 21 (NRC), used in or with any nuclear installation or activity; or (2) in medical applications or used on humans. Should any Product(s) be used in or with any nuclear installation or activity, medical application, used on humans, or misused in any way, OMEGA assumes no responsibility as set forth in our basic WARRANTY/DISCLAIMER language, and, additionally, purchaser will indemnify OMEGA and hold OMEGA harmless from any liability or damage whatsoever arising out of the use of the Product(s) in such a manner.

RETURN REQUESTS / INQUIRIES

Direct all warranty and repair requests/inquiries to the OMEGA Customer Service Department. BEFORE RETURNING ANY PRODUCT(S) TO OMEGA, PURCHASER MUST OBTAIN AN AUTHORIZED RETURN (AR) NUMBER FROM OMEGA'S CUSTOMER SERVICE DEPARTMENT (IN ORDER TO AVOID PROCESSING DELAYS). The assigned AR number should then be marked on the outside of the return package and on any correspondence.

The purchaser is responsible for shipping charges, freight, insurance and proper packaging to prevent breakage in transit.

FOR **WARRANTY** RETURNS, please have the following information available BEFORE contacting OMEGA:

1. Purchase Order number under which the product was PURCHASED,
2. Model and serial number of the product under warranty, and
3. Repair instructions and/or specific problems relative to the product.

FOR **NON-WARRANTY** REPAIRS, consult OMEGA for current repair charges. Have the following information available BEFORE contacting OMEGA:

1. Purchase Order number to cover the COST of the repair,
2. Model and serial number of the product, and
3. Repair instructions and/or specific problems relative to the product.

OMEGA's policy is to make running changes, not model changes, whenever an improvement is possible. This affords our customers the latest in technology and engineering. OMEGA is a registered trademark of OMEGA ENGINEERING, INC.

© Copyright 2013 OMEGA ENGINEERING, INC. All rights reserved. This document may not be copied, photocopied, reproduced, translated, or reduced to any electronic medium or machine-readable form, in whole or in part, without the prior written consent of OMEGA ENGINEERING, INC.

Title: Understanding Twisted Pair Cable Technology**No: GEN17-1****Date: Saturday, 25 June, 2005****SUMMARY:**

This Connectivity Information Sheet will explain some of the more important factors on how twisted pair cables work.

MORE INFORMATION:

In the late 1970s, twisted pair cabling originated in the computer industry as a means of transmitting digital data over computer networks. This cable was designed to be a medium for relatively slow computer data communication. Digital data signals are relatively forgiving and can tolerate considerable interference and degradation before affecting the integrity of the signal. It is only recently that twisted pair cable began to be used to carry analog video signals, which are much more demanding.

As this trend continues to gain acceptance and become more common, we must gain the knowledge necessary to deploy it consistently in a professional environment. It is important to understand known twisted pair cable issues and testing methods so we know how to recognize and resolve installation performance issues. Using the highest quality cable, proper installation techniques, and thorough testing will maximize the quality of the image being displayed in a presentation environment and minimize expensive and time consuming troubleshooting.

There have been significant changes in the technology and performance of twisted pair cable since its inception. The development of high-speed data transfer rates for network applications and bandwidth-consuming multimedia signals has necessitated significant improvements in the overall performance of twisted pair cable. Twisted pair cable is being used for data applications for networks such as 10baseT; 100baseT; Gigabit Ethernet; and multimedia video and audio. The most common names for these cables are Category 5 (CAT 5), Category 5e, and much higher performance cable like Category 6 and Category 7. In the data world Category 5e presently supports Local Area Networks (LANs) for 100 Mbps.

Category 6 supports up to 250 Mbps and some manufacturers now claim to support up to 350 Mbps and higher. These cables support Gigabit Ethernet and many multimedia applications.

This paper will explain some of the more important factors on how twisted pair cables work; specifically it will cover the following:

Clarify and explain some of the issues involving twisted pair cable

- Electromagnetic Emissions
- Common Mode Noise

Describe some of the tests used for meeting Category 5 and Category 6 requirements and testing for performance results that pertain to the use of Minicom products

- Wiremap
- Length
- Attenuation

- Return Loss
- Near-End Crosstalk
- Equal Level Far-End Crosstalk.

Any system – whether it uses coaxial cable or twisted pair cable – that integrates source materials and a display device for the purpose of sharing information is a presentation system. Optimal image quality in a presentation environment requires special attention to all components and factors, including the type and quality of cable used as well as the cable transmission method. Maximizing the advantages of using Category 5, 5e, or 6 systems to run analog video signals while minimizing the disadvantages, requires understanding twisted pair technology, potential installation issues, and cable tests.

Electromagnetic Emissions and Common Mode Noise

Let's take a look at how twisted pair works and what issues should be considered when selecting it for your multimedia application. This twisted pair cable we are going to discuss is made of four twisted pair wires. One problem with twisted pair wire is electromagnetic emissions at high frequencies. These emissions can couple into adjacent twisted pairs. The second issue is the ability of the cable to eliminate common mode noise. Common mode noise is electrical interference induced into the cable with equal amounts of energy, in the same polarity, on both wires of a twisted pair.

This can come from sources like electric motors, air-conditioners, power transformers, fluorescent lighting ballasts, etc.

The cable designer will optimize the common mode noise rejection and the reduction of transmitted signal electromagnetic emissions by maintaining certain twist ratios (twists per foot), which are in the form of different twist ratios between pairs, and clockwise and counter-clockwise twisting between pairs within a common sheath. Each wire is covered with a dielectric insulation, and the diameter of the center conductor and its centering within the dielectric insulator are very important in maintaining uniform impedance. It is also important to note that the twisting action helps keep the wires as close together as possible.

In a well-designed and balanced multi-pair Category 5/5e/6/7 cable with consistent twist ratios and matched pair lengths, the electromagnetic interference (EMI) being emitted from the pair is reduced significantly. In addition, common mode noise from external interference and adjacent pair crosstalk is significantly improved. To see how this is important, we first must understand what happens when a balanced signal is applied to a twisted pair of wires. When a transmitter applies a balanced analog audio or video signal to a twisted pair wire, the signal is the same amplitude (voltage level) on both wires, but the signal on one of the wires is inverted to the opposite polarity. When the signal on one wire is going in a positive direction, the signal on the other wire is going in a negative direction. This is referred to as differential mode. See Figure 1.

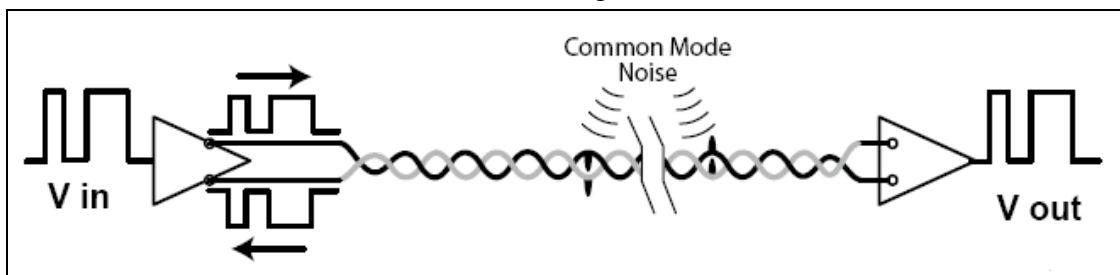


Figure 1. Common mode noise: The noise is at the same level traveling in the same direction at the same time. The noise will cancel at the receiver.

All induced common mode noise from adjacent wire pairs, as well as from other external sources such as motors, transformers, and other external sources, will cause the same noise signal to be induced into both wires equally and of the same polarity. This will cause electrons to flow in the same direction through both wires of the twisted pair, and the noise will cancel at the receiver. In balanced transmissions, the receiver is operating in a differential mode. This means it is looking for a difference between the two input signals to form an output signal. The receiver has a positive and negative input, sometimes referred to as the Tip and Ring inputs, respectively. The differential receiver performs a simple math function: it inverts the sign (polarity) of the signal at the negative input to a positive value and adds the value of the two input signals together.

Let's try it out with a signal value of +0.35 volts at the positive input and a signal value of -0.35 volts at the negative input. Now change the sign of the negative input to a +0.35 and add the two inputs together – the result is a +0.7 volts. See Figure 2.

When common mode noise is present on the twisted pair, the noise is equal in amplitude and always of the same polarity on both wires. The differential receiver processes this common mode noise in the same way as it did the signal. If we have +0.015 volts of common mode noise at both inputs, change the sign of the common mode noise at the negative input to -0.015 volts, and add the two inputs together. They will cancel out and only the original signal will be present at the output of the receiver. This would still be true if the common mode noise were negative at both inputs

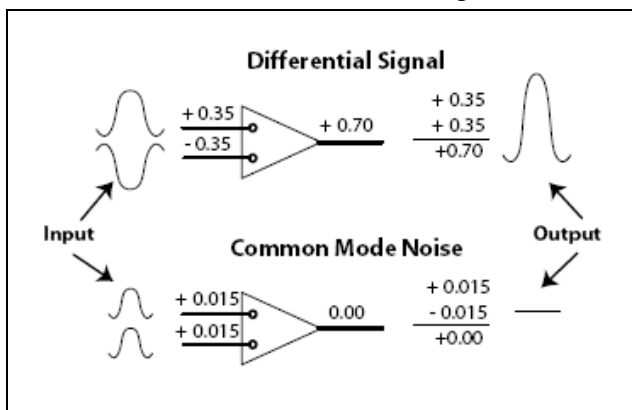


Figure 2. How common mode noise is cancelled at the receiver.

If for any reason the wires in a twisted pair were to become separated – like from a sharp bend during installation – the noise will strike the wires at slightly different angles, causing the induced signals (noise) to be slightly different in each wire. This difference will not cancel out at the receiver and, thus, will become part of the signal. At the same time, this separation will form a loop (See Figure 3) and will act as a loop antenna, picking up additional unwanted noise/crosstalk.

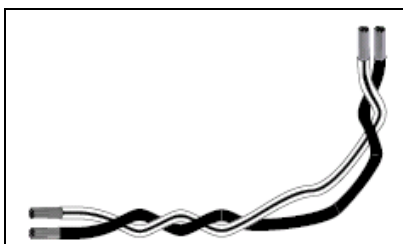


Figure 3. Twisted pair showing damaged twist pattern.

Cable Testing

Now that we have an understanding of how this cable works, we'll talk about how we're going to be sure that our new multimedia twisted pair cable installation is going to work, after we hook up Minicom CAT5 Transmitter and Receiver to display device. Just wait a minute, this is not a coax cable; it is not a "just crimp on some BNC connectors and turn everything on" type of application. As people in the data world know, it is very important that this cable run be tested to meet the stringent requirements of the CAT6 specification (the higher the quality of cable is, the higher the performance that results). To do this, we're going to use a hand-held Level Three cable tester and verify that the installation meets the requirements of Category 6. (Level Three tests for parameters up to the Category 6 standard, while Level Two tests for parameters up to the Category 5e standard.) This test will automatically perform a series of tests we're going to discuss.

The main tests that we need to be concerned with for our applications are the following:

- Wiremap
- Length
- Attenuation
- Return Loss
- Near-End Crosstalk
- Equal Level Far-End Crosstalk.

Wiremap Test

The Wiremap Test is used to identify installation-wiring errors:

- Proper pin termination at each end
- Continuity to the remote end
- Shorts between any two or more conductors
- Crossed pairs
- Split pairs
- Reversed pairs
- Any other mis-wiring.

Attenuation Test

The loss of signal strength (or voltage) in the cable is called attenuation. The more attenuation there is, the less signal there will be present at the receiver. The attenuation is measured in decibels (dB). Attenuation increases with distance and frequency. For every 6dB of loss, the original signal will be half the original amplitude. See table below.

Decibels vs. Voltage					
dB	Voltage Ratio	dB	Voltage Ratio	dB	Voltage Ratio
0	1V	-9	0.355	-18	0.125
-1	0.891	-10	0.316	-19	0.112
-2	0.794	-11	0.282	-20	0.100
-3	0.707	-12	0.250	-30	0.032
-4	0.631	-13	0.224	-40	0.010
-5	0.562	-14	0.200	-50	0.003

-6	0.500	-15	0.178	-60	0.001
-7	0.447	-16	0.158	-80	0.000
-8	0.398	-17	0.141		

Length Test

Structured cable systems for the data world have a length limit of 100 meters (328 feet) total. (Note: this restriction does not directly apply to the transmission of analog signals.)

The length test will provide us with the physical length of each pair and the delay time in nanoseconds. The delay is the time it takes for the signal to travel the entire length of the cable. This delay is a percentage of the speed of light called the Nominal Velocity of Propagation (NVP). Typical NVP varies from 60-90 percent of the speed of light from cable to cable. The delay skew is the difference in time it takes for a signal to travel down the shortest pair to the time it takes to travel down the longest pair. Lengths of wire pairs often vary within the same twisted pair cable due to small differences in twist tension and rates. The delay skew is measured in nanoseconds (ns) and feet.

For most data network applications, the delay skew limit is 45 ns; this is not acceptable for analog RGB signals. The delay skew information is very important when sending analog RGB signals over twisted pair wires and needs to be as close to zero as possible.

Depending on the resolution, the delay skew resulting from a length difference of three feet will most likely need compensation. Measurements of a typical 1024 x 768 signal with a refresh rate of 60 Hz (pixel clock of 65 MHz) showed the pixel duration to be approximately 15 ns.

For an image running at 1280 x 1024 pixels, with a refresh rate of 60 Hz (pixel clock of 135 MHz), the pixel duration was approximately 8 ns.

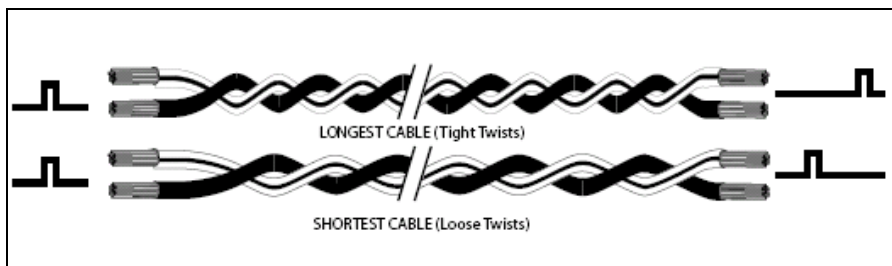


Figure 4. Delay skew: The signal traveling on the longest cable will arrive later than the signal traveling on the shortest cable, so the signals will arrive at different times.

Using Belden Media Twist cable for our reference, each foot has a delay of 1.451 ns. If there were a delay skew of five feet between a pair of wires, the delay in nanoseconds would be 7.255 (5 feet x 1.451 ns). This would be very close to one pixel width off at the 1280 x 1024 rate and half a pixel width off at the 1024 x 768 rate. If this delay skew is not compensated for, the image will appear to be out of convergence because the red, green, and blue signals will arrive at different times. See Figure 4. Delay skew is caused by differences in length between one or more of the pairs.

When transmitting multimedia analog information, we are not limited to the 100 meters (328 feet) maximum length specification for data networks (data networks are digital and have different standards). However, we need to understand that when performing a Level Three test on cable lengths that are much longer, certain tests will fail. The Length Test will always fail, and the Attenuation Test will also fail at some point. This is because these testers were designed to be used for data communications signals instead of analog signals.

The important information we need from these measurements is the delay skew in feet between the pairs in order to make the necessary compensation.

Twisted pair cable test equipment measures and reports wire pair length. (Test results on the various pair lengths can be used in equalizing pair skew.) The NVP is very close to that of conventional coax. The similarities in NVP mean that an additional length of coax equal to the length of pair skew (a 1:1 ratio), placed on the receiver's output, equalizes the effects of pair skew. For example, if there are two pairs, one with a length of 100 meters, the second with a length of 102 meters, then a 2-meter length of coaxial cable may be added at the end of the first pair's original cable run of 100 meters.

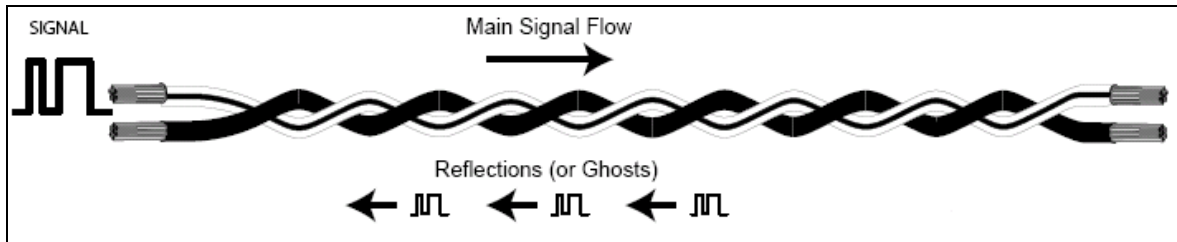


Figure 5. Reflected energy caused by impedance variations.

Return Loss Test

Return loss is a measurement of the reflected signal back toward the transmitter. This reflected energy is caused by variations of impedance in the cable and connectors. See Figure 5. This would be the equivalent of an electrical echo of the original signal. It is like when your TV is switched to a weak station and you see that the image is full of ghosts. These ghosts are nothing more than reflections of the original image. This same problem can happen with poorly terminated or damaged coax cables. The greater the variations in impedance, the greater the return loss readings. When running this test, it is important to verify that the return loss reading from all four pairs not only pass the return loss test, but also have nearly the same results. If three pairs pass with a substantial margin and the fourth pair barely passes, this might indicate a poor crimp or contact on an RJ45 connector along the transmission path. Other high return loss might be caused by damage made to the cable during installation.

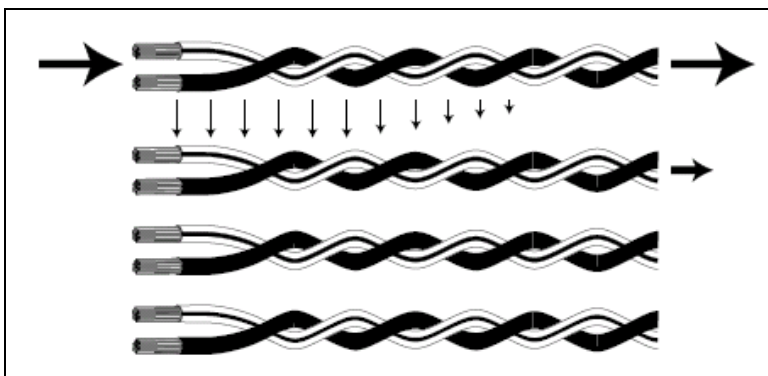


Figure 6. How Near-End Crosstalk is created.

Near-End Crosstalk (NEXT)

The NEXT measurement is the amount of signal that is induced into an adjacent twisted pair at the transmission end by the electromagnetic field created by the signal being transmitted through an adjacent pair at the same end. See Figure 6. The induced signal is strongest at this end partially because the transmitted signal is strongest at the transmitter

end. The transmitted signal gets attenuated as it travels through the cable and is weakest at the receiver, or far end. The untwisting of the cable that is required to make the termination makes this the most vulnerable part of the assembly process. Electromagnetic emissions become greater with increases in the frequency of the signal, and thus, crosstalk increases with increases in frequency. During the operation of 100-megabit and one-gigabit data systems, both ends are required to transmit and receive data simultaneously. This means that where the electromagnetic emissions are the strongest – at the transmitter – they are also very close to a receiver. With Minicom products, all signals are sent from the near end and received at the far end.

The near-end crosstalk gets attenuated somewhat by the impedance of the cable, prior to reaching the receiver. Proper termination practices and high quality cable and connectors play a very important part in keeping NEXT to a minimum.

ELFEXT (Equal Level Far-End Crosstalk)

ELFEXT is a very important measurement for our application. This is the crosstalk that reaches the receiver and has automatically had its results compensated for by variations in cable length. A short run will have less attenuation and therefore have a higher Far-End Crosstalk (FEXT) reading than a longer cable. The ELFEXT measurement automatically adjusts the FEXT results for the difference in cable lengths. If you were to test one cable of 30 meters and another at 70 meters, you would want to know how much crosstalk is reaching the receivers.

It is increasingly important for system contractors, designers, and installers to maintain skills and knowledge of system and infrastructure options. Many of the alternatives available, including twisted pair cable, have significant pitfalls that can be expensive or even disastrous to discover during a system installation. Twisted pair cable is a very attractive technology that enables unique and interesting interconnections when understood and deployed correctly.

In this paper we have discussed the workings of twisted pair cable technology. Problems such as electromagnetic emissions and common mode noise can be reduced with the use of well designed twisted pair cables and installation techniques that properly maintain a cable's twists and form. Rigorous cable testing verifies that the cable at hand meets the requirements of the standard required, Category 5, 5e, 6 or 7.

Understanding the capabilities and characteristics of twisted pair cable is only part of the system. It is equally important to carefully select the transmitter and receiver equipment and understand the effect they can have on system performance. Minicom manufactures a complete line of twisted pair cable extension and distribution equipment and makes available knowledgeable staff prepared to assist in the understanding and deployment of this and other technologies.

COMMENTS:

See Connectivity Information Sheet GEN18-1 for explanation of the skew and how to compensate it.

SUSPENSION LOADS

Front Suspension / Steering

Frontal Loading
Side Loading
Vertical Loading

Rear Suspension

Frontal Loading
Side Loading
Vertical Loading
Rear Loading

CHASSIS LOADS

Chassis

Top Roll Hoop Loading (End-O)
Front Loading
Side Loading
Rear Loading
Loading from shocks

Composites

Skid Plate

DRIVETRAIN LOADS

Drivetrain

Impulse on driveshafts from dropping with revved engine

APPENDIX H:
CALIBRATION DATA

Calibration Summary

Link Pre-Calibration

Amplification	Slope (lbf/V)						Offset (lbf)					
	L1	L2	L3	L4	L5	L6	L1	L2	L3	L4	L5	L6
Low	-1722	-1710	-1596	N/A	-1731	N/A	8412	8226	7875	N/A	8475	N/A
Mid	-992	-1144	-1077	N/A	-1165	N/A	4810	5407	5284	N/A	5648	N/A
High	-422	-411	-387	N/A	-421	N/A	1975	1751	1846	N/A	1933	N/A

Link Post-Calibration

Amplification	Slope (lbf/V)						Offset (lbf)					
	L1	L2	L3	L4	L5	L6	L1	L2	L3	L4	L5	L6
Low	-1685	-1479	-1118	-1675	-1789	-1396	8403	7145	5689	8345	9027	6859

Spindle Pre-Calibration

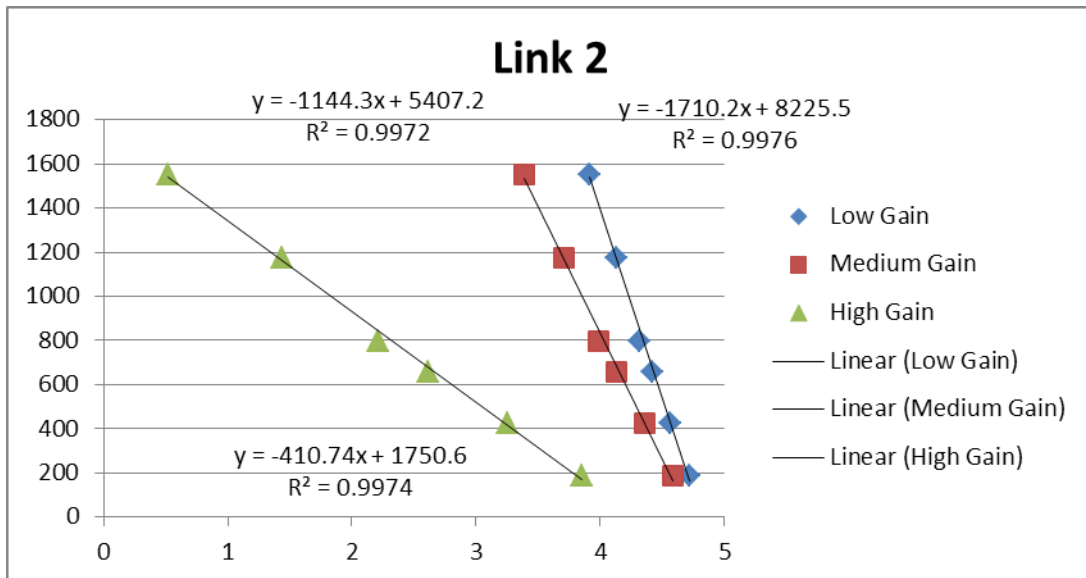
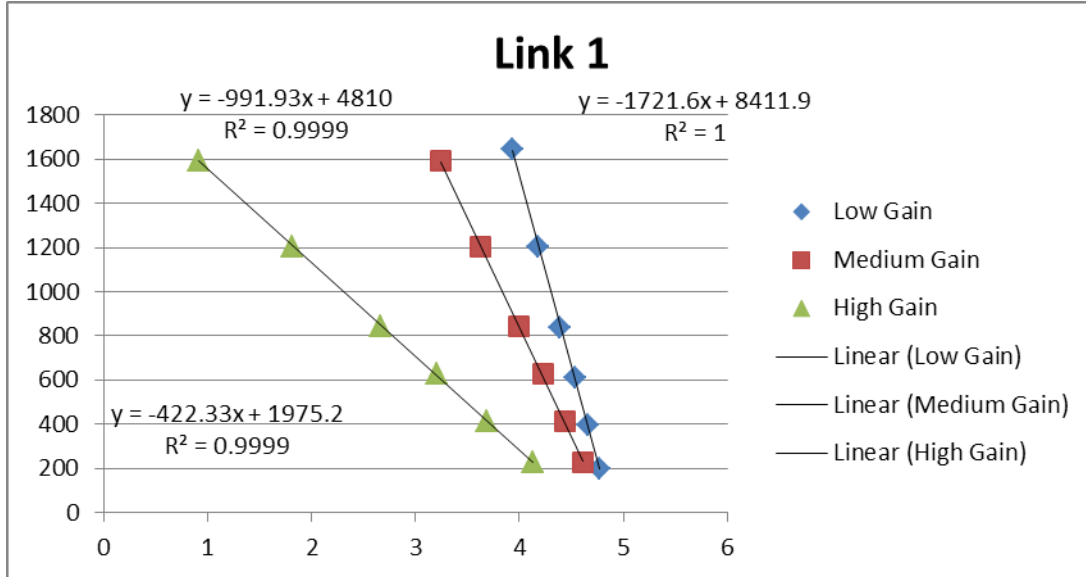
Amplification	Slope (psi/V)			Offset (psi)		
	Top	Rear	Bottom	Top	Rear	Bottom
Low	-18599	-17159	-23743	88727	84700	115885
Mid	-12464	-11422	-16219	58248	56359	78686
High	-4453	-4089	-5703	18467	20141	26794

Spindle Post-Calibration

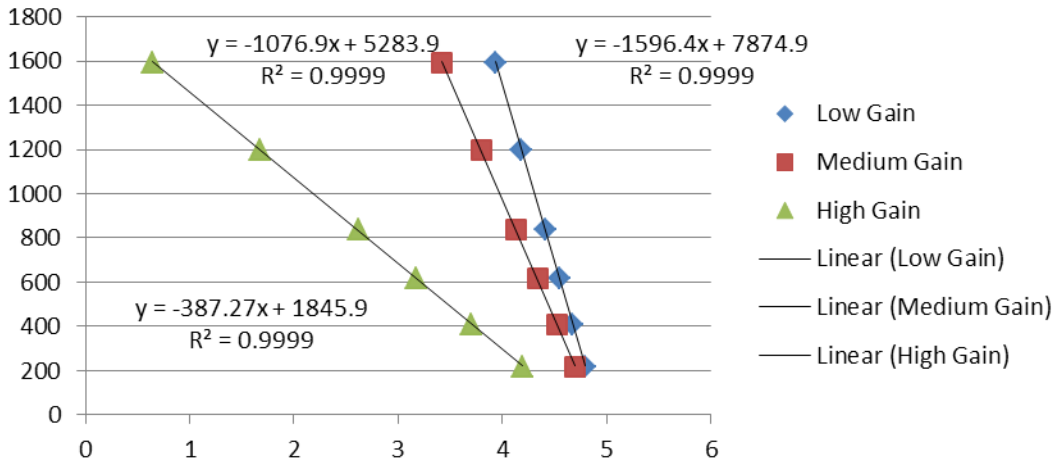
Amplification	Slope (psi/V)			Offset (psi)		
	Top	Rear	Bottom	Top	Rear	Bottom
Low	-18370	-9034	-22169	90532	42703	125557

For all plots for link calibrations, the y-axis is tensile load in lbf and the x-axis is the voltage in volts.
 For all plots for spindle calibrations, the y-axis is tensile stress in psi and the x-axis is the voltage in volts.

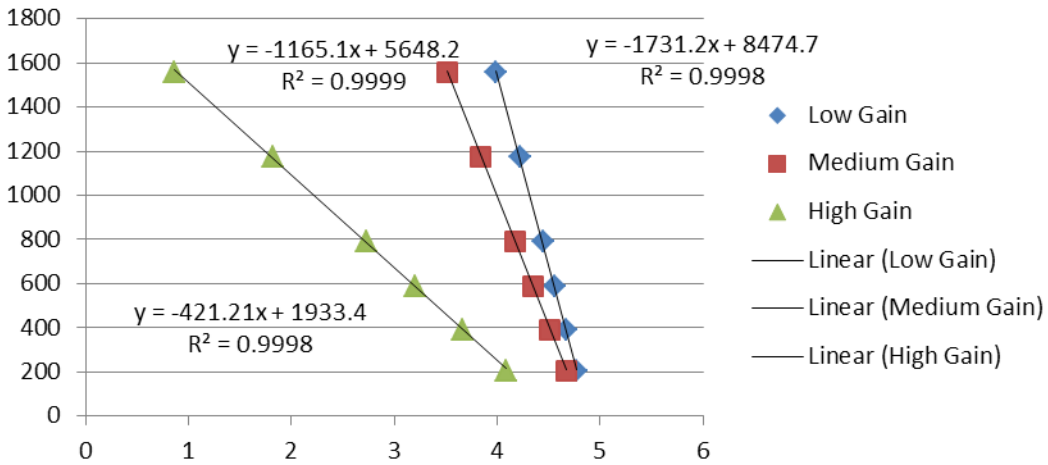
Links Calibration



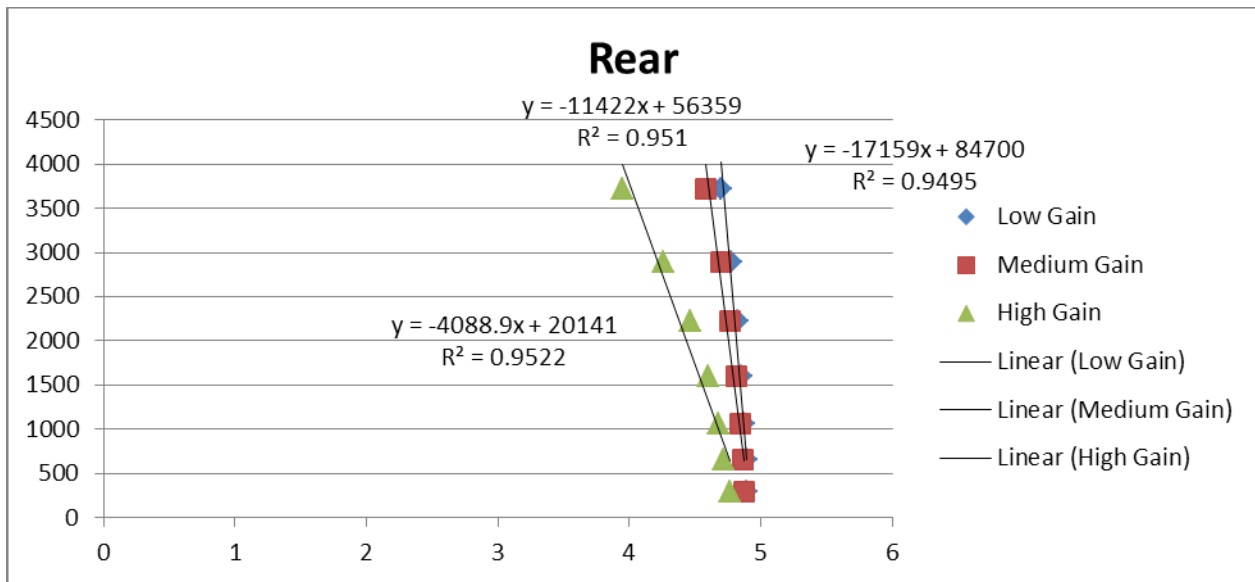
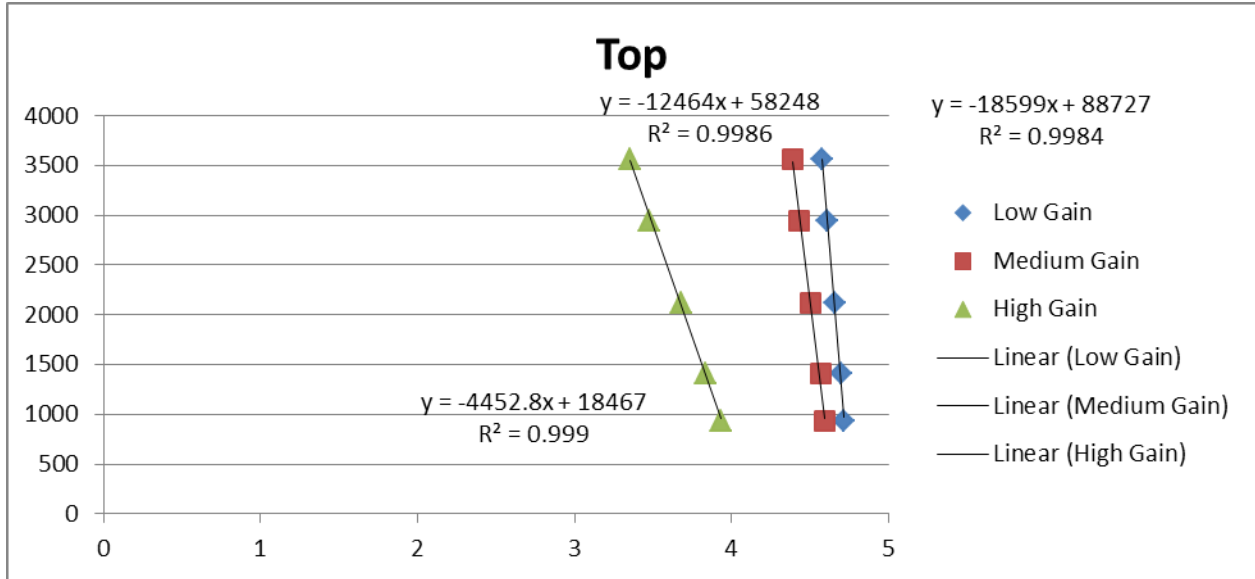
Link 3



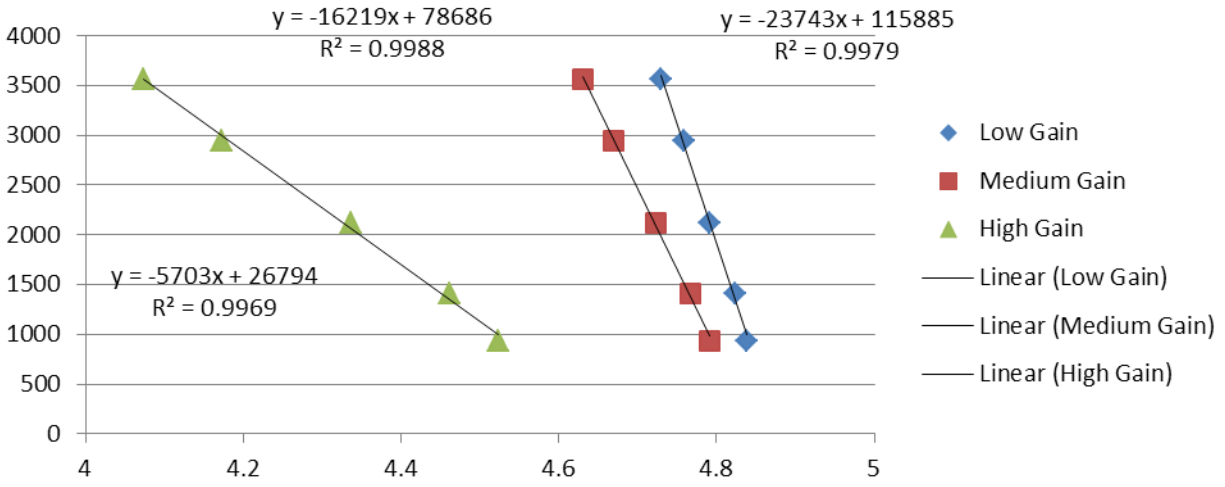
Link 5



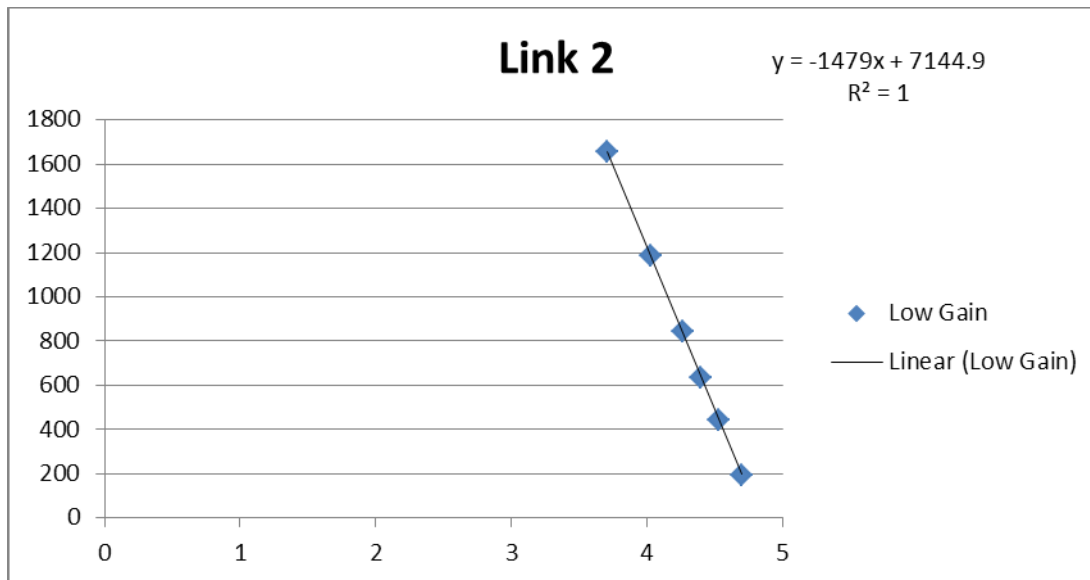
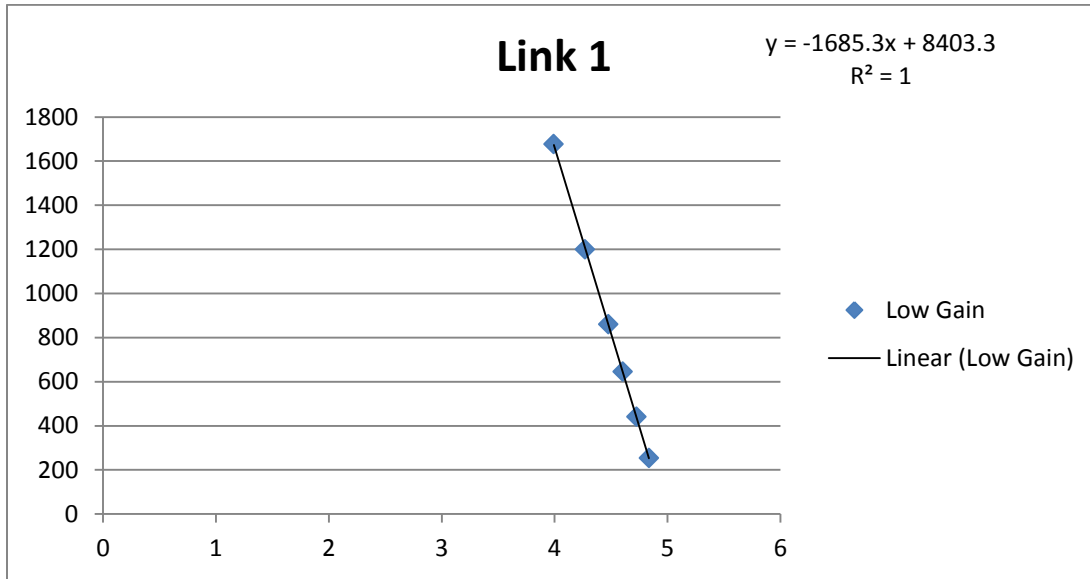
Spindle Calibration

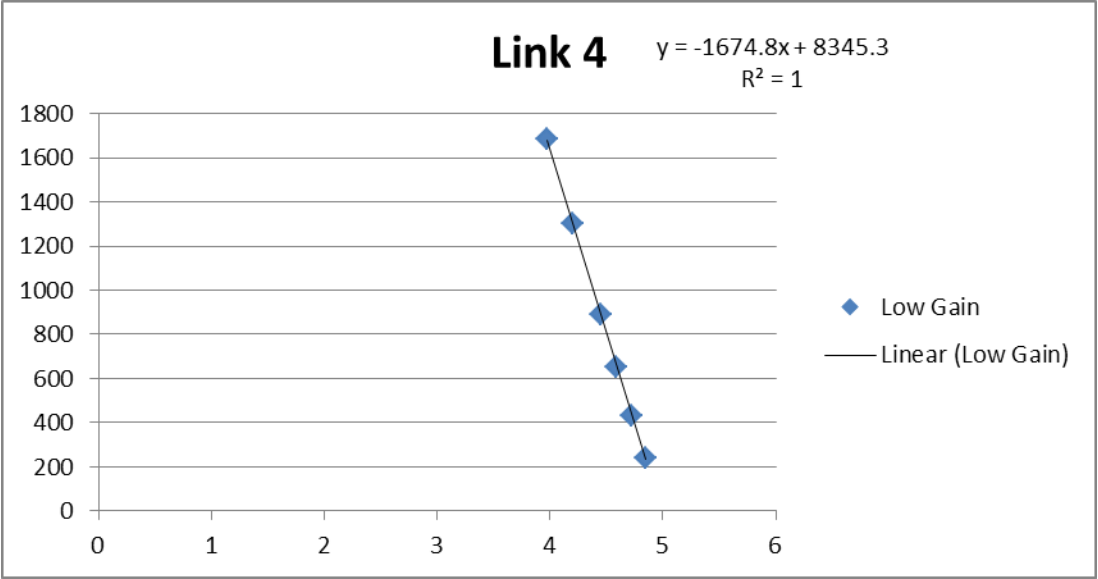
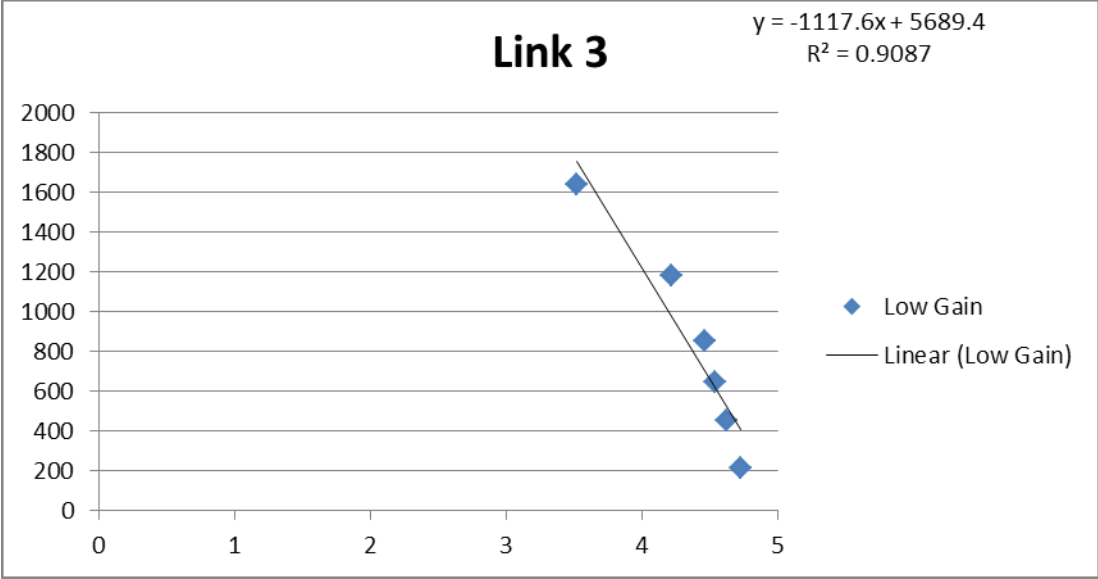


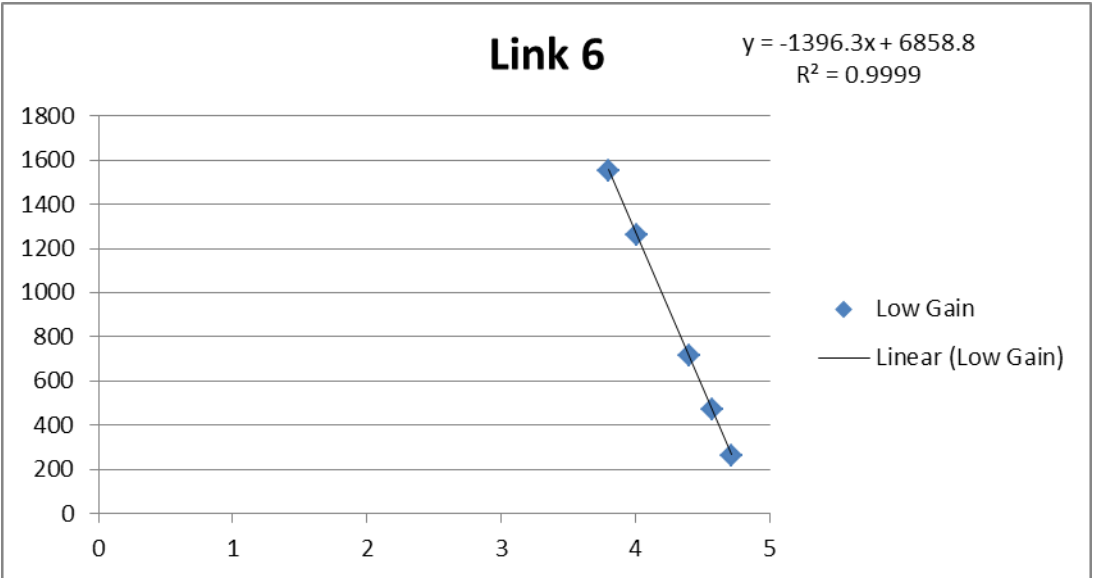
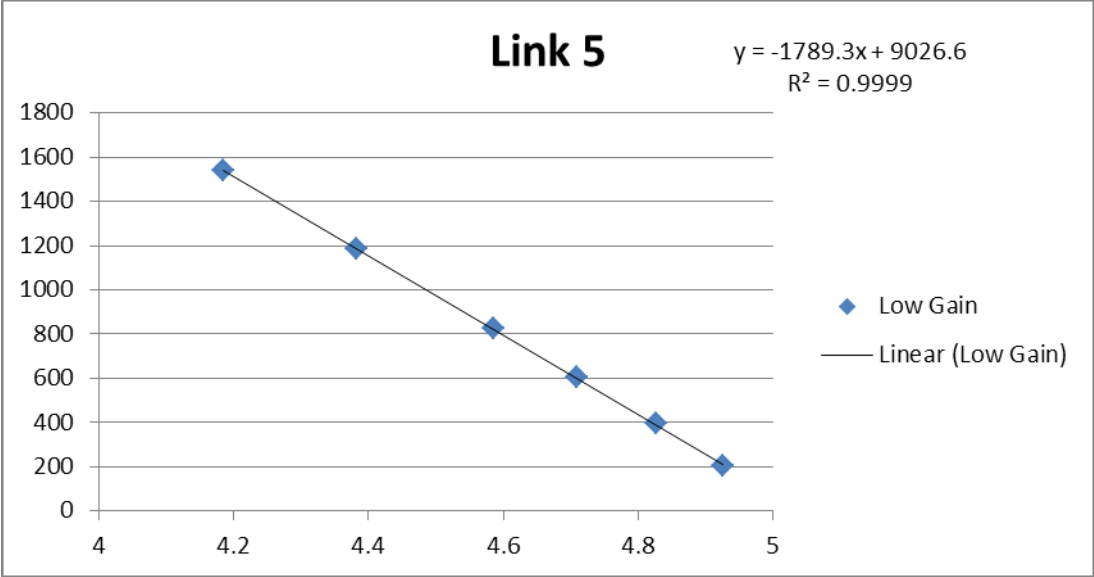
Bottom



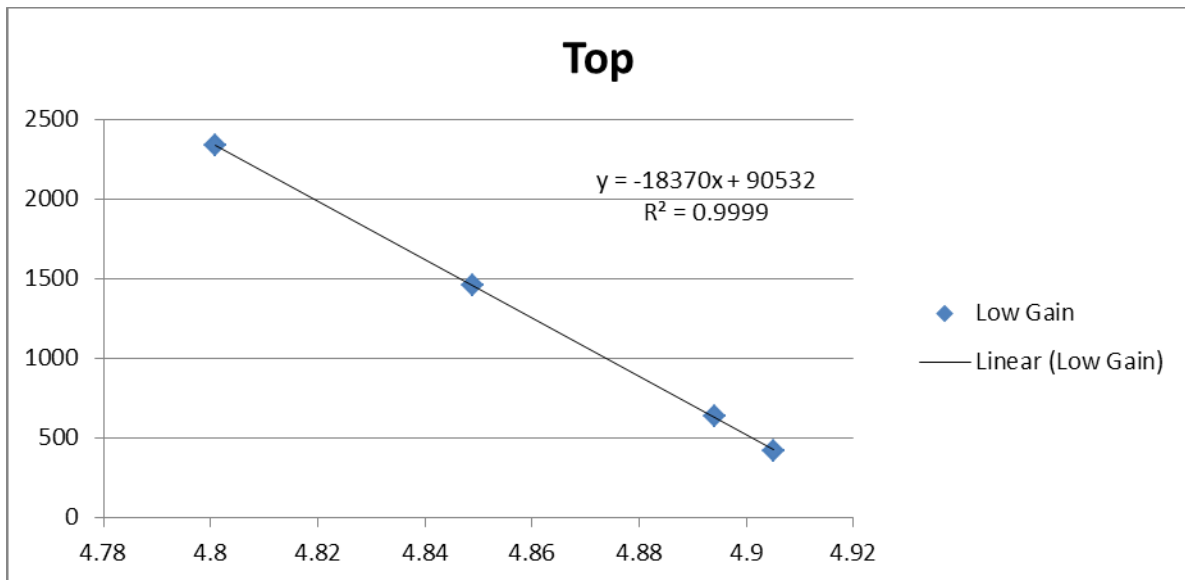
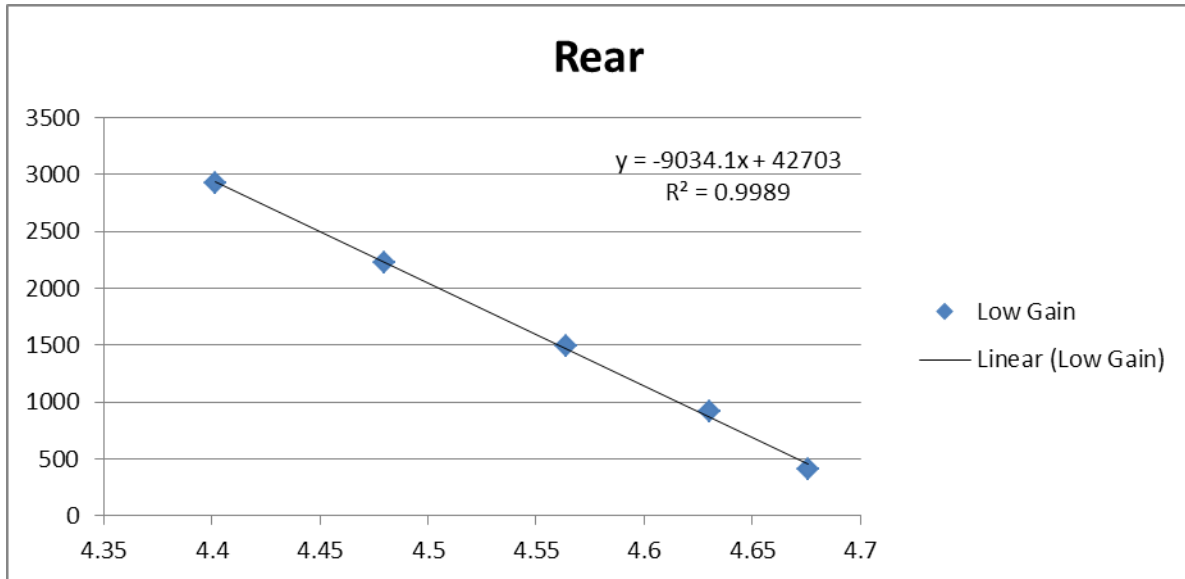
Re-calibration of Links



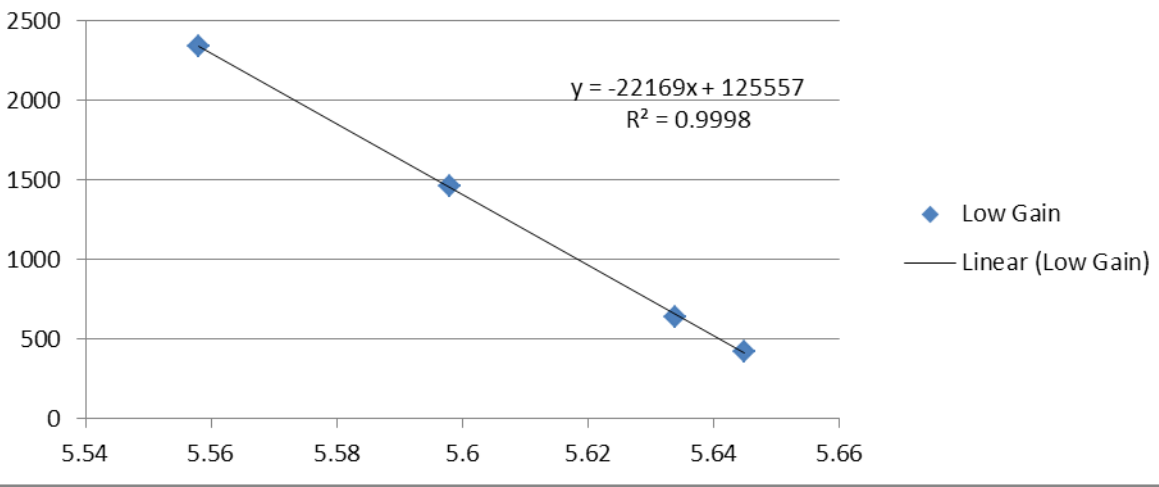




Re-calibration of Spindle

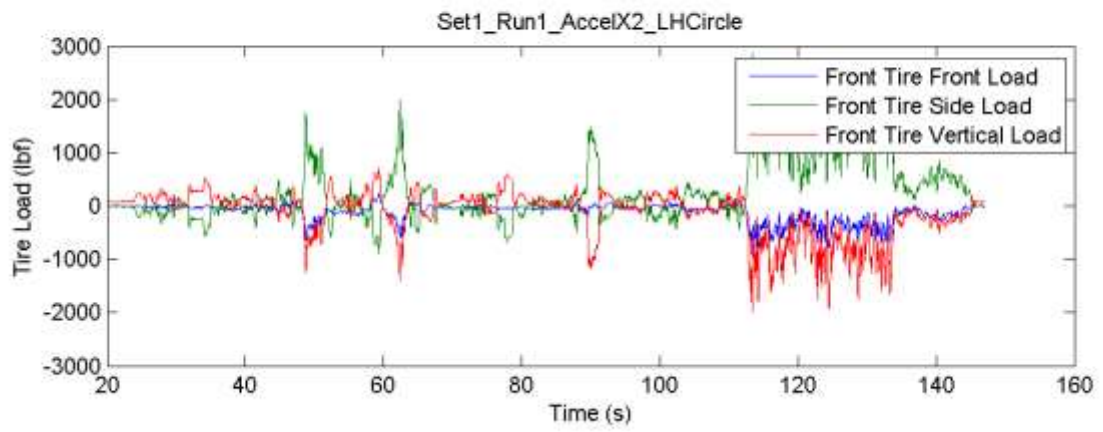
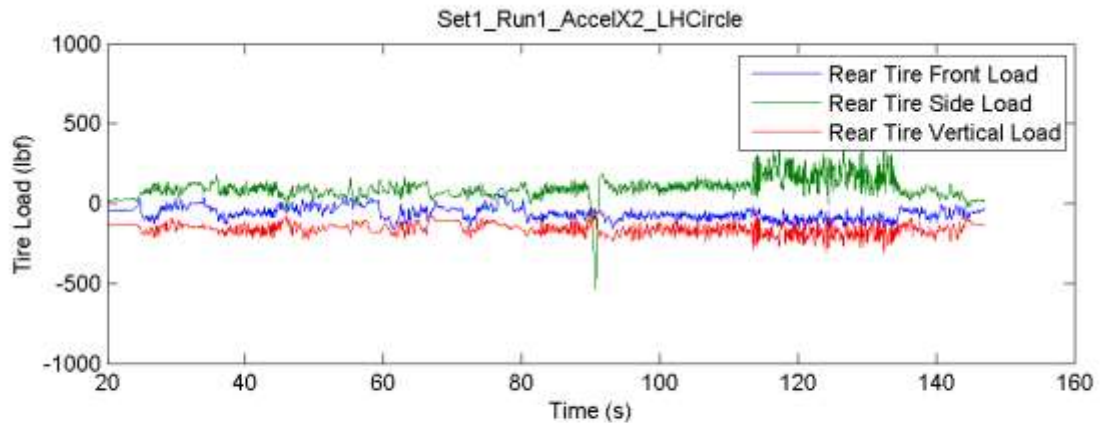


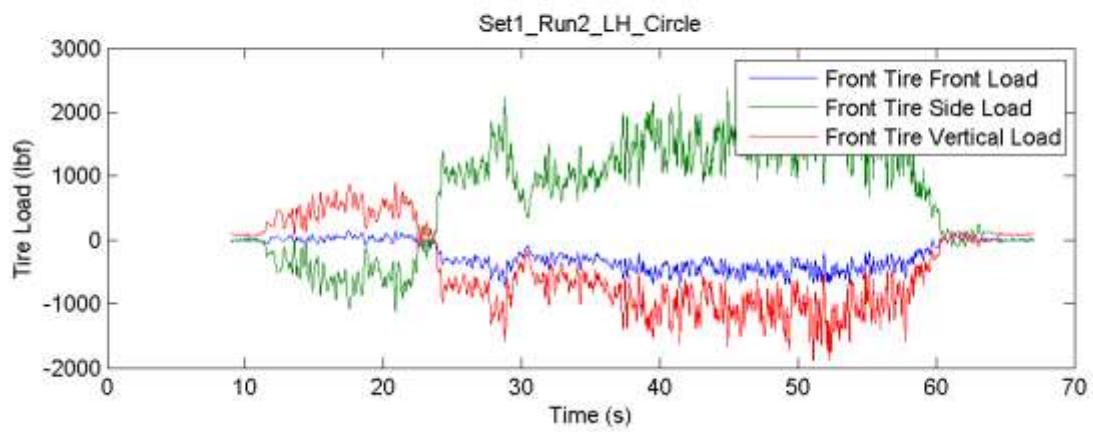
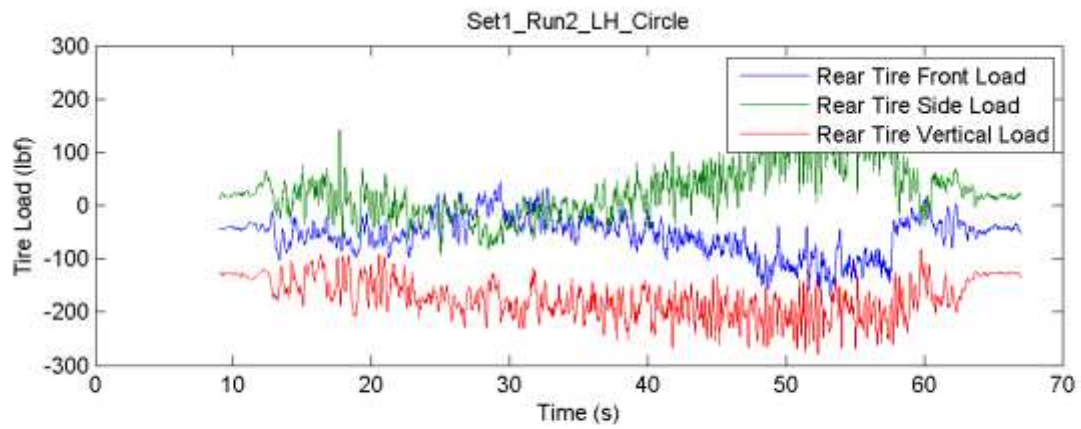
Bottom

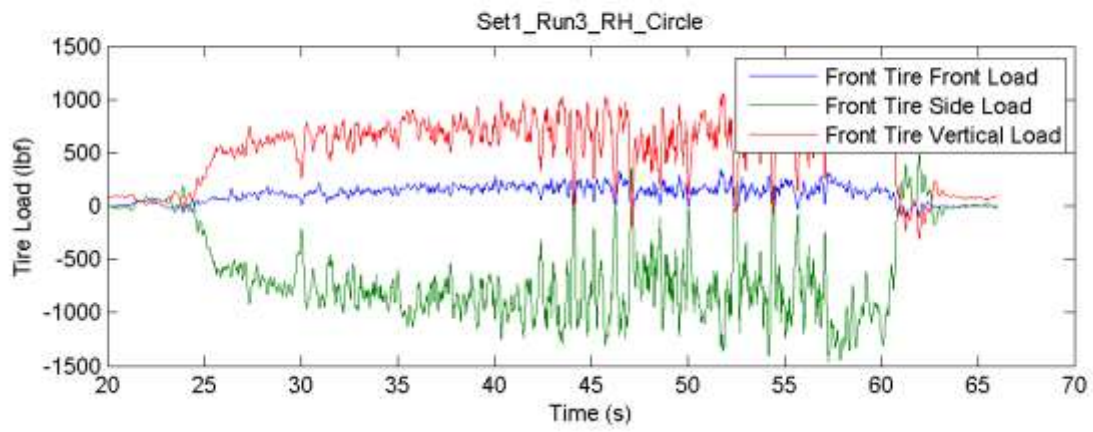
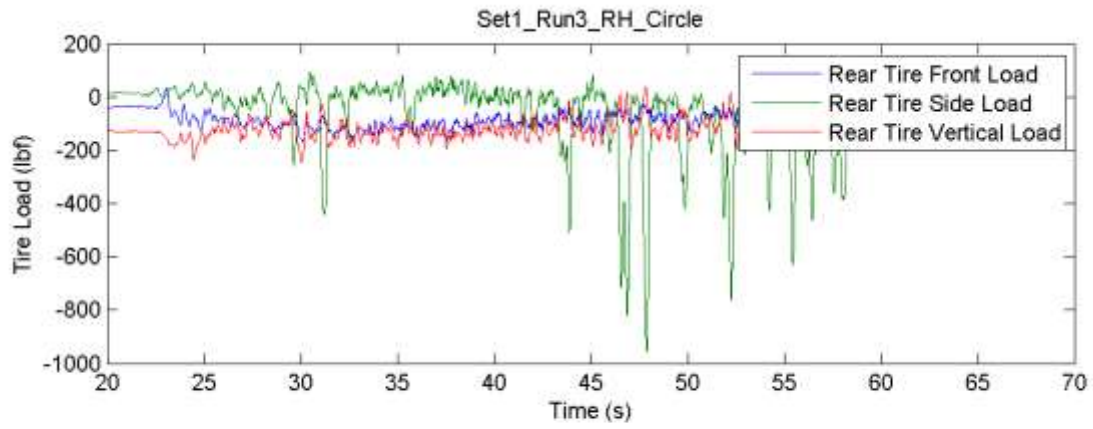


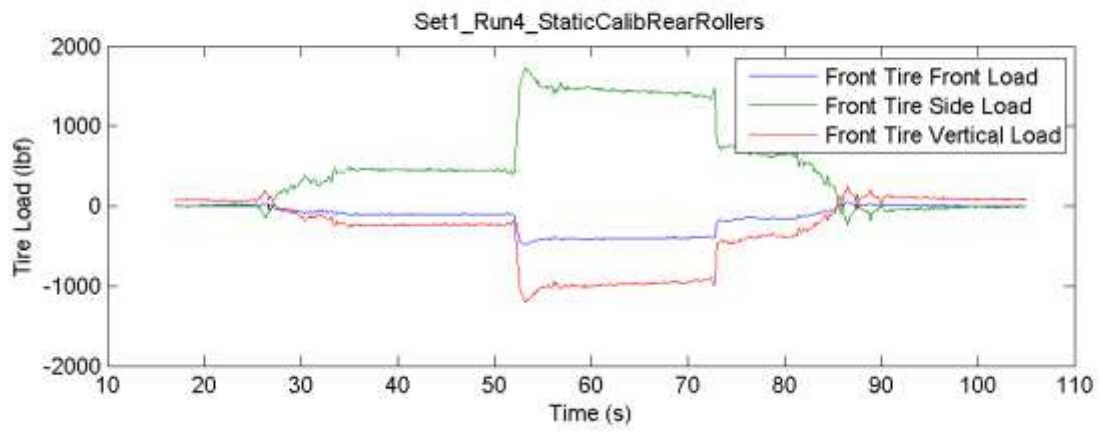
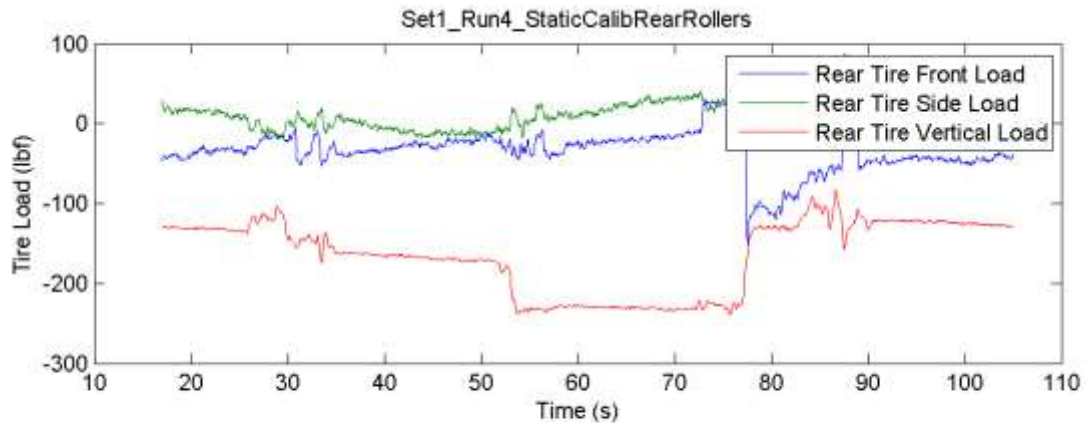
APPENDIX I:

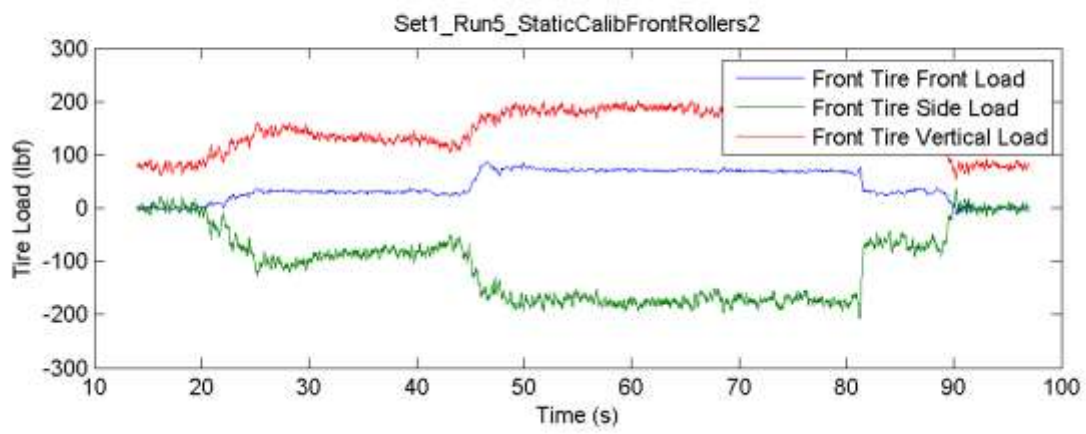
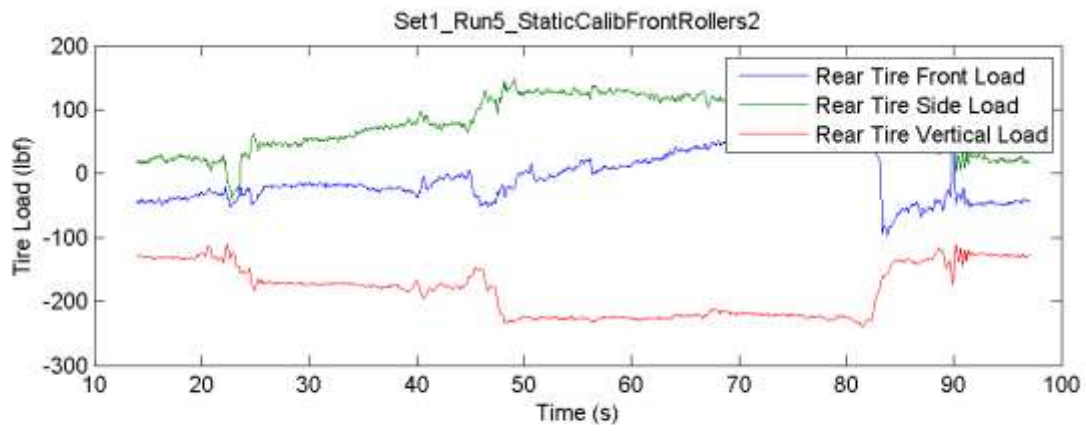
MATLAB PLOTS

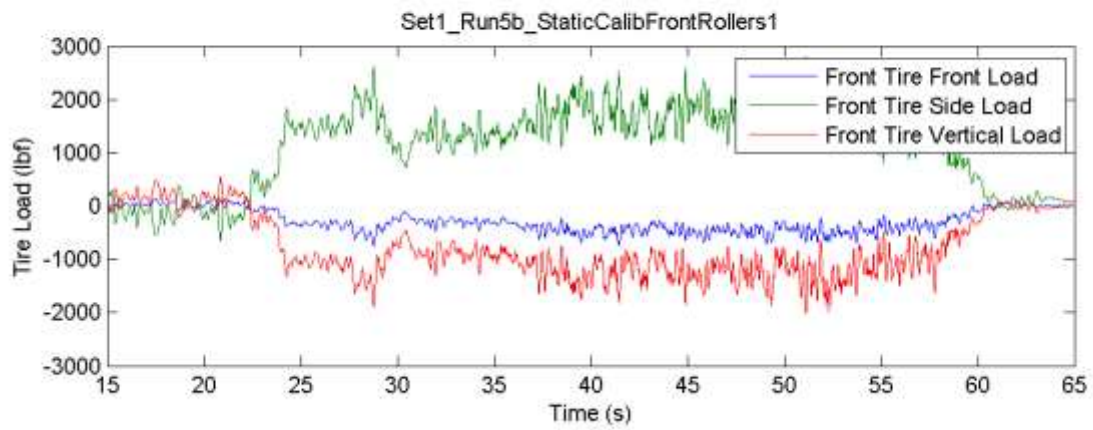
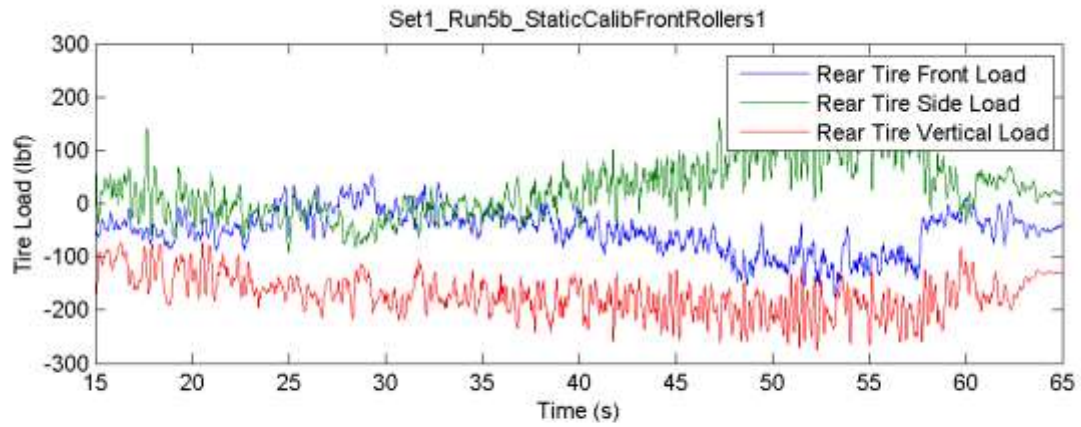


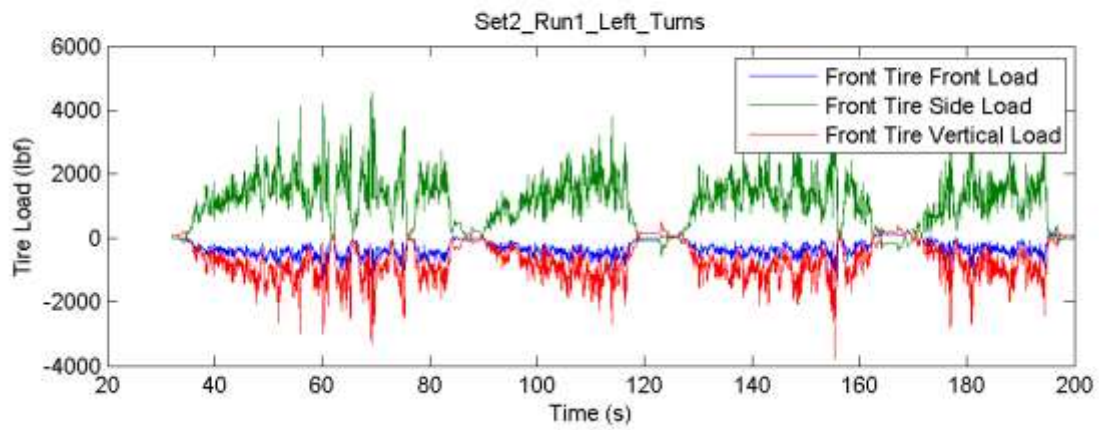
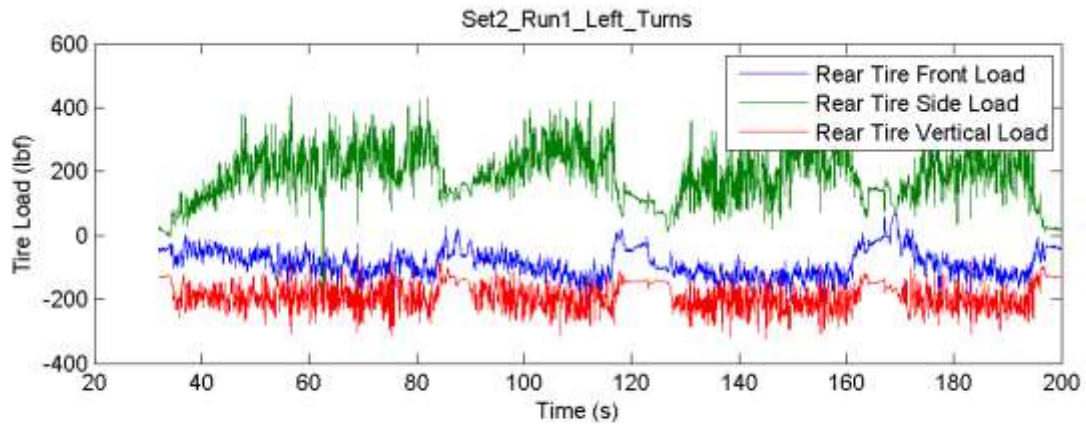


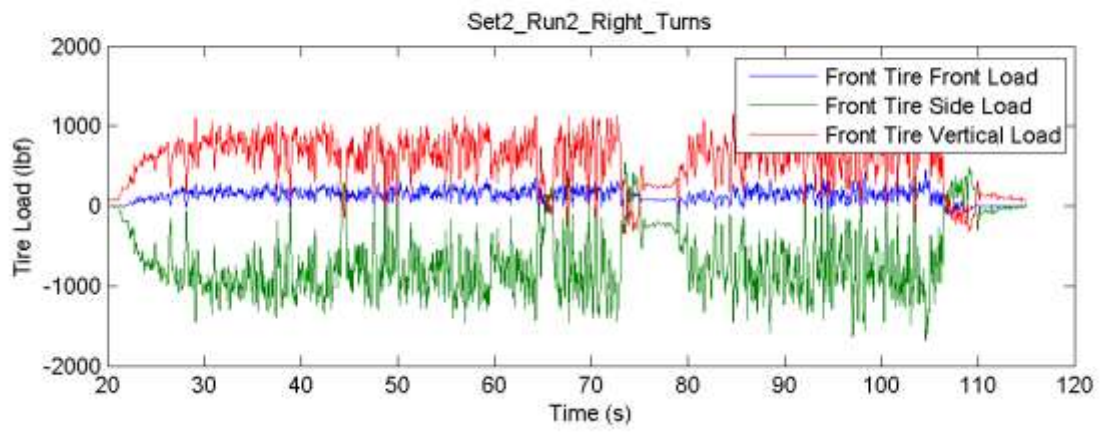
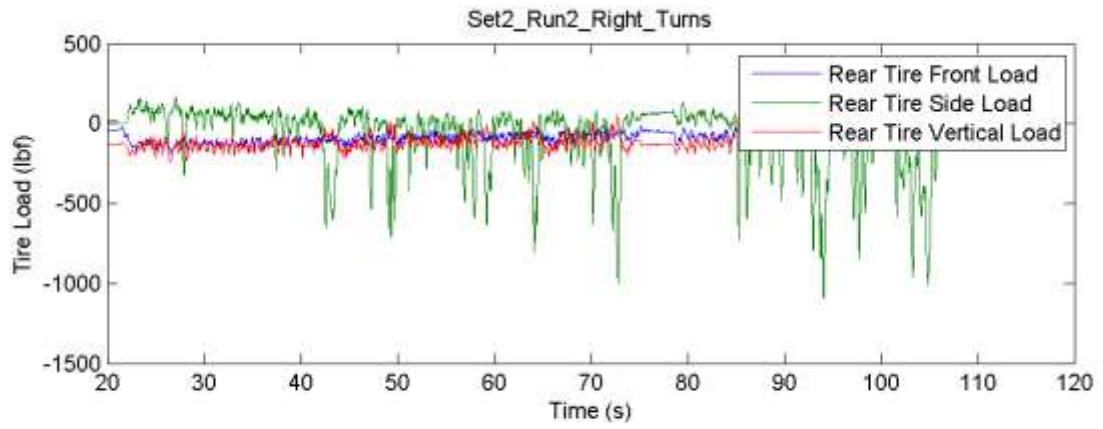


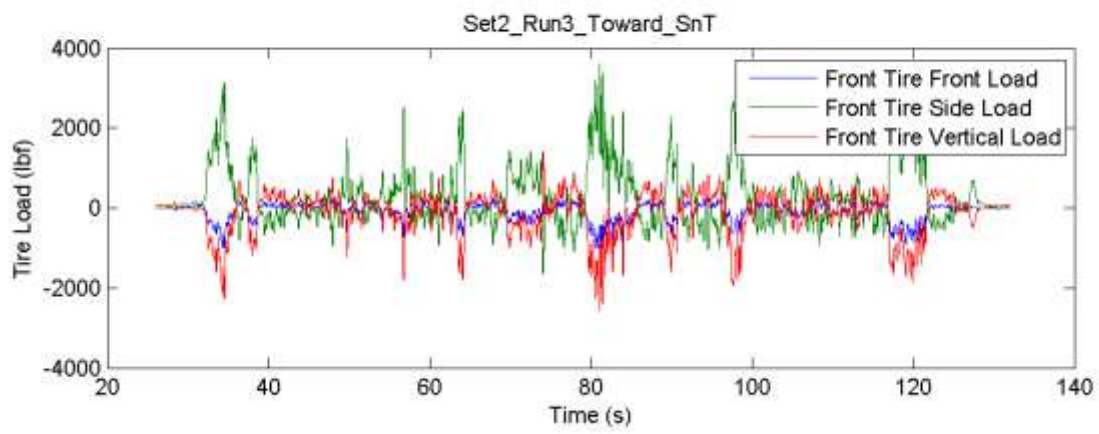
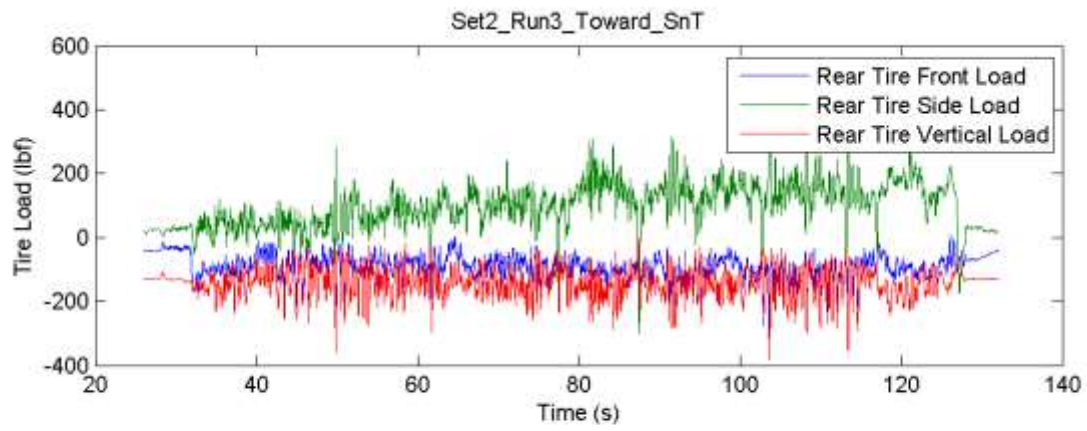


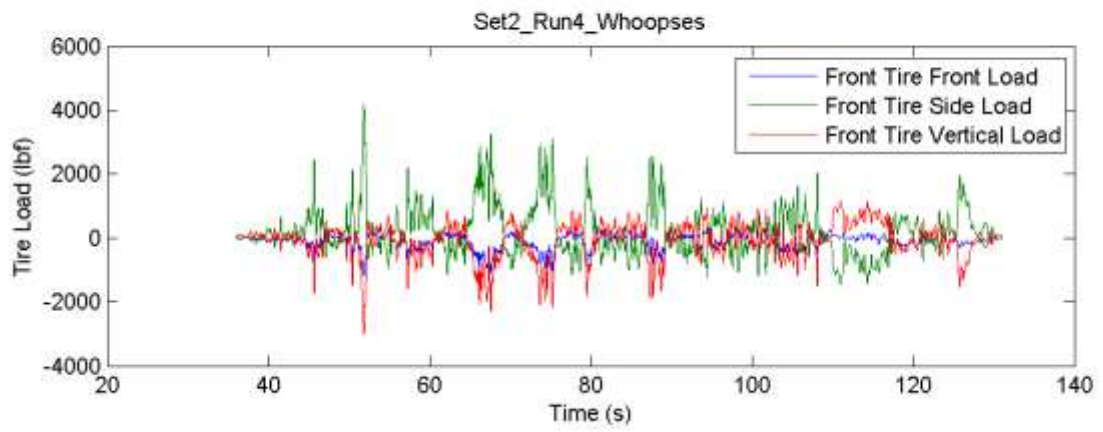
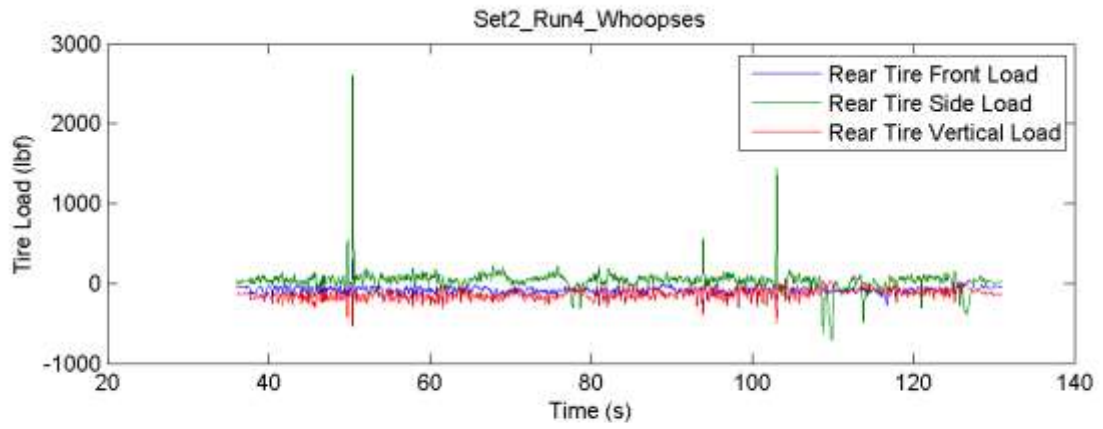


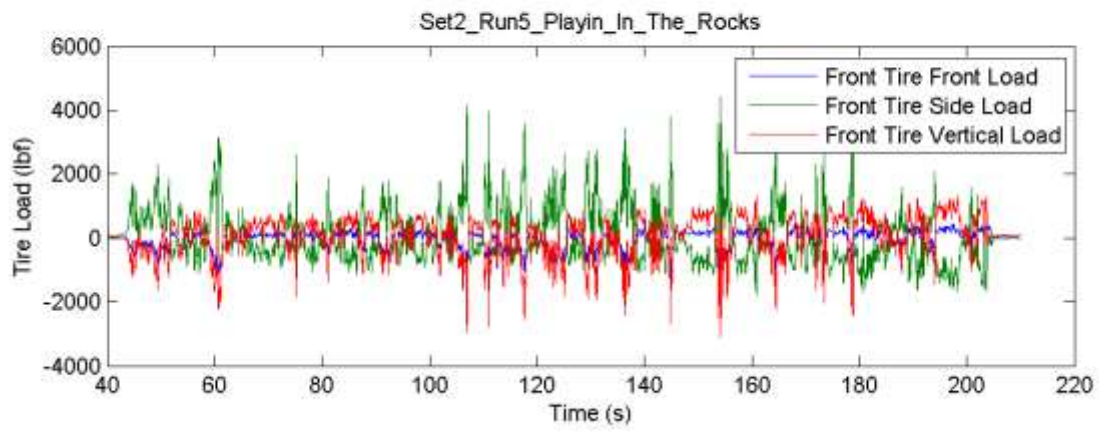
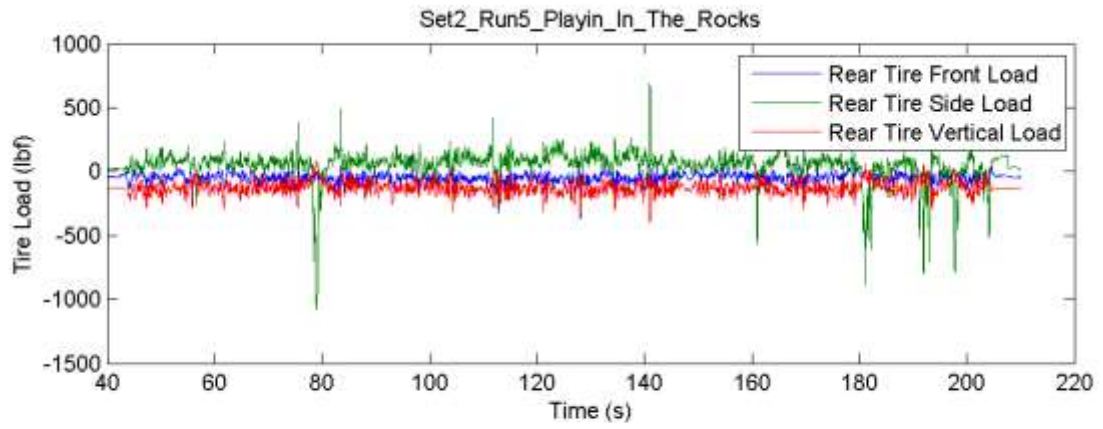


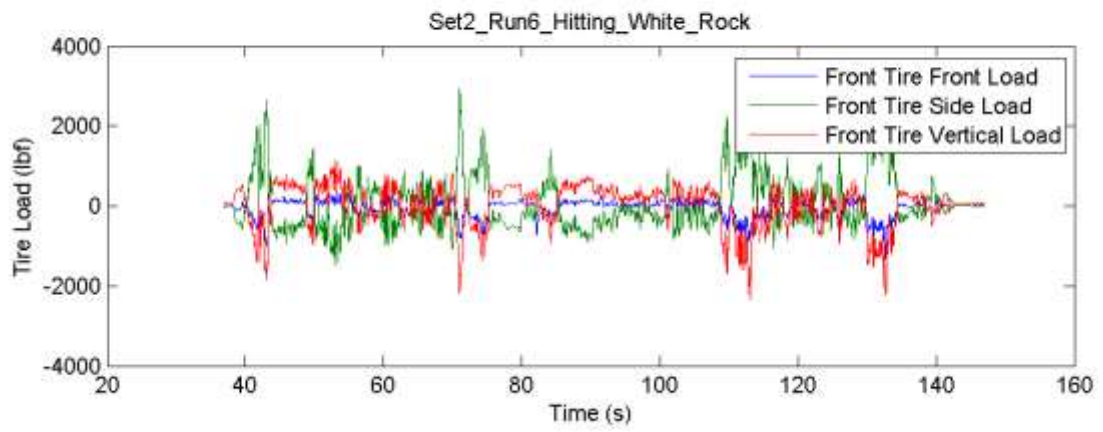
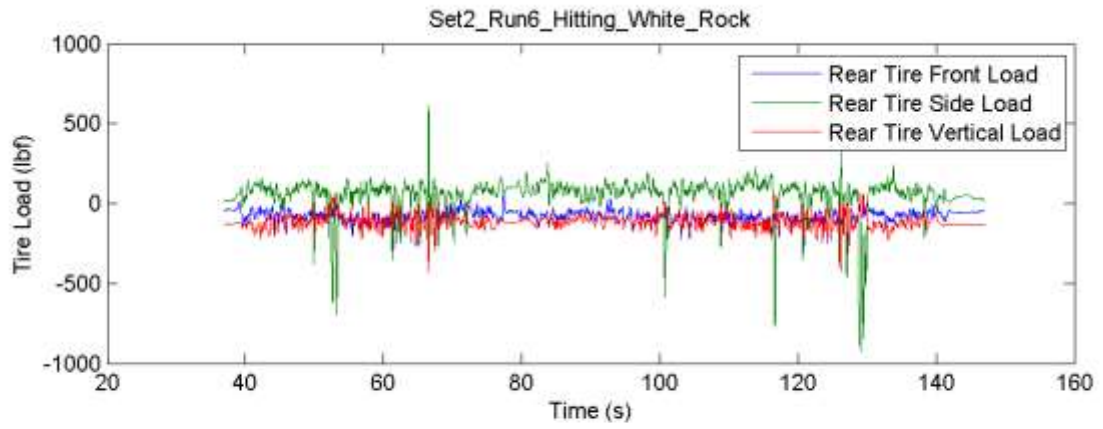


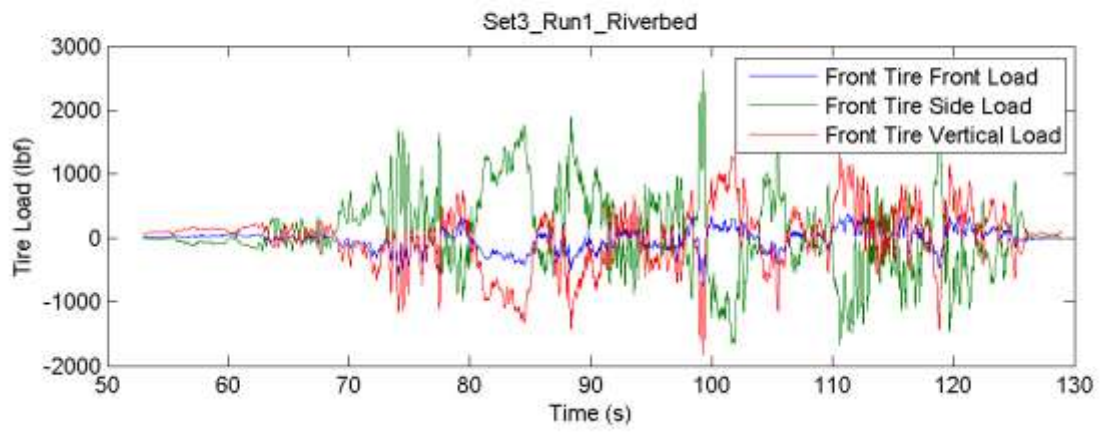
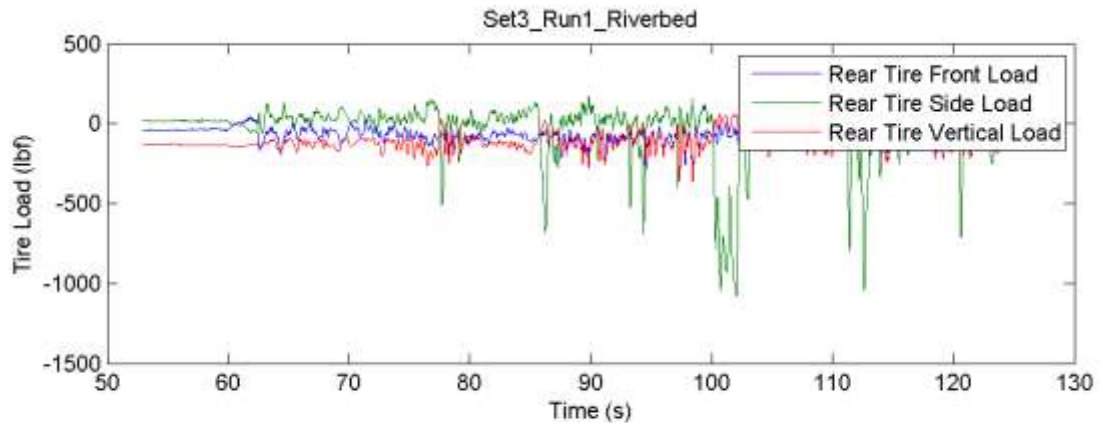


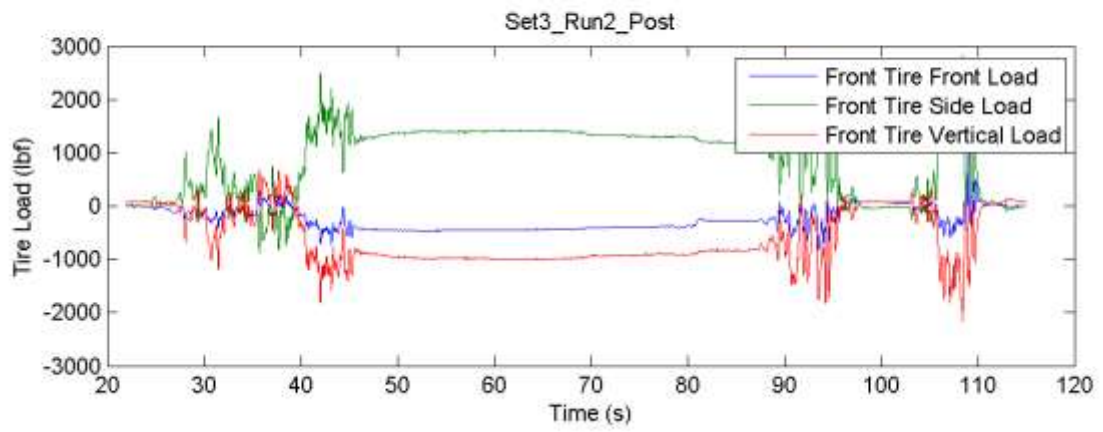
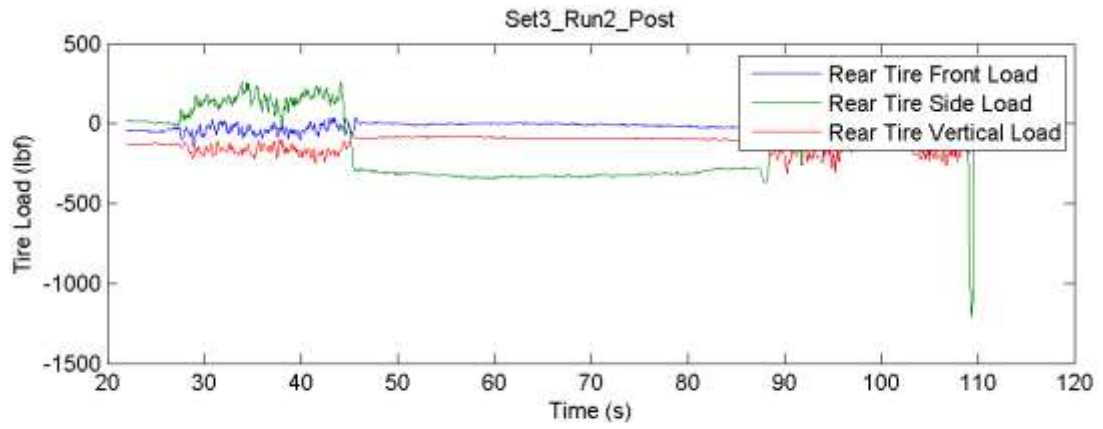


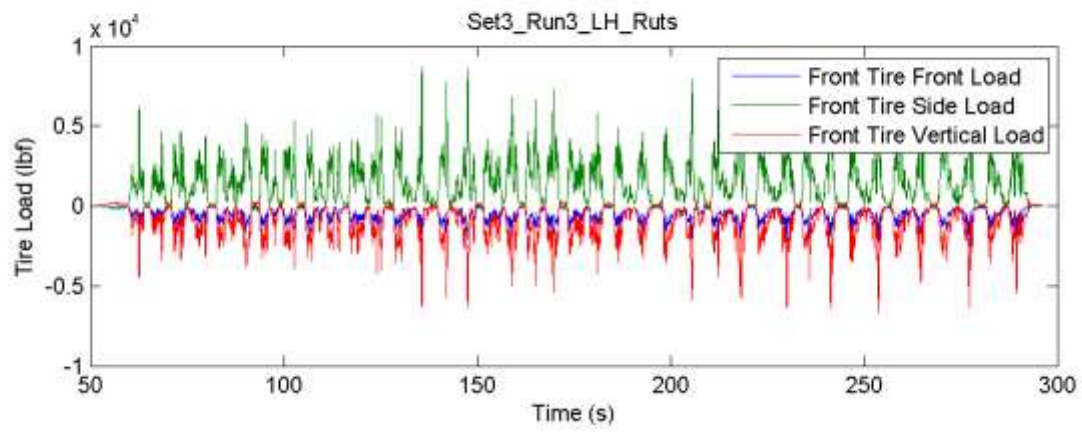
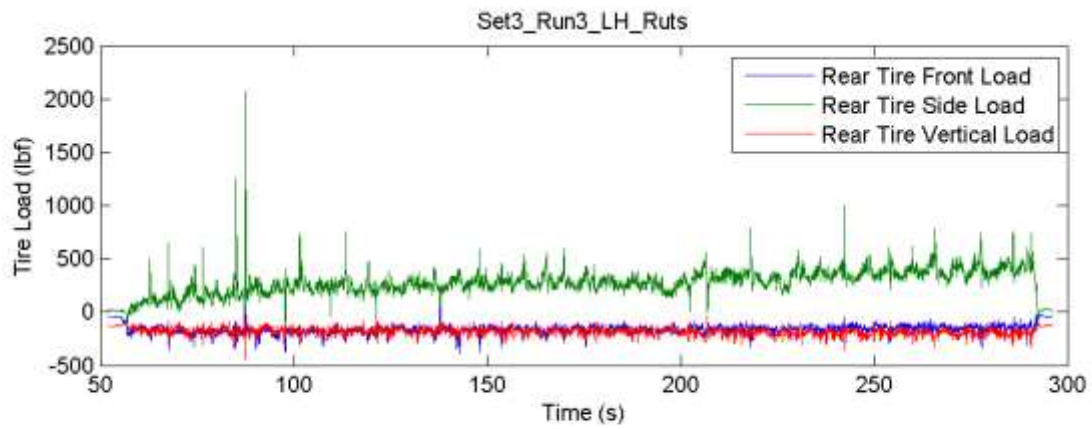


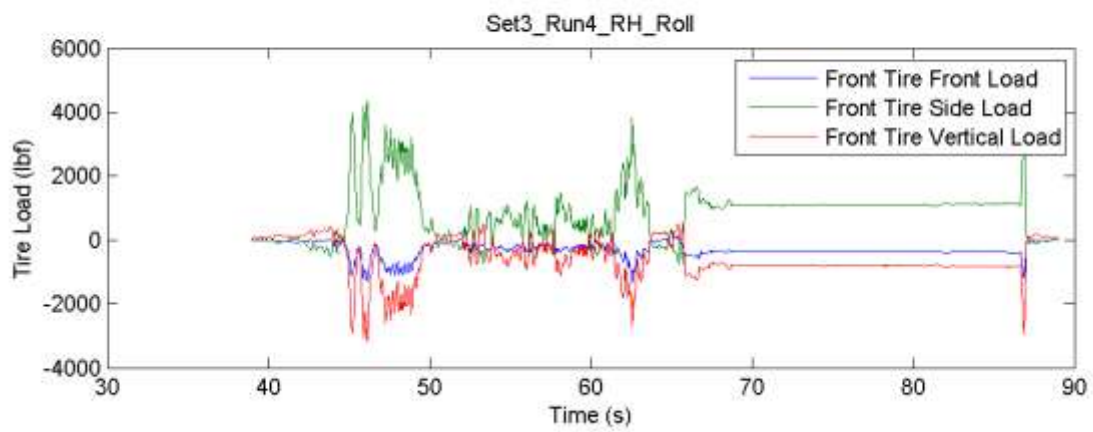
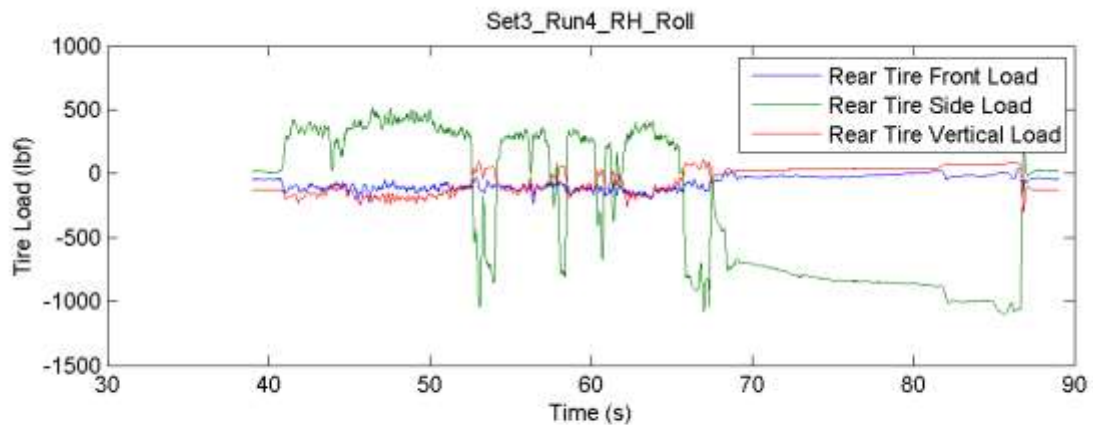


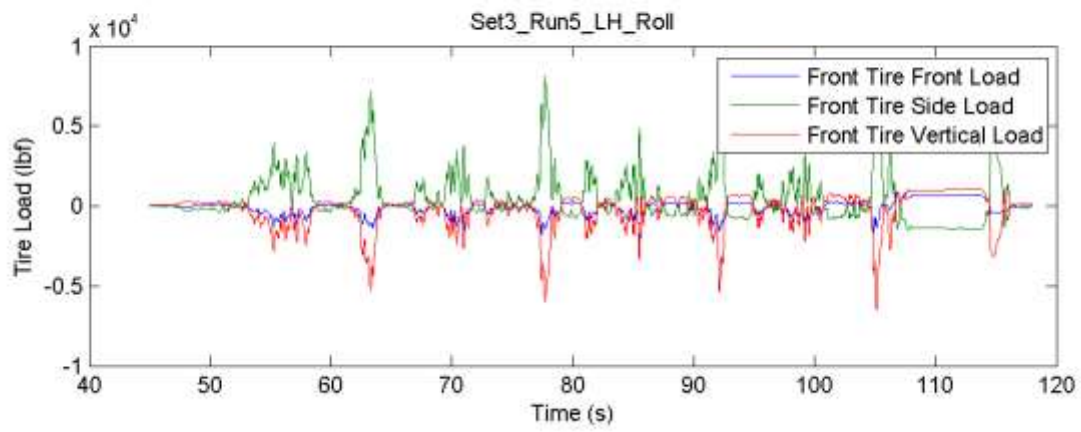
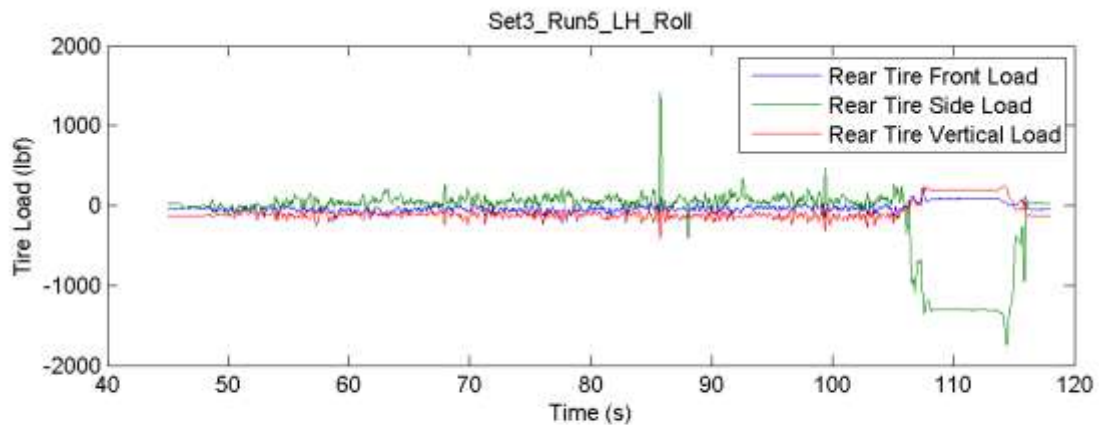


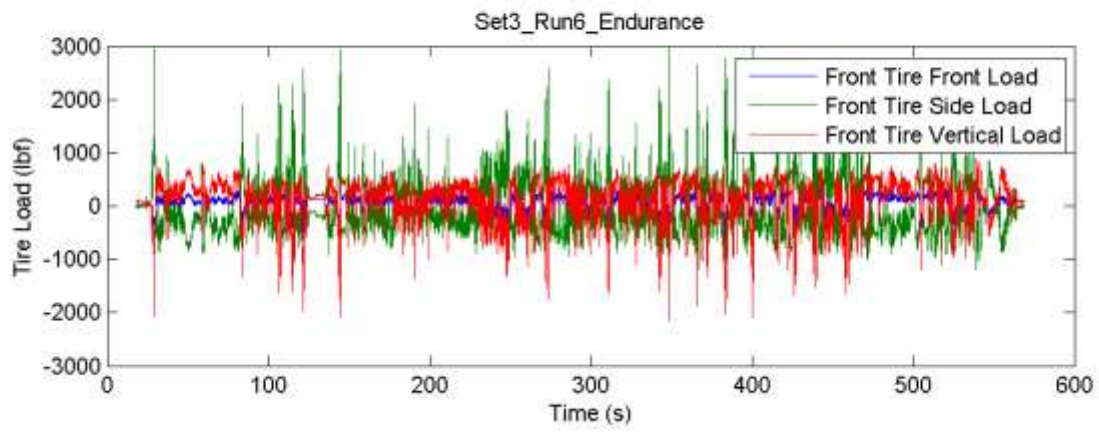
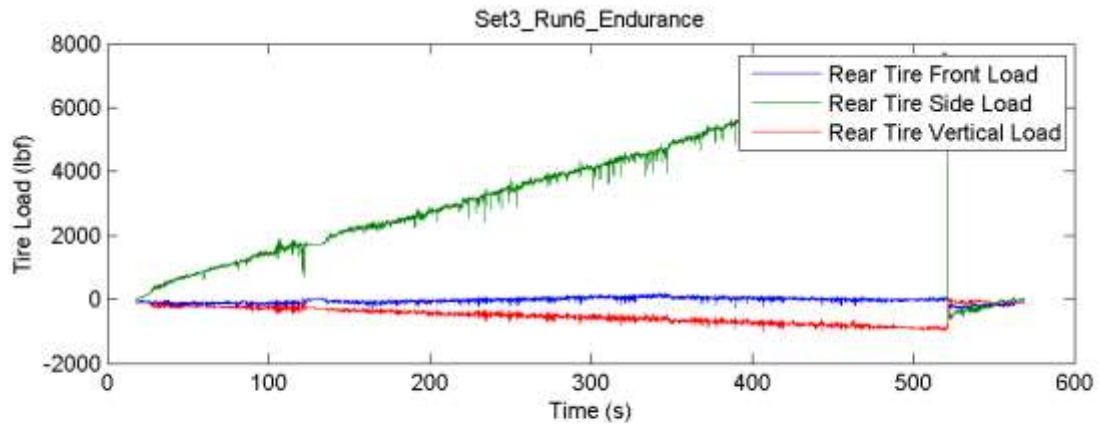


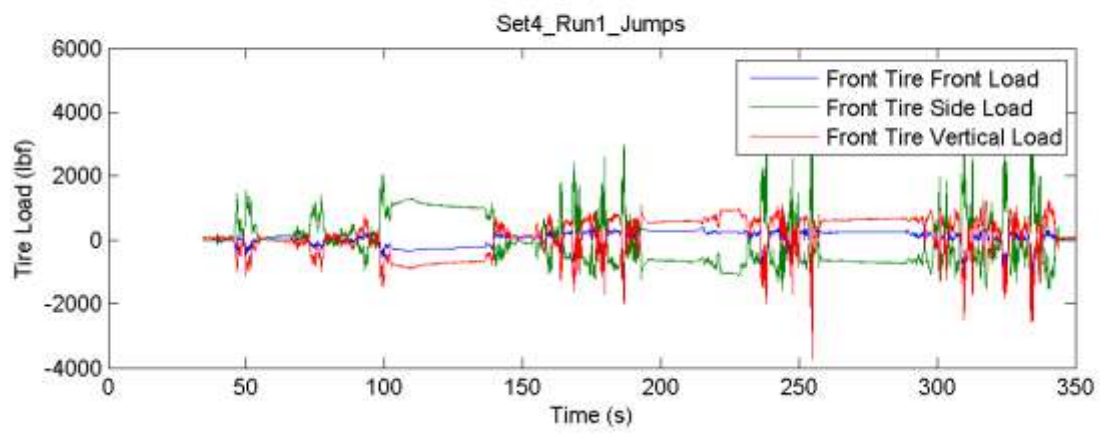
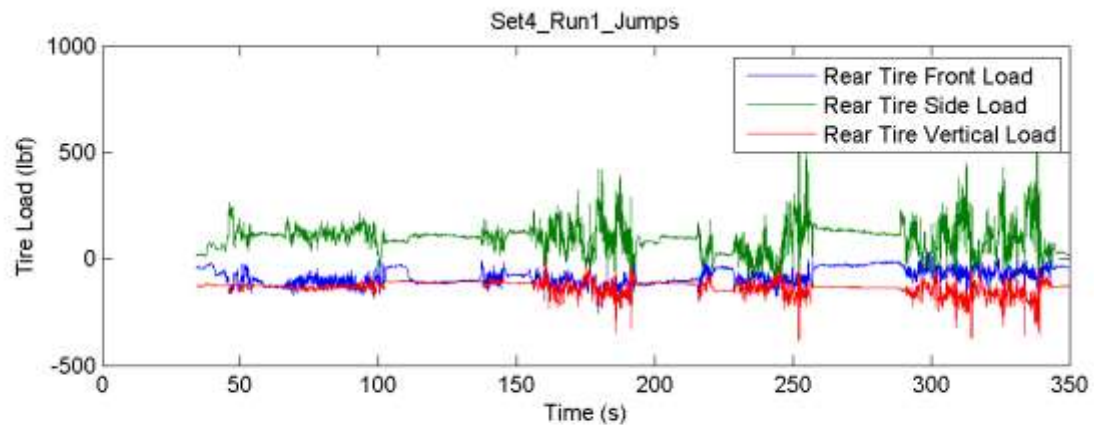


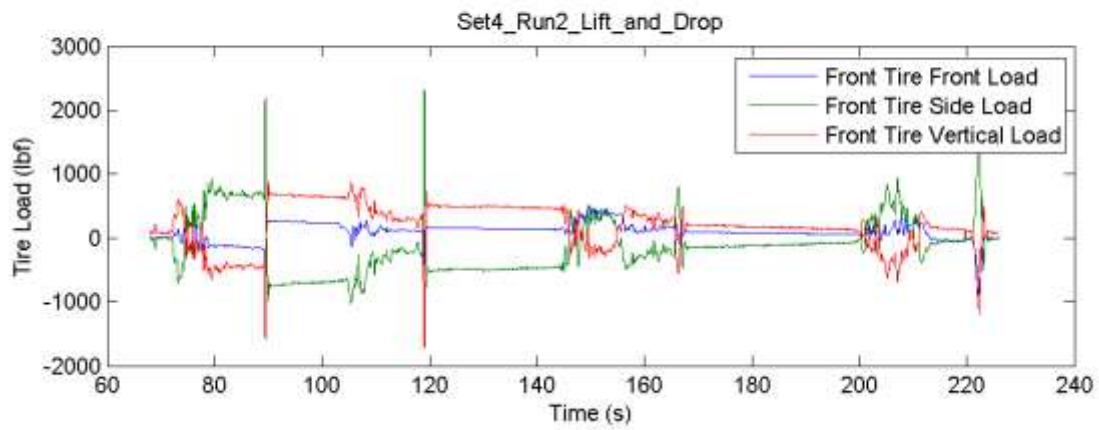
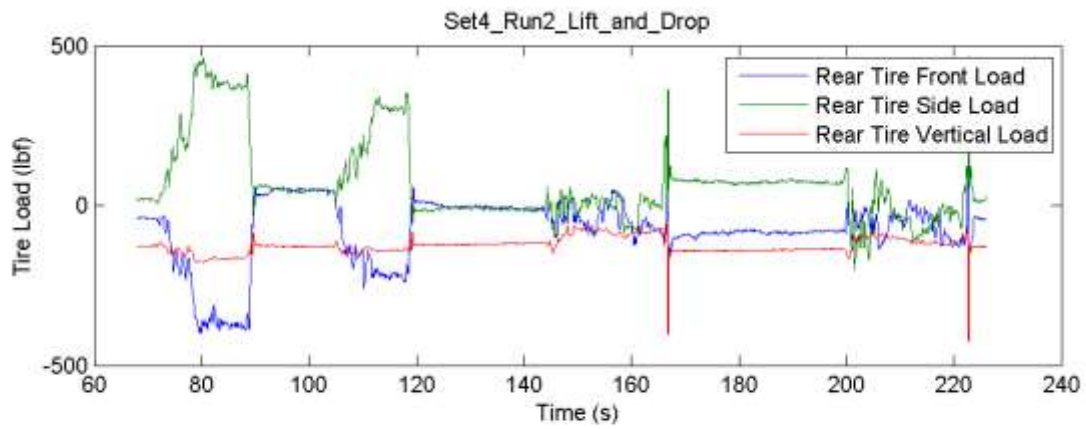


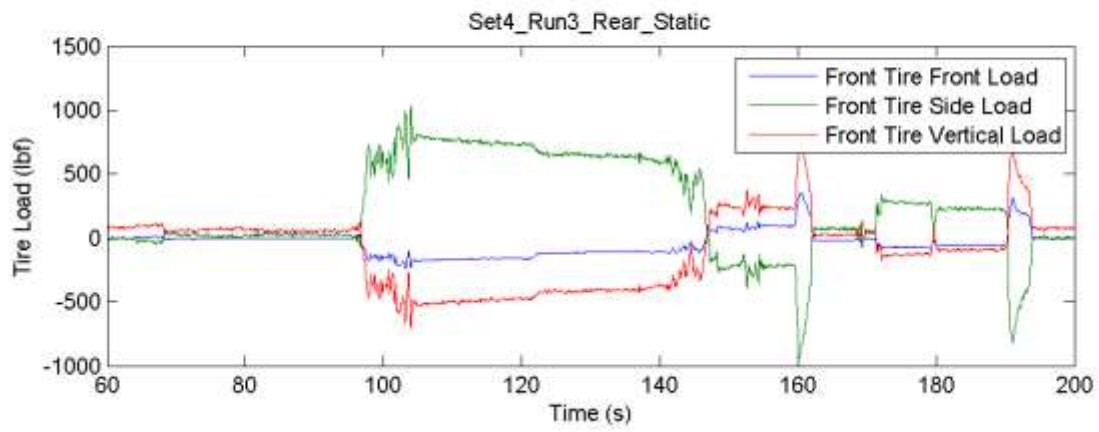
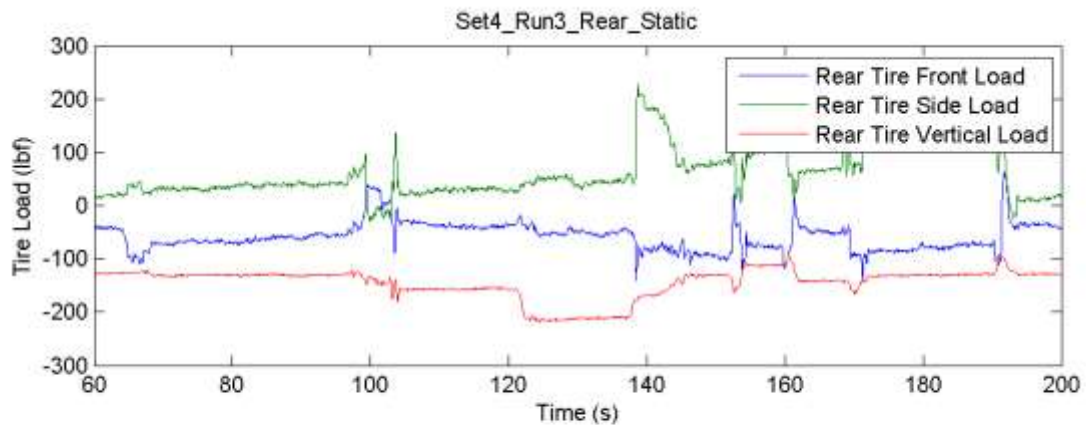


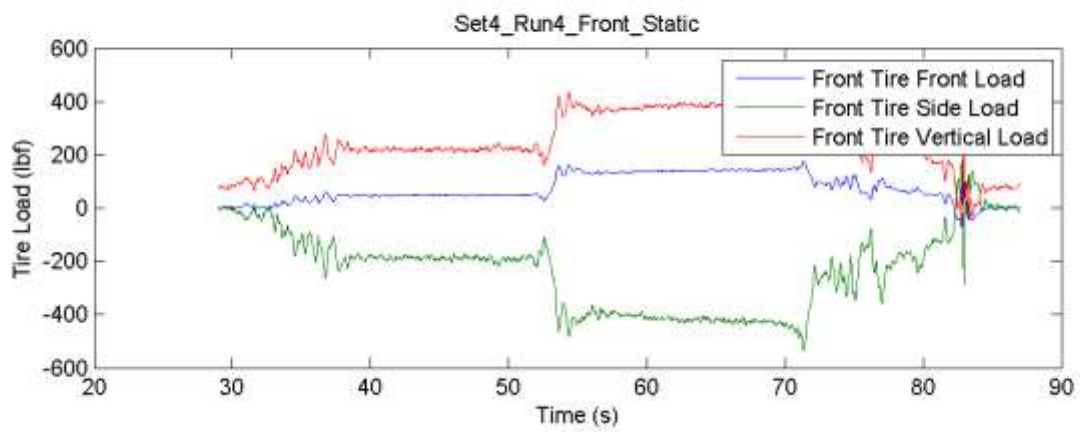
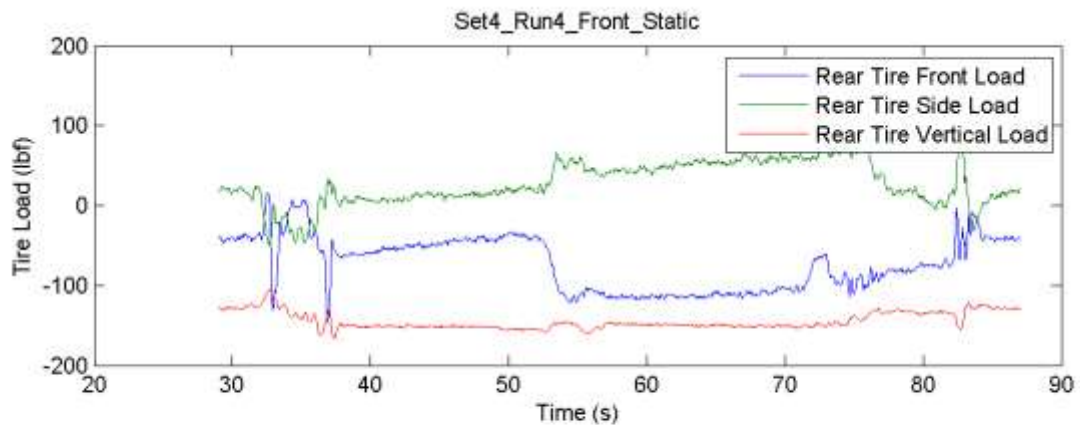












APPENDIX J:
MATLAB SCRIPT FILES

Appendix J - Matlab Analysis, Filtering, and Plots

Get Loaded Senior Project - By: Ryan Flatland, Nick Bonafede, Christian George - Published on: September 7, 2015

Contents

- [Initializations and Loading Data](#)
- [Allocations for Analysis](#)
- [Finding offsets](#)
- [Finding Link Loads and Spindle Stress](#)
- [Finding Wheel Loads](#)
- [Output](#)

Initializations and Loading Data

```

clc; clf; clear all;
load('Data_Out.mat','Data_Out');

%for CurrentRun = 1:22;
CurrentRun = 1;

% Note: checking the voltages, for some reason Link 1 and 2 are only
% reading at 100Hz, additionally, they are reading slightly different values
% than the raw data table while all the other channels are spot on.

% Array of strings with run name
Run = fieldnames(Data_Out(1));
temp = size(Run);
Runs = temp(1);
% Array of strings with data option names
Fields = fieldnames(Data_Out(1).(char(Run(1))));
>Data_Out.(char(Run(1))).(char(Fields(2)))(70)

CalibTimeStart = [20, 9, 20, 17, 14, 15, 32, 20, 26, 36, 40, 37, 53, 22, 52, 39, 45,
18, 34, 68, 60, 29];
%Starting time (s)
CalibTimeEnd = [147, 67, 66, 105, 97, 65, 200, 115, 132, 131, 210, 147, 129, 115, 296, 89, 118, 5
69, 350, 226, 200, 87];
%Ending time (s)
TIMEINC = 0.01; %DAQ time interval in seconds
AVERAGINGSTEPS = 100;

% Link Data and Allocations
LinkSlope = [-1721;-1710;-1596;-1674;-1731;-1396];
StaticLinkLoad = [-27,-19,-10,88,98,199];

LinkStartVal = zeros(Runs,6);
LinkStartOffset = zeros(Runs,6);
LinkEndVal = zeros(Runs,6);
LinkEndOffset = zeros(Runs,6);
LinkOffsetDrift = zeros(Runs,6);

```

```

% Spindle Data and Allocations
SpindleSlope = [-18599,-17159,-23743];
%Simple My/I with 137lbf vertical at 1.5" offset
StaticSpindleStress = [-2304,0,2304]; %psi

SpindleStartVal = zeros(Runs,3);
SpindleStartOffset = zeros(Runs,3);
SpindleEndVal = zeros(Runs,3);
SpindleEndOffset = zeros(Runs,3);
SpindleOffsetDrift = zeros(Runs,3);

```

Allocations for Analysis

```

RunLength = (CalibTimeEnd(CurrentRun) - CalibTimeStart(CurrentRun)) * (1/TIMEINC);

% Storage of Voltages
LinkVoltage = zeros(6,round(RunLength));
SpindleVoltage = zeros(3,round(RunLength));

% Storage of link loads
LinkLoad = zeros(6,round(RunLength));
SpindleStress = zeros(3,round(RunLength));

% Storage of computed loads
ForceRearFront = zeros(1,round(RunLength));
ForceRearSide = zeros(1,round(RunLength));
ForceRearVert = zeros(1,round(RunLength));
ForceFrontFront = zeros(1,round(RunLength));
ForceFrontSide = zeros(1,round(RunLength));
ForceFrontVert = zeros(1,round(RunLength));

```

Finding offsets

```

% For each run
for r = 1:Runs
    % Start offset for each link
    for j = 1:6
        sum = 0.00;
        i = 0;
        steps = AVERAGINGSTEPS;
        for i = -steps/2:steps/2
            curTime = CalibTimeStart(r) + i * TIMEINC;
            pos = round(curTime * (1/TIMEINC) + 1);
            sum = sum + Data_Out.(char(Run(r))).(char(Fields(1+j)))(pos);
        end
        LinkStartVal(r,j) = sum / (steps+1);
        LinkStartOffset(r,j) = StaticLinkLoad(j) - LinkStartVal(r,j) * LinkSlope(j);
    end
    % End offset for each link
    for j = 1:6
        sum = 0.00;
        i = 0;
        steps = AVERAGINGSTEPS;
        for i = -steps/2:steps/2

```

```

        curTime = CalibTimeEnd(r) + i * TIMEINC;
        pos = round(curTime * (1/TIMEINC) + 1);
        sum = sum + Data_Out.(char(Run(r))).(char(Fields(1+j)))(pos);
    end
    LinkEndVal(r,j) = sum / (steps+1);
    LinkEndOffset(r,j) = StaticLinkLoad(j) - LinkEndVal(r,j) * LinkSlope(j);
    LinkOffsetDrift(r,j) = LinkEndOffset(r,j) - LinkStartOffset(r,j);
end

% Start Offset for each spindle gauge
for j = 1:3
    sum = 0.00;
    i = 0;
    steps = AVERAGINGSTEPS;
    for i = -steps/2:steps/2
        curTime = CalibTimeStart(r) + i * TIMEINC;
        pos = round(curTime * (1/TIMEINC) + 1);
        sum = sum + Data_Out.(char(Run(r))).(char(Fields(8+j)))(pos);
    end
    SpindleStartVal(r,j) = sum / (steps+1);
    SpindleStartOffset(r,j) = StaticSpindleStress(j) - SpindleStartVal(r,j) * SpindleSlope(j);
end
% End Offset for each spindle gauge
for j = 1:3
    sum = 0.00;
    i = 0;
    steps = AVERAGINGSTEPS;
    for i = -steps/2:steps/2
        curTime = CalibTimeEnd(r) + i * TIMEINC;
        pos = round(curTime * (1/TIMEINC) + 1);
        sum = sum + Data_Out.(char(Run(r))).(char(Fields(8+j)))(pos);
    end
    SpindleEndVal(r,j) = sum / (steps+1);
    SpindleEndOffset(r,j) = StaticSpindleStress(j) - SpindleEndVal(r,j) * SpindleSlope(j);
    SpindleOffsetDrift(r,j) = SpindleEndOffset(r,j) - SpindleStartOffset(r,j);
end
end
end

```

Finding Link Loads and Spindle Stress

```

for r = CurrentRun
% Debug

% Finding Loads
for j = 1:6
    % Number of steps in the run
    steps = (CalibTimeEnd(r) - CalibTimeStart(r)) * (1/TIMEINC);
    stepOffset = CalibTimeStart(r) * (1/TIMEINC);
    for i = 1:steps
        per = i / steps; % Percentage along run
        curLinkOffset = per * LinkEndOffset(r,j) + (1 - per) * LinkStartOffset(r,j);

        pos = round(stepOffset + i);

        % Finding Link Loads
        LinkVoltage(j,i) = Data_Out.(char(Run(r))).(char(Fields(1+j)))(pos);
    end
end
end

```



```

LinkLoad(j,i) = LinkVoltage(j,i) * LinkSlope(j) + curLinkOffset;

% Finding Spindle Stress
if j < 4
    curSpindOffset = per * SpindleEndOffset(r,j) + (1 - per) * SpindleStartOffset(r,j);
    SpindleVoltage(j,i) = Data_Out.(char(Run(r))).(char(Fields(8+j)))(pos);
    SpindleStress(j,i) = SpindleVoltage(j,i) * SpindleSlope(j) + curSpindOffset;
end
end
end
end

```

Finding Wheel Loads

```

% Try forcing link loads
%LinkLoad(1,1) = -27;
%LinkLoad(2,1) = -19;
%LinkLoad(3,1) = -10;
%LinkLoad(4,1) = 88;
%LinkLoad(5,1) = 98;
%LinkLoad(6,1) = 199; % Is this a plus or minus? Plus - shock in
%compression (-) will put link 6 in tension (+).

steps = (CalibTimeEnd(r) - CalibTimeStart(r)) * (1/TIMEINC);
C1 = 1.5; % inch - Lateral offset from contact patch to gauges
C2 = 10; % inch - wheel radius
C3 = 0.547815; % in^2 - spindle cross sectional area
C4 = 0.044596; % in^4 - spindle I
C5 = 0.4176; % in - spindle radius

filter = 0; % half width of noise filter where applicable

for r = CurrentRun
    % Loop through each timestep on the run
    for i = 1:steps
        % Calculation of forces on Rear Tire
        ForceRearFront(1,i) = -1 * (LinkLoad(1,i) * -0.92634 + ...
            LinkLoad(2,i) * 0.185279 + ...
            LinkLoad(3,i) * 0.029687 + ...
            LinkLoad(4,i) * 0.187015 + ...
            LinkLoad(5,i) * -0.91683 + ...
            -1 * LinkLoad(6,i) * -0.47263);
        ForceRearSide(1,i) = -1 * (LinkLoad(1,i) * 0.375651 + ...
            LinkLoad(2,i) * 0.981109 + ...
            LinkLoad(3,i) * 0.99424 + ...
            LinkLoad(4,i) * 0.979033 + ...
            LinkLoad(5,i) * 0.3894 + ...
            -1 * LinkLoad(6,i) * 0.520447);
        ForceRearVert(1,i) = -1 * (LinkLoad(1,i) * -0.0289 + ...
            LinkLoad(2,i) * -0.05564 + ...
            LinkLoad(3,i) * -0.10298 + ...
            LinkLoad(4,i) * -0.08074 + ...
            LinkLoad(5,i) * -0.08824 + ...
            -1 * LinkLoad(6,i) * -0.71117);
    end
end

%{
    % Solving with the whole matrix... If we have 6 knowns and 3

```

```

% unknowns then we don't have to care about moments, right?
% Matrix including link unit vector and summed moments
% From Rear_Suspension_Force_Calculator_Ryan.m
%      Mr = [-0.943718025585254,0.225924564477908,0.0534027418730375,0.223698395848650,-0.930087
188508591,-0.255350837715847;...
%          -0.00554535164606722,-0.0126214840490452,-0.104424879590289,-0.140592567223314,-0.1
31706476230619,-0.876003579740481;...
%          -0.330704607256371,-0.974063031485061,-0.993097976879923,-0.964465011151933,-0.3429
15770840448,-0.409162165845863;...
%          -0.338689913626708,-0.992237968515686,2.33237311558979,4.86098801174608,1.610650471
14026,0;...
%          1.52430626047095,-2.27345743581831,-4.79411533847681,-2.25105571232592,1.5107834368
7259,0;...
%          0.940945349762221,-0.200681596379818,0.629525032736468,1.45560171265204,-4.94881097
778541,0];
%      %Link Magnitudes
%      F = [LinkLoad(1,i);
%          LinkLoad(2,i);
%          LinkLoad(3,i);
%          LinkLoad(4,i);
%          LinkLoad(5,i);
%          -1*LinkLoad(6,i)]; % remember to invert the shock magnitude
%
%      GroundForce = Mr * F;
%      ForceRearFront(1,i) = -GroundForce(1); % Positive back
%      ForceRearVert(1,i) = GroundForce(2); % Positive up
%      ForceRearSide(1,i) = GroundForce(3); % Positive in

% Calculation of forces on Front Tire
ForceFrontFront(1,i) = (1 / C1) * ((C4/2/C2) * (SpindleStress(1,i) + SpindleStress(3,i) - .
..
%          2 * SpindleStress(2,i)));
ForceFrontSide(1,i) = -1 * C3 / 2 * SpindleStress(1,i) + SpindleStress(3,i);
ForceFrontVert(1,i) = (1 / C1) * (-(C3/2) * (SpindleStress(1,i) + SpindleStress(3,i)) * C2
- ...
%          (C4/2/C2) * (SpindleStress(1,i) - SpindleStress(3,i)))
%}

% Calculation of forces on Front Tire
ForceFrontSide(1,i) = -(SpindleStress(1,i)+SpindleStress(3,i))*(C3/2);
%-( ( 1/C3) + (1/(C3*C1)) + (C2*C5/(C1*C4)) - ...
% (C2*C5/C4) )^-1 ) * (SpindleStress(1,i) + (SpindleStress(3,i)/C1));
ForceFrontVert(1,i) = ((C3*C2+C4/C5)*SpindleStress(1,i) + (C3*C2-C4/C5)*SpindleStress(3,i))
/(2*C1);
% (C4/(C1*C5)) * (SpindleStress(3,i) + ForceFrontSide(1,i) ...
% * ( 1/C3) + (C2*C5/C4) );
ForceFrontFront(1,i) = (.5*SpindleStress(1,i)-SpindleStress(2,i)+.5*SpindleStress(3,i))*C4/
(C1*C5);
%-(C4/(C1*C5)) * (SpindleStress(2,i) + (ForceFrontSide(1,i)/C3));

end
end

```

Output

```
Time = linspace(CalibTimeStart(r),CalibTimeEnd(r),RunLength);
```

```
% Filtered
```

```

%%{
figure(1)
subplot(2,1,1)
plot (Time,sgolayfilt(ForceRearFront(1,:),1,17), Time,sgolayfilt(ForceRearSide(1,:),1,17), Time,sgo
layfilt(ForceRearVert(1,:),1,17))
title(Run(r),'interpreter', 'none')
xlabel('Time (s)')
ylabel('Tire Load (lbf)')
legend('Rear Tire Front Load','Rear Tire Side Load','Rear Tire Vertical Load',1)
print('figure','-dpng')

%figure(2)
subplot(2,1,2)
plot (Time,sgolayfilt(ForceFrontFront(1,:),1,17), Time,sgolayfilt(ForceFrontSide(1,:),1,17), Time,
100+sgolayfilt(ForceFrontVert(1,:),1,17)/8)
title(Run(r),'interpreter', 'none')
xlabel('Time (s)')
ylabel('Tire Load (lbf)')
legend('Front Tire Front Load','Front Tire Side Load','Front Tire Vertical Load',1)
%}

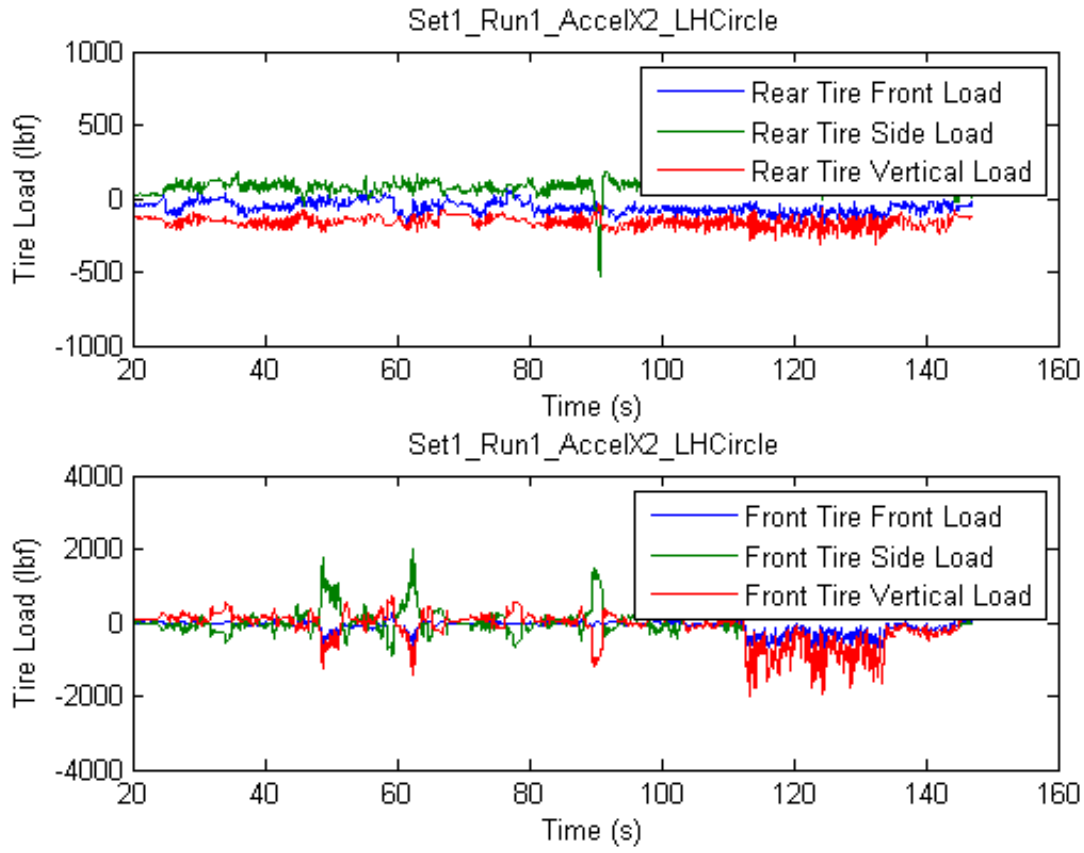
print(char(Run(r)),'-dpng') %Print Plots to .PNG

%end

% Unfiltered
%{
figure(1)
plot (Time,ForceRearFront(1,:), Time,ForceRearSide(1,:), Time,ForceRearVert(1,:))
title(Run(r),'interpreter', 'none')
xlabel('Time (s)')
ylabel('Tire Load (lbf)')
legend('Rear Tire Front Load','Rear Tire Side Load','Rear Tire Vertical Load')

figure(2)
plot (Time,ForceFrontFront(1,:), Time,ForceFrontSide(1,:), Time, ForceFrontVert(1,:))%
title(Run(r),'interpreter', 'none')
xlabel('Time (s)')
ylabel('Tire Load (lbf)')
legend('Front Tire Front Load','Front Tire Side Load','Front Tire Vertical Load',2)
%}

```



Published with MATLAB® R2013a